

THESIS

Cosmological and astrophysical aspects  
of massive spin-2 field

Katsuki AOKI

青木 勝輝



*Waseda University*

*Graduate School of Advanced Science and Engineering*

*Department of Pure and Applied Physics*

*Research on Theoretical Astrophysics and Cosmology*

February 2017



# Contents

|          |   |           |
|----------|---|-----------|
| <b>1</b> | <b>Introduction</b>   | <b>1</b>  |
| <b>2</b> | <b>Linear massive gravity</b>   | <b>5</b>  |
| 2.1      | Free field Lagrangian . . . . .                                       | 5         |
| 2.2      | vDVZ discontinuity . . . . .  | 8         |
| 2.3      | Stüeckelberg trick and decoupling limit . . . . .                     | 10        |
| 2.4      | Fierz-Pauli theory on curved background . . . . .                     | 11        |
| 2.5      | Experimental constraints on graviton mass . . . . .                   | 13        |
| <b>3</b> | <b>Nonlinear massive gravity and bigravity</b>                        | <b>17</b> |
| 3.1      | Nonlinear self-interactions . . . . .                                 | 17        |
| 3.1.1    | Hamiltonian analysis in general relativity . . . . .                  | 17        |
| 3.1.2    | Hamiltonian analysis in massive gravity . . . . .                     | 18        |
| 3.2      | de Rham-Gabadadze-Tolley theory . . . . .                             | 20        |
| 3.3      | Bigravity theory . . . . .  | 24        |
| 3.3.1    | Hassan-Rosen bigravity . . . . .                                      | 24        |
| 3.3.2    | Homothetic solutions . . . . .  | 25        |
| 3.3.3    | Linearization of bigravity theory . . . . .                           | 28        |
| 3.4      | Energy-momentum tensor of gravitons in bigravity . . . . .            | 29        |
| <b>4</b> | <b>Decoupling limits and Vainshtein mechanism</b>                     | <b>35</b> |
| 4.1      | Nonlinear Stüeckelberg fields . . . . .                               | 35        |
| 4.2      | Below the scale $\Lambda_3$ . . . . .                                 | 36        |
| 4.3      | $\Lambda_3$ decoupling limit . . . . .                                | 38        |
| 4.4      | Vainshtein mechanism . . . . .  | 40        |
| 4.5      | $\Lambda_2$ decoupling limit . . . . .                                | 43        |
| 4.5.1    | Non-compact nonlinear sigma model . . . . .                           | 45        |
| 4.5.2    | Effective action inside the Vainshtein radius . . . . .               | 46        |
| 4.5.3    | No-go result of stable background without vector excitation . . . . . | 47        |
| <b>5</b> | <b>Attractor universe</b>   | <b>51</b> |
| 5.1      | FLRW universe . . . . .   | 51        |
| 5.2      | Attractors . . . . .  | 54        |
| 5.3      | Dynamics of the universe with twin matter . . . . .                   | 56        |
| 5.4      | Cosmic no hair conjecture . . . . .                                   | 61        |
| <b>6</b> | <b>Stability in the early universe</b>                                | <b>65</b> |
| 6.1      | Ghost condensate and cosmological Vainshtein mechanism . . . . .      | 65        |
| 6.2      | Scalar graviton with nonlinear effects . . . . .                      | 67        |
| 6.2.1    | Adiabatic mode solution . . . . .                                     | 68        |
| 6.2.2    | Stability conditions of scalar graviton . . . . .                     | 71        |
| 6.3      | Perturbations with matter effects . . . . .                           | 74        |
| 6.3.1    | Adiabatic mode with matter perturbations . . . . .                    | 75        |
| 6.3.2    | GR phase . . . . .  | 76        |
| 6.3.3    | Bigravity phase . . . . .   | 77        |

|          |  |            |
|----------|--|------------|
| 6.4      | Transition from GR to bigravity . . . . .                                | 78         |
| <b>7</b> | <b>On dark matter</b>  | <b>83</b>  |
| 7.1      | Dark matter from $f$ -sector . . . . .                                   | 84         |
| 7.1.1    | Cosmic pie . . . . .   | 85         |
| 7.1.2    | Dark matter halo . . . . .   | 87         |
| 7.1.3    | Cosmic structure formation . . . . .                                     | 90         |
| 7.2      | Massive graviton as dark matter . . . . .                                | 99         |
| 7.2.1    | Production of massive gravitons . . . . .                                | 100        |
| 7.2.2    | Present abundance and gravitational waves . . . . .                      | 104        |
| <b>8</b> | <b>Astrophysical objects and Vainshtein screening</b>                    | <b>107</b> |
| 8.1      | Static and spherically symmetric spacetime . . . . .                     | 108        |
| 8.2      | Weak field approximation . . . . .                                       | 110        |
| 8.3      | Relativistic stars . . . . .   | 114        |
| 8.3.1    | Regular compact objects in $\Lambda_2$ decoupling limit . . . . .        | 114        |
| 8.3.2    | Regular compact objects: numerical results . . . . .                     | 123        |
| 8.4      | Perturbations around static and spherically symmetric solution . . . . . | 127        |
| 8.4.1    | Odd parity perturbations . . . . .                                       | 128        |
| 8.4.2    | Even parity perturbations . . . . .                                      | 128        |
| <b>9</b> | <b>Summary</b>   | <b>133</b> |
| <b>A</b> | <b>Constrained systems</b>   | <b>137</b> |
| A.1      | Lagrangian formulation . . . . .   | 137        |
| A.2      | Hamiltonian formulation . . . . .  | 138        |
| A.3      | Field theory . . . . .   | 141        |
| <b>B</b> | <b>Instabilities</b>   | <b>143</b> |
| B.1      | Ghost instability . . . . .  | 143        |
| B.2      | Gradient instability . . . . .   | 143        |
| B.3      | Tachyonic instability . . . . .  | 144        |
| B.4      | Ostrogradsky instability . . . . .                                       | 144        |

# Chapter 1

## Introduction

General Relativity (GR) is now widely accepted as the standard theory of gravity. GR has passed a number of observational and experimental tests and the robustness of GR has been confirmed with high accuracy, especially in Solar-System [1,2]. Despite these successes of GR alternative theories of gravity have been discussed from both theoretical and observational prospects.

A fundamental issue in physics is whether a graviton has a mass or not. According to the Lovelock's theorem, GR is the unique theory of gravity whose equation of motion is given by a symmetric second rank tensor which is divergence free and constructed from only the metric tensor with up to its second order derivatives in four dimensions [3]. From the particle physics perspective, GR is thought as the unique theory of a massless spin-2 field; that is, the carrier of the gravitational force, called graviton, is a massless spin-2 particle. However, the non-existence of the mass of the graviton is not a trivial assumption since we know, for example, the carriers of the electroweak forces are massive particles via the Higgs mechanism. Needless to say, some constraints on the graviton mass have been obtained from the observations which agree with the predictions of GR [4,5]. For instance, the existence of the massive graviton should change the gravitational law from the inverse square law. The inverse square law of the gravitational force has been confirmed from the laboratory scales ( $\sim 10^{-4}$  cm) to the Solar System scales ( $\sim 10^{17}$  cm), thus the graviton mass may not exist in the range  $10^{-2}$  eV  $\lesssim m \lesssim 10^{-23}$  eV. Nevertheless, the existence of the graviton mass has not been excluded in a wide range of scales and the massive graviton will provide significant deviations from the standard scenario. In particular, we mainly focus on the case in which the carriers of the gravitational force are given by a massive graviton and a massless graviton because this kind of theory might be natural to include a massive graviton as we will see later (Chapter 3).

Fierz and Pauli proposed a linearized theory of massive spin-2 field in 1939, called Fierz-Pauli theory [6]. Since the gravity should be described by a nonlinear theory of the metric tensor, the Fierz-Pauli theory has to be extended into nonlinear orders when we interpret this massive spin-2 field as the graviton. Another reason for the requirement of the nonlinear extension is to obtain a continuous restoration from the massive field into the massless field by taking the massless limit. The number of degrees of freedom of the massive spin-2 field is five which is larger than that of the massless spin-2 field. It is known that an additional degree of freedom is not decoupled even in the massless limit at the linear order and then the Newtonian gravity is not recovered which is called the van Dam-Veltman-Zakharov (vDVZ) discontinuity [7,8]. Vainshtein then proposed that the vDVZ discontinuity can be evaded by taking into account nonlinear mass terms, and the extra mode is screened inside the so-called Vainshtein radius, to recover the standard gravitational interaction mediated only by the helicity-2 modes [9]. Boulware and Deser pointed out, however, that such nonlinear extensions ruin the structure of the FP theory and introduce the ghost instability associated with the sixth degree of freedom [10]. Although this nonlinear ghost, often called Boulware-Deser (BD) ghost, appears in any simple nonlinear extensions of the FP massive gravity theory, it was shown in 2010 by de Rham, Gabadadze, and Tolley that the special choice of the mass term can eliminate such a ghost state at the decoupling limit [11,12], and later the proof was extended to fully nonlinear orders [13–16]. Furthermore, the nonlinear ghost-free massive gravity, often dubbed dRGT theory, is generalized to the bigravity theory [17]

and the multigravity theory [18] which contain massive graviton(s) as well as a massless graviton. See [19–22] for reviews.

Although the theoretical development of the massive graviton is independent on any cosmological reasons, the nonlinear theories of massive graviton are often discussed in the context of cosmology. Recent observation has confirmed the big bang scenario of the expanding Universe. The cosmological parameters are determined very precisely [23]. However, those observations reveal new unsolved mysteries in cosmology, i.e., the accelerated expansion of the Universe and the existence of dark matter. The discovery of these problems may suggest that a theory beyond standard physic is required.

The basic assumptions of the big bang cosmology are the cosmological principle (homogeneity and isotropy of the Universe) and the dynamics of the Universe is described by GR. The current accelerating expansion of the Universe could be caused by an unknown “energy” dubbed dark energy. The simplest candidate of dark energy is a cosmological constant (the vacuum expectation value of some fields). The matter contents of the Universe may be phenomenologically given by standard model particles, the cosmological constant  $\Lambda$ , and cold dark matter (CDM). However, the theoretically expected value of a cosmological constant is too large to explain the observed value of dark energy [24]. The origin of the accelerating expansion is one of the biggest mysteries in modern cosmology [25, 26]. An alternative approach is that this acceleration is caused by a “modification” of the gravity from GR at the infrared regime (see [27–29] for reviews). On the other hand, the origin of dark matter is also one of the biggest problems. Although many dark matter candidates have been proposed in the context of the particle physic (see [30, 31] for reviews), any dark matter particles have not been discovered yet [32–37]. The existence of dark matter is confirmed via only gravitational interactions. Hence, exploring dark matter candidate in the context of gravity is also a considerable approach. The modified theories of gravity could give solutions to the cosmological problems.

The modification of the gravity is strongly constrained by Solar System tests of the gravity. For example, one may easily construct a theory of gravity which explains the present acceleration of the Universe by the modification of the gravity instead of dark energy; however, in general, the modification may change the local gravitational law as well. The effects of the modification of gravity have to be screened at the Solar System level. Various screening mechanisms have been proposed. One natural theory with such a screening mechanism is the massive gravity with a tiny graviton mass because we may ignore the mass term in scales within the Compton wavelength. However, as we mentioned above, the linear massive gravity is not restored into GR due to the additional degree of freedom. The restoration to GR may be realized by nonlinear interactions in scales below the Vainshtein radius.

The effect of the spacetime curvature is significant for the massive spin-2 field. The Fierz-Pauli theory can be extended in a curved spacetime, although it is originally proposed in the Minkowski spacetime. A simple case is that the spacetime is given by a maximally symmetric spacetime. In this case two facts are well-known: (i) in de Sitter spacetime, the helicity-zero mode of the massive graviton becomes a ghost, called Higuchi ghost, when the Higuchi bound is violated [38, 39], and (ii) there is no vDVZ discontinuity in the anti-de Sitter spacetime [40, 41]. The Higuchi bound reads a lower bound of the graviton mass in order not to be a ghost state. Therefore, the linear massive spin-2 field has no healthy massless limit in the de Sitter spacetime. In the anti-de Sitter spacetime, on the other hand, the field has a continuous massless limit even though nonlinear interactions are not taken into account. In particular, the Higuchi ghost is relevant to discussions of the cosmology since similar type linear instabilities generally exist even in Friedmann-Lemaître-Robertson-Walker (FLRW) spacetimes [42] and the early stage of the Universe may yield the violation of the Higuchi bound. Of course, these discussions are based on the Fierz-Pauli theory which may not be directly applied into those in the dRGT theory or in the nonlinear bigravity theory. Nevertheless, one should confirm whether the Higuchi ghost exists or not and pay attention to a mechanism to evade the ghost if exists.

In this thesis, focusing on the bigravity theory which contains a massive graviton as well as a massless graviton, we discuss both cosmological and astrophysical aspects of the massive graviton.

The reasons for cosmological studies are related to the accelerating expansion of the Universe or the origin of dark matter. The bigravity can yield various phenomenological features depending on the graviton mass. The dynamics of the Universe should be changed by the graviton mass

and then the accelerating expansion could be obtained by the tiny graviton mass as  $m \sim 10^{-33}$  eV [43–52]. Another possibility is to explain the origin of dark matter when the graviton mass is heavy enough. When a matter field is introduced in the “dark” sector, it acts as the dark matter in the physical sector through the gravitational interactions for the gravitons with  $m \gtrsim 10^{-27}$  eV [51, 53]. Furthermore, the massive graviton itself is also a candidate of dark matter when the graviton mass is  $10^{-23}$  eV  $\lesssim m \lesssim 10^7$  eV [54] (see also [55, 56]).

When we focus on the early stage of the Universe, the Higuchi type instability will be problematic. Indeed, the papers [57–62] showed that the homogeneous and isotropic solutions are unstable due to the Higuchi type instability in bigravity. However, this instability may be resolved by the cosmological Vainshtein mechanism [63]. We found the cosmological solution in which the helicity-zero mode forms a condensed state around which the helicity-zero mode does not suffer from the Higuchi type instability. The cosmological Vainshtein mechanism yields that the continuous massless limit can be taken without the Higuchi type instability even in the cosmological background.

On the other hand, an astrophysical reason is to confirm the consistency with the predictions of GR in Solar System, i.e., the existence of the Vainshtein mechanism which is essential to making the graviton with  $m \lesssim 10^{-23}$  eV consistent with the Solar System observations. According to the Vainshtein mechanism, the nonlinear theories of massive graviton must be restored into GR in small scales. Vainshtein mechanism in massive gravity/bigravity has been discussed in [63–86]. In bigravity the Vainshtein screening of the extra degrees of freedom seems to be realized for the spacetime around a star [79, 82, 85] and also the early universe [63] in which only the scalar degree of freedom has an important role for the screening. However, we show that any Ricci flat Vainshtein screening solution is unstable when we take into account the excitation of the scalar graviton only [86]. Since the Vainshtein screening solution with the vector degrees of freedom has not been found so far, the existence of the Vainshtein mechanism in vacuum spacetimes is still an open question.

## Structure of the thesis

Before showing our cosmological and astrophysical studies we devote general properties of massive graviton in Chapters 2, 3, and 4.

In Chapter 2 we consider the linear theory of the massive graviton. We will show why the Fierz-Pauli theory is the unique ghost-free theory of the massive spin-2 field and why the Fierz-Pauli theory exhibits the vDVZ discontinuity and the Higuchi ghost. The observational constraints on the graviton mass are also discussed in this chapter because these constraints are obtained based on the linear theory.

We review the dRGT theory as well as the nonlinear bigravity theory in Chapter 3. First, we count the number of the degree of freedom in generic nonlinear massive gravity and confirm that there exists an additional mode. Then we introduce the Lagrangian of the dRGT theory and briefly review the ghost-freeness of the dRGT theory. The bigravity theory is a straightforward extension of the dRGT theory. We shall see that the theory contains a massless graviton and a massive graviton by considering linear perturbations around a specific solution of the bigravity theory. Furthermore, calculating second order perturbations, we define the energy-momentum tensors of gravitons.

In Chapter 4 we discuss the Vainshtein mechanism. We will introduce two limits: the  $\Lambda_3$  decoupling limit and the  $\Lambda_2$  decoupling limit. The scale  $\Lambda_3$  is associated with the lowest strong coupling scale of the massive graviton in the Minkowski spacetime [11, 12]. The scales below  $\Lambda_3$  are prohibited due to the ghost-freeness of the theory. In the  $\Lambda_3$  decoupling limit the helicity-zero mode is not explicitly decoupled from the helicity-two modes. On the other hand, the helicity-zero mode is expected to be decoupled due to the Vainshtein screening. The Vainshtein mechanism may cause the increasing of the strong coupling scale. As a result, we may take the  $\Lambda_2$  decoupling limit where the scale  $\Lambda_2$  gives the strong coupling scale around backgrounds in which the Vainshtein mechanism is implemented [83, 84, 86]. The helicity-zero mode is decoupled in the  $\Lambda_2$  decoupling limit. However, we will show that only the excitation of the helicity-zero mode suffers from the instability in Ricci flat spacetimes. In vacuum regions of the spacetime, the helicity-one modes

would be required to obtain a successful Vainshtein mechanism.

Our cosmological studies are summarized in Chapters 5, 6, and 7. In Chapter 5 we discuss the dynamics of the homogeneous and isotropic universe and show both accelerating and decelerating solutions are obtained as attractors in the late stage of the universe. The discussions about the Higuchi type instability is devoted in Chapter 6. We find a stable cosmological solution in a simple ansatz. In Chapter 7 we consider two possibilities to explain dark matter in the context of the bigravity theory. We also discuss some observational aspects of our dark matter scenarios. These cosmological studies show that the bigravity theory can give a solution to the dark components of the Universe and also that the bigravity theory can be consistent with the big bang cosmology.

We consider static and spherically symmetric solutions and discuss astrophysical aspects of the bigravity theory in Chapter 8. First, we review the results obtained in the weak field approximation. The Vainshtein screening seems to be realized in the weak gravitational field. However, we show that the Vainshtein screening can be broken due to the appearance of a curvature singularity in the strong gravitational field. Furthermore, we also show that the weak field solutions are unstable which is consistent with the general consequence discussed in Chapter 4. Therefore, the Vainshtein screening is indeed unsuccessful in the static and spherically symmetric solutions in the bigravity theory.

We summarize our results and give future prospects in Chapter 9.

Since knowledge about constrained systems is used to discuss spin-2 fields, we briefly review basics about the Lagrangian and the Hamiltonian formulations in constrained systems in Appendix A. In Appendix B, we summarize instabilities of a field: the ghost instability, the gradient instability, the tachyonic instability, and the Ostrogradsky instability.

## Notation

The metric signature is  $(-, +, \dots, +)$  and the curvature tensors are defined by  $R^\mu{}_{\alpha\beta\gamma} = \partial_\alpha \Gamma^\mu{}_{\beta\gamma} - \dots$  and  $R_{\mu\nu} = R^\alpha{}_{\mu\alpha\nu}$ . The symmetrization and the anti-symmetrization are normalized:  $A_{(\mu}B_{\nu)} = \frac{1}{2}(A_\mu B_\nu + A_\nu B_\mu)$  and  $A_{[\mu}B_{\nu]} = \frac{1}{2}(A_\mu B_\nu - A_\nu B_\mu)$ . Unless otherwise stated, we use the natural units  $c = \hbar = 1$ .



## Chapter 2

# Linear massive gravity

### 2.1 Free field Lagrangian

We consider linear tensor theories with a Lorentz invariance propagating on Minkowski background in four dimensions <sup>1</sup>. We introduce a symmetric Lorentz tensor  $h_{\mu\nu}$  with mass dimension one, and consider a quadratic action of  $h_{\mu\nu}$  which yields a linear order equation of motion of  $h_{\mu\nu}$ . Assuming the Lorentz invariance and the equivalence upon integration by parts, the generic kinetic term can be rewritten as

$$\mathcal{L}_{\text{kin}}^{\text{spin}-2} = \frac{1}{2} \partial^\alpha h^{\mu\nu} (a_1 \partial_\alpha h_{\mu\nu} + 2a_2 \partial_{(\mu} h_{\nu)\alpha} + a_3 \partial_\alpha h \eta_{\mu\nu} + 2a_4 \partial_{(\mu} h \eta_{\nu)\alpha}), \quad (2.1.1)$$

where  $a_1, a_2, a_3, a_4$  are constants and  $h = h^\mu{}_\mu$ . Note that one should not introduce any higher derivative terms to avoid the Ostrogradsky's instability (See Appendix B.4 for the Ostrogradsky's theorem). The Lagrangian (2.1.1) seems not to contain any higher derivative terms. However, arbitrary coefficients lead to the Ostrogradsky instability arising from higher derivatives of vector and/or scalar modes of  $h_{\mu\nu}$ . We decompose the symmetric tensor  $h_{\mu\nu}$  into a transverse tensor  $h_{\mu\nu}^T$  and a vector field  $\chi_\mu$ ,

$$h_{\mu\nu} = h_{\mu\nu}^T + 2\partial_{(\mu} \chi_{\nu)}. \quad (2.1.2)$$

Substituting this expression into the Lagrangian (2.1.1), the Lagrangian contains higher derivative terms as

$$\mathcal{L}_{\text{kin}}^{\text{spin}-2} \supset (a_1 + a_2) \chi^\mu \square^2 \chi_\mu + (a_1 + 3a_2 + 2a_3 + 4a_4) \chi^\mu \square \partial_\mu \partial_\nu \chi^\nu - 2(a_3 + a_4) h^T \square \partial_\alpha \chi^\alpha. \quad (2.1.3)$$

Therefore, the generic kinetic term of the tensor field suffers from the Ostrogradski instability even if the original Lagrangian does not contain higher derivatives of  $h_{\mu\nu}$ . To preserve the theory from the Ostrogradski instability, the coefficients have to satisfy

$$a_1 = -a_2 = -a_3 = a_4. \quad (2.1.4)$$

Setting  $a_1 = -1/4$  to follow standard conventions, the unique ghost-free kinetic term is given by the linearized Einstein-Hilbert term

$$\mathcal{L}_{\text{kin}}^{\text{spin}-2} = \mathcal{L}_{\text{EH}} := -\frac{1}{4} h^{\mu\nu} \mathcal{E}_{\mu\nu, \alpha\beta} h^{\alpha\beta}, \quad (2.1.5)$$

where

$$\mathcal{E}_{\mu\nu, \alpha\beta} h^{\alpha\beta} = -\frac{1}{2} \partial^2 h_{\mu\nu} - \frac{1}{2} \partial_\mu \partial_\nu h + \partial_\alpha \partial_{(\nu} h^\alpha{}_{\mu)} + \frac{1}{2} \eta_{\mu\nu} (\partial^2 h - \partial_\alpha \partial_\beta h^{\alpha\beta}), \quad (2.1.6)$$

is the Lichnerowicz operator. For the Einstein-Hilbert action, the appearance of the higher derivatives is prohibited by the gauge invariance under the transformation

$$h_{\mu\nu} \rightarrow h_{\mu\nu} + 2\partial_{(\mu} \xi_{\nu)}. \quad (2.1.7)$$

---

<sup>1</sup>The statement discussed here can be straightforwardly generalized into any dimensional spacetime.

The gauge invariance indeed leads to that the vector field  $\chi_\mu$  turns to be a gauge mode. The higher derivatives of the physical variables do not appear in the Einstein-Hilbert action.

Next, we consider the mass terms of the tensor field. The possible Lorentz invariant mass terms are

$$\mathcal{L}_{\text{mass}}^{\text{spin}-2} = -\frac{m^2}{8}(h_{\mu\nu}h^{\mu\nu} + \alpha h^2). \quad (2.1.8)$$

Similarly to the case of generic kinetic terms, higher derivative terms would appear even if the mass term do not contain derivatives. Thus,  $\alpha$  should be determined by the Ostrogradsky-free condition. We decompose  $h_{\mu\nu}$  into the transverse tensor  $h_{\mu\nu}^T$ , the transverse vector  $\chi_\mu^T$  and the scalar  $\chi$ ,

$$h_{\mu\nu} = h_{\mu\nu}^T + 2\partial_{(\mu}\chi_{\nu)}^T + 2\partial_\mu\partial_\nu\chi. \quad (2.1.9)$$

The higher derivative terms appear in

$$\mathcal{L}_{\text{mass}}^{\text{spin}-2} \supset -m^2(\alpha + 1)((\square\chi)^2 - 2\chi^{T\mu}\square\partial_\mu\chi), \quad (2.1.10)$$

thus, the higher derivatives are canceled out only when

$$\alpha = -1. \quad (2.1.11)$$

As a result, the ghost-free Lorentz invariant mass term is uniquely given by the Fierz-Pauli mass term [6],

$$\mathcal{L}_{\text{mass}}^{\text{spin}-2} = \mathcal{L}_{\text{FP}} := -\frac{m^2}{8}(h_{\mu\nu}h^{\mu\nu} - h^2), \quad (2.1.12)$$

where the parameter  $m$  describes the mass of the tensor field  $h_{\mu\nu}$ . Adding to the ghost-free kinetic term, the Fierz-Pauli Lagrangian is given by

$$\mathcal{L} = -\frac{1}{4}h^{\mu\nu}\mathcal{E}_{\mu\nu,\alpha\beta}h^{\alpha\beta} - \frac{m^2}{8}(h_{\mu\nu}h^{\mu\nu} - h^2), \quad (2.1.13)$$

which is the unique ghost-free Lorentz invariant theory of the massive tensor field.

Note that the Fierz-Pauli mass term is not gauge invariant. The appearance of the unstable mode is protected by the existence of a non-trivial constraint instead of the gauge invariance. To see this statement, we back to the Lagrangian

$$\mathcal{L} = -\frac{1}{4}h^{\mu\nu}\mathcal{E}_{\mu\nu,\alpha\beta}h^{\alpha\beta} - \frac{m^2}{8}(h_{\mu\nu}h^{\mu\nu} + \alpha h^2). \quad (2.1.14)$$

The variation with respect to  $h_{\mu\nu}$  gives the field equation

$$\mathcal{E}_{\mu\nu}^{\alpha\beta}h_{\alpha\beta} + \frac{m^2}{2}(h_{\mu\nu} + \alpha\eta_{\mu\nu}h) = 0. \quad (2.1.15)$$

Multiplying the field equation by  $\partial^\mu$ , we get the constraint equation

$$\partial^\mu(h_{\mu\nu} + \alpha\eta_{\mu\nu}h) = 0. \quad (2.1.16)$$

The trace of the field equation leads

$$\square h - \partial_\alpha\partial_\beta h^{\alpha\beta} + \frac{m^2}{2}(1 + 4\alpha)h = 0. \quad (2.1.17)$$

Combining Eq. (2.1.17) with Eq. (2.1.16), we obtain the equation for the trace of  $h_{\mu\nu}$

$$(1 + \alpha)\square h + \frac{m^2}{2}(1 + 4\alpha)h = 0. \quad (2.1.18)$$

Hence the trace of  $h_{\mu\nu}$  is dynamical when  $\alpha \neq -1$  for which there is an additional degree of freedom in addition to ones of the massive spin-2 field. On the other hand,  $h$  is non-dynamical only when  $\alpha = -1$ , and the degree of freedom actually coincides with those of the massive spin-2 field. We note that the trace part indeed corresponds to the unstable mode, which can be seen by introducing the tensor

$$h_{\mu\nu}^{TT} = h_{\mu\nu} - \frac{2(1+\alpha)}{3m^2} \partial_\mu \partial_\nu h - \frac{1}{3}(1+\alpha)\eta_{\mu\nu}h, \quad (2.1.19)$$

where  $h_{\mu\nu}^{TT}$  is transverse-traceless by using the equations of motion. The Lagrangian is rewritten as

$$\mathcal{L} = -\frac{1}{8} (\partial_\alpha h_{\mu\nu}^{TT})^2 + \frac{(1+\alpha)^2}{12} (\partial_\alpha h)^2 + \dots. \quad (2.1.20)$$

Hence the kinetic term of  $h$  has an opposite sign, and then  $h$  suffers from the ghost instability. When  $\alpha = -1$ ,  $h$  is not a dynamical variable because the equation (2.1.18) is replaced with a constraint equation. As a result, only when  $\alpha = -1$ , there exists a non-trivial constraint equation which removes the ghost mode. There is no such a constraint equation for the general mass term, which is a reason for the existence of Boulware-Deser ghost [10]. We will revisit this problem in the case of nonlinear mass terms in Section 3.1.

The linearized Einstein-Hilbert action describes the motion of the massless tensor field, while the Fierz-Pauli action indeed gives the equation of motion of the massive tensor field. First, we discuss the Einstein-Hilbert action in which unphysical degrees of freedom (i.e., gauge degrees of freedom) exist. For the gauge transformation (2.1.7), the quantity  $\bar{h}_{\mu\nu} := h_{\mu\nu} - \frac{1}{2}\eta_{\mu\nu}h$  transforms as

$$\partial^\mu \bar{h}_{\mu\nu}^{\text{new}} = \partial^\mu \bar{h}_{\mu\nu}^{\text{old}} - \square \chi_\nu.$$

Hence one can choose the harmonic gauge

$$\partial^\mu \bar{h}_{\mu\nu} = \partial^\mu \left( h_{\mu\nu} - \frac{1}{2}\eta_{\mu\nu}h \right) = 0, \quad (2.1.21)$$

with an appropriate gauge function  $\chi_\nu$ . In the harmonic gauge, the linearized Einstein equation without a source is given by

$$\square \bar{h}_{\mu\nu} = 0. \quad (2.1.22)$$

However, the harmonic gauge is not complete gauge fixing since the quantity  $\partial^\mu \bar{h}_{\mu\nu}$  is still invariant under the gauge transformation with the gauge function satisfying  $\square \chi_\mu = 0$ . In the Fourier space, the linearized Einstein equation and the condition  $\square \chi_\mu = 0$  yield

$$\bar{h}_{\mu\nu} = \sum_k \bar{h}_{\mu\nu}^{(k)} e^{ik_\mu x^\mu}, \quad \chi_\mu = \sum_k \chi_\mu^{(k)} e^{ik_\mu x^\mu}, \quad (2.1.23)$$

with  $k^\mu k_\mu = 0$ , where  $\bar{h}_{\mu\nu}^{(k)}$  and  $\chi_\mu^{(k)}$  are Fourier coefficients for the momentum  $k^\mu$ . By using the residual gauge freedom, one can choose the transverse-traceless gauge

$$\partial_\mu h^{\mu\nu} = 0, \quad h^\mu{}_\mu = 0, \quad u^\mu h_{\mu\nu} = 0,$$

where  $u^\mu$  is a constant timelike vector. Then the equation of motion is simply given by the massless Klein-Gorden equation

$$\square h_{\mu\nu} = 0. \quad (2.1.24)$$

The gauge fixing conditions give eight conditions on ten components of  $h_{\mu\nu}$ . Thus, the gauge fixed variable has only two independent components which is indeed same as the number of the

polarizations of the massless spin-2 field. For instance, when we choose the vector  $u^\mu = (1, 0, 0, 0)$  and consider a plane wave traveling in the  $z$  direction  $k^\mu = (\omega, 0, 0, \omega)$ ,  $h_{\mu\nu}$  is expressed as

$$h_{\mu\nu} = \begin{pmatrix} 0 & 0 & 0 & 0 \\ 0 & h_+ & h_\times & 0 \\ 0 & h_\times & -h_+ & 0 \\ 0 & 0 & 0 & 0 \end{pmatrix} e^{ik_\mu x^\mu}, \quad (2.1.25)$$

where  $h_+$  and  $h_\times$  express two independent polarizations.

In the case of the Fierz-Pauli action, there is no gauge freedom but there exist constraint equations on  $h_{\mu\nu}$ . In the vacuum, Eqs. (2.1.16) and (2.1.18) with  $\alpha = -1$  give the transverse-traceless condition

$$\partial_\mu h^{\mu\nu} = 0, \quad h = 0. \quad (2.1.26)$$

Then, the field equation is reduced into the massive Klein-Gordon equation

$$(\square - m^2)h_{\mu\nu} = 0. \quad (2.1.27)$$

We note that the transverse-traceless condition (2.1.26) give only five conditions on  $h_{\mu\nu}$ . Therefore, the residual degrees of freedom of  $h_{\mu\nu}$  are five which is the same number as the number of the polarizations of the massive spin-2 field.

## 2.2 vDVZ discontinuity

In the previous section, we discuss free propagating massless and massive tensor fields. Here, we introduce a matter coupling

$$\mathcal{L}_m = \frac{\kappa}{2} h_{\mu\nu} T^{\mu\nu}, \quad (2.2.1)$$

where  $T^{\mu\nu}$  is the energy-momentum tensor of a matter field and  $\kappa := \sqrt{8\pi G}$  is the gravitational coupling constant. Intuitively, the massive field is restored into the corresponding massless field by taking a massless limit. However, in the tensor field, the massless limit of the tensor field does not coincide with the massless one, which is known as the van Dam-Veltman-Zakharov (vDVZ) discontinuity [7, 8].

Let us find solutions of massless and massive tensor field with a source. We assume the energy-momentum tensor of the matter is conserved, i.e.,  $\partial_\mu T^{\mu\nu} = 0$ . The equation of motion of the massless tensor field with a source is expressed by

$$\partial^2 h_{\text{massless}}^{\mu\nu} = -2\kappa \left( T^{\mu\nu} - \frac{1}{2} \eta^{\mu\nu} T \right), \quad (2.2.2)$$

where we have chosen the harmonic gauge

$$\partial_\mu h_{\text{massless}}^{\mu\nu} = \frac{1}{2} \partial^\nu h_{\text{massless}}. \quad (2.2.3)$$

On the other hand, the equation of motion for the massive graviton is given by

$$(\partial^2 - m^2)h_{\text{massive}}^{\mu\nu} = -2\kappa \left( T^{\mu\nu} - \frac{1}{3} \left( \eta^{\mu\nu} - \frac{\partial^\mu \partial^\nu}{m^2} \right) T \right), \quad (2.2.4)$$

where the massive graviton must satisfy the constraint equations

$$\partial_\mu h_{\text{massive}}^{\mu\nu} = \partial^\nu h_{\text{massive}}, \quad \frac{m^2}{2} h_{\text{massive}} = -\frac{\kappa}{3} T. \quad (2.2.5)$$

We define a tensor  $\tilde{h}_{\text{massive}}^{\mu\nu}$  as

$$h_{\mu\nu}^{\text{massive}} = \tilde{h}_{\mu\nu}^{\text{massive}} + 2\partial_\mu \partial_\nu \tilde{\phi}, \quad (2.2.6)$$

where  $\tilde{\phi}$  is assumed to satisfy

$$(\partial^2 - m^2)\tilde{\phi} = -\frac{\kappa}{3m^2}T. \quad (2.2.7)$$

Then the equation of motion of  $\tilde{h}_{\text{massive}}^{\mu\nu}$  is given by

$$(\partial^2 - m^2)\tilde{h}_{\text{massive}}^{\mu\nu} = -2\kappa \left( T^{\mu\nu} - \frac{1}{3}\eta^{\mu\nu}T \right), \quad (2.2.8)$$

Note that, although the massive tensor field has no gauge symmetry, the matter action is invariant under (2.2.6):

$$\mathcal{L}_m = \frac{\kappa}{2}h_{\mu\nu}^{\text{massive}}T^{\mu\nu} = \frac{\kappa}{2}\tilde{h}_{\mu\nu}^{\text{massive}}T^{\mu\nu} + \text{total divergence}. \quad (2.2.9)$$

Therefore, the matter field is not affected by  $\tilde{\phi}$ . To discuss the tensor field observed by a matter, it is sufficient to find a solution of  $\tilde{h}_{\mu\nu}^{\text{massive}}$  rather than  $h_{\mu\nu}^{\text{massive}}$ .

The source terms of the massless and massive field equations are different which suggests the existence of the vDVZ discontinuity. Indeed, the solution of the massive field is not restored into the one of the massless field. To see explicitly the existence of the vDVZ discontinuity, we consider a point source at the origin

$$T^{\mu\nu} = M\delta_0^\mu\delta_0^\nu\delta^{(3)}(\mathbf{0}), \quad (2.2.10)$$

where  $M$  is the mass of the source. The solution of the massless field is given by

$$\kappa h_{00}^{\text{massless}} = \frac{2GM}{r}, \quad \kappa h_{0i}^{\text{massless}} = 0, \quad \kappa h_{ij}^{\text{massless}} = \frac{2GM}{r}\delta_{ij}, \quad (2.2.11)$$

where  $r = \sqrt{x^i x_i}$ . On the other hand, the solution of the massive field is given by

$$\kappa \tilde{h}_{00}^{\text{massive}} = \frac{4}{3}\frac{2GM}{r}e^{-mr}, \quad \kappa \tilde{h}_{0i}^{\text{massive}} = 0, \quad \kappa \tilde{h}_{ij}^{\text{massive}} = \frac{2}{3}\frac{2GM}{r}e^{-mr}\delta_{ij}, \quad \kappa \tilde{\phi} = -\frac{2GM}{3m^2 r}e^{-mr}, \quad (2.2.12)$$

and then

$$\begin{aligned} \kappa h_{00}^{\text{massive}} &= \frac{4}{3}\frac{2GM}{r}e^{-mr}, \\ \kappa h_{0i}^{\text{massive}} &= 0, \\ \kappa h_{ij}^{\text{massive}} &= \frac{2}{3}\frac{2GM}{r}e^{-mr} \left[ \frac{1+mr+m^2r^2}{m^2r^2}\delta_{ij} - \frac{x_i x_j}{m^2r^4}(3+3mr+m^2r^2) \right]. \end{aligned} \quad (2.2.13)$$

Hence the physical prediction from the massive field is not restored into one from the massless field in the massless limit,

$$h_{00}^{\text{massless}} \neq \tilde{h}_{00}^{\text{massive}}|_{m \rightarrow 0}, \quad h_{ij}^{\text{massless}} \neq \tilde{h}_{ij}^{\text{massive}}|_{m \rightarrow 0}. \quad (2.2.14)$$

The result implies that, when the gravity is mediated by a massive tensor field, the massive graviton conflicts with the solar system experiment even if the graviton mass is tiny.

The above argument is based on the linear theory of the massive tensor field, however, from the expression (2.2.13), one can find a linear approximation is no longer valid in the massless limit. In the scale  $r \ll m^{-1}$ ,  $(ij)$ -component of  $h_{ij}^{\text{massive}}$  is approximated by

$$\kappa h_{ij}^{\text{massive}} \approx \frac{4}{3}\frac{GM}{m^2 r^3}(\delta_{ij} - 3x_i x_j). \quad (2.2.15)$$

Therefore the linear approximation ( $\kappa h_{\mu\nu} \ll 1$ ) is valid only when

$$r \gg r_V := \left( \frac{GM}{m^2} \right), \quad (2.2.16)$$

where  $r_V$  is called the Vainshtein radius. For instance, when we set the graviton mass to be a cosmological scale as  $m^{-1} \sim 10^{28}$  cm, the Vainshtein radius for the sun ( $r_S \sim 10^5$  cm) is

$$r_V \sim 10^{20} \text{ cm} \sim 0.01 \text{ kpc},$$

which is much greater than 1 AU ( $\sim 10^{13}$  cm). Therefore, even in the weak gravitational field regime, the nonlinear interactions of scalar graviton have to be taken into account. Below the Vainshtein radius, the nonlinear interactions become relevant and then there would be no discontinuity due to, so-called, the Vainshtein mechanism [9] which we shall discuss in Chapter 4 and Chapter 8.

### 2.3 Stüeckelberg trick and decoupling limit

In the previous section, we have shown that the massive tensor field has the vDVZ discontinuity by constructing an explicit solution. In this section, we revisit the vDVZ discontinuity by introducing, so called, Stüeckelberg field which will make it clear why the massive field is not restored to the corresponding massless field even in the massless limit.

In four dimensions, the degrees of freedom of the massless tensor field are only two: there are two polarizations of helicity-2 modes. On the other hand, the massive tensor field contains five degrees of freedom: one helicity-0, two helicity-1, and two helicity-2 modes. Therefore taking a direct limit from the Fierz-Pauli Lagrangian to the Einstein-Hilbert Lagrangian is not smooth massless limit because degrees of freedom of helicity-0 and helicity-1 modes are lost. The smooth limit must be that the degrees of freedom are neither added nor lost. To find a correct limit, the trick is introducing the gauge symmetry by introducing new fields, which is called Stüeckelberg trick.

The original Lagrangian of the massive tensor field is given by

$$\mathcal{L} = -\frac{1}{4}h^{\mu\nu}\mathcal{E}_{\mu\nu}^{\alpha\beta}h_{\alpha\beta} - \frac{m^2}{8}(h_{\mu\nu}h^{\mu\nu} - h^2) + \frac{\kappa}{2}h_{\mu\nu}T^{\mu\nu}, \quad (2.3.1)$$

in which there is no gauge symmetry. To yield a gauge symmetry, we introduce a vector field  $A_\mu$  with the replacement

$$h_{\mu\nu} \rightarrow h_{\mu\nu} + 2\partial_{(\mu}A_{\nu)}. \quad (2.3.2)$$

Under this replacement, the kinetic term and the matter coupling term are unchanged, while the mass term is changed. The replaced Lagrangian is expressed by

$$\mathcal{L} = -\frac{1}{4}h^{\mu\nu}\mathcal{E}_{\mu\nu}^{\alpha\beta}h_{\alpha\beta} - \frac{m^2}{8}(h_{\mu\nu}h^{\mu\nu} - h^2) - \frac{m^2}{8}F_{\mu\nu}F^{\mu\nu} - \frac{m^2}{2}(h^{\mu\nu}\partial_\mu A_\nu - h\partial_\mu A^\mu) + \frac{\kappa}{2}h^{\mu\nu}T_{\mu\nu}, \quad (2.3.3)$$

where  $F_{\mu\nu} = 2\partial_{[\mu}A_{\nu]}$ . One can see this Lagrangian is invariant under the transformation

$$h_{\mu\nu} \rightarrow h_{\mu\nu} + 2\partial_{(\mu}\xi_{\nu)}, \quad A_\mu \rightarrow A_\mu - \xi_\mu. \quad (2.3.4)$$

Choosing the unitary gauge  $A_\mu = 0$ , the original Lagrangian is obtained. Therefore, two theories (2.3.1) and (2.3.3) are equivalent. Introducing only the vector Stüeckelberg field is not sufficient since the original theory contains the helicity-0 mode as well. We again take the Stüeckelberg trick for the vector field  $A_\mu$ , i.e., we replace the vector field with

$$A_\mu \rightarrow A_\mu + \partial_\mu\phi. \quad (2.3.5)$$

Then the Lagrangian is replaced with

$$\begin{aligned} \mathcal{L} = & -\frac{1}{4}h^{\mu\nu}\mathcal{E}_{\mu\nu}^{\alpha\beta}h_{\alpha\beta} - \frac{m^2}{8}(h_{\mu\nu}h^{\mu\nu} - h^2) - \frac{m^2}{8}F_{\mu\nu}F^{\mu\nu} \\ & - \frac{m^2}{2}(h^{\mu\nu}\partial_\mu A_\nu - h\partial_\mu A^\mu) - \frac{m^2}{2}(h^{\mu\nu}\partial_\mu\partial_\nu\phi - h\partial_\mu\partial^\mu\phi) + \frac{\kappa}{2}h^{\mu\nu}T_{\mu\nu}, \end{aligned} \quad (2.3.6)$$

where this Lagrangian has two gauge symmetries: one is (2.3.4) and another is

$$A_\mu \rightarrow A_\mu + \partial_\mu \chi, \quad \phi \rightarrow \phi - \chi. \quad (2.3.7)$$

Hence the number of degrees of freedom are unchanged, and the original Lagrangian is obtained by choosing the unitary gauge  $A_\mu = 0, \phi = 0$ .

Next, we take a decoupling limit in which the fields decouple from some of them with keeping the number of degrees of freedom. The direct  $m \rightarrow 0$  limit loses the degrees of freedom of  $\phi$  and  $A_\mu$ . Hence we first normalize the fields  $A_\mu$  and  $\phi$  as follows:

$$A_\mu \rightarrow \frac{1}{m} A_\mu, \quad \phi \rightarrow \frac{1}{m^2} \phi. \quad (2.3.8)$$

Then we take the  $m \rightarrow 0$  limit:

$$\begin{aligned} \mathcal{L} &= -\frac{1}{4} h^{\mu\nu} \mathcal{E}_{\mu\nu}^{\alpha\beta} h_{\alpha\beta} - \frac{m^2}{8} (h_{\mu\nu} h^{\mu\nu} - h^2) - \frac{1}{8} F_{\mu\nu} F^{\mu\nu} \\ &\quad - \frac{m}{2} (h^{\mu\nu} \partial_\mu A_\nu - h \partial_\mu A^\mu) - \frac{1}{2} (h^{\mu\nu} \partial_\mu \partial_\nu \phi - h \partial_\mu \partial^\mu \phi) + \frac{\kappa}{2} h^{\mu\nu} T_{\mu\nu}, \\ \xrightarrow{m \rightarrow 0} \mathcal{L}_{m \rightarrow 0} &= -\frac{1}{4} h^{\mu\nu} \mathcal{E}_{\mu\nu}^{\alpha\beta} h_{\alpha\beta} - \frac{1}{8} F_{\mu\nu} F^{\mu\nu} - \frac{1}{2} (h^{\mu\nu} \partial_\mu \partial_\nu \phi - h \partial_\mu \partial^\mu \phi) + \frac{\kappa}{2} h^{\mu\nu} T_{\mu\nu}. \end{aligned} \quad (2.3.9)$$

The decoupling limit Lagrangian has two independent gauge symmetry

$$h_{\mu\nu} \rightarrow h_{\mu\nu} + 2\partial_{(\mu} \xi_{\nu)}, \quad (2.3.10)$$

$$A_\mu \rightarrow A_\mu + \partial_\mu \chi, \quad (2.3.11)$$

which are the same ones of the massless vector field and the massless tensor field. The number degrees of freedom of the decoupling limit Lagrangian is actually same as one of the original Lagrangian. Note that, although the vector field  $A_\mu$  decouples from the tensor field, the scalar field does not decouple from the tensor field which is the origin of the vDVZ discontinuity. It becomes more clear by introducing a tensor field by

$$h_{\mu\nu} = H_{\mu\nu} + \phi \eta_{\mu\nu}. \quad (2.3.12)$$

The Lagrangian is given by

$$\mathcal{L} = -\frac{1}{4} H^{\mu\nu} \mathcal{E}_{\mu\nu}^{\alpha\beta} H_{\alpha\beta} - \frac{1}{8} F_{\mu\nu} F^{\mu\nu} - \frac{3}{4} (\partial\phi)^2 + \frac{\kappa}{2} H^{\mu\nu} T_{\mu\nu} + \frac{\kappa}{2} \phi T. \quad (2.3.13)$$

where the scalar field couples to matter field. As a result, the gravity is mediated not only by the tensor field, but also by the scalar field even in the decoupling limit. The existence of the fifth force mediated by the scalar graviton is the origin of the vDVZ discontinuity.

## 2.4 Fierz-Pauli theory on curved background

So far, we have considered the linear massive tensor field on the Minkowski background. In this section, we shall study a linear massive tensor field propagating on a fixed curved background. The linear action of the massive tensor field is given by the quadratic order Einstein-Hilbert action around the curved background with the Fierz-Pauli mass term:

$$\begin{aligned} S &= \int d^4x \sqrt{-g} [\mathcal{L}_{\text{EH}} + \mathcal{L}_{\text{FP}}] \\ &= \int d^4x \sqrt{-g} \left[ -\frac{1}{4} h^{\mu\nu} \mathcal{E}_{\mu\nu, \alpha\beta} h^{\alpha\beta} - \frac{\Lambda}{4} (h^2 - 2h_{\mu\nu} h^{\mu\nu}) - \frac{m^2}{8} (h_{\mu\nu} h^{\mu\nu} - h^2) \right], \end{aligned} \quad (2.4.1)$$

where  $\Lambda$  is a cosmological constant and

$$\begin{aligned} \mathcal{E}_{\mu\nu, \alpha\beta} h^{\alpha\beta} &= -\frac{1}{2} \square h_{\mu\nu} - \frac{1}{2} \nabla_\mu \nabla_\nu h + \nabla_\alpha \nabla_{(\nu} h^\alpha_{\mu)} + \frac{1}{2} g_{\mu\nu} (\square h - \nabla_\alpha \nabla_\beta h^{\alpha\beta}) \\ &\quad - 2 \left( h^\alpha_{(\mu} R_{\nu)\alpha} - \frac{1}{2} h R_{\mu\nu} \right) - \frac{1}{4} (\bar{g}_{\mu\nu} h - 2h_{\mu\nu}) R. \end{aligned} \quad (2.4.2)$$

The massive tensor field does not have a gauge symmetry, since the mass term breaks the diffeomorphism. As in the case of the flat background, the gauge symmetry can be explicitly restored by introducing the Stückelberg fields  $A_\mu$  and  $\phi$  as

$$h_{\mu\nu} = H_{\mu\nu} + 2\nabla_{(\mu}A_{\nu)} + 2\nabla_\mu\nabla_\nu\phi. \quad (2.4.3)$$

The variable  $h_{\mu\nu}$  is invariant under the following gauge transformations:

$$H_{\mu\nu} \rightarrow H_{\mu\nu} + 2\nabla_{(\mu}\xi_{\nu)}, \quad A_\mu \rightarrow A_\mu - \xi_\mu, \quad (2.4.4)$$

and

$$A_\mu \rightarrow A_\mu + \nabla_\mu\chi, \quad \phi \rightarrow \phi - \chi. \quad (2.4.5)$$

We can interpret  $H_{\mu\nu}$ ,  $A_\mu$ , and  $\phi$  as tensor, vector, and scalar modes, respectively.

The Einstein-Hilbert action preserves the diffeomorphism invariance, and therefore neither  $A_\mu$  nor  $\phi$  appears in  $S_{\text{EH}}$ . On the other hand, the FP mass term is rewritten by using the Stückelberg fields as

$$\begin{aligned} \mathcal{L}_{\text{FP}} = & -\frac{m^2}{8}(H_{\mu\nu}H^{\mu\nu} - H^2) - \frac{m^2}{8}F_{\mu\nu}F^{\mu\nu} + \frac{m^2}{2}R_{\mu\nu}A^\mu A^\nu - \frac{m^2}{2}(H^{\mu\nu}\nabla_\mu A_\nu - H\nabla_\mu A^\mu) \\ & + \frac{m^2}{2}R^{\mu\nu}\nabla_\mu\phi\nabla_\nu\phi + m^2R_{\mu\nu}A^\mu\nabla^\nu\phi - \frac{m^2}{2}(H^{\mu\nu}\nabla_\mu\nabla_\nu\phi - H\Box\phi) \end{aligned} \quad (2.4.6)$$

where  $F_{\mu\nu} = 2\nabla_{[\mu}A_{\nu]}$ . Note that the interaction terms between the tensor and the scalar graviton modes produce the vDVZ discontinuity around the flat background as shown in the previous section. On the other hand, the vDVZ discontinuity does not occur around a curved background in the massless limit [40, 41].

In order to see the absence of the vDVZ discontinuity, we take a canonical normalization for the vector mode as

$$A_\mu \rightarrow \frac{1}{m}A_\mu$$

and for the scalar graviton mode as

$$\phi \rightarrow \frac{1}{m\sqrt{R_0}}\phi,$$

instead of the normalization  $\phi \rightarrow \phi/m^2$ , where a positive constant  $R_0$  denotes a typical scale of the background Ricci tensor, i.e.  $R_0 \sim O(R_{\mu\nu})$ . Then the scalar part of the action becomes

$$S_2 \supset \int d^4x \sqrt{-g} \left[ \frac{R^{\mu\nu}}{2R_0} \nabla_\mu\phi\nabla_\nu\phi + \frac{R_{\mu\nu}}{\sqrt{R_0}} A^\mu\nabla^\nu\phi - \frac{m}{2\sqrt{R_0}} (H^{\mu\nu}\nabla_\mu\nabla_\nu\phi - H\Box\phi) \right]. \quad (2.4.7)$$

Therefore, when the effective graviton mass is negligible compared with the background Ricci curvature (i.e.  $m^2 \ll R_0$ ), the interaction between tensor and scalar modes vanishes, and then there is no vDVZ discontinuity.

However, the kinetic term of the scalar graviton is modified from the standard one in such a massless limit. Hence the ghost instability or the gradient instability may appear, depending on the background Ricci curvature. For simplicity, we assume a maximally symmetric spacetime:

$$R_{\mu\nu} = \frac{1}{4}Rg_{\mu\nu}, \quad R = 4\Lambda. \quad (2.4.8)$$

Using the normalizations

$$A_\mu \rightarrow \frac{1}{m}A_\mu, \quad \phi \rightarrow \frac{1}{m^2}\phi, \quad (2.4.9)$$

and the redefinition of the variable

$$H_{\mu\nu} = \mathcal{H}_{\mu\nu} + \phi g_{\mu\nu}, \quad (2.4.10)$$



the action is given by

$$S = \int d^4x \sqrt{-g} \left[ \mathcal{L}_{\text{EH}}[\mathcal{H}] - \frac{m^2}{8} (\mathcal{H}_{\mu\nu} \mathcal{H}^{\mu\nu} - \mathcal{H}^2) - \frac{1}{8} F^2 + \frac{R}{4} A_\mu A^\mu - \frac{m}{2} (\mathcal{H}_{\mu\nu} \nabla^\mu A^\nu - \mathcal{H} \nabla_\mu A^\mu) - \frac{3}{4} \left( 1 - \frac{R}{6m^2} \right) ((\partial\phi)^2 - m^2 \phi \mathcal{H} - 2m\phi \nabla_\mu A^\mu - 4m^2 \phi^2) \right]. \quad (2.4.11)$$

Hence the scalar mode would be a ghost when

$$1 - \frac{R}{6m^2} < 0. \quad (2.4.12)$$

If the background spacetime is the AdS spacetime, there is no ghost even in the limit  $m \rightarrow 0$  and there is no vDVZ discontinuity. However, in the de Sitter background, the helicity-0 mode becomes a ghost so-called the Higuchi ghost in the limit  $m \rightarrow 0$ . The action is free from the ghost when the Higuchi bound

$$3m^2 - 2\Lambda > 0, \quad (2.4.13)$$

is satisfied [38, 39], so the mass has the lower bound to be free from the ghost instability. At the exact bound value  $3m^2 = 2\Lambda$ , the helicity-0 mode is decoupled and a new gauge symmetry appears which is called partially massless [87, 88].

When the background spacetime is the FLRW spacetime

$$d\bar{s}_g^2 = a^2(-d\eta^2 + d\mathbf{x}^2), \quad (2.4.14)$$

the ghost or the gradient instability appears depending on the dynamics of the background spacetime [42] which we call the Higuchi type instability. The kinetic term is expressed by

$$R^{\mu\nu} \nabla_\mu \pi \nabla_\nu \pi = \frac{3H^2}{2a^2} (1 + 3w) \left[ (\partial_\eta \phi)^2 - \frac{w-1}{1+3w} (\partial_i \phi)^2 \right], \quad (2.4.15)$$

where  $w$  is the effective equation-of-state parameter of the background universe defined by

$$w = -1 - \frac{2H'}{3aH^2}, \quad (2.4.16)$$

and  $H = a'/a^2$  is the Hubble parameter where a prime is the derivative with respect to the conformal time  $\eta$ . Therefore the Higuchi ghost type instability appears for  $w < -1/3$ , while the gradient instability is found for  $-1/3 < w < 1$ . This fact indicates that an instability is unavoidable if the background spacetime consists of an ordinary matter components ( $w < 1$ ).

However, such an instability is quite obscure in the physical interpretation, since the natural expectation would be that the massive theory should be restored to its corresponding massless theory when the energy scale of the background spacetime is higher than the mass. The instability may simply hint the possibility that the linear perturbations are no longer valid as in the case of vDVZ discontinuity which we shall discuss in Chapter 6.

## 2.5 Experimental constraints on graviton mass

If the gravitational theory contains a massive graviton, one can discuss the graviton mass bound from several experiments of the gravity. There are mainly two general features of the massive graviton: the existence of the Yukawa-type potential and the modification of the dispersion relation of the gravitational wave. These effects can be seen from the linear massive gravity and the linear theory gives some constraints on the graviton mass; however, as already mentioned, the linear theory cannot be used in scales below the Vainshtein radius. In the nonlinear regime, the Vainshtein mechanism may give the restoration to predictions of GR. Even if the screening mechanism works, a tiny deviation from GR should exist and it could constrain the graviton mass but the Vainshtein mechanism is still subject to discussion (see Chapter 4 and Chapter 8). Hence, in this section, we briefly discuss the constraints on the graviton mass only based on the linear

theory of the massive gravity (see the reviews [1, 4, 5] and references therein for further discussions of the graviton mass bound).

We can consider several gravitational theories with a massive graviton: one is the carrier of the gravitational force is only the massive graviton and others are cases when the gravitational force is mediated by massive gravitons and also the massless graviton. In the case of only massive graviton, we can obtain strong upper bounds on the graviton mass since the gravitational force has the Yukawa suppression in scales beyond the Compton wavelength; thus, large-scale gravitating systems, e.g., galaxies and galaxy clusters, give a tight constraint on the graviton mass although the constraints depend on the distributions of dark matter. However, for the bigravity and the multi-gravity, these constraints cannot be used since the gravitational force can be propagated by the massless graviton. Furthermore, if the massless graviton dominates the gravitational interactions between matter in such theories, one cannot obtain any constraints on the graviton mass in the case of weakly coupling massive graviton (see Fig. 2.1).

First, we discuss the case of the theory with only massive graviton. In this case, as mentioned above, one of the tightest constraints comes from the consideration of galactic and cluster dynamics [89] which gives

$$m \lesssim 10^{-29} \text{ eV}, \quad \lambda \gtrsim 10^{24} \text{ cm}, \quad (2.5.1)$$

where  $\lambda = \frac{\hbar}{mc}$  is the (reduced) Compton wavelength of the massive graviton. However, this constraint depends on the distribution of dark matter. The most rigorous model independent constraint on the Yukawa-type modification can be derived from solar system dynamics [90]. The solid bound on the graviton mass from solar system is

$$m < 7.2 \times 10^{-23} \text{ eV}, \quad \lambda > 2.8 \times 10^{17} \text{ cm}. \quad (2.5.2)$$

Another type of constraint can be obtained by the direct detection of the gravitational wave. Recently, Advanced LIGO detected the gravitational waves GW150914 from a binary black hole merger [91]. For the massive gravitational wave, the lower frequency gravitational waves travel slower than the higher ones. The graviton mass can be constrained by this difference of the propagating speed of the gravitational waves. The analysis of GW150914 [2, 92] gives the bound

$$m < 1.2 \times 10^{-22} \text{ eV}, \quad \lambda > 1.7 \times 10^{17} \text{ cm}. \quad (2.5.3)$$

We note that, while the solar system constrains the existence of the Yukawa-type modification of the gravity, GW150914 gives the constraint on the modification of the dispersion relation. These constraints give rigorous and independent bounds on the graviton mass.

In this thesis, we will mainly focus on the bigravity theory which contains one massless graviton and one massive graviton. Hence we then discuss the graviton mass constraints in the bigravity theory. In general, the gravitational potential in the bigravity theory can be given by

$$\Phi = -\frac{GM}{r} \left( 1 + \alpha e^{-r/\lambda} \right). \quad (2.5.4)$$

In the case of  $\alpha \gtrsim 1$ , the graviton mass bounds for a large scale modification are obtained from the solar system experiments similarly to the case of the only massive graviton. On the other hand, one important difference from the case of the only massive graviton is that the graviton mass can be heavy, i.e., a short scale modification of gravity is also possible. Since the Yukawa potential can be ignored in the scale  $r \gg \lambda$ , the Newtonian behavior is reproduced at such a scale. The laboratory scale experiments on the gravity constrain the existence of such a massive graviton with the mass around  $10^{-2}$  eV or lighter than it. Furthermore, if the graviton mass is about TeV scale, the graviton mass can be constrained from the LHC. Since the graviton universally couples with standard model particles, the massive graviton can be produced by some particle collision. The produced massive graviton rapidly decays to other standard model particles if the mass scale of the coupling to matter is TeV scale. The experimental constraints on the gravitational potential (2.5.4) and on the massive graviton production are summarized in Fig. 2.1 from [4].

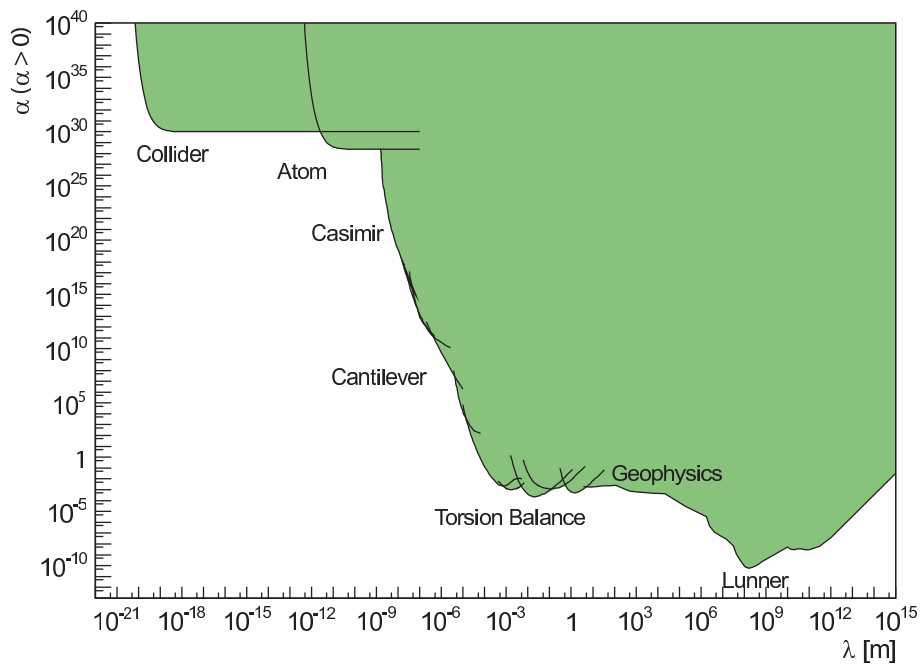


Figure 2.1: Experimental constraints on the gravitational potential (2.5.4) adapted from Ref. [4]. The colored region is the excluded area at 95% confidence level (see [4] and references therein for details).



## Chapter 3

# Nonlinear massive gravity and bigravity

### 3.1 Nonlinear self-interactions

As discussed in Sec. 2.2, the Fierz-Pauli theory is no longer valid below the Vainshtein radius; thus, nonlinear extensions of the Fierz-Pauli theory are needed and the nonlinear interactions have to be taken into account. However, generic nonlinear extensions of the Fierz-Pauli theory lead to an additional degree of freedom [10]. In this section, we count degrees of freedom of the general nonlinear massive gravity by using the Hamiltonian formulation and show the appearance of the additional degree of freedom for generic nonlinear interactions. The Hamiltonian formulation in a constrained system is summarized in Appendix A.

#### 3.1.1 Hamiltonian analysis in general relativity

First, we briefly discuss the Hamiltonian formulation in  $D = (d + 1)$ -dimensional GR. In the Hamiltonian formulation, it is necessary to foliate the  $(d + 1)$ -dimensional spacetime with a family of  $d$ -dimensional spacelike hypersurfaces. Hence we use the ADM decomposition

$$ds^2 = -N^2 dt^2 + g_{ij}(dx^i + N^i dt)(dx^j + N^j dt), \quad (3.1.1)$$

with the lapse function  $N$ , the shift vector  $N^i$ , and the  $d$ -dimensional induced metric  $g_{ij}$  on the spacelike hypersurface. Then the Einstein-Hilbert action is expressed as

$$\mathcal{L}_{\text{EH}} = \sqrt{-g}R = \sqrt{\det(g_{ij})}N({}^dR + K^{ij}K_{ij} - K^2) + \text{boundary terms}, \quad (3.1.2)$$

where  ${}^dR$  is the intrinsic curvature and  $K_{ij}$  is the extrinsic curvature. While the intrinsic curvature  ${}^dR$  does not contain the time derivative, the extrinsic curvature can be expressed by

$$K_{ij} = \frac{1}{2N}(\dot{g}_{ij} - 2D_{(i}N_{j)}), \quad (3.1.3)$$

where  $D_i$  is the covariant derivative in  $g_{ij}$ ; thus the extrinsic curvature contains the time derivative of  $g_{ij}$ . The momentum conjugate to  $g_{ij}$  is defined by

$$\begin{aligned} \pi^{ij} &= \frac{\delta}{\delta \dot{g}_{ij}}(\sqrt{-g}R) \\ &= \sqrt{\det(g_{ij})}(K^{ij} - K g^{ij}). \end{aligned} \quad (3.1.4)$$

Since the Einstein-Hilbert action does not contain the time derivative of the lapse and the shift, the momentum conjugates to them yield primary constraints

$$\pi_0 = \frac{\delta}{\delta \dot{N}}(\sqrt{-g}R) \approx 0, \quad (3.1.5)$$

$$\pi_i = \frac{\delta}{\delta \dot{N}^i}(\sqrt{-g}R) \approx 0. \quad (3.1.6)$$

As a result, the Hamiltonian in GR is given by

$$\mathcal{H}_T = \pi_0 v^0 + \pi_i v^i + \mathcal{H}, \quad (3.1.7)$$

$$\mathcal{H} = -NR_0 - N^i R_i, \quad (3.1.8)$$

where  $v^0$  and  $v^i$  are Lagrangian multipliers and

$$R_0 = \sqrt{\det(g_{ij})} {}^d R + \frac{1}{\sqrt{\det(g_{ij})}} \left( \frac{1}{2} \pi^i \pi^j - \pi^{ij} \pi_{ij} \right), \quad (3.1.9)$$

$$R_i = 2\sqrt{\det(g_{ij})} g_{ij} D_k \left( \frac{\pi^{jk}}{\sqrt{\det(g_{ij})}} \right). \quad (3.1.10)$$

The primary constraints should be preserved after a time evolution, so these conditions generate secondary constraints

$$\dot{\pi}_0 = \{\pi_0, H_T\} = R_0 \approx 0, \quad (3.1.11)$$

$$\dot{\pi}_i = \{\pi_i, H_T\} = R_i \approx 0, \quad (3.1.12)$$

where  $H_T = \int d^d x \mathcal{H}_T$ . Note that the preservations of secondary constraints are weakly satisfied, thus they do not yield any constraint.

We find  $D$  primary constraints and  $D$  secondary constraints in GR. Poisson brackets of them are calculated by

$$\{\pi_\alpha, R_\beta\} \approx 0, \quad (3.1.13)$$

and

$$\{R_0(x), R_0(y)\} = - \left[ R^i(x) \frac{\partial}{\partial x^i} \delta^{(d)}(x-y) - R^i(y) \frac{\partial}{\partial y^i} \delta^{(d)}(x-y) \right] \approx 0, \quad (3.1.14)$$

$$\{R_0(x), R_i(y)\} = -R_0(y) \frac{\partial}{\partial x^i} \delta^{(d)}(x-y) \approx 0, \quad (3.1.15)$$

$$\{R_i(x), R_j(y)\} = - \left[ R_j(x) \frac{\partial}{\partial x^i} \delta^{(d)}(x-y) - R_i(y) \frac{\partial}{\partial y^j} \delta^{(d)}(x-y) \right] \approx 0, \quad (3.1.16)$$

where we denote  $\pi_\alpha = (\pi_0, \pi_i)$ ,  $R_\beta = (R_0, R_i)$ . All Poisson bracket are weakly zero, thus all constraints are first class which is indeed associated with the general covariance of GR. As a result, we find  $2D$  primary constraints in terms of  $D(D+1)$  canonical variables. The degrees of freedom of GR in the phase space is thus

$$D(D+1) - 2 \times 2D = D(D-3),$$

which corresponds to  $D(D-3)/2$  independent degrees of freedom in the field space. This result is indeed same as the number of the polarizations of the massless spin-2 field in  $D$  dimensions.

### 3.1.2 Hamiltonian analysis in massive gravity

Next, we move to the case of the massive gravity. We assume the Lagrangian of the general nonlinear massive gravity as

$$\mathcal{L}_{\text{mGR}} = \mathcal{L}_{\text{EH}} + \mathcal{L}_{\text{mass}}(N, N^i, g_{ij}). \quad (3.1.17)$$

where  $\mathcal{L}_{\text{mass}}(N, N^i, g_{ij})$  is assumed not to contain derivatives. Hence primary constrains are same as the case of GR

$$\pi_0 \approx 0, \quad \pi_i \approx 0, \quad (3.1.18)$$

and then the Hamiltonian is given by

$$\mathcal{H}_T = \pi_0 v^0 + \pi_i v^i + \mathcal{H}_{\text{GR}} - \mathcal{L}_{\text{mass}}, \quad (3.1.19)$$

$$\mathcal{H}_{\text{GR}} = -NR_0 - N^i R_i. \quad (3.1.20)$$

The preservations of the primary constraints generate secondary constraint. While the mass term does not affect the primary constraints, the mass term contribute the secondary constraints:

$$\mathcal{C}_\alpha(x) = \{\pi_\alpha(x), H_T\} = R_\alpha(x) + \tilde{\mathcal{C}}_\alpha(x) \approx 0, \quad (3.1.21)$$

where we define

$$\tilde{\mathcal{C}}_\alpha(x) = \frac{\delta \mathcal{L}_{\text{mass}}(x)}{\delta N^\alpha(x)}, \quad (3.1.22)$$

and we denote  $N^\alpha = (N, N^i)$ . In general, the Poisson brackets of the constraints are no longer weakly zero thus all constraints are second class. Furthermore, the preservations of the secondary constraints are not trivially satisfied differently from the case of GR. The preservations of the secondary constraints hold when

$$\begin{aligned} \mathcal{D}_\alpha(x) &= \{\mathcal{C}_\alpha(x), H_T\} \\ &\approx \{\mathcal{C}_\alpha(x), H\} + \int d^3y \{\tilde{\mathcal{C}}_\alpha(x), \pi_\beta(y)\} v^\beta(y) \\ &= \{\mathcal{C}_\alpha(x), H\} + L_{\alpha\beta} v^\beta(x) \approx 0, \end{aligned} \quad (3.1.23)$$

where

$$L_{\alpha\beta} := \{\tilde{\mathcal{C}}_\alpha(x), \pi_\beta(x)\} = \frac{\delta^2 \mathcal{L}_{\text{mass}}}{\delta N^\alpha \delta N^\beta}. \quad (3.1.24)$$

For general mass terms, the determinant of  $L_{\alpha\beta}$  is nonzero, thus there exists the inverse matrix  $(L^{-1})^{\alpha\beta}$  and then the Lagrangian multipliers are determined by

$$v^\alpha = -(L^{-1})^{\alpha\beta} \{\mathcal{C}_\beta(x), H\}. \quad (3.1.25)$$

Hence Eq. (3.1.23) is not constraint on the canonical variables but the equation to determine the Lagrangian multipliers.

As a result, we have  $2D$  second class constraints in terms of  $D(D+1)$  canonical variables. The degrees of freedom of the nonlinear massive gravity is thus

$$D(D+1) - 2D = D(D-1),$$

in the phase space, or  $D(D-1)/2$  in the field space. On the other hand, the number of polarizations of the massive spin-2 field in  $D$  dimensions is given by

$$\frac{(D+1)(D-2)}{2} = \frac{D(D-1)}{2} - 1.$$

Therefore the general nonlinear massive gravity contains an additional scalar degree of freedom as well as ones of the massive spin-2 field. As shown in Section 2.1, this additional scalar corresponds to the ghost mode, so-called Boulware-Deser ghost [10].

However, as also discussed in Section 2.1, the additional scalar can be eliminated by a nontrivial constraint. When the determinant of  $L_{\alpha\beta}$  is nonzero, the preservations of the secondary constraints yield the equations to determine the Lagrangian multipliers. However when the determinant of  $L_{\alpha\beta}$  is weakly zero, some of the Lagrangian multipliers are undetermined by (3.1.23). Instead, some of (3.1.23) give tertiary constraints on the canonical variables. To eliminate one degree of freedom in the field space, two constraints are required in the phase space. Since there exist an even number of second class constraints in general, even if there is only one tertiary constraint, the preservation of the tertiary constraint may generate a quaternary constraint. Hence, if

$$\det(L_{\alpha\beta}) \approx 0, \quad (3.1.26)$$

is satisfied, the BD ghost could be eliminated. Indeed, we shall see in next section that the ghost-free nonlinear massive gravity satisfies this condition.

### 3.2 de Rham-Gabadadze-Tolley theory

As discussed in the previous section, the generic nonlinear interactions lead to the BD ghost. However, de Rham, Gabadadze, and Tolley pointed out that the special choice of the mass term can eliminate the BD ghost and proposed the ghost-free nonlinear massive gravity often dubbed the dRGT theory [11, 12]. Although they showed the ghost-freeness in the decoupling limit which will be detailed in Section 4.3, the proof was extended at fully nonlinear orders [13–16].

To construct the mass term of the metric  $g_{\mu\nu}$ , we need a fictitious metric for the Stückelberg fields called the fiducial metric  $f_{\mu\nu}$  which is assumed to be non-dynamical in the dRGT theory. Then the action of the dRGT theory is given by

$$S = \frac{1}{2\kappa_g^2} \int d^4x \sqrt{-g} \left[ R - 2m^2 \sum_{n=0}^4 c_n \mathcal{U}_n(\mathcal{K}) \right], \quad (3.2.1)$$

with

$$\mathcal{K}^\mu{}_\nu = \delta^\mu{}_\nu - \gamma^\mu{}_\nu, \quad (3.2.2)$$

where  $\gamma^\mu{}_\nu$  is a squat root of  $g^{-1}f$  defined by the relation

$$\gamma^\mu{}_\rho \gamma^\rho{}_\nu = g^{\mu\rho} f_{\rho\nu}. \quad (3.2.3)$$

The ghost-free mass term are constructed by the elementary symmetric polynomials of the eigenvalues of the matrix  $\mathcal{K}$ . We define

$$\mathcal{U}_0(X) = 1, \quad (3.2.4)$$

$$\mathcal{U}_1(X) = [X] = \sum_i \lambda_i, \quad (3.2.5)$$

$$\mathcal{U}_2(X) = \frac{1}{2}([X]^2 - [X^2]) = \sum_{i<j} \lambda_i \lambda_j, \quad (3.2.6)$$

$$\mathcal{U}_3(X) = \frac{1}{3!}([X]^3 - 3[X][X^2] + 2[X^3]) = \sum_{i<j<k} \lambda_i \lambda_j \lambda_k, \quad (3.2.7)$$

$$\mathcal{U}_4(X) = \frac{1}{4!}([X]^4 - 6[X]^2[X^2] + 3[X^2]^2 + 8[X][X^3] - 6[X^4]) = \lambda_1 \lambda_2 \lambda_3 \lambda_4, \quad (3.2.8)$$

where  $\lambda_i$  are eigenvalues of the matrix  $X^\mu{}_\nu$  and we use the notations  $X^{n\mu}{}_\nu = X^\mu{}_{\alpha_2} X^{\alpha_2}{}_{\alpha_3} \cdots X^{\alpha_n}{}_\nu$  and  $[X^n] = X^{n\mu}{}_\mu$ . We have introduced the constant term  $\mathcal{U}_0$  and the tadpole term  $\mathcal{U}_1$ , for completeness. The absence of the constant term and the tadpole term (i.e.,  $c_0 = c_1 = 0$ ) guarantees the existence of the Minkowski vacuum with the Minkowski fiducial metric. Alternatively, these quantities are expressed by

$$\mathcal{U}_0(X) = -\frac{1}{4!} \epsilon_{\mu\nu\rho\sigma} \epsilon^{\mu\nu\rho\sigma} \quad (3.2.9)$$

$$\mathcal{U}_1(X) = -\frac{1}{3!} \epsilon_{\mu\nu\rho\sigma} \epsilon^{\alpha\nu\rho\sigma} X^\mu{}_\alpha, \quad (3.2.10)$$

$$\mathcal{U}_2(X) = -\frac{1}{4} \epsilon_{\mu\nu\rho\sigma} \epsilon^{\alpha\beta\rho\sigma} X^\mu{}_\alpha X^\nu{}_\beta, \quad (3.2.11)$$

$$\mathcal{U}_3(X) = -\frac{1}{3!} \epsilon_{\mu\nu\rho\sigma} \epsilon^{\alpha\beta\gamma\sigma} X^\mu{}_\alpha X^\nu{}_\beta X^\rho{}_\gamma, \quad (3.2.12)$$

$$\mathcal{U}_4(X) = -\frac{1}{4!} \epsilon_{\mu\nu\rho\sigma} \epsilon^{\alpha\beta\gamma\delta} X^\mu{}_\alpha X^\nu{}_\beta X^\rho{}_\gamma X^\sigma{}_\delta. \quad (3.2.13)$$

Note that the potential term can be expressed by the elementary symmetric polynomials of the eigenvalues of the matrix  $\gamma$ :

$$\sum_{n=0}^4 c_n \mathcal{U}_n(\mathcal{K}) = \sum_{n=0}^4 b_n \mathcal{U}_n(\gamma), \quad (3.2.14)$$



with the relations between the coefficients  $c_n$  and  $b_n$

$$\begin{aligned} c_0 &= b_0 + 4b_1 + 6b_2 + 4b_3 + b_4, \\ c_1 &= -(b_1 + 3b_2 + 3b_3 + b_4), \\ c_2 &= b_2 + 2b_3 + b_4, \\ c_3 &= -(b_3 + b_4), \\ c_4 &= b_4. \end{aligned} \tag{3.2.15}$$

The existence of the Minkowski vacuum is realized when the coefficients  $b_n$  satisfy

$$c_0 = b_0 + 3b_1 + 3b_2 + b_3 = 0, \quad -c_1 = b_1 + 3b_2 + 3b_3 + b_4 = 0. \tag{3.2.16}$$

A normalization of  $m$  to be the graviton mass around the Minkowski vacuum ( $c_0 = c_1 = 0$ ) gives

$$c_2 = b_2 + 2b_3 + b_4 = -1, \tag{3.2.17}$$

in which the dRGT mass term is expanded to the Fierz-Pauli mass term at the quadratic order of  $h_{\mu\nu} := g_{\mu\nu} - \eta_{\mu\nu}$  with the graviton mass  $m$ .

In order to take the square root to obtain the explicit form of  $\gamma^\mu{}_\nu$ , it is useful to introduce the vielbein systems,  $\{e_\mu^{(a)}\}$  and  $\{\omega_\mu^{(a)}\}$ , which are define by

$$g_{\mu\nu} = \eta_{ab} e_\mu^{(a)} e_\nu^{(b)}, \quad f_{\mu\nu} = \eta_{ab} \omega_\mu^{(a)} \omega_\nu^{(b)}. \tag{3.2.18}$$

We then redefine the square root  $\gamma^\mu{}_\nu$  as

$$\gamma^\mu{}_\nu = \epsilon \eta_{ab} e^{\mu(a)} \omega_\nu^{(b)}, \tag{3.2.19}$$

where  $\epsilon = \pm 1$  comes from the square root. Changing the sign of  $\epsilon$  corresponds to the following transformation

$$\gamma^\mu{}_\nu \leftrightarrow -\gamma^\mu{}_\nu, \tag{3.2.20}$$

for which the interaction term is invariant by changing the sign of the coupling constant as

$$b_n \leftrightarrow (-1)^n b_n. \tag{3.2.21}$$

Hence, we shall only consider the case of  $\epsilon = +1$  unless we reintroduce  $\epsilon$  explicitly. While the metric contains only 10 degrees of freedom, the vielbein contains 16 degrees of freedom. The additional 6 freedom comes from the gauge freedom of the local Lorentz symmetry of vielbein

$$e_\mu^{(a)} \rightarrow \Lambda^{(a)}{}_{(b)} e_\mu^{(b)}, \tag{3.2.22}$$

where  $\Lambda^{(a)}{}_{(b)}$  represents the transformations of local boost and local rotation of the vielbein. Two definitions (3.2.3) and (3.2.19) are completely equivalent if we impose an additional constraint on the vielbeins, called the symmetric vielbein condition,

$$e_{(a)}^\mu \omega_{\mu(b)} = e_{(b)}^\mu \omega_{\mu(a)}, \tag{3.2.23}$$

which eliminates 6 degrees of freedom of the local Lorentz symmetry of vielbeins. Therefore, the dRGT theory in the vielbein system contains only 6 gauge freedom associated with the local Lorentz symmetry although the theory contains two independent vielbeins<sup>1</sup>.

Note that, as shown in [18], even if we do not assume the symmetric vielbein condition, the condition can be obtained from the variation with respect to  $\Lambda^{(a)}{}_{(b)}$  when we assume the dRGT mass term defined on the vielbein system. This formulation is called unconstrained vielbein formulation. The equivalence is broken when we introduce the doubly coupled matter field which couples to

---

<sup>1</sup>We notice again that the vielbein  $\omega_\mu^{(a)}$  is not a dynamical field in the dRGT theory but a fictitious non-dynamical field. In bigravity discussed in next section, the vielbein  $\omega_\mu^{(a)}$  is also a dynamical field.

both vielbeins  $e_\mu^{(a)}$  and  $\omega_\mu^{(a)}$  [93]. In this thesis, however, we do not consider the doubly coupled matter field thus the vielbein system is equivalent to the metric system.

Let us see the ghost-freeness of the dRGT theory. The structure of the dRGT mass term will be clear when we use the decoupling limit. The decoupling limit makes it clear why the generic mass terms give a ghost mode and why the dRGT mass term can eliminate such a ghost mode. However, we now do not use the decoupling limit. We discuss the general proof of the ghost-freeness of the dRGT mass term without the decoupling limit. The discussions on the decoupling limit will be done in next chapter.

Just for simplicity, we focus on the simplest case of the action

$$S = \frac{1}{2\kappa_g^2} \int d^4x \sqrt{-g} (R - 2m^2[\gamma]) . \quad (3.2.24)$$

Two metrics are decomposed into

$$ds_g^2 = -N^2 dt^2 + g_{ij}(dx^i + N^i dt)(dx^j + N^j dt) , \quad (3.2.25)$$

$$ds_f^2 = -M^2 dt^2 + f_{ij}(dx^i + M^i dt)(dx^j + M^j dt) . \quad (3.2.26)$$

Then one can calculate

$$N^2 g^{-1} f = \mathbf{E}_0 + N \mathbf{E}_1 + N^2 \mathbf{E}_2 , \quad (3.2.27)$$

$$N \gamma = \mathbf{A} + N \mathbf{B} , \quad (3.2.28)$$

where

$$\mathbf{E}_0 = \begin{pmatrix} a_0 & a_j \\ -a_0 c^i & -c^i a_j \end{pmatrix} , \quad (3.2.29)$$

$$\mathbf{E}_1 = \begin{pmatrix} M^k d_k & d_k \\ -a_0 d^i - c^i M^k d_k & -a_j d^i - c^i d_j \end{pmatrix} , \quad (3.2.30)$$

$$\mathbf{E}_2 = \begin{pmatrix} 0 & 0 \\ x M^k D^i_\ell D^\ell_k & x D^i_k D^k_j \end{pmatrix} , \quad (3.2.31)$$

$$\mathbf{A} = \frac{1}{M \sqrt{x}} \begin{pmatrix} a_0 & a_j \\ -a_0 c^i & -c^i a_j \end{pmatrix} , \quad (3.2.32)$$

$$\mathbf{B} = \sqrt{x} \begin{pmatrix} 0 & 0 \\ M^k D^i_k & D^i_j \end{pmatrix} , \quad (3.2.33)$$

with the quantities

$$a_0 = M^2 + M M^i f_{ij} n^j , \quad (3.2.34)$$

$$a_i = M f_{ki} n^k , \quad (3.2.35)$$

$$c^i = M n^i + M^i , \quad (3.2.36)$$

$$d^i = D^i_k n^k , \quad d_i = f_{ki} d^k , \quad (3.2.37)$$

$$x = \frac{a_0 - c^k a_k}{M^2} = 1 - n^i f_{ij} n^j , \quad (3.2.38)$$

and  $n^i, D^i_j$  are defined by the relations

$$N^i - M^i = (M \delta^i_j + N D^i_j) n^j , \quad (3.2.39)$$

$$\sqrt{x} D^i_j = \sqrt{(g^{ik} - d^i d^k) f_{kj}} , \quad (3.2.40)$$

Then the potential term is expressed by

$$\sqrt{-g}[\gamma] = M \sqrt{x \det(g_{ij})} + N \sqrt{x \det(g_{ij})} [D] . \quad (3.2.41)$$

The independent variables are given by  $(N, N^i, g_{ij})$ , however one can chose  $(N, n^i, g_{ij})$  as independent variables instead of the original variables. This change of variables is valid when the transformation is not singular, i.e.,

$$\det \left[ \frac{\delta N^i}{\delta n^j} \right] = \det \left[ M \delta^i_j + N \frac{\delta(D^i_k n^k)}{\delta n^j} \right] \neq 0 \quad (3.2.42)$$

By using the variables  $(N, n^i, g_{ij})$ , the Lagrangian is given by

$$\mathcal{L} = \pi^{ij} \dot{g}_{ij} + (M n^i + M^i) R_i + N(R^0 + R_i D^i_j n^j) - 2m^2 \sqrt{x \det(g_{ij})} (M + N[D]), \quad (3.2.43)$$

and then the Hamiltonian is expressed by

$$\mathcal{H}_T = \pi_0 v^0 + \pi_i v^i + \mathcal{H}, \quad (3.2.44)$$

$$\mathcal{H} = -(M n^i + M^i) R_i - N(R_0 + R_i D^i_j n^j) + 2m^2 \sqrt{x \det(g_{ij})} (M + N[D]), \quad (3.2.45)$$

where the primary constraints are

$$\pi_\alpha \approx 0. \quad (3.2.46)$$

The preservations of the primary constrains yield secondary constraints

$$\begin{aligned} \dot{\pi}_0 &= \{\pi_0, \mathcal{H}_T\} = -\frac{\delta \mathcal{H}}{\delta N} \\ &= R_0 + R_i D^i_j n^j - 2m^2 \sqrt{x \det(g_{ij})} [D] \approx 0, \end{aligned} \quad (3.2.47)$$

$$\begin{aligned} \dot{\pi}_i &= \{\pi_i, \mathcal{H}_T\} = -\frac{\delta \mathcal{H}}{\delta n^i} \\ &= \mathcal{C}_j \left( M \delta^j_i + N \frac{\delta(D^j_k n^k)}{\delta n^i} \right) \approx 0. \end{aligned} \quad (3.2.48)$$

Note that the non-singular condition (3.2.42) prohibits the parenthesis in the second equation vanishes. Hence the secondary constraints are given by

$$\mathcal{C}_0 := R_0 + R_i D^i_j n^j - 2m^2 \sqrt{x \det(g_{ij})} [D] \approx 0, \quad (3.2.49)$$

$$\mathcal{C}_i := R_i - 2m^2 \sqrt{\det(g_{ij})/x} n^k f_{ki} \approx 0, \quad (3.2.50)$$

where we use

$$\frac{\delta \sqrt{x}}{\delta n^i} = -x^{-1/2} f_{ik} n^k, \quad (3.2.51)$$

$$\frac{\delta [D]}{\delta n^i} = -x^{-1/2} n^k f_{kj} \frac{\delta}{\delta n^i} (n^\ell D^j_\ell) \quad (3.2.52)$$

As discussed in the previous section, the BD ghost can be eliminated when the matrix

$$L_{\alpha\beta} = \frac{\delta \mathcal{L}}{\delta n^\alpha n^\beta} \quad (3.2.53)$$

has one zero eigenvalue, where  $n^\alpha = (N, n^i)$ . The matrix is calculated as

$$L_{00} = 0, \quad L_{0i} = \mathcal{C}_j \frac{\delta(D^j_k n^k)}{\delta n^i}. \quad (3.2.54)$$

and then  $L_{0i}$  is zero by using the secondary constraints. As a result,  $\det(L) \approx 0$  is satisfied and the dRGT theory is free from the BD ghost.

The dRGT theory has no BD ghost, however, it has still been problematic in the context of cosmology. It was revealed that the original dRGT theory does not admit any non-trivial flat or

closed FLRW universe if the fiducial metric for the Stüeckelberg fields is Minkowski's one [94]. While this issue can be resolved either by open FLRW solutions [95] or by replacing the Minkowski fiducial metric with an FLRW one [96], it was later shown that all homogeneous and isotropic FLRW solutions in the dRGT theory are unstable due to either a linear ghost or a new type of nonlinear ghost [97–99]. Therefore to discuss the cosmology, one should consider a curved fiducial metric or generalize the theory. When we take a curved fiducial geometry, e.g. the FLRW or an inhomogeneous background, it may be natural to promote it to a dynamical one. In fact, the dRGT massive gravity theory has been generalized to such a theory with two dynamical metrics which we discuss in the next section.

### 3.3 Bigravity theory

#### 3.3.1 Hassan-Rosen bigravity

The dRGT theory contains a non-dynamical metric  $f_{\mu\nu}$ . This metric can be dynamical when the Einstein-Hilbert action for  $f_{\mu\nu}$  is added and this generalization of the theory, called a bigravity theory, is still free from the BD ghost shown by Hassan and Rosen [17]. As we will see later, while the dRGT theory contains only a massive spin-2 field, the bigravity theory contains a massless spin-2 field as well as a massive spin-2 field, with total seven degrees of freedom in the gravity sector.

The gravitational part of the bigravity is given by

$$S_{\text{grav}} = \frac{1}{2\kappa_g^2} \int d^4x \sqrt{-g} R(g) + \frac{1}{2\kappa_f^2} \int d^4x \sqrt{-f} \mathcal{R}(f) - \frac{m^2}{\kappa^2} \int d^4x \sqrt{-g} \sum_{n=0}^4 b_n \mathcal{U}_n(\gamma), \quad (3.3.1)$$

where  $g_{\mu\nu}$  and  $f_{\mu\nu}$  are two dynamical metrics, and  $R(g)$  and  $\mathcal{R}(f)$  are their Ricci scalars. The parameters  $\kappa_g^2 = 8\pi G$  and  $\kappa_f^2 = 8\pi \mathcal{G}$  are the corresponding gravitational constants, while  $\kappa$  is defined by  $\kappa^2 = \kappa_g^2 + \kappa_f^2$ .

The matter action  $S_m$  can be divided into three types:

$$S_m = S_g(g, \psi_g) + S_f(f, \psi_f) + S_d(g, f, \psi_d), \quad (3.3.2)$$

where first two types of matter fields couple to either  $g_{\mu\nu}$  or  $f_{\mu\nu}$ , while the third type couples to both metrics. The matter fields that couple to only one metric do not spoil the structure of the gravitational part of the theory that eliminates the (would-be) BD ghost. On the other hand, matter fields that couple to both metrics generically reintroduce the BD ghost. Although one can construct a ghost-free double matter coupling via an effective composite metric at low energy scales, such a coupling gives a ghost at high energy scales [93, 100–106]. This would imply that the matter should couple to only one metric. One way to avoid the difficulty of the double matter coupling was proposed in the context of the partially constrained vielbein formulation that breaks Lorentz invariance at the cosmological scale [107], making it possible to couple matter fields simultaneously to both metrics without the BD ghost at all scales. In this thesis, however, we focus on the single matter coupling:

$$S_m = S_g(g, \psi_g) + S_f(f, \psi_f), \quad (3.3.3)$$

This restriction guarantees the weak equivalence principle as well as the ghost free condition. We call the  $g$ -matter  $\psi_g$  and the  $f$ -matter  $\psi_f$  twin matter fluids.

Taking the variation of the action with respect to  $g_{\mu\nu}$  and  $f_{\mu\nu}$ , we find two sets of the Einstein equations:

$$G^\mu{}_\nu = \kappa_g^2 (T_g^{[\gamma]\mu}{}_\nu + T_g^{[m]\mu}{}_\nu), \quad (3.3.4)$$

$$\mathcal{G}^\mu{}_\nu = \kappa_f^2 (T_f^{[\gamma]\mu}{}_\nu + T_f^{[m]\mu}{}_\nu), \quad (3.3.5)$$

where  $G^\mu{}_\nu$  and  $\mathcal{G}^\mu{}_\nu$  are the Einstein tensors for  $g_{\mu\nu}$  and  $f_{\mu\nu}$ , respectively. The matter energy-momentum tensors are given by

$$T_g^{[m]}{}_{\mu\nu} = -2 \frac{\delta S_g^{[m]}}{\delta g^{\mu\nu}}, \quad T_f^{[m]}{}_{\mu\nu} = -2 \frac{\delta S_f^{[m]}}{\delta f^{\mu\nu}}. \quad (3.3.6)$$

The  $\gamma$ -“energy-momentum” tensors from the interaction term are given by

$$T_g^{[\gamma]\mu}{}_{\nu} = \frac{m^2}{\kappa^2} (\tau^{\mu}{}_{\nu} - \mathcal{U} \delta^{\mu}{}_{\nu}), \quad (3.3.7)$$

$$T_f^{[\gamma]\mu}{}_{\nu} = -\frac{\sqrt{-g}}{\sqrt{-f}} \frac{m^2}{\kappa^2} \tau^{\mu}{}_{\nu}, \quad (3.3.8)$$

with

$$\begin{aligned} \tau^{\mu}{}_{\nu} = & \{b_1 \mathcal{U}_0 + b_2 \mathcal{U}_1 + b_3 \mathcal{U}_2 + b_4 \mathcal{U}_3\} \gamma^{\mu}{}_{\nu} \\ & - \{b_2 \mathcal{U}_0 + b_3 \mathcal{U}_1 + b_4 \mathcal{U}_2\} (\gamma^2)^{\mu}{}_{\nu} \\ & + \{b_3 \mathcal{U}_0 + b_4 \mathcal{U}_1\} (\gamma^3)^{\mu}{}_{\nu} \\ & - b_4 \mathcal{U}_0 (\gamma^4)^{\mu}{}_{\nu}. \end{aligned} \quad (3.3.9)$$

The energy-momenta of matter fields are assumed to be conserved individually as

$$\overset{(g)}{\nabla}_{\mu} T_g^{[m]\mu}{}_{\nu} = 0, \quad \overset{(f)}{\nabla}_{\mu} T_f^{[m]\mu}{}_{\nu} = 0, \quad (3.3.10)$$

where  $\overset{(g)}{\nabla}_{\mu}$  and  $\overset{(f)}{\nabla}_{\mu}$  are covariant derivatives with respect to  $g_{\mu\nu}$  and  $f_{\mu\nu}$ . From the contracted Bianchi identities for (3.3.4) and (3.3.5), the conservation of the  $\gamma$ -“energy-momenta” is also guaranteed as

$$\overset{(g)}{\nabla}_{\mu} T_g^{[\gamma]\mu}{}_{\nu} = 0, \quad \overset{(f)}{\nabla}_{\mu} T_f^{[\gamma]\mu}{}_{\nu} = 0. \quad (3.3.11)$$

### 3.3.2 Homothetic solutions

First we give one simple solution, in which we assume that two metrics are proportional;

$$f_{\mu\nu} = K^2 g_{\mu\nu}, \quad (3.3.12)$$

where  $K$  is a scalar function. In this case, since we find the tensor  $\gamma^{\mu}{}_{\nu} = K \delta^{\mu}{}_{\nu}$ , the  $\gamma$ -“energy-momentum” is given by

$$\begin{aligned} \kappa_g^2 T_g^{[\gamma]\mu}{}_{\nu} &= -\Lambda_g(K) \delta^{\mu}{}_{\nu}, \\ \kappa_f^2 T_f^{[\gamma]\mu}{}_{\nu} &= -\Lambda_f(K) \delta^{\mu}{}_{\nu}, \end{aligned}$$

where

$$\begin{aligned} \Lambda_g(K) &= m^2 \frac{\kappa_g^2}{\kappa^2} (b_0 + 3b_1 K + 3b_2 K^2 + b_3 K^3), \\ \Lambda_f(K) &= m^2 \frac{\kappa_f^2}{\kappa^2} (b_4 + 3b_3 K^{-1} + 3b_2 K^{-2} + b_1 K^{-3}). \end{aligned} \quad (3.3.13)$$

From the energy-momentum conservation (3.3.11), we find that  $K$  is a constant. As a result, we find two sets of the Einstein equations with cosmological constants  $\Lambda_g$  and  $\Lambda_f$ :

$$G_{\mu\nu}(g) + \Lambda_g g_{\mu\nu} = \kappa_g^2 T_g^{[m]}{}_{\mu\nu}, \quad (3.3.14)$$

$$G_{\mu\nu}(f) + \Lambda_f f_{\mu\nu} = \kappa_f^2 T_f^{[m]}{}_{\mu\nu}. \quad (3.3.15)$$

Since two metrics are proportional, we have the constraints on the cosmological constants and matter fields as

$$\Lambda_g(K) = K^2 \Lambda_f(K), \quad (3.3.16)$$

$$\kappa_g^2 T_g^{[m]\mu}{}_{\nu} = K^2 \kappa_f^2 T_f^{[m]\mu}{}_{\nu}. \quad (3.3.17)$$

The quartic equation (3.3.16) for  $K$  has at most four real roots, which give four different cosmological constants. The basic equations (3.3.14) (or (3.3.15)) are just the Einstein equations in GR with a cosmological constant. Hence any solutions in GR with a cosmological constant are always the solutions in the present bigravity theory. We shall call these solutions homothetic solutions because of the proportionality of two metrics.

In the vacuum case, there exist Minkowski, de Sitter, and anti-de Sitter solutions depending on the sign of the cosmological constant. Since  $K$  has at most four branches, the vacuum solution cannot be determined uniquely. It implies that, even if we assume the existence of the Minkowski vacuum in the bigravity theory, it could admit de Sitter vacuum as another branch of the vacuum solution. The typical value of the emerged cosmological constant would be an order of magnitude of the graviton mass square which implies that the present acceleration of the Universe can be explained by the graviton mass. So before discussing more details of bigravity, we summarize when the bigravity theory admits the de Sitter vacuum as well as the Minkowski vacuum [51, 108].

To admit the trivial Minkowski vacuum, we set

$$c_0 = c_1 = 0, \quad c_2 = -1, \quad (3.3.18)$$

where the parameters  $c_i$  are defined by (3.2.15). Note that the setting  $c_2 = -1$  is not relevant to the existence of the Minkowski vacuum, but it gives a normalization such that the parameter  $m$  corresponds to the graviton mass propagating on the Minkowski vacuum. Then the coupling constants  $b_i$  are given by two parameters  $c_3$  and  $c_4$  as

$$\begin{aligned} b_0 &= 4c_3 + c_4 - 6, \\ b_1 &= 3 - 3c_3 - c_4, \\ b_2 &= 2c_3 + c_4 - 1, \\ b_3 &= -(c_3 + c_4), \\ b_4 &= c_4. \end{aligned} \quad (3.3.19)$$

In this case, one can easily find

$$\Lambda_g(1) = \Lambda_f(1) = 0, \quad (3.3.20)$$

thus  $K = 1$  gives a root of the quartic equation (3.3.16) with zero cosmological constant. The rest three roots of the equation (3.3.16) can be all real or one real and two complex. The de Sitter solution can be found when the coupling constants satisfy

$$2c_3^2 + 3c_4 > 0. \quad (3.3.21)$$

This parameter space is classified into five regions depending on the sign of  $K$  and the magnitude relations of the roots  $K$ . The de Sitter vacuum with  $K > 0$  is found when

$$\begin{aligned} c_3 < 0, \quad c_3 + c_4 < 0, \quad 2c_3^2 + 3c_4 > 0 & \quad [\text{region (1)}], \\ c_3 > 3, \quad 3c_3 + c_4 < 3, \quad 2c_3^2 + 3c_4 > 0 & \quad [\text{region (2)}]. \end{aligned}$$

We show the typical examples (Models A and B) for these regions in Table 3.1: For the coupling constants which satisfy

$$\begin{aligned} c_3 + c_4 > 0, \quad 3c_3 + c_4 < 3, \quad 2c_3^2 + 3c_4 > 0 & \quad [\text{region (3a)}], \\ c_3 + c_4 < 0, \quad 3c_3 + c_4 > 3, \quad 2c_3^2 + 3c_4 > 0 & \quad [\text{region (3b)}], \\ c_3 + c_4 > 0, \quad 3c_3 + c_4 > 3, \quad 2c_3^2 + 3c_4 > 0 & \quad [\text{region (3c)}], \end{aligned}$$

we obtain one de Sitter solution for  $K_{(\text{dS})} < 0$ . In Table 3.2, we show some examples (Models C, D, and E).

In Fig.3.1, we show the regions (1), (2) and (3) where de Sitter solution exists are shown on the  $c_3$ - $c_4$  plane. In the white region in Fig.3.1, there is no de Sitter solution. There exist either three or one AdS spacetimes.

As a result, the bigravity theory can admit the de Sitter vacuum as well as the Minkowski vacuum in an appropriate parameter space. However, the existence of several vacua give a question:

| Model | $(c_3, c_4)$ | region | $K$         | $\Lambda_g$    | vacuum           |
|-------|--------------|--------|-------------|----------------|------------------|
| A     | $(-1, 0)$    | (1)    | $-0.523476$ | $-11.0162m^2$  | AdS <sub>1</sub> |
|       |              |        | 1           | 0              | M                |
|       |              |        | 1.67319     | $-0.19723m^2$  | AdS <sub>2</sub> |
|       |              |        | 6.85028     | $6.2134m^2$    | dS               |
| B     | $(4, -10)$   | (2)    | $-1.91031$  | $-40.2009m^2$  | AdS <sub>1</sub> |
|       |              |        | 1           | 0              | M                |
|       |              |        | 0.145979    | $0.132407m^2$  | dS               |
|       |              |        | 0.59766     | $-0.070451m^2$ | AdS <sub>2</sub> |

Table 3.1: In the parameter regions (1) and (2), there exists one de Sitter solution with  $K_{(\text{dS})} > 0$ . In addition, we find three other vacuum solutions (two anti-de Sitter (AdS) solutions as well as a trivial Minkowski spacetime). We assume  $\kappa_f = \kappa_g$ .

| model | $(c_3, c_4)$ | region | $K$             | $\Lambda_g$               | vacuum           |
|-------|--------------|--------|-----------------|---------------------------|------------------|
| C     | $(1/2, 0)$   | (3a)   | $-2 - \sqrt{3}$ | $\frac{3}{2}\sqrt{3}m^2$  | dS               |
|       |              |        | $-2 + \sqrt{3}$ | $-\frac{3}{2}\sqrt{3}m^2$ | AdS <sub>1</sub> |
|       |              |        | 1               | 0                         | M                |
|       |              |        | 3               | $-2m^2$                   | AdS <sub>2</sub> |
| D     | $(5/2, -4)$  | (3b)   | $-2 - \sqrt{3}$ | $-36.1866m^2$             | AdS <sub>1</sub> |
|       |              |        | $-2 + \sqrt{3}$ | $0.186534m^2$             | dS               |
|       |              |        | 1/3             | $-\frac{2}{9}m^2$         | AdS <sub>2</sub> |
|       |              |        | 1               | 0                         | M                |
| E     | $(3, 0)$     | (3c)   | $-0.761557$     | $14.8663m^2$              | dS               |
|       |              |        | 0.636672        | $-0.077027m^2$            | AdS <sub>1</sub> |
|       |              |        | 1               | 0                         | M                |
|       |              |        | 4.12489         | $-11.7893m^2$             | AdS <sub>2</sub> |

Table 3.2: In the parameter region (3), there exists one de Sitter solution with  $K_{(\text{dS})} < 0$ . We also find three other vacuum solutions (two AdS solutions as well as a trivial Minkowski spacetime). The region (3) is divided into three sub-regions ((3a), (3b) and (3c)) depending on the properties of the solutions. We assume  $\kappa_f = \kappa_g$ .

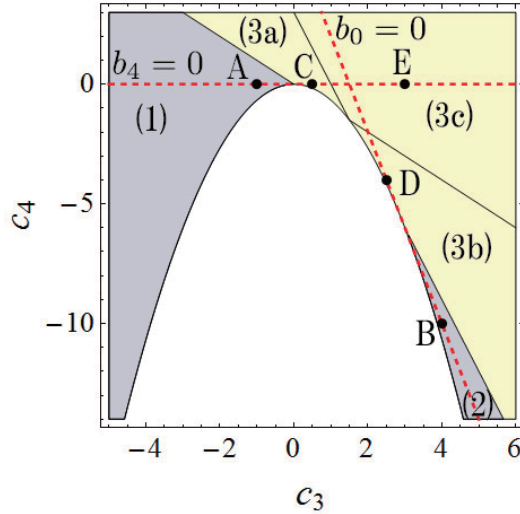


Figure 3.1: The de Sitter solutions with  $K > 0$  and  $K < 0$  are found in the regions (1) and (2) and in the region (3), respectively. The region (3) is divided into three sub-regions ((3a), (3b) and (3c)).

Is the de Sitter spacetime an attractor as the universe expands? To explain the current accelerating expansion of the Universe by the graviton mass, the de Sitter branch must be an attractor. On the other hand, if the graviton mass does not explain the accelerating expansion (e.g., the case when the graviton mass is quite large compared to the current energy density of the Universe), the Minkowski branch must be an attractor. Indeed, the universe evolves into the de Sitter branch (or the Minkowski branch) for general initial data which will be discussed in Chapter 5.

### 3.3.3 Linearization of bigravity theory

The bigravity theory contains one massless graviton and one massive graviton. This becomes clear when we look at the linear perturbations around a homothetic solution. The unperturbed solution is assumed to be homothetic, i.e.,

$$f_{\mu\nu}^{(0)} = K^2 g_{\mu\nu}^{(0)}, \quad (3.3.22)$$

where (0) indicates background quantities. This provides solutions to the unperturbed part of the two Einstein equations (3.3.14) and (3.3.15). A constant  $K$  is determined by the quartic equation (3.3.16), and the matter energy-momenta satisfy the unperturbed part of (3.3.17). We then consider the following perturbations:

$$g_{\mu\nu} = g_{\mu\nu}^{(0)} + \delta g_{\mu\nu}, \quad (3.3.23)$$

$$f_{\mu\nu} = f_{\mu\nu}^{(0)} + K^2 \delta f_{\mu\nu} = K^2 \left( g_{\mu\nu}^{(0)} + \delta f_{\mu\nu} \right) \quad (3.3.24)$$

where  $|\delta g_{\mu\nu}|, |\delta f_{\mu\nu}| \ll |g_{\mu\nu}^{(0)}|$ . The suffixes of  $\delta g_{\mu\nu}$  as well as  $\delta f_{\mu\nu}$  are raised and lowered by the background metric  $g_{\mu\nu}^{(0)}$ .

We obtain the quadratic action for the perturbations of the metrics as,

$$\begin{aligned} S_2 &= \int d^4x \sqrt{-\bar{g}} \left[ \frac{1}{\kappa_g^2} \mathcal{L}_{\text{EH}}[\delta g; \Lambda_g] + \frac{K^2}{\kappa_f^2} \mathcal{L}_{\text{EH}}[\delta f; \Lambda_g] + \mathcal{L}_{\text{FP}}[\varphi; m_{\text{eff}}^2] \right] \\ &= \int d^4x \sqrt{-\bar{g}} \mathcal{L}_{\text{EH}}[h; \Lambda_g] + \int d^4x \sqrt{-\bar{g}} \left[ \mathcal{L}_{\text{EH}}[\varphi; \Lambda_g] + \mathcal{L}_{\text{FP}}[\varphi; m_{\text{eff}}^2] \right], \end{aligned} \quad (3.3.25)$$

where the massless and massive graviton modes with mass dimension one are defined by

$$h_{\mu\nu} = \frac{\kappa_f}{K \kappa_g \kappa_-} \delta g_{\mu\nu} + \frac{K \kappa_g}{\kappa_f \kappa_-} \delta f_{\mu\nu}, \quad (3.3.26)$$

$$\varphi_{\mu\nu} = \frac{1}{\kappa_-} (\delta g_{\mu\nu} - \delta f_{\mu\nu}), \quad (3.3.27)$$

with  $\kappa_-^2 = \kappa_g^2 + K^{-2} \kappa_f^2$ . The effective graviton mass  $m_{\text{eff}}$  in a homothetic background spacetime is defined by

$$m_g^2 := \frac{m^2 \kappa_g^2}{\kappa^2} (b_1 K + 2b_2 K^2 + b_3 K^3), \quad (3.3.28)$$

$$m_f^2 := \frac{m^2 \kappa_f^2}{K^2 \kappa^2} (b_1 K + 2b_2 K^2 + b_3 K^3), \quad (3.3.29)$$

$$\begin{aligned} m_{\text{eff}}^2 &:= m_g^2 + m_f^2 \\ &= \frac{m^2}{\kappa^2} \left( \kappa_g^2 + \frac{\kappa_f^2}{K^2} \right) (b_1 K + 2b_2 K^2 + b_3 K^3). \end{aligned} \quad (3.3.30)$$

The quadratic Einstein-Hilbert Lagrangian and the FP mass term for a metric perturbation  $\chi_{\mu\nu}$  are defined by

$$\mathcal{L}_{\text{EH}}[\chi; \Lambda_g] = -\frac{1}{4} \chi^{\mu\nu} \mathcal{E}_{\mu\nu, \alpha\beta} \chi^{\alpha\beta} - \frac{\Lambda_g}{4} (\chi^2 - 2\chi_{\mu\nu} \chi^{\mu\nu}), \quad (3.3.31)$$

$$\mathcal{L}_{\text{FP}}[\chi; m_{\text{eff}}^2] = -\frac{m_{\text{eff}}^2}{8} (\chi_{\mu\nu} \chi^{\mu\nu} - \chi^2). \quad (3.3.32)$$



It is now explicit from (3.3.25) that the bigravity theory contains one massless and one massive graviton since the action for  $h_{\mu\nu}$  is given by the linearized Einstein-Hilbert action and the action for  $\varphi_{\mu\nu}$  is given by the Fierz-Pauli action defined on a fixed curve spacetime.

### 3.4 Energy-momentum tensor of gravitons in bigravity

In the previous section, we showed the quadratic action of the bigravity can be decomposed into the massless graviton and the massive graviton. Although these are decoupled at linear order, the massless graviton and the massive graviton are coupled at non-linear order. The nonlinear terms give a backreaction into the gravitational field, e.g., localized massive gravitons may form the gravitational field. In GR, as derived by Isaacson [109], the energy-momentum tensor of the high-frequency gravitational wave can be defined by evaluating the nonlinear terms of the Einstein equation. Therefore, even in bigravity, we could define the energy-momentum tensors of both massless and massive gravitons which may give backreactions into the gravitational field. In this section, we define the energy-momentum tensors of gravitons in bigravity based on our paper [54].

As is well known in GR, the division of the spacetime geometry into a background and gravitational waves requires a separation of scales for the two: the length or/and time scale associated with the perturbation should be sufficiently shorter than the scale associated with the smooth background [109]. In this situation the energy-momentum tensor of gravitational waves is defined by the second order part of the perturbed Einstein equation averaged over a length or/and time scale between the two scales. The same assumption and procedure can be employed to define the energy-momentum tensor of the massless graviton in the context of bigravity.

Here we assume sufficiently high-frequency/momentum gravitational waves compared with the spacetime geometry. When we consider high-frequency/momentum waves, the motion of such waves could be decoupled from the dynamics of a background and they freely propagate around the background. So, first we discuss the free propagating massless and massive gravitational waves. For simplicity, we assume the background spacetime is the  $K = 1$  Minkowski spacetime with the coupling constant (3.2.15). The generalization to a curved background could be straightforward when the frequency/momentum is sufficiently higher than the inverse of the curvature scale of the background.

The quadratic action is expressed as

$$\begin{aligned} S_2 &= \int d^4x \left[ \frac{1}{\kappa_g^2} \mathcal{L}_{\text{EH}}[\delta g] + \frac{1}{\kappa_f^2} \mathcal{L}_{\text{EH}}[\delta f] + \mathcal{L}_{\text{FP}}[\varphi] + \frac{1}{2} \delta g_{\mu\nu} T_m^{\mu\nu} \right] \\ &= \int d^4x \left[ \mathcal{L}_{\text{EH}}[h] + \frac{1}{2M_{\text{Pl}}} h_{\mu\nu} T_m^{\mu\nu} \right] + \int d^4x \left[ \mathcal{L}_{\text{EH}}[\varphi] + \mathcal{L}_{\text{FP}}[\varphi] + \frac{1}{2M_G} \varphi_{\mu\nu} T_m^{\mu\nu} \right], \end{aligned} \quad (3.4.1)$$

where  $T_m^{\mu\nu}$  is the matter energy-momentum tensor which is introduced to compare the energy-momentum tensor of matter with those of gravitons<sup>2</sup>. The gravitational coupling constants are defined by

$$M_{\text{Pl}} := \frac{\kappa}{\kappa_g \kappa_f}, \quad M_G := \frac{\kappa}{\kappa_g^2} = \frac{\kappa_f}{\kappa_g} M_{\text{Pl}}. \quad (3.4.2)$$

Note that we have assumed the matter contribute to only low-frequency/momentum modes. The matter does not contribute to the motion of the high-frequency waves thus high-frequency/momentum modes freely propagate around the background. Hence, the equations of motion of high-frequency waves at linear order are given by

$$\mathcal{E}_{\mu\nu, \alpha\beta} h^{\alpha\beta} = 0, \quad (3.4.3)$$

$$\mathcal{E}_{\mu\nu, \alpha\beta} \varphi^{\alpha\beta} + \frac{m^2}{2} (\varphi_{\mu\nu} - \varphi \eta_{\mu\nu}) = 0. \quad (3.4.4)$$

---

<sup>2</sup>For simplicity, we introduce a matter field couple with only  $g_{\mu\nu}$ . Although we can also introduce a matter field couple with  $f_{\mu\nu}$ , it is not so important for the discussion here

Since the massless graviton has a gauge symmetry, we can choose the transverse-traceless gauge for the massless eigenstate, i.e.,

$$\partial_\mu h^\mu{}_\nu = 0, \quad h = 0, \quad h_{\mu\nu} u^\nu = 0, \quad (3.4.5)$$

where  $u^\mu$  is a timelike vector. Since the massive graviton does not enjoy the gauge symmetry, we cannot impose any gauge condition for the massive graviton. However, in vacuum, we can obtain the transverse-traceless condition from the equation of motion:

$$\partial_\mu \varphi^\mu{}_\nu = 0, \quad \varphi = 0. \quad (3.4.6)$$

As a result, the equations of motion are expressed as

$$\partial^2 h_{\mu\nu} = 0, \quad (3.4.7)$$

$$(\partial^2 - m^2)\varphi_{\mu\nu} = 0. \quad (3.4.8)$$

The equations are the Klein-Gordon equations with and without the mass term, thus we can easily find their solutions. However, the explicit forms of the solutions are not necessary to evaluate the energy-momentum tensor.

As mentioned above, the graviton energy-momentum tensor can be defined by evaluating nonlinear terms of the Einstein equation. In the case of GR, there is no ambiguity to define the energy-momentum tensor since there is only one Einstein equation. However, in the case of bigravity, there are two Einstein equations thus it is not clear how to define the energy-momentum tensor from nonlinear terms of the Einstein equations. Therefore, we first consider another definition of the energy-momentum tensor: the ‘‘canonical’’ energy-momentum tensor which is defined from the Noether’s theorem.

In the classical field theory, when the Lagrangian is given, the canonical energy-momentum tensor can be defined from the Noether’s theorem. However, since the Lagrangian has a freedom to add a total divergence term, the energy-momentum tensor cannot be defined uniquely. To remove this ambiguity, we define the canonical energy-momentum tensor by averaging over a spacetime region. Hence we define the canonical energy-momentum tensor of a symmetric tensor field  $\chi_\mu$  as

$$\Theta_\chi^{\mu\nu} := \left\langle -\frac{\delta \mathcal{L}_\chi}{\delta(\partial_\mu \chi_{\alpha\beta})} \partial^\nu \chi_{\alpha\beta} + \eta^{\mu\nu} \mathcal{L}_\chi \right\rangle, \quad (3.4.9)$$

where the symbol  $\langle \dots \rangle$  denotes an average over a spacetime region with a size larger than the corresponding scale of the perturbation but smaller than the scale of the background, defined through an appropriate window function. Specifically, the assumption of a large hierarchy of scales makes it possible for us to ignore boundary terms of  $\langle \dots \rangle$  and perform integration by part, e.g., as

$$\langle \partial_\rho \chi_{\mu\nu} \chi_{\alpha\beta} \rangle = -\underbrace{\langle \chi_{\mu\nu} \partial_\rho \chi_{\alpha\beta} \rangle}_{\mathcal{O}(\lambda^{-1} \chi^2)} + \mathcal{O}(L^{-1} \chi^2) \approx -\langle \chi_{\mu\nu} \partial_\rho \chi_{\alpha\beta} \rangle, \quad (3.4.10)$$

where  $L, \lambda$  are scales of the average and the perturbations, respectively, which are assumed to be  $L \gg \lambda$ . For the massless graviton  $h_{\mu\nu}$ , the Lagrangian is given by the linearized Einstein-Hilbert action. Assuming the transverse-traceless gauge, the canonical energy-momentum tensor is calculated by

$$\begin{aligned} \Theta_{\text{gw}}^{\mu\nu} &= \left\langle -\frac{\delta \mathcal{L}_{\text{EH}}}{\delta(\partial_\mu h_{\alpha\beta})} \partial^\nu h_{\alpha\beta} + \eta^{\mu\nu} \mathcal{L}_{\text{EH}} \right\rangle \\ &= \frac{1}{4} \langle \partial^\mu h^{\alpha\beta} \partial^\nu h_{\alpha\beta} \rangle + \frac{1}{8} \eta^{\mu\nu} \langle h_{\alpha\beta} \partial^2 h^{\alpha\beta} \rangle. \end{aligned} \quad (3.4.11)$$

The second term vanishes from the field equation (3.4.7), and then the canonical energy-momentum tensor of the massless graviton is given by

$$\Theta_{\text{gw}}^{\mu\nu} = \frac{1}{4} \langle \partial^\mu h^{\alpha\beta} \partial^\nu h_{\alpha\beta} \rangle. \quad (3.4.12)$$

The canonical energy-momentum tensor of the massive graviton can be obtained in a way similar to the case of the massless graviton. By using the field equation (3.4.8) and the transverse-traceless condition (3.4.6), the canonical energy-momentum tensor is given by

$$\begin{aligned}\Theta_G^{\mu\nu} &= \left\langle -\frac{\delta(\mathcal{L}_{\text{EH}} + \mathcal{L}_{\text{FP}})}{\delta(\partial_\mu \varphi_{\alpha\beta})} \partial^\nu \varphi_{\alpha\beta} + \eta^{\mu\nu} (\mathcal{L}_{\text{EH}} + \mathcal{L}_{\text{FP}}) \right\rangle \\ &= \frac{1}{4} \langle \partial^\mu \varphi^{\alpha\beta} \partial^\nu \varphi_{\alpha\beta} \rangle.\end{aligned}\quad (3.4.13)$$

We note the averaging and the integration by part used to derive the energy-momentum tensor. For the massless graviton with the transverse-traceless gauge (3.4.6), in both GR and bigravity, the integration by part can be applied to the time derivative as well as the spatial derivatives even if the average is over a spatial region, provided that the gravitational wave over the region of integration can be considered as a wave propagating to one direction. For example, in a region sufficiently far from a finite-size source a solution to the wave equation propagating to, say, the  $z$  direction is written as  $F(t-z)$  and thus  $\partial_t$  applied to it can be replaced by  $-\partial_z$  before performing the spatial integration by part and then  $\partial_z$  acted on another function of the form  $G(t-z)$  can be replaced by  $-\partial_t$ . On the other hand, this argument does not apply to the massive graviton since a wave of a massive field changes its shape as it propagates in one direction. Moreover, even for the massless graviton, in either GR or bigravity, this argument does not seem to be valid for stochastic gravitational waves, which come from every direction to every point. We thus employ an average over a spacetime region to make it possible to do integration by part.

In general relativity, the energy-momentum tensor of the graviton defined from Noether's theorem is also obtained from the nonlinear part of the Einstein equation. Here we consider up to second order of the perturbation. For a transverse-traceless perturbation  $\chi_{\mu\nu} := M_{\text{pl}}(g_{\mu\nu} - \eta_{\mu\nu})$ , the second order part of the Ricci tensor is given by

$$M_{\text{pl}}^2 \delta R_{\mu\nu}^{(2)} = \frac{1}{4} \chi^{\alpha\beta}{}_{,\mu} \chi_{\alpha\beta,\nu} - \frac{1}{2} \chi_{\mu\alpha,\beta} \chi_{\nu}{}^{\beta,\alpha} + \frac{1}{2} \chi_{\mu}{}^{\alpha,\beta} \chi_{\nu\alpha,\beta} + \frac{1}{2} \chi^{\alpha\beta} (\chi_{\alpha\beta,\mu\nu} - 2\chi_{\alpha(\mu,\nu)\beta} + \chi_{\mu\nu,\alpha\beta}), \quad (3.4.14)$$

where we have imposed the transverse-traceless gauge condition. We define the energy-momentum tensor of the graviton as

$$T_\chi^{\mu\nu} := M_{\text{pl}}^2 \langle \delta G^{\mu\nu}(\chi) \rangle = - \left( \eta^{\mu\alpha} \eta^{\nu\beta} - \frac{1}{2} \eta^{\mu\nu} \eta^{\alpha\beta} \right) M_{\text{pl}}^2 \langle \delta R_{\alpha\beta}(\chi) \rangle. \quad (3.4.15)$$

Integrating by part (under the high-frequency/momentum approximation) and using the equation of motion  $\chi_{\alpha\beta,\gamma}{}^\gamma = 0$ , one can obtain

$$T_\chi^{\mu\nu} = \frac{1}{4} \langle \chi^{\alpha\beta,\mu} \chi_{\alpha\beta,\nu} \rangle, \quad (3.4.16)$$

which is the same as the result from the Noether's theorem. Including the energy-momentum tensors of the graviton as well as the matter, the Einstein equation is expressed as

$$\mathcal{E}^{\mu\nu,\alpha\beta} \chi_{\alpha\beta} = \frac{1}{M_{\text{pl}}} (T_{\text{m}}^{\mu\nu} + T_\chi^{\mu\nu}). \quad (3.4.17)$$

Hence the energy-momentum tensor of the graviton is a source of the gravitational field. Note that the conservation law of the energy-momentum tensor is guaranteed without taking an average over a spacetime region. The divergence of  $T_\chi^{\mu\nu}$  is calculated as

$$\partial_\nu T_\chi^{\mu\nu} = \left( \frac{1}{4} \chi^{\alpha\beta,\mu} - \frac{1}{2} \chi^{\mu\alpha,\beta} \right) \chi_{\alpha\beta,\gamma}{}^\gamma, \quad (3.4.18)$$

which is zero due to the field equation.

The canonical energy-momentum tensor of the massive graviton would be a source of the gravitational field in bigravity. We expand the equations (3.3.4) and (3.3.5) around the Minkowski vacuum up to the second order of perturbations. We use the transverse-traceless gauge for the

massless graviton continuously. The second order parts of  $T_g^{[\gamma]\mu\nu}$  and  $T_f^{[\gamma]\mu\nu}$  in terms of the mass eigenstates are given by

$$\begin{aligned} \delta T_g^{(2)[\gamma]\mu\nu} &= \frac{m^2}{8\kappa^2} [(9\kappa_g^2 + \kappa_f^2 - 2c_3\kappa^2)\varphi^{\mu\alpha}\varphi^\nu{}_\alpha - (4\kappa_g^2 - c_3\kappa^2)\varphi^{\alpha\beta}\varphi_{\alpha\beta}\eta^{\mu\nu}] \\ &\quad + m^2 \frac{\kappa_g\kappa_f}{\kappa^2} \left[ \frac{1}{4}\varphi^{\alpha(\mu}h^{\nu)}{}_\alpha - \frac{1}{2}h^{\alpha\beta}\varphi_{\alpha\beta}\eta^{\mu\nu} \right], \end{aligned} \quad (3.4.19)$$

$$\begin{aligned} \delta T_f^{(2)[\gamma]\mu\nu} &= \frac{m^2}{8\kappa^2} [(-5\kappa_g^2 + 3\kappa_f^2 + 2c_3\kappa^2)\varphi^{\mu\alpha}\varphi^\nu{}_\alpha - (-3\kappa_g^2 + \kappa_f^2 + c_3\kappa^2)\varphi^{\alpha\beta}\varphi_{\alpha\beta}\eta^{\mu\nu}] \\ &\quad + m^2 \frac{\kappa_g\kappa_f}{\kappa^2} \left[ -\frac{1}{4}\varphi^{\alpha(\mu}h^{\nu)}{}_\alpha + \frac{1}{2}h^{\alpha\beta}\varphi_{\alpha\beta}\eta^{\mu\nu} \right], \end{aligned} \quad (3.4.20)$$

where we use  $h^\mu{}_\mu = 0$  and  $\varphi^\mu{}_\mu = 0$ . Note that although both  $T_g^{[\gamma]\mu\nu}$  and  $T_f^{[\gamma]\mu\nu}$  are complicated, the sum is simply given by

$$\delta T_g^{(2)[\gamma]\mu\nu} + \delta T_f^{(2)[\gamma]\mu\nu} = \frac{m^2}{2}\varphi^{\mu\alpha}\varphi^\nu{}_\alpha - \frac{m^2}{8}\varphi^{\alpha\beta}\varphi_{\alpha\beta}\eta^{\mu\nu}. \quad (3.4.21)$$

We find the canonical energy-momentum tensors of massless and massive gravitons are obtained as source terms of the field equation of the massless graviton with the coupling constant  $M_{\text{pl}}$ . Including the energy-momentum tensors, the equation of motion of the massless graviton is expressed by

$$\mathcal{E}^{\mu\nu,\alpha\beta}h_{\alpha\beta} = \frac{1}{M_{\text{pl}}}(T_{\text{m}}^{\mu\nu} + T_{\text{gw}}^{\mu\nu} + T_G^{\mu\nu}), \quad (3.4.22)$$

where the energy-momentum tensors of the massless graviton and the massive graviton are defined by

$$\begin{aligned} T_{\text{gw}}^{\mu\nu} &:= -M_{\text{pl}}^2\delta G^{\mu\nu(2)}(h) \\ &= -\frac{1}{4}h^{\alpha\beta,\mu}h_{\alpha\beta}{}^{,\nu} + \frac{1}{2}h^\mu{}_{\alpha,\beta}h^{\nu\beta,\alpha} - \frac{1}{2}h^{\mu\alpha,\beta}h^\nu{}_{\alpha,\beta} \\ &\quad - h^{\alpha(\mu}h^{\nu)}{}_{\alpha,\beta}{}^{,\beta} - \frac{1}{2}h^{\alpha\beta}(h_{\alpha\beta}{}^{,\mu\nu} - 2h^{\mu}{}_{\alpha}{}^{,\nu)}{}_\beta + h^{\mu\nu}{}_{,\alpha\beta} \\ &\quad + \eta^{\mu\nu} \left( \frac{3}{8}h_{\alpha\beta,\gamma}h^{\alpha\beta,\gamma} - \frac{1}{4}h_{\alpha\beta,\gamma}h^{\alpha\gamma,\beta} + \frac{1}{2}h^{\alpha\beta}h_{\alpha\beta,\gamma}{}^{,\gamma} \right), \end{aligned} \quad (3.4.23)$$

$$\begin{aligned} T_G^{\mu\nu} &:= -\frac{1}{\kappa^2}\delta G^{\mu\nu(2)}(\varphi) + \delta T_g^{(2)[\gamma]\mu\nu} + \delta T_f^{(2)[\gamma]\mu\nu} \\ &= -\frac{1}{4}\varphi^{\alpha\beta,\mu}\varphi_{\alpha\beta}{}^{,\nu} + \frac{1}{2}\varphi^\mu{}_{\alpha,\beta}\varphi^{\nu\beta,\alpha} - \frac{1}{2}\varphi^{\mu\alpha,\beta}\varphi^\nu{}_{\alpha,\beta} \\ &\quad - \varphi^{\alpha(\mu}\varphi^{\nu)}{}_{\alpha,\beta}{}^{,\beta} - \frac{1}{2}\varphi^{\alpha\beta}(\varphi_{\alpha\beta}{}^{,\mu\nu} - 2\varphi^{\mu}{}_{\alpha}{}^{,\nu)}{}_\beta + \varphi^{\mu\nu}{}_{,\alpha\beta} \\ &\quad + \eta^{\mu\nu} \left( \frac{3}{8}\varphi_{\alpha\beta,\gamma}\varphi^{\alpha\beta,\gamma} - \frac{1}{4}\varphi_{\alpha\beta,\gamma}\varphi^{\alpha\gamma,\beta} + \frac{1}{2}\varphi^{\alpha\beta}\varphi_{\alpha\beta,\gamma}{}^{,\gamma} \right) \\ &\quad + \frac{m^2}{2}\varphi^{\mu\alpha}\varphi^\nu{}_\alpha - \frac{m^2}{8}\varphi^{\alpha\beta}\varphi_{\alpha\beta}\eta^{\mu\nu}. \end{aligned} \quad (3.4.24)$$

Averaging over a spacetime region, the energy-momentum tensors are reduced into

$$T_{\text{gw}}^{\mu\nu} = \frac{1}{4}\langle h^{\alpha\beta,\mu}h_{\alpha\beta}{}^{,\nu} \rangle, \quad (3.4.25)$$

$$T_G^{\mu\nu} = \frac{1}{4}\langle \varphi^{\alpha\beta,\mu}\varphi_{\alpha\beta}{}^{,\nu} \rangle, \quad (3.4.26)$$

which are indeed the same as the canonical energy-momentum tensors defined from Noether's theorem. The energy-momentum tensors  $T_{\text{gw}}^{\mu\nu}$  and  $T_G^{\mu\nu}$  satisfy the conservation laws without the

average over a spacetime region. The energy-momentum tensor of the massless graviton is the same as that in the case of GR, while the divergence of that of the massive graviton is calculated by

$$\partial_\nu T_G^{\mu\nu} = \left( \frac{1}{4} \varphi^{\alpha\beta,\mu} - \frac{1}{2} \varphi^{\mu\alpha,\beta} \right) (\varphi_{\alpha\beta,\gamma}{}^{,\gamma} - m^2 \varphi_{\alpha\beta}). \quad (3.4.27)$$

Hence the conservation law of the energy-momentum tensor of the massive graviton is guaranteed as well. As a result, we conclude that, in bigravity, both massless and massive gravitons are sources of the gravity mediated by the massless graviton rather than either  $g_{\mu\nu}$ ,  $f_{\mu\nu}$  or the massive graviton.

Note that the coupling strength is given by only  $M_{\text{pl}}$  in the Einstein equation of the massless graviton (3.4.22). The coupling  $M_G$  gives the coupling strength between the massive graviton and matter. Therefore, although the massive graviton is decoupled from the matter at the linear order in the limit  $M_G \rightarrow \infty$ , the massive graviton is not decoupled from the massless graviton in this limit. We also note that there is no mixing term between  $h_{\mu\nu}$  and  $\varphi_{\mu\nu}$  in the equation (3.4.22). It indicates that the cubic order Lagrangian would be schematically given by

$$\mathcal{L}_3 = \frac{1}{M_{\text{pl}}} h \partial^2 h^2 + \frac{1}{M_{\text{pl}}} h (\partial^2 \varphi^2 + m^2 \varphi^2) + \frac{1}{M_G} \varphi (\partial^2 \varphi^2 + m^2 \varphi^2). \quad (3.4.28)$$

This structure shows that the massive graviton cannot decay to two massless gravitons although it decay to some particles via the interaction  $\frac{1}{M_G} \varphi_{\mu\nu} T_m^{\mu\nu}$ . The discussions about the limit  $M_G \rightarrow \infty$  and the cubic order Lagrangian are more detailed in [55, 56].



## Chapter 4

# Decoupling limits and Vainshtein mechanism

The massive graviton generally contains five polarizations: one helicity-0 mode, two helicity-1 modes, and two helicity-2 modes. As discussed in Section 2.3, the Stückelberg trick is useful to discuss these modes in the Fierz-Pauli theory. For example, one can see the helicity-0 mode is not decoupled from the helicity-2 mode even in the massless limit. In this Chapter we consider this kind of analysis in the dRGT massive gravity and the bigravity. We shall derive an effective theory by taking a decoupling limit: In a limit, one can ignore the irrelevant interactions with keeping the number of degree of freedom in which some of degrees of freedom could be decoupled from other ones. The Stückelberg trick and the decoupling limit make it easy to see not only the appearance and disappearance of the BD ghost but also the existence of the Vainshtein mechanism.

### 4.1 Nonlinear Stückelberg fields

In this section, we introduce Stückelberg fields in order that the action of massive gravity recovers the gauge symmetry. In the Fierz-Pauli theory, it is sufficient to introduce the Stückelberg fields at linear order. However, to discuss nonlinear theories of massive gravity, we should extend Stückelberg fields to nonlinear orders.

Clearly, the metric perturbation usually defined by  $\delta g_{\mu\nu} := g_{\mu\nu} - g_{\mu\nu}^{(0)}$  is not a covariant quantity. To define a perturbation as a covariant quantity, we introduce Stückelberg fields as scalar quantities  $\phi^a$  ( $a = 0, 1, 2, 3$ ) and define the tensor

$$H_{\mu\nu} := g_{\mu\nu} - \partial_\mu \phi^a \partial_\nu \phi^b g_{ab}^{(0)}(\phi), \quad (4.1.1)$$

where the suffixes of  $H_{\mu\nu}$  are raised and lowered by the metric  $g_{\mu\nu}$ . Since the quantities  $\phi^a$  transform as scalars under diffeomorphisms  $x^\mu \rightarrow X^\alpha(x)$ , the quantity  $f_{\mu\nu} := \partial_\mu \phi^a \partial_\nu \phi^b g_{ab}^{(0)}(\phi)$  transforms like a metric tensor, so we call  $f_{\mu\nu}$  the fiducial metric. We define the unitary gauge where the Stückelberg fields are  $\phi^a = \delta_\mu^a x^\mu$  in which we simply obtain  $H_{\mu\nu} = \delta g_{\mu\nu}$ . Hence, the tensor  $H_{\mu\nu}$  can be recognized as a covariant form of the perturbation  $\delta g_{\mu\nu}$  by introducing the nonlinear Stückelberg fields. Using the covariant quantities, we can construct a covariant form of generic nonlinear interactions. We have two covariant quantities  $g_{\mu\nu}$  and  $H_{\mu\nu}$  (or  $f_{\mu\nu}$ ) under diffeomorphisms. Then a covariant form of generic nonlinear interactions is given by

$$\mathcal{L}_{\text{NL}} = \mathcal{L}_{\text{NL}}(g, H) = \mathcal{L}_{\text{NL}}(g, f). \quad (4.1.2)$$

In the case of the flat fiducial metric  $f_{\mu\nu} = \partial_\mu \phi^a \partial_\nu \phi^b \eta_{ab}$ , the Stückelberg fields can be split as  $\phi^a = \delta_a^\mu (x^a + \pi^a)$  and then  $f_{\mu\nu}$  is expressed by

$$f_{\mu\nu} = \eta_{\mu\nu}(x) + 2\partial_{(\mu} \pi_{\nu)}(x) + \partial_\mu \pi_\alpha(x) \partial_\nu \pi^\alpha(x), \quad (4.1.3)$$

where  $\pi_\mu$  is a vector field on the Minkowski spacetime. In this case the tensor  $H_{\mu\nu}$  is written as

$$H_{\mu\nu} = \frac{h_{\mu\nu}}{M_{\text{pl}}} - 2\partial_{(\mu}\pi_{\nu)} - \partial_\mu\pi_\alpha\partial_\nu\pi^\alpha, \quad (4.1.4)$$

with  $h_{\mu\nu} := M_{\text{pl}}(g_{\mu\nu} - \eta_{\mu\nu})$ . Since  $\pi_\mu$  is the vector field, introducing new Stüeckelberg fields  $A_\mu$  and  $\pi$ , we can also split it as

$$\pi_\mu = \frac{A_\mu}{mM_{\text{pl}}} + \frac{\partial_\mu\pi}{m^2M_{\text{pl}}}. \quad (4.1.5)$$

Then the tensor  $H_{\mu\nu}$  can be decomposed into  $\pi$ ,  $A_\mu$  and  $h_{\mu\nu}$  which can be regarded as the helicity-0, the helicity-1 and the helicity-2 modes, respectively.

## 4.2 Below the scale $\Lambda_3$

Before discussing the dRGT theory, we back to the general massive gravity. Generic nonlinear interactions lead to the BD ghost as discussed in Section 3.1 which can be also seen in the decoupling limit as the Ostrogradski instability [110, 111]. For simplicity, we only focus on the case of the massive gravity around the Minkowski background until Section 4.4.

As explicitly shown in Section 2.3, the special structure of the Fierz-Pauli mass term schematically leads to

$$\mathcal{L}_{\text{FP}} = m^2M_{\text{pl}}^2\delta g^2 = m^2h^2 + mh\partial A + h\partial\partial\pi + (\partial A)^2, \quad (4.2.1)$$

which does not contain any higher derivative terms, thus the Fierz-Pauli action is free from the Ostrogradski instability. However generic nonlinear interactions, given by

$$\begin{aligned} \mathcal{L}_{\text{NL}}(g, H) &= m^2M_{\text{pl}}^2 \sum \left( \frac{h}{M_{\text{pl}}} \right)^j \left( \frac{\partial A}{mM_{\text{pl}}} \right)^k \left( \frac{\partial^2\pi}{m^2M_{\text{pl}}} \right)^\ell \\ &= \sum \Lambda_{j,k,\ell}^{-(j+2k+3\ell-4)} h^j (\partial A)^k (\partial\partial\pi)^\ell, \end{aligned} \quad (4.2.2)$$

where

$$\Lambda_{j,k,\ell} = \left( m^{k+2\ell-2} M_{\text{pl}}^{j+k+\ell-2} \right)^{1/(j+2k+3\ell-4)}, \quad (4.2.3)$$

with  $j, k, \ell \in \mathbb{N}$  and  $j+k+\ell > 2$ , may contain higher derivative terms leading to the Ostrogradski instability.

The lowest interaction scale is  $\Lambda_5 := \Lambda_{j=0,k=0,\ell=3} = (m^4M_{\text{pl}})^{1/5}$  arising from the interactions  $(\partial^2\pi)^3$ . Clearly, this type of interactions contains higher derivatives. Therefore, to be free from the Ostrogradski instability, the interactions at the scale  $\Lambda_5$  must be eliminated. However, even if such a dangerous interaction is absent, there are infinite dangerous interactions  $(\partial^2\pi)^\ell$  with the coupling scale  $\Lambda_{j=0,k=0,\ell>3}$  at the scales

$$\Lambda_5 = (m^4M_{\text{pl}})^{1/5} < \Lambda_{j=0,k=0,\ell>3} < \Lambda_{j=0,k=0,\ell\rightarrow\infty} = \Lambda_3 = (m^2M_{\text{pl}})^{1/3}, \quad (4.2.4)$$

which lead to the Ostrogradski instability. Therefore, interactions below the scale  $\Lambda_3$  must be absent in the ghost-free nonlinear massive gravity. Note that interactions with  $j > 0$  or  $k > 0$  give large energy scale interactions. So we focus on only the helicity-0 sector of the massive graviton.

The most dangerous terms arises from the form of  $(\partial^2\pi)^\ell$ . Thus we only focus on only self-interactions of the scalar part here. Neglecting the vector and the tensor parts, the tensors are given by

$$g_{\mu\nu} \approx \eta_{\mu\nu}, \quad H_{\mu\nu} \approx -\frac{2}{m^2M_{\text{pl}}}\Pi_{\mu\nu} - \frac{1}{m^4M_{\text{pl}}^2}\eta^{\alpha\beta}\Pi_{\mu\alpha}\Pi_{\beta\nu}, \quad (4.2.5)$$



where  $\Pi_{\mu\nu} := \partial_\mu \partial_\nu \pi$ . Then the nonlinear interaction is constructed by a function of  $\eta_{\mu\nu}$  and  $\Pi_{\mu\nu}$ . We expand the nonlinear interactions in terms of  $\Pi_{\mu\nu}$  up to cubic order, for example,

$$\mathcal{L}_{\text{NL}} = \mathcal{L}_2 + \mathcal{L}_3 + \mathcal{O}(\Pi^4), \quad (4.2.6)$$

where the Lorentz invariance leads to

$$\begin{aligned} \mathcal{L}_2(g, H) &= -m^2 M_{\text{pl}}^2 (\beta_1 [H^2] + \beta_2 [H]^2) \\ &\approx -\frac{1}{m^2} (\beta_1 [\Pi^2] + \beta_2 [\Pi]^2), \end{aligned} \quad (4.2.7)$$

$$\begin{aligned} \mathcal{L}_3(g, H) &= -m^2 M_{\text{pl}}^2 (\gamma_1 [H^3] + \gamma_2 [H][H^2] + \gamma_3 [H]^3) \\ &\approx -\frac{1}{m^4 M_{\text{pl}}} (\gamma_1 [\Pi^3] + \gamma_2 [\Pi][\Pi^2] + \gamma_3 [\Pi]^3), \end{aligned} \quad (4.2.8)$$

with the notations  $\Pi^{n\mu}{}_\nu = \Pi^\mu{}_{\alpha_2} \Pi^{\alpha_2}{}_{\alpha_3} \cdots \Pi^{\alpha_n}{}_\nu$  and  $[\Pi^n] = \Pi^{n\mu}{}_\mu$ , and  $\beta_1, \beta_2, \gamma_1, \gamma_2$  and  $\gamma_3$  are arbitrary constants. Those are general forms of quadratic and cubic Lagrangian constructed by  $\Pi_{\mu\nu}$  and  $\eta_{\mu\nu}$  with the Lorentz invariance. Note that the generic quadratic order interaction contains the higher derivatives as a form of  $(\partial\partial\pi)^2$ . However, in the case of the Fierz-Pauli combination ( $\beta_2 = -\beta_1$ ), the quadratic order interaction becomes the total divergence term and then the action does not contain the higher derivative terms. Indeed, the quadratic term is explicitly calculated as

$$[\Pi^2] - [\Pi]^2 = -\epsilon_{\mu\nu\rho\sigma} \epsilon^{\alpha\beta\rho\sigma} \Pi^\mu{}_\alpha \Pi^\nu{}_\nu = -\partial^\mu (\epsilon_{\mu\nu\rho\sigma} \epsilon^{\alpha\beta\rho\sigma} \partial_\alpha \pi \partial^\nu \partial_\beta \pi) + \epsilon_{\mu\nu\rho\sigma} \epsilon^{\alpha\beta\rho\sigma} \partial_\alpha \pi \partial^\mu \partial^\nu \partial_\beta \pi,$$

where the last term vanishes due to the property of the antisymmetric tensor. Similarly to the Fierz-Pauli combination, the following combinations are total divergence terms:

$$\begin{aligned} \mathcal{U}_0(\Pi) &= -\frac{1}{4!} \epsilon_{\mu\nu\rho\sigma} \epsilon^{\mu\nu\rho\sigma} \\ &= 1, \end{aligned} \quad (4.2.9)$$

$$\begin{aligned} \mathcal{U}_1(\Pi) &= -\frac{1}{3!} \epsilon_{\mu\nu\rho\sigma} \epsilon^{\alpha\nu\rho\sigma} \Pi^\mu{}_\alpha \\ &= [\Pi], \end{aligned} \quad (4.2.10)$$

$$\begin{aligned} \mathcal{U}_2(\Pi) &= -\frac{1}{4} \epsilon_{\mu\nu\rho\sigma} \epsilon^{\alpha\beta\rho\sigma} \Pi^\mu{}_\alpha \Pi^\nu{}_\beta \\ &= \frac{1}{2!} ([\Pi]^2 - [\Pi^2]), \end{aligned} \quad (4.2.11)$$

$$\begin{aligned} \mathcal{U}_3(\Pi) &= -\frac{1}{3!} \epsilon_{\mu\nu\rho\sigma} \epsilon^{\alpha\beta\gamma\sigma} \Pi^\mu{}_\alpha \Pi^\nu{}_\beta \Pi^\rho{}_\gamma \\ &= \frac{1}{3!} ([\Pi]^3 - 3[\Pi][\Pi^2] + 2[\Pi^3]), \end{aligned} \quad (4.2.12)$$

$$\begin{aligned} \mathcal{U}_4(\Pi) &= -\frac{1}{4!} \epsilon_{\mu\nu\rho\sigma} \epsilon^{\alpha\beta\gamma\delta} \Pi^\mu{}_\alpha \Pi^\nu{}_\beta \Pi^\rho{}_\gamma \Pi^\sigma{}_\delta \\ &= \frac{1}{4!} ([\Pi^4] - 6[\Pi^2][\Pi]^2 + 8[\Pi^3][\Pi] + 3[\Pi^2]^2 - 6[\Pi^4]). \end{aligned} \quad (4.2.13)$$

Therefore, the cubic order interaction is the total divergence term when we chose  $\gamma_2 = -3\gamma_1$  and  $\gamma_3 = 2\gamma_1$ . This procedure can be done at quartic order. On the other hand, clearly from the property of the antisymmetric tensor, one cannot construct such terms at quintic order or more higher orders. Since the original action of massive gravity should be constructed by  $g_{\mu\nu}$  and  $f_{\mu\nu}$  (or  $H_{\mu\nu}$ ), we should rewrite the total divergence combinations by using  $g_{\mu\nu}$  and  $f_{\mu\nu}$  without appearance of higher orders of  $\Pi_{\mu\nu}$ . So, we introduce a tensor  $\gamma^\mu{}_\nu := \sqrt{g^{\mu\rho} f_{\rho\nu}}$  defined by the relation

$$\sqrt{g^{\mu\rho} f_{\rho\sigma}} \sqrt{g^{\sigma\rho} f_{\rho\nu}} = g^{\mu\rho} f_{\rho\nu}. \quad (4.2.14)$$

In the case of (4.2.5), this square root of the matrix is explicitly given by

$$\sqrt{g^{\mu\rho} f_{\rho\nu}} \approx \delta^\mu{}_\nu + \frac{\Pi^\mu{}_\nu}{m^2 M_{\text{pl}}}. \quad (4.2.15)$$

Hence, the ghost-free nonlinear interactions would be given by

$$\mathcal{L}_{\text{GFNL}} = c_2 \mathcal{U}_2(\mathcal{K}) + c_3 \mathcal{U}_3(\mathcal{K}) + c_4 \mathcal{U}_4(\mathcal{K}), \quad (4.2.16)$$

which is nothing but the dRGT mass term, where  $\mathcal{K}^\mu{}_\nu$  is defined by (3.2.2). Note that, although we do not include a constant term  $\mathcal{U}_0(\mathcal{K})$  and a tadpole term  $\mathcal{U}_1(\mathcal{K})$  in order that the Minkowski spacetime is a vacuum solution, the ghost-free interactions can be extended to include them.

As a result, we have confirmed that the dangerous terms may appear below the scale  $\Lambda_3$  but they are absent in the ghost-free massive gravity. The dRGT interaction does not contain self-interactions of the scalar part  $\pi$ . However, the non-existence of the self-interaction of  $\pi$  leads to the vDVZ discontinuity in the Fierz-Pauli theory since the scalar part appears in the interaction between  $h_{\mu\nu}$  and  $\pi$  which cannot disappear even in the massless limit. We hope this interaction is screened when the nonlinear interactions are taken into account. Hence, we shall discuss the nonlinear interactions between  $h_{\mu\nu}$  and  $\pi$  in next section which interactions should be relevant to the screening of the fifth force.

### 4.3 $\Lambda_3$ decoupling limit

The dRGT theory is constructed by using the square root of the matrix which leads to a infinite order polynomial of  $H_{\mu\nu}$  as

$$\mathcal{K}^\mu{}_\nu = - \sum_{n=1}^{\infty} \bar{d}_n (H^n)^\mu{}_\nu, \quad (4.3.1)$$

with

$$\bar{d}_n = \frac{(2n)!}{(1-2n)(n!)^2 4^n}. \quad (4.3.2)$$

However, as shown in previous section, when we focus on only the scalar part, the matrix  $\mathcal{K}^\mu{}_\nu$  is simply given by a finite expression

$$\mathcal{K}_{\mu\nu}|_{h=A=0} = \frac{1}{m^2 M_{\text{pl}}} \Pi_{\mu\nu}. \quad (4.3.3)$$

In this section we discuss the interactions between the tensor part and the scalar part by taking, so called, the  $\Lambda_3$  decoupling limit [112] which also give a finite expression when we do not take into account the vector part [11].

The  $\Lambda_3$  decoupling limit is defined by the limit

$$M_{\text{pl}} \rightarrow \infty, \quad m \rightarrow 0, \quad \Lambda_3 := (m^2 M_{\text{pl}})^{1/3} : \text{finite}, \quad (4.3.4)$$

in which all interactions beyond the scale of  $\Lambda_3$  disappear. Relevant interactions in this limit are given by forms of  $h(\partial^2\pi)^\ell$  or  $(\partial A)^2(\partial^2\pi)^\ell$ . Since the vector part is decoupled from the tensor part in the  $\Lambda_3$  decoupling limit, only the tensor-scalar interactions seem to be important for the vDVZ discontinuity and the Vainshtein mechanism. Therefore, we only focus on the interactions of the form of  $h(\partial^2\pi)^\ell$ . The complete  $\Lambda_3$  decoupling limit including the vector part in the dRGT theory is shown in [113], and the  $\Lambda_3$  decoupling limit in the bigravity is discussed in [114].

Note that, as discussed later in §. 4.5.3, the scalar graviton is not sufficient to obtain a stable Vainshtein screening solution. The vector graviton should have an important role for the Vainshtein mechanism. However, since an explicit example of the Vainshtein screening solution including the vector graviton has not been found so far, the role of the vector graviton is not clear. In this and next sections, thus, we only consider the role of the scalar graviton for the Vainshtein mechanism. Nevertheless, the scalar graviton is worth noting for the Vainshtein mechanism.

Let us derive the interactions of the form of  $h(\partial^2\pi)^\ell$ . By using the relation

$$\left. \frac{\delta[\mathcal{K}^n]}{\delta h^{\mu\nu}} \right|_{h=A=0} = \frac{n}{2} \left( \frac{1}{\Lambda_3^{3(n-1)}} \Pi^{\mu\nu n-1} - \frac{1}{\Lambda_3^{3n}} \Pi^{\mu\nu n} \right), \quad (4.3.5)$$

we can obtain

$$\frac{\delta}{\delta h^{\mu\nu}} \sqrt{-g} \mathcal{L}(\mathcal{K}) \Big|_{h=A=0} = \frac{1}{2} \left( X_{\mu\nu}^{(1)} + \frac{\beta_2}{\Lambda_3^3} X_{\mu\nu}^{(2)} + \frac{\beta_3}{\Lambda_3^6} X_{\mu\nu}^{(3)} \right), \quad (4.3.6)$$

where we define

$$\begin{aligned} X_{\mu\nu}^{(1)} &= -\frac{1}{2!} \epsilon_{\mu}^{\alpha\beta\gamma} \epsilon_{\nu\alpha'\beta'\gamma} \Pi_{\alpha}^{\alpha'} \\ &= [\Pi] \eta_{\mu\nu} - \Pi_{\mu\nu}, \end{aligned} \quad (4.3.7)$$

$$\begin{aligned} X_{\mu\nu}^{(2)} &= -\frac{1}{2!} \epsilon_{\mu}^{\alpha\beta\gamma} \epsilon_{\nu\alpha'\beta'\gamma} \Pi_{\alpha}^{\alpha'} \Pi_{\beta'}^{\beta} \\ &= \frac{1}{2} \eta_{\mu\nu} ([\Pi]^2 - [\Pi^2]) + \Pi_{\mu\nu}^2 - [\Pi] \Pi_{\mu\nu}, \end{aligned} \quad (4.3.8)$$

$$\begin{aligned} X_{\mu\nu}^{(3)} &= -\frac{1}{3!} \epsilon_{\mu}^{\alpha\beta\gamma} \epsilon_{\nu\alpha'\beta'\gamma'} \Pi_{\alpha}^{\alpha'} \Pi_{\beta}^{\beta'} \Pi_{\gamma'}^{\gamma} \\ &= \frac{1}{6} ([\Pi]^3 - 3[\Pi][\Pi^2] + 2[\Pi^3]) - \Pi_{\mu\nu}^3 + [\Pi] \Pi_{\mu\nu}^2 - \frac{1}{2} ([\Pi]^2 - [\Pi^2]), \end{aligned} \quad (4.3.9)$$

and

$$\beta_2 = c_3 - 1, \quad \beta_3 = -(c_3 + c_4). \quad (4.3.10)$$

Then the effective action with the  $\Lambda_3$  decoupling limit is given by

$$\mathcal{L}_{\text{eff}} = -\frac{1}{4} h^{\mu\nu} \mathcal{E}_{\mu\nu,\alpha\beta} h^{\alpha\beta} - \frac{1}{2} h^{\mu\nu} \left( X_{\mu\nu}^{(1)} + \frac{\beta_2}{\Lambda_3^3} X_{\mu\nu}^{(2)} + \frac{\beta_3}{\Lambda_3^6} X_{\mu\nu}^{(3)} \right) + \frac{1}{2M_{\text{pl}}} h^{\mu\nu} T_{\mu\nu}. \quad (4.3.11)$$

Note that, although the interactions  $h(\partial^2\pi)^2$  or  $h(\partial^2\pi)^3$  seem to contain higher derivatives, the special combinations do not lead to any higher derivatives in the equation of motion. Indeed, the equation of motion of  $h_{\mu\nu}$  trivially contains up to section order derivatives, and the variation with respect to  $\pi$  gives

$$\begin{aligned} &M_{\text{pl}} \epsilon^{\alpha\beta\gamma\delta} \epsilon_{\mu\nu\rho\sigma} R^{(1)\mu\nu}_{\alpha\beta} \left( \delta^{\rho}_{\gamma} \delta^{\sigma}_{\delta} + \frac{2\beta_2}{\Lambda_3^3} \Pi^{\rho}_{\gamma} \delta^{\sigma}_{\delta} + \frac{\beta_3}{\Lambda_3^6} \Pi^{\rho}_{\gamma} \Pi^{\sigma}_{\delta} \right) \\ &= \epsilon^{\alpha\beta\gamma\delta} \epsilon_{\mu\nu\rho\sigma} \partial^{\mu} \left[ (\partial_{\beta} h^{\nu}_{\alpha} - \partial_{\alpha} h^{\nu}_{\beta}) \left( \delta^{\rho}_{\gamma} \delta^{\sigma}_{\delta} + \frac{2\beta_2}{\Lambda_3^3} \Pi^{\rho}_{\gamma} \delta^{\sigma}_{\delta} + \frac{\beta_3}{\Lambda_3^6} \Pi^{\rho}_{\gamma} \Pi^{\sigma}_{\delta} \right) \right] = 0, \end{aligned} \quad (4.3.12)$$

which does not contain third or more higher order derivatives, where

$$R^{(1)\mu\nu}_{\alpha\beta} = \frac{1}{M_{\text{pl}}} (\partial_{\mu} \partial_{[\beta} h_{\alpha]\nu} + \partial_{\nu} \partial_{[\alpha} h_{\beta]\mu}), \quad (4.3.13)$$

is the linearized Riemann curvature. Hence, this action is free from the Ostrogradski instability which is consistent with the BD ghost-freeness of the dRGT theory.

In the Fierz-Pauli theory, one can obtain an unmix action by taking a linearized conformal transformation in which the scalar-tensor interaction vanishes. In the dRGT theory, although it is possible to obtain an unmix action up to the cubic order by a field redefinition, the interaction  $hX^{(3)}$  cannot vanish. By performing the field redefinition as

$$h_{\mu\nu} = \tilde{h}_{\mu\nu} - \pi \eta_{\mu\nu} + \frac{\beta_2}{\Lambda_3^3} \partial_{\mu} \pi \partial_{\nu} \pi, \quad (4.3.14)$$

the action is rewritten as

$$\begin{aligned} \mathcal{L}_{\text{eff}} &= -\frac{1}{4} \tilde{h}^{\mu\nu} \mathcal{E}_{\mu\nu,\alpha\beta} \tilde{h}^{\alpha\beta} + \sum_{n=2}^5 \frac{\alpha_n}{\Lambda_3^{3(n-2)}} \mathcal{L}_n^{\text{gal}} - \frac{1}{2} \frac{\beta_3}{\Lambda_3^6} \tilde{h}^{\mu\nu} X_{\mu\nu}^{(3)} \\ &+ \frac{1}{2M_{\text{pl}}} \tilde{h}_{\mu\nu} \tilde{T}^{\mu\nu} - \frac{1}{2M_{\text{pl}}} \pi T + \frac{\beta_3}{2M_{\text{pl}} \Lambda_3^3} \partial_{\mu} \pi \partial_{\nu} \pi T^{\mu\nu}, \end{aligned} \quad (4.3.15)$$

where

$$\mathcal{L}_2^{\text{gal}} = -\frac{1}{2}(\partial\pi)^2, \quad (4.3.16)$$

$$\mathcal{L}_3^{\text{gal}} = -\frac{1}{2}(\partial\pi)^2[\Pi], \quad (4.3.17)$$

$$\mathcal{L}_4^{\text{gal}} = -\frac{1}{2}(\partial\pi)^2([\Pi]^2 - [\Pi^2]), \quad (4.3.18)$$

$$\mathcal{L}_5^{\text{gal}} = -\frac{1}{12}(\partial\pi)^2([\Pi]^3 - 3[\Pi][\Pi^2] + 2[\Pi^3]). \quad (4.3.19)$$

The dimensionless coefficients  $\alpha_n$  are given by

$$\alpha_2 = \frac{3}{2}, \quad (4.3.20)$$

$$\alpha_3 = \frac{3}{2}\beta_2, \quad (4.3.21)$$

$$\alpha_4 = \frac{1}{2}\beta_2^2 - 2\beta_3, \quad (4.3.22)$$

$$\alpha_5 = -15\beta_2\beta_3. \quad (4.3.23)$$

One can see that the action contains nonlinear derivative interactions of the scalar graviton  $\pi$  which are important for the Vainshtein mechanism discussed in next section.

Note that the terms  $\mathcal{L}_n, hX^{(n)}$  are called Galileon interactions since they are invariant under a Galilean like transformation for the field as

$$\pi \rightarrow \pi + c + v_\mu x^\mu, \quad (4.3.24)$$

with a constant  $c$  and a constant vector  $v_\mu$ . The Galieon type interactions were originally introduced in Ref. [115] as a generalization of the decoupling limit of the Dvali-Gabadadze-Porrati (DGP) theory [116–118]. The generalization of the Galileon scalar field including the gravity leads to the general scalar-tensor theories, called the Horndeski theory and beyond Horndeski theories [119–125]. The Horndeski theory is the most general scalar-tensor theory with the equations of motion up to second order derivatives, while beyond Horndeski theories are more general scalar-tensor theories with higher order derivative equations of motion but without the Ostrogradski instability. Clearly from that the effective action of the massive gravity is reduced into the Galileon type scalar-tensor theory, the Vainshtein mechanism has an important role not only in the massive gravity but also in some classes of the scalar-tensor theories which have non-linear second order derivative interactions. For example, the effective theory of the Horndeski theory for the Vainshtein mechanism around the Minkowski spacetime is given by

$$\mathcal{L}_H = -\frac{1}{4}h^{\mu\nu}\mathcal{E}_{\mu\nu,\alpha\beta}h^{\alpha\beta} + \sum_{n=2}^5 \frac{\tilde{\alpha}_n}{\Lambda^{3(n-2)}}\mathcal{L}_n^{\text{gal}} - \frac{1}{2}\sum_{n=1}^3 \frac{\tilde{\beta}_n}{\Lambda^{3(n-1)}}h^{\mu\nu}X_{\mu\nu}^{(n)} + \frac{1}{2M_{\text{pl}}}h_{\mu\nu}T^{\mu\nu}, \quad (4.3.25)$$

where  $\Lambda$  gives the strong coupling scale and the coefficients  $\tilde{\alpha}_n$  and  $\tilde{\beta}_n$  are determined by the Horndeski action [126] (see [127–129] for effective theories for the Vainshtein mechanism around a cosmological background).

## 4.4 Vainshtein mechanism

The Vainshtein mechanism is a mechanism to screen the fifth force mediated by the scalar field by nonlinear second order derivative interactions. In the linear theory, the field profile of the scalar field with a point source is proportional to  $r^{-1}$  and then the second order derivative of the scalar field is typically proportional to  $r^{-3}$  where  $r$  is the distance from the source. Since  $\partial^2\pi$  becomes larger near the source (it increases faster than other type interactions such as the first derivative interactions or the non-derivative interactions), the nonlinear second order derivative interactions

could dominate over the linear terms inside some radius, called the Vainshtein radius. As already mentioned in Section 2.2, in the massive gravity, the Vainshtein radius is given by

$$r_V = \left( \frac{GM}{m^2} \right),$$

where  $M$  is the gravitational mass of the source. The typical value of the Vainshtein radius is about  $10^{20}$  cm for the sun with the cosmological scale graviton mass. The Vainshtein mechanism in massive gravity and bigravity has been discussed in [63–79, 81, 82, 85].

Since the nonlinear interactions are important for the Vainshtein mechanism, one cannot use perturbative expansions and one has to take into account full nonlinear orders to discuss the Vainshtein mechanism. The massive gravity contains the infinite number of interactions although they can be resummed as finite terms by using the square root of the matrix. Therefore, the general discussion for the Vainshtein mechanism is too difficult to analyze it. However, as shown in the previous section, the massive gravity can be reduced to the finite order expression by taking the  $\Lambda_3$  decoupling limit without the vector graviton. The effective action is given by a scalar-tensor theory with Galileon type interactions which would be relevant to the Vainshtein mechanism. In what follows, thus, we will discuss the Vainshtein mechanism based on a Galileon scalar theory.

We thus consider the cubic Galileon theory

$$\mathcal{L} = -\frac{1}{2}(\partial\pi)^2 - \frac{1}{\Lambda^3}(\partial\pi)^2\Box\pi + \frac{1}{M_{\text{pl}}}\pi T, \quad (4.4.1)$$

where  $T$  is the trace of the energy-momentum tensor of the source. The constant  $\Lambda$  gives the strong coupling scale which controls the energy scale of the nonlinear interaction. As mentioned above, the Galileon interaction  $(\partial\pi)^2\Box\pi$  will dominate over the standard kinetic term  $(\partial\pi)^2$  close to the source with  $\partial^2\pi \gg \Lambda^3$ . Hence one cannot use perturbative expansions around  $\pi = 0$ . However, it is possible to use the perturbation around some background configuration. When we split the energy-momentum tensor into a background contribution  $T_0$  and a perturbation  $\delta T$  with  $T_0 \gg \delta T$ , the scalar field is also split into a background configuration  $\pi_0$  and a perturbation  $\phi$  as

$$\pi = \pi_0 + \phi. \quad (4.4.2)$$

The quadratic action for the perturbation  $\phi$  is then

$$\mathcal{L}_2 = -\frac{1}{2}Z^{\mu\nu}(\pi_0)\partial_\mu\phi\partial_\nu\phi + \frac{1}{M_{\text{pl}}}\phi\delta T \quad (4.4.3)$$

where the effective metric  $Z^{\mu\nu}$  is give by

$$Z^{\mu\nu} := \eta^{\mu\nu} + \frac{1}{\Lambda^3}X^{(1)\mu\nu}(\pi_0). \quad (4.4.4)$$

Note that the effective metric is symbolically  $Z \sim 1 + \partial^2\pi_0/\Lambda^3$ . Hence, while the effective metric is order unity in the linear regime ( $\partial^2\pi_0 \ll \Lambda^3$ ), the effective metric has a large value in the nonlinear regime ( $\partial^2\pi_0 \gg \Lambda^3$ ).

The idea of the screening is that the effective coupling between the scalar field and the matter is suppressed by the background configuration of the scalar field. The canonically normalized perturbation of the scalar field is given by

$$\tilde{\phi} = \sqrt{Z}\phi, \quad (4.4.5)$$

where  $Z$  is a constant to express the typical value of  $Z^{\mu\nu}$  in some local region. In terms of the normalized field, the action is

$$\mathcal{L}_2 = -\frac{1}{2}\frac{Z^{\mu\nu}}{Z}\partial_\mu\tilde{\phi}\partial_\nu\tilde{\phi} + \frac{1}{M_{\text{eff}}}\tilde{\phi}\delta T, \quad (4.4.6)$$

where the effective coupling constant to the matter is defined by

$$M_{\text{eff}} := \sqrt{Z}M_{\text{pl}}. \quad (4.4.7)$$

In the linear regime  $Z \sim 1$ , the effective coupling constant recovers the original coupling constant. However, the energy scale of the effective coupling becomes higher than the original one in the nonlinear regime  $Z \gg 1$  which leads to the coupling to the matter is suppressed. Hence the effective coupling to the matter depends on the configuration of the background and it can be screened in the nonlinear regime. In particular, the strong coupling scale  $\Lambda$  is related to the graviton mass as  $\Lambda = (m^2 M_{\text{pl}})^{1/3}$ , the massless limit  $m \rightarrow 0$  leads to  $Z \rightarrow \infty$  which means the coupling to the matter vanishes.

Another importance of the Vainshtein mechanism is that the strong coupling scale also depends on the background configuration. In terms of the canonical normalized perturbation, the full action is given by

$$\mathcal{L} = -\frac{1}{2} \frac{Z^{\mu\nu}}{Z} \partial_\mu \tilde{\phi} \partial_\nu \tilde{\phi} - \frac{1}{\Lambda_{\text{eff}}^3} (\partial \tilde{\phi})^2 \square \tilde{\phi} + \frac{1}{M_{\text{eff}}} \tilde{\phi} \delta T, \quad (4.4.8)$$

where the effective strong coupling scale is

$$\Lambda_{\text{eff}} := \sqrt{Z} \Lambda. \quad (4.4.9)$$

Hence the strong coupling scale rises in  $Z \gg 1$  which implies that the lowest energy scale of the theory turns to the scale  $\Lambda_{\text{eff}}$  instead of  $\Lambda$  inside the Vainshtein radius and then there exists another decoupling limit associated with the new scale  $\Lambda_{\text{eff}}$ . Indeed, we will introduce another decoupling limit, called the  $\Lambda_2$  decoupling limit recently proposed by [83, 84] in next section. As discussed in our paper [86], the  $\Lambda_2$  decoupling limit around a curved spacetime gives an effective action inside the Vainshtein radius in which the Vainshtein mechanism is already implemented.

So far, we have included only the self-interaction of the scalar field. However, the massive gravity contains the interactions as  $hX^{(n)}$ . Specifically, one cannot obtain the unmixed action of the scalar and the tensor fields even taking the field redefinition when  $hX^{(3)}$  is included. The existence of the mixing terms gives a qualitatively different effect from the self-interactions of the scalar field. For completeness, we consider the general action (4.3.25). The case of the massive gravity is obtained when  $\tilde{\alpha}_n = 0$  and  $\Lambda = (m^2 M_{\text{pl}})^{1/3}$ . Similarly to above discussion, the energy-momentum tensor, the scalar field, and the tensor field are split into background quantities and perturbations. Note that the linearized Einstein equation is given by

$$\mathcal{E}_{\mu\nu, \alpha\beta} h_0^{\alpha\beta} + \sum_{n=1}^3 \frac{\tilde{\beta}_n}{\Lambda^{3(n-1)}} X_{\mu\nu}^{(n)}(\pi_0) = \frac{1}{M_{\text{pl}}} T_{0\mu\nu}, \quad (4.4.10)$$

where  $h_0^{\mu\nu}$ ,  $\pi_0$ , and  $T_{0\mu\nu}$  are background quantities. To obtain a successful Vainshtein screening, the contributions from the scalar field to the Einstein equation should be sub-dominant. Hence, the metric perturbation and the scalar field should satisfy the following inequalities:

$$\partial^2 h_0 \gg \partial^2 \pi_0, \quad \frac{1}{\Lambda^3} (\partial^2 \pi_0)^2, \quad \frac{1}{\Lambda^6} (\partial^2 \pi_0)^3. \quad (4.4.11)$$

These inequalities lead to that when the scale of the scalar field reaches the strong coupling scale, i.e.,  $\partial^2 \pi_0 \sim \Lambda^3$ , the tensor field should satisfy the inequality

$$\partial^2 h_0 \gg \Lambda^3. \quad (4.4.12)$$

The quadratic Lagrangian for the scalar fluctuation is then

$$\mathcal{L}_2 = -\frac{1}{2} (Z_{\text{gal}}^{\mu\nu} + Z_h^{\mu\nu}) \partial_\mu \phi \partial_\nu \phi + \mathcal{O}(\delta h \partial^2 \delta \phi), \quad (4.4.13)$$

where

$$Z_{\text{gal}}^{\mu\nu} = \tilde{\alpha}_2 \eta^{\mu\nu} + \sum_{n=1}^3 \frac{\tilde{\alpha}_{n+2}}{\Lambda^{3n}} X^{(n)\mu\nu}(\pi_0), \quad (4.4.14)$$

$$Z_h^{\mu\nu} = -\frac{M_{\text{pl}}}{4\Lambda^3} \epsilon^{\mu\alpha\beta\gamma} \epsilon^{\nu\alpha'\beta'\gamma'} R^{(1)\alpha'\beta'}_{\alpha\beta}(h_0) \left( \tilde{\beta}_2 \delta^{\gamma'}_{\gamma} + \frac{\tilde{\beta}_3}{\Lambda^3} \Pi^{\gamma'}_{\gamma}(\pi_0) \right). \quad (4.4.15)$$

Note that the kinetic mixing just gives a negligible contribution for the scalar field when the Vainshtein mechanism works, i.e.,  $Z_{\text{gal}} \gg 1$  or  $Z_h \gg 1$ . The inequalities (4.4.11) and (4.4.12) suggest

$$Z_{\text{gal}}^{\mu\nu} \ll Z_h^{\mu\nu}, \quad (4.4.16)$$

thus the contributions from the self-interactions are also sub-dominant. We note that, when  $\tilde{\beta}_3 = 0$ , the matrix  $Z_h^{\mu\nu}$  is comparable to  $Z_{\text{gal}}^{\mu\nu}$  in vacuum region since the Einstein equation gives

$$Z_h^{\mu\nu} = -\frac{M_{\text{pl}}\tilde{\beta}_2}{\Lambda^3}G_{\mu\nu}^{(1)}(h_0) = \tilde{\beta}_2 \sum_{n=1}^2 \frac{\tilde{\beta}_n}{\Lambda^{3n}} X^{(n)}(\pi_0),$$

where  $G_{\mu\nu}^{(1)}$  is the linearized Einstein tensor. Hence, the self-interactions give non-negligible contributions in vacuum region when  $\tilde{\beta}_3 = 0$ . However, the case of  $\tilde{\beta}_3 \neq 0$ , the self-interactions can be ignored and then the effective metric is approximated by  $Z_h^{\mu\nu}$ . In this case,  $\partial^2\pi_0 \gg \Lambda^3$  is not necessary to obtain  $Z_h \gg 1$ . The inequality  $M_{\text{pl}}R^{(1)}(h_0) \sim \partial^2 h_0 \gg \Lambda^3$  gives a large value of the effective metric  $Z_h^{\mu\nu}$  even when

$$\partial^2\pi_0 \sim \Lambda^3. \quad (4.4.17)$$

The curvature is typically  $R^{(1)} \sim GM/r^3$  for the point source then  $M_{\text{pl}}R^{(1)}(h_0) \gg \Lambda^3$  is realized in the region

$$r \ll \left(\frac{M_{\text{pl}}}{\Lambda^3}GM\right)^{1/3}, \quad (4.4.18)$$

which is nothing but the space region inside the Vainshtein radius of the massive gravity  $r_V := (GM/m^2)^{1/3}$  when  $\Lambda = (m^2 M_{\text{pl}})^{1/3}$ .

Furthermore, the fact that the nonlinear interactions should be included in  $R \gg m^2$  suggests something about the Higuchi instability. The Higuchi instability occurs when the universe satisfies  $R \sim H^2 \gtrsim m^2$ . When the scalar graviton grows exponentially due to the Higuchi instability, all relevant nonlinear interactions have to be taken into account when the scalar graviton reaches  $\partial^2\pi \sim \Lambda_3^3$ . Then, the scalar graviton may condense into the value  $\partial^2\pi \sim \Lambda_3^3$ . If this scenario is possible, the Higuchi instability does not affect any observable quantities since the Vainshtein mechanism screens all effects from the scalar graviton. Therefore, the Higuchi instability does not spoil a successful background dynamics if the ‘‘cosmological’’ Vainshtein mechanism works. In Chapter 6, we will discuss whether such a condensation state exists in a simple set up.

## 4.5 $\Lambda_2$ decoupling limit

Although the lowest strong coupling scale of the dRGT theory is  $\Lambda_3$  around the Minkowski vacuum, as discussed in previous section, the lowest scale can rise when the Vainshtein mechanism works. Therefore, there would be another decoupling limit associated with the new scale around a non-trivial background in which there may exist a smooth GR limit. In this section, we consider the  $\Lambda_2$  decoupling limit proposed by [83,84] which considered the limit around a non-trivial Minkowski background in which there exists a smooth GR limit where the Stüeckelberg fields have some non-trivial expectation value

$$g_{\mu\nu} = \eta_{\mu\nu} + \mathcal{O}(m^2), \quad \phi^a = \bar{\phi}^a(x) \neq x^a. \quad (4.5.1)$$

Our paper [86] extended the  $\Lambda_2$  decoupling limit around the Minkowski one to the limit around a curved one in which an effective theory inside the Vainshtein radius can be obtained.

Before discussing the Vainshtein mechanism in  $\Lambda_2$  decoupling limit, let us consider a simple case with a smooth GR limit. An example of a massive gravity with a smooth GR limit is the Fierz-Pauli theory defined on AdS spacetime as mentioned in Section 2.4. Around the AdS background, the scalar graviton gets a kinetic term due to the curvature of the AdS spacetime. While the strong

coupling scale of the scalar graviton is  $\Lambda_3 := (m^2 M_{\text{pl}})^{1/3}$  around the Minkowski spacetime, the strong coupling scale rises to  $\Lambda_* := (m M_{\text{pl}}/L)^{1/3}$  when  $L^{-1} \gg m$  where  $L$  is the AdS radius. This increasing of the strong coupling scale is similar to that in the Vainshtein mechanism. Indeed, as shown in Section 2.4, the Fierz-Pauli theory on AdS spacetime has no vDVZ discontinuity and then there exists a smooth GR limit due to the increasing of the strong coupling scale.

A difference between the Minkowski background and a curved background is that the vector graviton gets the mass term as  $R_{\mu\nu} A^\mu A^\nu$ . When the vector graviton has no mass term, the longitudinal mode of the vector is just a gauge mode. Therefore, the interactions between the scalar graviton and the tensor graviton must remain to keep the degree of freedom of the scalar graviton in the case of Fierz-Pauli theory on the Minkowski background. On the other hand, the longitudinal mode is a physical mode when there is a mass term and the scalar Stüeckelberg field is not necessary to be introduced. The Fierz-Pauli mass term on a curve spacetime is then

$$\mathcal{L}_{\text{FP,AdS}} = -\frac{m^2}{8}(h_{\mu\nu}h^{\mu\nu} - h^2) - \frac{1}{8}F_{\mu\nu}F^{\mu\nu} + \frac{1}{2}R_{\mu\nu}A^\mu A^\nu - \frac{m}{2}(h^{\mu\nu}\nabla_\mu A_\nu - h\nabla_\mu A^\mu). \quad (4.5.2)$$

The limit  $m \rightarrow 0$  is a smooth limit since the gauge breaking term  $R_{\mu\nu}A^\mu A^\nu$  remains. Furthermore, the limit cuts the interactions between the tensor one and the vector one. Therefore, the limit  $m \rightarrow 0$  gives a smooth GR limit if  $R_{\mu\nu}A^\mu A^\nu$  does not produce any instability (e.g., the AdS background).

Let us, then, consider the case of the dRGT mass term when the vector Stüeckelberg field is introduced but the scalar Stüeckelberg field is not introduced around some appropriate background. In this situation the scale  $\Lambda_3$  does not appear since the interactions with the scale  $\Lambda_3$  arise from interactions between the scalar mode and other modes. The scalar mode is encoded in the vector graviton as the longitudinal mode, so we have only self-interactions of the vector graviton or interactions between the tensor graviton and the vector graviton. Then the interactions are

$$\mathcal{L}_{\text{dRGT}} = \sum_{j,k} \Lambda_{j,k}^{-(j+2k+4\ell-4)} R_0^\ell h^j (\partial A)^k A^{2\ell}, \quad (4.5.3)$$

with

$$\Lambda_{j,k} = \left( m^{k+2\ell-2} M_{\text{pl}}^{j+k+2\ell-2} \right)^{1/(j+2k+4\ell-4)}. \quad (4.5.4)$$

and  $R_0$  represents the scale of the background curvature. Note that, up to quadratic order with  $R_0 = 0$ , i.e., the case of the Fierz-Pauli mass term, the interactions are

$$\mathcal{L}_{\text{FP}} = -\frac{m^2}{8}(h_{\mu\nu}h^{\mu\nu} - h^2) - \frac{1}{8}F_{\mu\nu}F^{\mu\nu} - \frac{m}{2}(h^{\mu\nu}\partial_\mu A_\nu - h\partial_\mu A^\mu). \quad (4.5.5)$$

The gauge breaking terms  $h\partial A$  vanish in the limit with  $m \rightarrow 0$ , thus, the scalar degrees of freedom is lost in the Fierz-Pauli case. However, nonlinear self-interactions of the vector graviton ( $j = 0, k \geq 3$ ) or the coupling to the curvature ( $j = 0, \ell \geq 1$ ), which may break the gauge invariance of the vector mode, have the scale  $\Lambda_2$  and then they remain in the  $\Lambda_2$  decoupling limit defined by

$$m \rightarrow 0, \quad M_{\text{pl}} \rightarrow \infty, \quad \Lambda_2 := (m M_{\text{pl}})^{1/2} : \text{finite}. \quad (4.5.6)$$

In the same limit, the couplings to the tensor mode ( $j \geq 1$ ) vanishes. Since the vDVZ discontinuity is caused by the existence of the coupling to the tensor graviton, the disappearance of such interactions leads to no vDVZ discontinuity. The  $\Lambda_2$  decoupling limit cuts the coupling to the tensor one, but it keeps the gauge breaking terms of the vector one. The  $\Lambda_2$  decoupling limit, thus, gives a smooth GR limit keeping correct degrees of freedom.

After the  $\Lambda_2$  decoupling limit the strong coupling scale of the scalar mode is no longer  $\Lambda_3$ . The scalar mode appears in the nonlinear interactions of the vector mode or in the coupling to the curvature. The strong coupling scale must depend on the expectation value of the vector mode or the scale of the curvature. To make the action after the  $\Lambda_2$  decoupling limit a viable effective theory, the new strong coupling scale has to be greater than  $\Lambda_3$ . For instance, the strong coupling scale around the AdS background is given by  $\Lambda_* = (m M_{\text{pl}}/L)^{1/3} \sim (m M_{\text{pl}} \sqrt{R})^{1/3}$  which is clearly greater than  $\Lambda_3$  in the  $\Lambda_2$  decoupling limit. Conversely, the  $\Lambda_2$  decoupling limit may give a viable



effective theory when  $R \gg m^2$  in which the strong coupling scale of the scalar mode would be higher than  $\Lambda_3$ . Since interior regions of the Vainshtein radius mean  $R \gg m^2$ , the  $\Lambda_2$  decoupling limit may give an effective theory inside the Vainshtein radius.

In what follow we discuss the  $\Lambda_2$  decoupling limit around some non-trivial background in the dRGT massive gravity and the bigravity. The tensor modes are decoupled from other modes by taking the  $\Lambda_2$  decoupling limit. Then the action for the tensor mode is given by that in GR, while the effective action for the Stückelberg fields is given by called the massive gravity nonlinear sigma model where the degrees of freedom of the scalar and the vector gravitons are encoded in four scalar fields. In particular, the  $\Lambda_2$  decoupling limit around a curved background gives an effective theory inside the Vainshtein radius.

### 4.5.1 Non-compact nonlinear sigma model

Nonlinear sigma models are effective theories obtained from various areas of physics [130, 131] which map from a base manifold to a target space. A typical action of a nonlinear sigma model is given by

$$S_{\text{NLSM}} = - \int d^4x \frac{1}{2} \eta^{\mu\nu} \partial_\mu \phi^a \partial_\nu \phi^b f_{ab}(\phi), \quad (4.5.7)$$

where  $f_{ab}$  is the target space metric and  $\phi^a$  are scalar fields. If the target space metric has a Lorentzian signature  $(-, +, \dots, +)$ , the minus sign leads to a ghost mode in one of  $\phi^a$ . Hence, to avoid an existence of a ghost degree of freedom, the target space metric of nonlinear sigma models should be positive definite. This requirement translates to the isometry group to be compact if the target space has some symmetry.

An exception of a nonlinear sigma model with a Lorentzian signature is the  $p$ -brane Nambu-Goto action

$$S_{\text{NG}} = - \frac{T_p}{2} \int d^{p+1}x \sqrt{-\det(\partial_\mu \phi^a \partial_\nu \phi^b f_{ab}(\phi))}, \quad (4.5.8)$$

where  $f_{ab}$  is a Lorentzian metric. The action has  $p + 1$  diffeomorphism along the brane world-volume which makes the (would-be) ghost mode a gauge mode. Hence, the (would-be) ghost degree of freedom is eliminated by first class constraints in the Nambu-Goto action.

The paper [83] pointed out that one can construct nonlinear sigma models with a Lorentzian target space in which the (would-be) ghost degree of freedom is eliminated by second class constraints. This class of “non-compact” nonlinear sigma models are given by

$$S_{\text{NLSM}} = \int d^Dx \sum_{n=1}^D b_n(\phi) \gamma^{\mu_1}_{[\mu_1} \gamma^{\mu_2}_{\mu_2} \cdots \gamma^{\mu_n}_{\mu_n]}, \quad (4.5.9)$$

where  $b_n(\phi^a)$  are arbitrary functions of  $\phi^a$  and  $\gamma^\mu_\mu$  is the square root of the matrix for  $N \geq D$  defined by

$$\gamma^\mu_\rho \gamma^\rho_\nu = g^{\mu\rho}(x) \partial_\mu \phi^a \partial_\nu \phi^b f_{ab}(\phi), \quad (4.5.10)$$

with a Lorentzian metric  $f_{ab}(\phi)$  and  $a = 0, 1, \dots, N - 1$ . Although the action is constructed by  $N$  scalar fields, this class of nonlinear sigma models just has  $N - 1$  degrees of freedom in general [84]. In particular, we call the cases  $D = N$  the massive gravity nonlinear sigma models since the action is related with the dRGT mass term where  $f_{ab}$  and  $\phi^a$  are recognized as the fiducial metric and the Stückelberg fields, respectively. Note that, in the non-compact nonlinear sigma models, the spacetime metric  $g_{\mu\nu}$  is not a dynamical field. The action just describes motions of  $\phi^a$ .

Let us focus on the massive gravity nonlinear sigma model with  $D = N = 4$  and  $b_n$  are constant. In this case, the action of the massive gravity nonlinear sigma model is nothing but the dRGT mass term in four dimensions. The massive gravity nonlinear sigma model has three degrees of freedom. On the other hand, the dRGT theory in four dimensions has five degrees of freedom: two tensor modes, two vector modes, and one scalar mode. Two additional degrees of freedom must come from the Einstein-Hilbert action so must be tensor degrees of freedom. Hence, the dRGT

mass term itself has scalar and vector degrees of freedom which is consistent with the previous discussion. This is one important difference from the Fierz-Pauli mass term since the scalar degree of freedom appears as coupling to the tensor degree of freedom in Fierz-Pauli mass term. The dRGT mass term carries the scalar and the vector degrees of freedom even if the tensor ones are not dynamical. Note that, however, the self-interactions of the scalar one are total divergence terms and the scalar-vector interaction does not appear at quadratic order in dRGT mass term around the Minkowski background. Hence, the scalar graviton is strong coupled around the trivial background

$$g_{\mu\nu} = \eta_{\mu\nu}, \quad \phi^a = x^a, \quad (4.5.11)$$

when the couplings to tensor modes are ignored. To avoid the strong coupling, it should be necessary that the Stückelberg fields have some non-trivial expectation value, or that the metric is curved. The papers [83,84] considered the case of the non-trivial Minkowski background (4.5.1) in which the vector modes are nonlinearly excited. On the other hand, our paper [86] discussed the case of a curved metric in which the scalar graviton is not strong coupled without vector excitations but the scalar graviton has an instability around a Ricci flat spacetime.

### 4.5.2 Effective action inside the Vainshtein radius

In this subsection, we show that massive gravity nonlinear sigma model gives an effective theory of the vector and scalar gravitons inside the Vainshtein radius for general massive/bi-gravity as long as we have the Vainshtein screening solutions. The results shown in this and next subsections are based on our paper [86].

Let us start with the bigravity action (3.3.1) and (3.3.3). Notice that our set-up of the bigravity is so general that it includes ghost-free massive gravity [11, 12] as a special case. It is obtained by fixing  $f$ -spacetime as the Minkowski one with the limit  $\kappa_f \rightarrow 0$  [132].

In what follows we set  $c_0 = c_1 = 0$  and  $c_2 = -1^1$ . We also introduce four Stückelberg fields  $\phi^a(x)$ , with which the metric  $f_{\mu\nu}$  can be written by

$$f_{\mu\nu}(x) = \frac{\partial\phi^a}{\partial x^\mu} \frac{\partial\phi^b}{\partial x^\nu} f_{ab}(\phi^a(x)), \quad (4.5.12)$$

to see the dynamics of the vector and scalar gravitons in a clear way.

It was shown in Refs. [83,84] that in the case of ghost-free massive gravity, about non-trivial vacua

$$g_{\mu\nu} = \eta_{\mu\nu} + \mathcal{O}(m^2), \quad \phi^a = \bar{\phi}^a(x) \neq x^a, \quad (4.5.13)$$

and in the  $\Lambda_2$  decoupling limit, given by

$$m, \kappa_g, \kappa_f \rightarrow 0, \quad \Lambda_2 \equiv \sqrt{m/\kappa_g} : \text{finite}, \quad (4.5.14)$$

an interesting effective theory for  $\phi^a$ , so-called the massive gravity nonlinear sigma model described by the following action

$$S_{\text{MG-NLS}}^{(0)} = -\Lambda_2^4 \int d^4x \sqrt{-\eta} \sum_{n=2}^4 c_n \mathcal{U}_n(\gamma_{\text{NLS}}), \quad (4.5.15)$$

$$\gamma_{\text{NLS}}{}^\mu{}_\rho \gamma_{\text{NLS}}{}^\rho{}_\nu = \eta^{\mu\rho}(x) \frac{\partial\phi^a}{\partial x^\rho} \frac{\partial\phi^b}{\partial x^\nu} \eta_{ab}(\phi). \quad (4.5.16)$$

is obtained.

One interesting property of this massive gravity nonlinear sigma model is that its strong coupling scale is given by  $\Lambda_2$ . This is higher than  $\Lambda_3 \equiv (m^2/\kappa_g)^{1/3}$  coming from the analysis around

<sup>1</sup>In general, the ghost-free interactions include a constant term  $\mathcal{U}_0$  and a tadpole term  $\mathcal{U}_1(\mathcal{K})$ . Although we drop them here, just for simplicity, including these terms does not change our main conclusion.

the trivial vacuum  $g_{\mu\nu} = \eta_{\mu\nu}$ ,  $\phi^a = x^a$ . Another interesting property is that the vector and scalar modes of graviton encoded in  $\phi^a$  decouple with matter fields even in the linear regime, which does not give vDVZ discontinuity and the Vainshtein mechanism is implemented automatically.

This suggests that as long as the Vainshtein screening works, even we start with more general set-up described by Eq. (3.3.1), that is, not limiting  $g_{\mu\nu}$  and  $f_{ab}$  to flat, not neglecting the  $f$ -matter fields, we can expect that the massive gravity nonlinear sigma model is obtained as an effective theory inside the Vainshtein radius. Actually, if the Vainshtein mechanism is working, the metrics can be expressed by

$$g_{\mu\nu} = g_{\mu\nu}^{\text{GR}} + \kappa_g \delta g_{\mu\nu}, \quad (4.5.17)$$

$$f_{ab} = f_{ab}^{\text{GR}} + \kappa_f \delta f_{ab}, \quad (4.5.18)$$

where  $g_{\mu\nu}^{\text{GR}}$  and  $f_{ab}^{\text{GR}}$  are solutions in GR with the matter actions  $S_g^{[\text{m}]}$  and  $S_f^{[\text{m}]}$ , respectively, and  $\delta g_{\mu\nu}$  and  $\delta f_{ab}$  should be treated as perturbations. Here,  $g_{\mu\nu}^{\text{GR}}(x)$  and  $f_{ab}^{\text{GR}}(\phi)$  are determined as functions of  $x^\mu$  and  $\phi^a$ , respectively, from which we can regard that  $g_{\mu\nu}^{\text{GR}}$  and  $f_{ab}^{\text{GR}}$  act as external forces. Then with the undetermined variables  $\phi^a, \delta g_{\mu\nu}, \delta f_{ab}$ , the action can be expanded as

$$S = S_{\text{GR}}(\delta g) + S_{\text{GR}}(\delta f) + S_{\text{MG-NLS}}(\phi^a; g^{\text{GR}}, f^{\text{GR}}) + \Lambda_2^4 \mathcal{O}(\kappa_g \delta g, \kappa_f \delta f). \quad (4.5.19)$$

where  $S_{\text{GR}}$  are the perturbed actions for the metric perturbations which are same as those in GR.  $S_{\text{MG-NLS}}$  is the action of the massive gravity nonlinear sigma model given by

$$S_{\text{MG-NLS}} = -\Lambda_2^4 \int d^4x \sqrt{-g_{\text{GR}}} \sum_{n=2}^4 c_n \mathcal{U}_n(\gamma_{\text{NLS}}), \quad (4.5.20)$$

which generalizes Eq. (4.5.20) with the following replacements:

$$\kappa_g \rightarrow \kappa, \quad \eta_{\mu\nu} \rightarrow g_{\mu\nu}^{\text{GR}}, \quad \eta_{ab} \rightarrow f_{ab}^{\text{GR}}. \quad (4.5.21)$$

One may worry that the tadpole terms of the metric perturbations give the backreaction from the Stüeckelberg fields to the spacetimes. Since the background spacetimes are given by the solutions in GR, they appear only through the interaction terms between the Stüeckelberg fields and the metric perturbations of order  $\Lambda_2^4 \mathcal{O}(\kappa_g \delta g, \kappa_f \delta f)$ . However, by taking the  $\Lambda_2$  decoupling limit given by Eq. (4.5.14), the contributions from the tadpole terms are negligible and then the Stüeckelberg fields and the metric perturbations are decoupled. Then, in this limit the Stüeckelberg fields are simply determined by the massive gravity nonlinear sigma model (4.5.20) and the spacetimes are completely same as those in GR. Therefore the massive gravity nonlinear sigma model with curved metrics is the effective action of the Stüeckelberg fields as long as the Vainshtein mechanism works and we have the same solutions as in GR.

Indeed, the Vainshtein screening solutions can be obtained by this effective action with curved metrics. The Vainshtein mechanism for the static and spherically symmetric spacetime is found with the interior and the exterior Schwarzschild metrics [85] (see also [79, 82]) and the cosmological Vainshtein mechanism is found with the Friedmann-Lemaître-Robertson-Walker metric [63]. Although we denoted the procedure of the  $\Lambda_2$  decoupling limit just as the massless limit in these papers, the limits used in [63, 85] are equivalent to the  $\Lambda_2$  decoupling limit shown above.

### 4.5.3 No-go result of stable background without vector excitation

In this section, we show that the scalar graviton generally suffers from a ghost and/or a gradient instability when there is no vector graviton excitation in the massive gravity nonlinear sigma model. For simplicity, we do not introduce the  $f$ -matter fields here thus we can assume  $f_{ab}^{\text{GR}}$  is the Minkowski spacetime. In this case, the Stüeckelberg field can be split as  $\phi^a = \delta_\mu^a(x^\mu + \pi^\mu)$ , then  $f_{\mu\nu}$  is expressed by

$$f_{\mu\nu} = \eta_{\mu\nu} + 2\partial_{(\mu}\pi_{\nu)} + \partial_\mu\pi_\alpha\partial_\nu\pi^\alpha, \quad (4.5.22)$$

where  $\pi_\mu$  is a vector field on the Minkowski spacetime. Furthermore, to see the existence of the instability, we assume a weak gravitational field and ignore the vector graviton excitation:

$$g_{\mu\nu}^{\text{GR}} = \eta_{\mu\nu} + h_{\mu\nu}^{\text{GR}}, \quad (4.5.23)$$

$$\pi_\mu = \partial_\mu \pi. \quad (4.5.24)$$

Note that we do not normalize the scalar graviton  $\pi$  to be mass dimension one in this subsection since the strong coupling scale of the scalar mode cannot be fixed.

In a similar way to the  $\Lambda_3$  decoupling limit, the action can be expanded as

$$\mathcal{L}_{\text{MG-NLS}} = -\frac{\Lambda_2^4}{2} h^{\text{GR} \mu\nu} \left( X_{\mu\nu}^{(1)} + \beta_2 X_{\mu\nu}^{(2)} + \beta_3 X_{\mu\nu}^{(3)} \right) + \mathcal{O}(h_{\text{GR}}^2). \quad (4.5.25)$$

Note that, differently from the case of  $\Lambda_3$  decoupling limit,  $h_{\mu\nu}^{\text{GR}}$  has been already fixed and it acts as an external force for the field  $\pi$ .

The field  $\pi$  can be split into the background configuration  $\bar{\pi}$  and the perturbation  $\delta\pi$  as

$$\pi = \bar{\pi} + \delta\pi, \quad (4.5.26)$$

with  $\delta\pi \ll \bar{\pi}$ .  $\bar{\pi}$  is determined by the the equation of motion

$$\begin{aligned} & \epsilon^{\alpha\beta\gamma\delta} \epsilon_{\mu\nu\rho\sigma} R^{(1)\mu\nu}{}_{\alpha\beta} \left( \delta^\rho{}_\gamma \delta^\sigma{}_\delta + 2\beta_2 \bar{\Pi}^\rho{}_\gamma \delta^\sigma{}_\delta + \beta_3 \bar{\Pi}^\rho{}_\gamma \bar{\Pi}^\sigma{}_\delta \right) \\ & = \epsilon^{\alpha\beta\gamma\delta} \epsilon_{\mu\nu\rho\sigma} \partial^\mu \left[ (\partial_\beta h^{\text{GR}\nu}{}_\alpha - \partial_\alpha h^{\text{GR}\nu}{}_\beta) (\delta^\rho{}_\gamma \delta^\sigma{}_\delta + 2\beta_2 \bar{\Pi}^\rho{}_\gamma \delta^\sigma{}_\delta + \beta_3 \bar{\Pi}^\rho{}_\gamma \bar{\Pi}^\sigma{}_\delta) \right] = 0, \end{aligned} \quad (4.5.27)$$

where  $R_{\mu\nu\alpha\beta}^{(1)}$  is the linearized Riemann curvature and  $\bar{\Pi}_{\mu\nu} = \partial_\mu \partial_\nu \bar{\pi}$ . Then the quadratic order action for the perturbation  $\delta\pi$  is given by

$$\mathcal{L}_2 = -\frac{1}{2} Z^{\mu\nu} \partial_\mu \delta\pi \partial_\nu \delta\pi + \mathcal{O}(h_{\text{GR}}^2), \quad (4.5.28)$$

where

$$Z^{\mu\nu} = -\frac{\Lambda_2^4}{4} \epsilon^{\mu\alpha\beta\gamma} \epsilon^\nu{}_{\alpha'\beta'\gamma'} R^{(1)\alpha'\beta'}{}_{\alpha\beta} (\beta_2 \delta^{\gamma'}{}_\gamma + \beta_3 \bar{\Pi}^{\gamma'}{}_\gamma). \quad (4.5.29)$$

We note

$$Z^{\mu\nu} = \beta_2 \times (\text{Ricci curvatures}) + \beta_3 \times \bar{\Pi} \times (\text{Riemann and Ricci curvatures}),$$

thus  $Z^{\mu\nu}$  is identically zero for a Ricci flat spacetime when  $\beta_3 = 0$ . For this case, we should take into account next order contributions of  $h_{\text{GR}}$ . In this section, however, we restrict our analysis to the case of  $\beta_3 \neq 0$  and assume  $Z^{\mu\nu}$  is not zero.

The no-ghost and no-gradient instability condition is given by the signs of eigenvalues of  $Z^{\mu\nu}$  are  $[-, +, +, +]$ , which is equivalent to all eigenvalues of  $Z^\mu{}_\nu$  are positive. Hence we obtain

$$Z^\mu{}_\mu > 0, \quad (4.5.30)$$

as a necessary condition of no-instabilities. However, we obtain

$$Z^\mu{}_\mu \propto \text{Ricci curvatures}.$$

Since the sum of the eigenvalues is zero for any Ricci flat spacetime, there is at least one negative eigenvalue of  $Z^\mu{}_\nu$ , which leads a ghost instability or a gradient instability. As a result, a ghost and/or a gradient instability appears for any Ricci flat background.

For instance, the static and spherically symmetric solution is given by

$$h_{tt}^{\text{GR}} = \frac{2GM}{r}, \quad h_{rr}^{\text{GR}} = \frac{2GM}{r}, \quad \text{others} = 0, \quad (4.5.31)$$

$$\partial_\mu \bar{\pi} = (0, r\mu(r), 0, 0), \quad \mu = \pm \frac{1}{\sqrt{\beta_3}} + \mathcal{O}(GM/r). \quad (4.5.32)$$

Then the matrix  $Z^{\mu\nu}$  is given by

$$Z^{\mu\nu} = \frac{GM\sqrt{\beta_3}}{r^3} \times \text{diag} \left[ 0, \mp 2, \pm \frac{1}{r^2}, \pm \frac{1}{r^2 \sin^2 \theta} \right]. \quad (4.5.33)$$

Hence the gradient instability appears from either the radial or the angular derivatives. Note that, since the  $(tt)$ -component of  $Z^{\mu\nu}$  is zero at leading order of  $GM/r$ , it seems that the scalar graviton is infinitely strong coupled. However the kinetic term indeed appears at the next order of  $GM/r$  and our effective action does not lose any degrees of freedom as we will see in Section 8.4.

Since the bigravity theory contains degrees of freedom of the vector graviton as well as one of the scalar graviton and these are coupled to each other in a general background, one cannot directly conclude the Vainshtein screening solution is unstable in a Ricci flat background spacetime. Therefore we shall discuss general perturbations including vector gravitons around the static and spherically symmetric background in the next section. Regardless of this, our result suggests that the Vainshtein screening solutions cannot be supported only by the scalar graviton and the excitation of the vector graviton has to be taken into account.

Note that our result can be also straightforwardly applied to the Horndeski theories. Based on the effective action for the Vainshtein mechanism, the paper [126] showed the static and spherically symmetric solution with the Vainshtein screening is unstable as long as the Horndeski theory includes so-called  $\mathcal{L}_5$  term. Actually, for the case of Horndeski theory, although other terms appear in the effective action, they have been shown to be sub-dominant in Section 4.4 if we assume that the Vainshtein screening is working.



## Chapter 5

# Attractor universe

One of the most attractive phenomenological application of the bigravity theory is to explain the accelerating expansion of the Universe without dark energy. As already shown in §. 3.3.2, the bigravity theory can admit the de Sitter solution as a vacuum solution where the typical value of the effective cosmological constant would be an order of magnitude of the graviton mass square. It implies that the bigravity theory may give the self-accelerating universe without dark energy at the late stage of the Universe. Indeed, based on the ghost-free bigravity theory, many authors have studied cosmological models [43–52] (see also [94–99, 133–137] for the cosmology in massive gravity). However, the vacuum solution in bigravity is not unique. Therefore, it is not trivial whether the accelerating expansion is naturally found in the late time for general initial data. This is related to the so-called cosmic no-hair conjecture in GR, in which de Sitter solution is an attractor for generic initial conditions if there exists a cosmological constant [138–149]. In this chapter, we analyze the details of the evolution of the universe including both matter fields and study whether the accelerating expansion is obtained as an attractor or not [51].

We explore whether the accelerating expansion of the universe is obtained as an attractor or not. Therefore, we focus on the case when the bigravity theory admits the Minkowski solution as well as the de Sitter solution as vacuum solutions. In this case, the five parameters  $b_i$  in the bigravity theory are given by only two free parameters  $c_3$  and  $c_4$  as (3.3.19) and the de Sitter vacuum is realized in the parameter space shown in Fig. 3.1. The parameter space is classified into five subspaces depending on the properties of the cosmological solutions shown below.

### 5.1 FLRW universe

Now we discuss the FLRW spacetime, which metrics are given by

$$ds_g^2 = -N_g^2(t)dt^2 + a_g^2(t) \left( \frac{dr^2}{1-kr^2} + r^2 d\Omega^2 \right), \quad (5.1.1)$$

$$ds_f^2 = -N_f^2(t)dt^2 + a_f^2(t) \left( \frac{dr^2}{1-kr^2} + r^2 d\Omega^2 \right), \quad (5.1.2)$$

where  $N_g$  and  $N_f$  are lapse functions, while  $a_g$  and  $a_f$  are scale factors for  $g_{\mu\nu}$  and  $f_{\mu\nu}$ , respectively. Since those variables must be positive, we choose the tetrads as

$$\{e_\mu^{(a)}\} = \text{diag} \left( N_g, \frac{a_g}{\sqrt{1-kr^2}}, a_g, a_g \sin \theta \right) \quad (5.1.3)$$

$$\{\omega_\mu^{(a)}\} = \text{diag} \left( N_f, \frac{a_f}{\sqrt{1-kr^2}}, a_f, a_f \sin \theta \right) \quad (5.1.4)$$

Then the gamma matrix defined by  $\gamma^\mu{}_\nu = \epsilon e_{(a)}^\mu \omega_\nu^{(a)}$  is given by

$$\gamma^\mu{}_\nu = \epsilon \text{diag} (A, B, B, B), \quad (5.1.5)$$

where  $A = N_f/N_g$ ,  $B = a_f/a_g$  and  $\epsilon = \pm 1$ . Setting  $\tilde{A} = \epsilon A$ ,  $\tilde{B} = \epsilon B$ , we find that the interaction energy-momentum tensors are given by

$$T_g^{[\gamma]\mu}{}_{\nu} = \text{diag} \left[ -\rho_g^{[\gamma]}, P_g^{[\gamma]}, P_g^{[\gamma]}, P_g^{[\gamma]} \right], \quad (5.1.6)$$

$$T_f^{[\gamma]\mu}{}_{\nu} = \text{diag} \left[ -\rho_f^{[\gamma]}, P_f^{[\gamma]}, P_f^{[\gamma]}, P_f^{[\gamma]} \right] \quad (5.1.7)$$

where

$$\rho_g^{[\gamma]} = \frac{m^2}{\kappa^2} (b_0 + 3b_1\tilde{B} + 3b_2\tilde{B}^2 + b_3\tilde{B}^3), \quad (5.1.8)$$

$$P_g^{[\gamma]} = -\frac{m^2}{\kappa^2} \left[ b_0 + b_1(\tilde{A} + 2\tilde{B}) + b_2(2\tilde{A}\tilde{B} + \tilde{B}^2) + b_3\tilde{A}\tilde{B}^2 \right], \quad (5.1.9)$$

$$\rho_f^{[\gamma]} = \frac{m^2}{\kappa^2} \left( b_4 + \frac{3b_3}{\tilde{B}} + \frac{3b_2}{\tilde{B}^2} + \frac{b_1}{\tilde{B}^3} \right), \quad (5.1.10)$$

$$P_f^{[\gamma]} = -\frac{m^2}{\kappa^2} \left[ b_4 + b_3 \left( \frac{1}{\tilde{A}} + \frac{2}{\tilde{B}} \right) + b_2 \left( \frac{2}{\tilde{A}\tilde{B}} + \frac{1}{\tilde{B}^2} \right) + \frac{b_1}{\tilde{A}\tilde{B}^2} \right]. \quad (5.1.11)$$

The cosmic times for  $g$ - and  $f$ -metrics are defined by

$$\tau_g = \int N_g(t) dt, \quad \tau_f = \int N_f(t) dt, \quad (5.1.12)$$

respectively. Using the gauge freedom, in what follows, we set  $N_g = 1$ , in which gauge choice, the time coordinate  $t$  is the same as the cosmic time of  $g$ -metric.

We assume that twin matter fields ( $g$ -matter and  $f$ -matter fluids) are described by perfect fluids

$$T_g^{[m]\mu}{}_{\nu} = \text{diag} \left[ -\rho_g(t), P_g(t), P_g(t), P_g(t) \right],$$

$$T_f^{[m]\mu}{}_{\nu} = \text{diag} \left[ -\rho_f(t), P_f(t), P_f(t), P_f(t) \right],$$

and assume that the universe consists of dust (non-relativistic matter) and radiation (relativistic matter) for twin matter fluids. From the conservation equations,

$$\dot{\rho}_g + 3\frac{\dot{a}_g}{a_g}(\rho_g + P_g) = 0,$$

$$\dot{\rho}_f + 3\frac{\dot{a}_f}{a_f}(\rho_f + P_f) = 0, \quad (5.1.13)$$

where the dot denotes the derivative with respect to  $t$ , the energy densities are described by the scale factors as

$$\kappa_g^2 \rho_g = \kappa_g^2 (\rho_{g,m} + \rho_{g,r}) = \frac{c_{g,m}}{a_g^3} + \frac{c_{g,r}}{a_g^4}$$

$$\kappa_f^2 \rho_f = \kappa_f^2 (\rho_{f,m} + \rho_{f,r}) = \frac{c_{f,m}}{a_f^3} + \frac{c_{f,r}}{a_f^4}, \quad (5.1.14)$$

where  $c_{g,m}$ ,  $c_{g,r}$ ,  $c_{f,m}$  and  $c_{f,r}$  are positive integration constants.

The Einstein equations with the metric ansatz (5.1.1) and (5.1.2) are reduced to the Friedmann equations:

$$H_g^2 + \frac{k}{a_g^2} = \frac{\kappa_g^2}{3} \left[ \rho_g^{[\gamma]} + \rho_g \right], \quad (5.1.15)$$

$$H_f^2 + \frac{k}{a_f^2} = \frac{\kappa_f^2}{3} \left[ \rho_f^{[\gamma]} + \rho_f \right], \quad (5.1.16)$$

where

$$H_g = \frac{\dot{a}_g}{a_g}, \quad H_f = \frac{\dot{a}_f}{N_f a_f} \quad (5.1.17)$$



are the Hubble expansion parameters.

The conservation equations for  $T_g^{[\gamma]\mu}{}_\nu$  and  $T_f^{[\gamma]\mu}{}_\nu$  are reduced to one equation:

$$\left(\frac{\dot{a}_f}{\dot{a}_g} - A\right) (b_1 + 2b_2\tilde{B} + b_3\tilde{B}^2) = 0. \quad (5.1.18)$$

These are two cases: The first parentheses vanishes or the second one does so. If the second parentheses vanishes,  $\tilde{B}$  is a constant, and then  $\rho_g^{[\gamma]}(\tilde{B})$  and  $\rho_f^{[\gamma]}(\tilde{B})$  are also constant. As a result, the Friedmann equations (5.1.15) and (5.1.16) are the same as the ordinary ones in GR with a cosmological constant. Since the evolution of the universe is well analyzed in GR, we will not discuss this case furthermore<sup>1</sup>. Thus, we assume that the first parentheses vanishes. This condition holds when

$$H_g = BH_f. \quad (5.1.19)$$

From two Friedmann equations (5.1.15), (5.1.16) with the condition (5.1.19), we find one algebraic equation

$$\kappa_g^2 \left[ \rho_g^{[\gamma]}(\tilde{B}) + \rho_g(a_g) \right] - \kappa_f^2 \tilde{B}^2 \left[ \rho_f^{[\gamma]}(\tilde{B}) + \rho_f(a_f) \right] = 0. \quad (5.1.20)$$

Since  $a_f = Ba_g = \epsilon\tilde{B}a_g$ , this equation gives the relation between  $\tilde{B}$  and  $a_g$ . It also provides us some information about the interaction term  $\rho_g^{[\gamma]}$  and  $\rho_f^{[\gamma]}$  in terms of twin matter fluids, which will be used in the discussion about dark matter later.

The above equation (5.1.20) with (5.1.14) is rewritten into a quartic equation for  $a_g$  as

$$\tilde{B}C_\Lambda(\tilde{B})a_g^4 + \tilde{B}C_m(\tilde{B})a_g + C_r(\tilde{B}) = 0, \quad (5.1.21)$$

where

$$\begin{aligned} C_\Lambda(\tilde{B}) &= \tilde{B} \left[ \kappa_g^2 \rho_g^{[\gamma]}(\tilde{B}) - \kappa_f^2 \tilde{B}^2 \rho_f^{[\gamma]}(\tilde{B}) \right] \\ &= \kappa_g^2 \tilde{B} \left( b_3 \tilde{B}^3 + 3b_2 \tilde{B}^2 + 3b_1 \tilde{B} + b_0 \right) - \kappa_f^2 \left( b_4 \tilde{B}^3 + 3b_3 \tilde{B}^2 + 3b_2 \tilde{B} + b_1 \right), \end{aligned} \quad (5.1.22)$$

$$C_m(\tilde{B}) = c_{g,m} \tilde{B} - \epsilon c_{f,m}, \quad (5.1.23)$$

$$C_r(\tilde{B}) = c_{g,r} \tilde{B}^2 - c_{f,r}. \quad (5.1.24)$$

Solving (5.1.21), we obtain the relation  $a_g = a_g(\tilde{B})$  and then  $a_f = \epsilon\tilde{B}a_g(\tilde{B})$ . Plugging this relation into the Friedmann equation (5.1.15), we find the equation for  $\tilde{B}$  as

$$\left(\frac{d\tilde{B}}{dt}\right)^2 + V_g(\tilde{B}) = 0, \quad (5.1.25)$$

where the potential for  $\tilde{B}$  is given by

$$V_g(\tilde{B}) = \frac{a_g^2}{a_g'^2} \left[ \frac{k}{a_g^2(\tilde{B})} - \frac{1}{3} \left( \kappa_g^2 \rho_g^{[\gamma]}(\tilde{B}) + \frac{c_{g,m}}{a_g^3(\tilde{B})} + \frac{c_{g,r}}{a_g^4(\tilde{B})} \right) \right]$$

with

$$a_g' = - \frac{\left( C_\Lambda + \tilde{B}C'_\Lambda \right) a_g^4 + (2c_{g,m}\tilde{B} - \epsilon c_{f,m})a_g + 2c_{g,r}\tilde{B}}{\tilde{B}(4C_\Lambda a_g^3 + C_m)}.$$

A prime denotes the derivative with respect to  $\tilde{B}$ .

<sup>1</sup>The behavior of the solution in the second case is same as that in dRGT theory. Since the cosmological solution in dRGT theory was shown pathological due to the ghost instability [97–99], the second case would contain the ghost instability.

## 5.2 Attractors

The matter and radiation densities become equal at the redshift  $z = z_{\text{eq}} \approx 3000$  in our universe. Hence, after  $z_{\text{eq}}$ , matter density is dominant in  $g$ -spacetime, which we assume in what follows since we are interested in the present acceleration of the universe. We also assume a flat Universe with  $k = 0$  from observation<sup>2</sup>.

We mainly discuss when radiation density in  $f$ -spacetime can be also ignored. In this case, (5.1.20) becomes

$$C_\Lambda(\tilde{B})a_g^3 + C_m(\tilde{B}) = 0, \quad (5.2.1)$$

which gives

$$a_g(\tilde{B}) = - \left( \frac{C_m(\tilde{B})}{C_\Lambda(\tilde{B})} \right)^{\frac{1}{3}}. \quad (5.2.2)$$

The potential for  $\tilde{B}$  is given by

$$V_g(\tilde{B}) = - \frac{3C_m C_\Lambda^2 \left[ \kappa_g^2 \rho_g^{[\gamma]} C_m - c_{g,m} C_\Lambda + 3k C_\Lambda^{\frac{2}{3}} C_m^{\frac{1}{3}} \right]}{(C_\Lambda C'_m - C_m C'_\Lambda)^2}. \quad (5.2.3)$$

If  $C_\Lambda(\tilde{B}) = 0$  as well as  $C_m(\tilde{B}) = 0$  initially,  $\tilde{B}$  is always constant and then we find the homothetic solution as an exact solution:

$$\begin{aligned} A &= B = |\tilde{B}_\ell|, \\ c_{f,m} &= |\tilde{B}_\ell| c_{g,m} \end{aligned} \quad (5.2.4)$$

We find the conventional matter dominant universe with/without a cosmological constant.

However,  $C_\Lambda(\tilde{B})$  does not usually vanish. For generic initial data, solving the equation (5.1.25) for  $\tilde{B}$ , we obtain the scale factor  $a_g$  by Eq. (5.2.2) with  $\tilde{B}(t)$ , and then another scale factor  $a_f$  by

$$a_f(\tilde{B}) = \epsilon \tilde{B} a_g(\tilde{B}). \quad (5.2.5)$$

The ratio  $A$  of the lapse functions is also given by

$$A(\tilde{B}) = \epsilon \left( \tilde{B} + \frac{3C_m C_\Lambda}{C_\Lambda C'_m - C_m C'_\Lambda} \right). \quad (5.2.6)$$

The potential  $V_g$  satisfies the following conditions at  $\tilde{B} = \tilde{B}_\ell$ :

$$V_g(\tilde{B}_\ell) = 0, \quad (5.2.7)$$

$$V'_g(\tilde{B}_\ell) = 0, \quad (5.2.8)$$

$$V''_g(\tilde{B}_\ell) = -6\Lambda_g(\tilde{B}_\ell). \quad (5.2.9)$$

The AdS solution with  $\Lambda_g < 0$  is isolated because the potential is not negative definite and then Eq.(5.1.25) is satisfied only at  $\tilde{B}_\ell = \tilde{B}_{(\text{AdS})}$ . For the case of  $\Lambda_g > 0$ , on the other hand, there are two allowed regions where the universe can exist; the left and right regions of the point  $\tilde{B}_\ell = \tilde{B}_{(\text{AdS})}$ . The potential near  $\tilde{B}_{(\text{AdS})}$  is shown in Fig. 5.1. The potential form depends on the ratio of matter densities  $r_m \equiv c_{f,m}/c_{g,m}$  as well as the coupling parameters  $\{b_i\}$ . Although there are two allowed regions in the equation of motion for  $\tilde{B}$ , one side is not physical, that is, it corresponds to the region where a scale factor becomes negative because from Eq. (5.2.2), we can evaluate the scale factor near  $\tilde{B} = \tilde{B}_{(\text{AdS})}$  as

$$\begin{aligned} a_g &= - \left[ \frac{c_{g,m} \tilde{B}_{(\text{AdS})} - \epsilon c_{f,m}}{C'_\Lambda(\tilde{B}_{(\text{AdS})})(\tilde{B} - \tilde{B}_{(\text{AdS})})} \right]^{1/3} \\ &\propto (\tilde{B} - \tilde{B}_{(\text{AdS})})^{-1/3} \end{aligned} \quad (5.2.10)$$

<sup>2</sup> Even if we consider the closed ( $k = 1$ ) or open ( $k = -1$ ) FLRW universe, our main result will not change.

which changes the sign at  $\tilde{B} = \tilde{B}_{(\text{dS})}$ . Here  $C'_\Lambda(\tilde{B}_{(\text{dS})})$  is a constant. Which side of regions is physical depends on the value of  $r_m$ . For example, for Model B ( $c_3 = 4$  and  $c_4 = -10$ ), if  $r_m < r_m^{(\text{dS})} = 0.145979$ , the left region is physically allowed, while for  $r_m > r_m^{(\text{dS})}$ , the right region becomes physically possible (see Fig. 5.1, in which we plot both cases of  $r_m = 0$ , and 0.3).

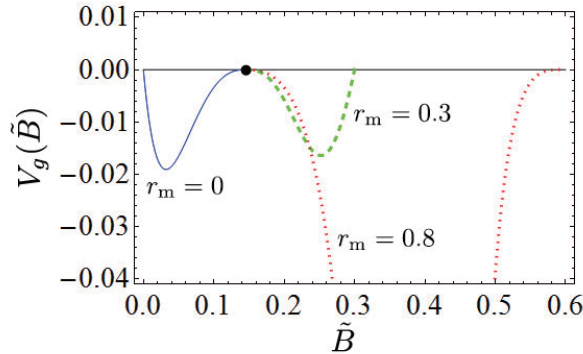


Figure 5.1: The potentials  $V_g(\tilde{B})$  for Model B ( $c_3 = 4, c_4 = -10$ ) with  $r_m = 0$  (the blue solid curve),  $r_m = 0.3$  (the green dashed curve), or  $r_m = 0.8$  (the red dotted curve). The black dot denotes de Sitter solution  $\tilde{B}_{(\text{dS})}$ .

In both cases,  $\tilde{B}$  evolves into  $\tilde{B}_{(\text{dS})}$  as an attractor. Near  $\tilde{B}_{(\text{dS})}$ , the potential is approximated as

$$V_g \approx -3\Lambda_g(\tilde{B} - \tilde{B}_{(\text{dS})})^2. \quad (5.2.11)$$

Hence we find the solution for  $\tilde{B}$  as

$$\tilde{B} \approx \tilde{B}_{(\text{dS})} + C_0 \exp[\pm\sqrt{3\Lambda_g}t], \quad (5.2.12)$$

where  $C_0$  is an integration constant. The plus sign corresponds to an unstable evolution rolling down from the potential peak, while the minus sign shows a stable solution which asymptotically approaches to  $\tilde{B}_{(\text{dS})}$ . The scale factor evolves as

$$a_g \propto \exp\left[\sqrt{\frac{\Lambda_g}{3}}t\right] \quad (5.2.13)$$

(see Fig. 5.2). Hence de Sitter accelerating universe is obtained as an attractor. Note that if  $r_{\text{cr}}^{(\text{dS})} < r_m (< r_m^{(\text{AdS})} = 1.67319)$ , where  $r_{\text{cr}}^{(\text{dS})} = 0.41105$ , the potential is unbounded from below and diverges at a finite value of  $\tilde{B}$ , where a singularity ( $\dot{\tilde{B}} = \infty$ ) appears as we will show later (see the potential with  $r_m = 0.8$  in Fig. 5.1).

For the case of  $\tilde{B}_{(\text{M})} = 1$ , we find

$$V_g(\tilde{B}_{(\text{M})}) = V'_g(\tilde{B}_{(\text{M})}) = V''_g(\tilde{B}_{(\text{M})}) = 0, \quad (5.2.14)$$

since  $\Lambda_g = 0$ . Evaluating also  $V'''_g(\tilde{B}_{(\text{M})})$  as

$$V'''_g(\tilde{B}_{(\text{M})}) = 54 \left( \frac{m_f^2 + m_g^2 r_m}{1 - r_m} \right), \quad (5.2.15)$$

we find that  $V'''_g$  is positive when  $r_m < 1$ , then the left region ( $\tilde{B} \leq \tilde{B}_{(\text{M})}$ ) is physically allowed, while the right region ( $\tilde{B} \geq \tilde{B}_{(\text{M})}$ ) is allowed if  $r_m > 1$ . In this case, the potential is approximated as

$$V_g = V_0(\tilde{B} - \tilde{B}_{(\text{M})})^3 \quad (5.2.16)$$

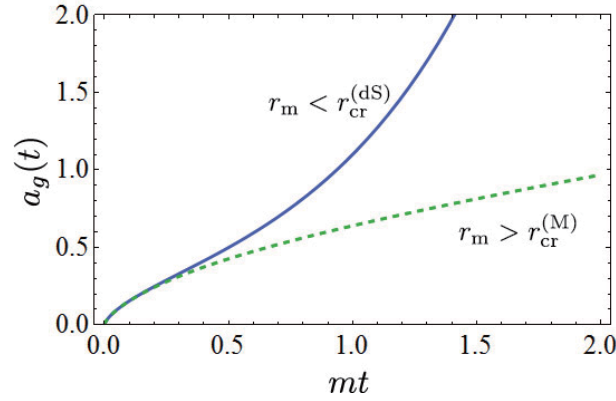


Figure 5.2: The evolution of the scale factor  $a_g$  for the case of  $c_3 = 4, c_4 = -10$ . The bottom curve corresponding to  $c_{f,m}/c_{g,m} = 2$  (dashed green) shows the evolution to dust dominated universe, while the top curve corresponding to  $c_{f,m}/c_{g,m} = 0$  (solid blue) shows the evolution to de Sitter spacetime.

with

$$V_0 = 9 \left( \frac{m_f^2 + m_g^2 r_m}{1 - r_m} \right). \quad (5.2.17)$$

Eq. (5.1.25) is integrated as

$$-V_0(\tilde{B} - \tilde{B}_{(M)}) = \frac{4}{(t - t_0)^2}, \quad (5.2.18)$$

where  $t_0$  is an integration constant. As a result, the asymptotic solution of the scale factor is

$$a_g \propto (\tilde{B} - \tilde{B}_{(M)})^{-1/3} \propto (t - t_0)^{2/3}, \quad (5.2.19)$$

which is that of dust matter dominated universe (see Fig. 5.2). When  $\tilde{B}_\ell = \tilde{B}_{(M)}$ , a dust matter dominated universe is found as an attractor.

### 5.3 Dynamics of the universe with twin matter

We are interested in whether the cosmic no-hair conjecture holds. Hence we analyze our system for various initial data and discuss which initial condition leads to de Sitter expansion. In order to discuss whether de Sitter accelerating universe is naturally achieved as an attractor or not, we survey all possible allowed initial data. Especially we focus on the ratio  $r_m$  of energy densities of twin matter fluids. The results are summarized on the  $r_m$ - $\tilde{B}$  plane. For the parameter region (1) and (2), we show two typical examples of Model A ( $c_3 = -1, c_4 = 0$ ) and of Model B ( $c_3 = 4, c_4 = -10$ ), in Figs. 5.3 and 5.4, respectively. For the region (3), we also present the typical results for Model C ( $c_3 = 1/2, c_4 = 0$ ), D ( $c_3 = 5/2, c_4 = -4$ ) and E ( $c_3 = 3, c_4 = 0$ ) in Figs. 5.5, 5.6 and 5.7, respectively.

The colored regions denote the ranges of physically allowed initial data. The universes in the stripe-shaded light-blue area evolve into de Sitter spacetime, while those in the crosshatched light-green area evolve into the dust matter dominated universe. The universes started from the gray shaded areas eventually find a future singularity.

We may probably easily understand that the spacetime evolves either de Sitter universe or the matter dominant universe, depending on the initial conditions, because two homothetic solutions are attractors. However, we also find singular spacetime for some initial data. Why a flat FLRW universe can evolve into a future singularity, which never happens in GR? To explain how the universe evolves into a singularity, we consider Model B ( $c_3 = 4$  and  $c_4 = -10$ ) (Fig. 5.4).

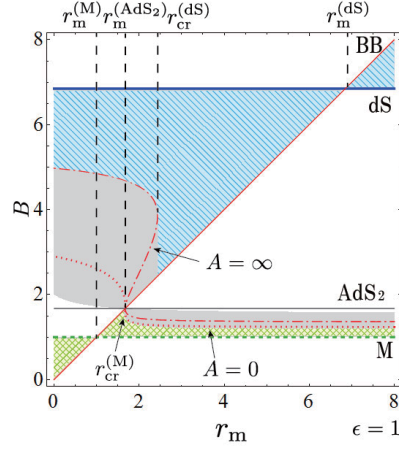


Figure 5.3: The attractor regions in the  $r_m$ - $\tilde{B}$  plane are shown for Model A ( $c_3 = -1, c_4 = 0$ ). The solid, dotted and dashed lines denote de Sitter, anti de Sitter and dust dominated universes, respectively.  $r_m^{(M)} = 1$ ,  $r_m^{(AdS_2)} = 1.67319$ , and  $r_m^{(dS)} = 6.85028$  give the boundary values, where the properties of dynamics change. The initial data in the striped-shaded light-blue and crosshatched light-green regions evolve into de Sitter and the dust dominated universe, respectively. BB denotes an initial Big Bang singularity ( $a_g = a_f = 0$ ). The spacetime started from the other colored region evolves into singularities, which are shown by dot-dashed curves. There exist two critical values  $r_{cr}^{(dS)} = 2.4328$  and  $r_{cr}^{(M)} = 1.67318$ . Beyond  $r_{cr}^{(dS)}$ , every spacetime evolves into de Sitter universe if  $B > r_m^{(AdS_2)}$ , while all spacetime with  $r_m < r_{cr}^{(M)}$  evolves into the matter dominant universe if  $B < r_m^{(AdS_2)}$ .

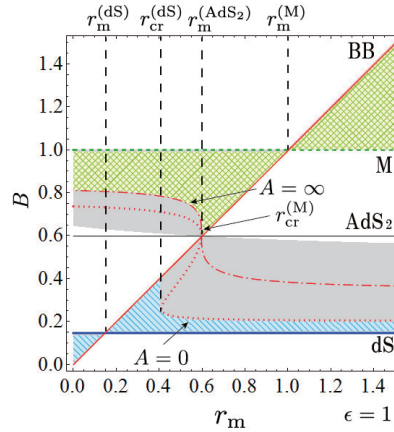


Figure 5.4: The same figure as Fig. 5.3 for Model B ( $c_3 = 4, c_4 = -10$ ). The boundary values are given by  $r_m^{(M)} = 1$ ,  $r_m^{(AdS_2)} = 0.59766$ , and  $r_m^{(dS)} = 0.145979$ . Below the critical value  $r_{cr}^{(dS)} = 0.41105$ , every spacetime evolves into de Sitter universe if  $B < r_m^{(AdS_2)}$ , while all spacetime with  $r_m > r_{cr}^{(M)} = 0.597663$  evolves into the matter dominant universe if  $B > r_m^{(AdS_2)}$ .

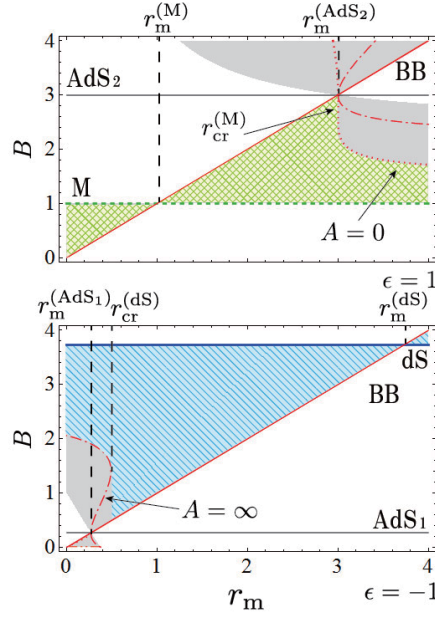


Figure 5.5: The same figure as Fig. 5.3 for Model C ( $c_3 = 1/2, c_4 = 0$ ). The de Sitter solution exists in the case of  $\epsilon = -1$ , while the matter dominant universe is found for  $\epsilon = 1$ . Hence we draw two figures of  $\epsilon = \pm 1$  separately. because there appears a singularity at  $\tilde{B} = 0$ , where  $\epsilon$  changes the sign. The boundary values are given by  $r_m^{(M)} = 1$ ,  $r_m^{(\text{AdS}_1)} = 2 - \sqrt{3}$ ,  $r_m^{(\text{AdS}_2)} = 3$ , and  $r_m^{(\text{dS})} = 2 + \sqrt{3}$ . Beyond the critical value  $r_{\text{cr}}^{(\text{dS})} = 0.489757$ , every spacetime evolves into de Sitter universe if  $\epsilon = -1$  and  $B > r_m^{(\text{AdS}_1)}$ , while all spacetime with  $r_m < r_{\text{cr}}^{(M)} = 2.99645$  evolves into the matter dominant universe if  $\epsilon = 1$  and  $B < r_m^{(\text{AdS}_2)}$ .

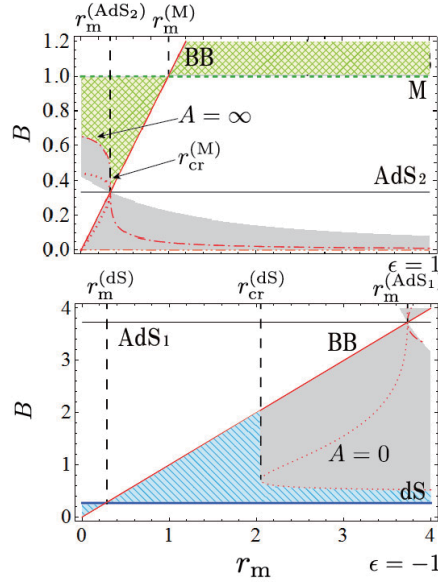


Figure 5.6: The same figure as Fig. 5.5 for Model D ( $c_3 = 5/2, c_4 = -4$ ) ( $\epsilon = -1$ ). The boundary values are given by  $r_m^{(M)} = 1$ ,  $r_m^{(\text{AdS}_1)} = 2 + \sqrt{3}$ ,  $r_m^{(\text{AdS}_2)} = 1/3$ , and  $r_m^{(\text{dS})} = 2 - \sqrt{3}$ . Below the critical value  $r_{\text{cr}}^{(\text{dS})} = 2.04183$ , every spacetime evolves into de Sitter universe if  $\epsilon = -1$  and  $B < r_m^{(\text{AdS}_1)}$ , while all spacetime with  $r_m > r_{\text{cr}}^{(M)} = 0.33729$  evolves into the matter dominant universe if  $\epsilon = 1$  and  $B > r_m^{(\text{AdS}_2)}$ .

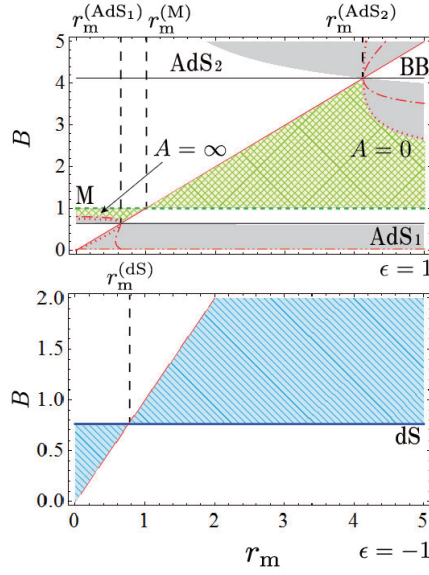


Figure 5.7: The same figure as Fig. 5.5 for Model E ( $c_3 = 3, c_4 = 0$ ). The boundary values are given by  $r_m^{(M)} = 1$ ,  $r_m^{(\text{AdS}_1)} = 0.636672$ ,  $r_m^{(\text{AdS}_2)} = 4.12489$ , and  $r_m^{(\text{dS})} = 0.761557$ . Every spacetime with  $\epsilon = -1$  evolves into de Sitter universe. The matter dominant universe is found for all spacetime with  $\epsilon = 1$  and  $r_m^{(\text{AdS}_1)} < r_m < r_m^{(\text{AdS}_2)}$

If  $r_m < r_{\text{cr}}^{(\text{dS})}$ , the universe starts from a big bang initial singularity and evolves into de Sitter spacetime. When  $r_{\text{cr}}^{(\text{dS})} < r_m < r_m^{(\text{AdS}_2)}$ , the evolution of  $a_g$  is the similar to the above case. Starting from a big bang initial data ( $a_g = 0$ ), it evolves into de Sitter spacetime. However, the behavior of  $a_f$  becomes strange. We show the time evolution of two scale factors in Figs. 5.8-5.10, in which we set  $r_m = 0.58$ .

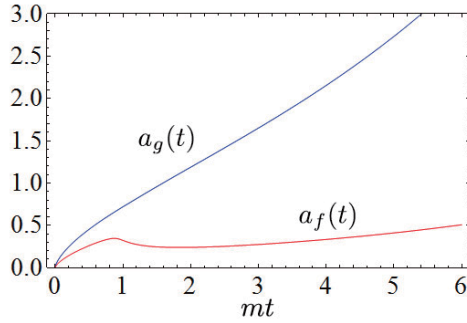


Figure 5.8: The time evolution of two scale factors  $a_g$  and  $a_f$  for Model B ( $c_3 = 4, c_4 = -10$ ) with  $c_{f,m}/c_{g,m} = 0.58$ .

$a_f$  first increases and then turns to decrease. It eventually increases again, resulting in an exponential expansion. In order to analyze the reason why the universe shows a transient collapse, we show the time evolution of  $A$  and  $B$  in Fig. 5.9. We find that  $A$  becomes negative when  $a_f$  decreases. It means that the time direction in this period turns to be reverse. It is the reason of the collapse.

However there appears a singularity when  $\tilde{A}$  vanishes, i.e.,  $\dot{a}_f = 0$ . Substituting  $\tilde{A} = \dot{a}_f/\dot{a}_g$

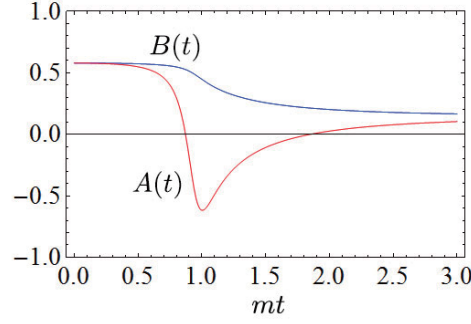


Figure 5.9: The time evolution of  $B(t)$  and  $A(t)$  for Model B with  $c_{f,m}/c_{g,m} = 0.58$ .

into the Ricci scalar  $\mathcal{R}(f)$ , we obtain

$$\begin{aligned}\mathcal{R}(f) &= 6 \left[ \frac{1}{N_f a_f} \left( \frac{\dot{a}_f}{N_f} \right)' + \frac{\dot{a}_f^2}{N_f^2 a_f^2} + \frac{k}{a_f^2} \right] \\ &= 6 \left( \frac{\dot{a}_g \ddot{a}_g}{a_f \dot{a}_f} + \frac{\dot{a}_g^2}{a_f^2} + \frac{k}{a_f^2} \right).\end{aligned}\quad (5.3.1)$$

$\ddot{a}_g$  does not vanish at  $\tilde{A} = 0$ , because the  $r$ - $r$  component of field equation of  $g_{\mu\nu}$  is given by

$$\begin{aligned}2 \frac{\ddot{a}_g}{a_g} + \frac{\dot{a}_g^2}{a_g^2} + \frac{k}{a_g^2} &= m_g^2 \left[ b_0 + b_1(\tilde{A} + 2\tilde{B}) \right. \\ &\quad \left. + b_2(2\tilde{A}\tilde{B} + \tilde{B}^2) + b_3\tilde{A}\tilde{B}^2 \right] - \kappa_g^2 P_g.\end{aligned}\quad (5.3.2)$$

Thus, the Ricci scalar  $\mathcal{R}(f)$  diverges at  $\dot{a}_f = 0$  ( $\tilde{A} = 0$ ) assuming  $\dot{a}_g \neq 0$ . Note that the Ricci scalar for  $g_{\mu\nu}$  is finite at this point. It implies that  $g$ -spacetime is regular whereas  $f$ -spacetime is singular at  $\tilde{A} = 0$ .

Note that it is possible to solve the equation for  $\tilde{B}$  by use of the potential  $V_g$  even we find a singularity in  $f$ -spacetime, because the interaction term does not diverge. However, it is impossible to solve the equation by use of the cosmic time  $\tau_f$  in  $f$ -spacetime. From Fig. 5.10, it is almost

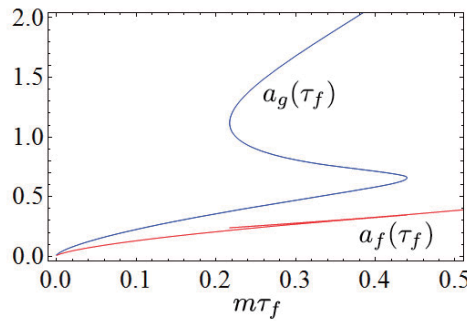


Figure 5.10: The time evolution of two scale factors  $a_g$  and  $a_f$  in terms of  $\tau_f$  for Model B with  $c_{f,m}/c_{g,m} = 0.58$ . Beyond the singularity, both scale factors decrease in time, and then increase again after another singularity.

trivial that a singularity appears at the turning points of  $a_f$ .

Fig.5.9 implies that  $t(\tau_f)$  is not single-valued although  $\tau_f(t)$  is a single-valued function. As a result, the variables such as  $a_g(\tau_f)$  or  $a_f(\tau_f)$  are not single-valued (see Fig.5.10).



The reverse of the above case also occurs, that is,  $f$ -spacetime is regular anytime except for a big bang singularity whereas  $g$ -spacetime becomes singular at  $\dot{a}_g = 0$ , when  $\tilde{A} = \infty$ . The sign of  $\tilde{A}$  also changes beyond this singularity. This happens in the case of Model A ( $c_3 = -1, c_4 = 0$ ).

In Figs. 5.3-5.7, we show the region of  $\tilde{A} < 0$ , on which boundaries (the solid and dashed curves for  $\tilde{A} = 0$   $\tilde{A} = \infty$ , respectively) singularities appear. Hence if the universe starts from the gray shaded area, it evolves into a singularity either at  $\tilde{A} = 0$  or at  $\tilde{A} = \infty$ . If the universe starts from a big bang singularity ( $a_g = a_f = 0$ : red solid line), it evolves into a negative lapse area through a singularity and eventually goes to a positive lapse area again, finding the de Sitter accelerating universe (or the matter dominated universe). For the other initial data in the gray area, the boundary does not correspond to a big bang singularity, but the universe is bounced at the boundary. Either this spacetime evolves directly into a singularity at  $\tilde{A} = \infty$ , or it first goes to the boundary and then it is bounced back to the singularity. Going through a negative lapse area, both cases eventually evolve into a positive lapse area again. In any case, however, a singularity formation cannot be avoided if the universe starts from the gray area.

As shown in Figs. 5.3-5.7, there exists critical values  $r_{\text{cr}}^{(\text{dS})}$  ( $r_{\text{cr}}^{(\text{M})}$ ) for  $r_{\text{m}} = c_{f,\text{m}}/c_{g,\text{m}}$ , beyond (or below) which both  $g$ - and  $f$ -spacetime are regular and then they evolve into de Sitter universe (or the dust matter dominated universe). The universe never evolves into a singularity. The critical value  $r_{\text{cr}}^{(\text{dS/M})}$  can be found as follows: It is given by an extreme value of boundary curve of  $\tilde{A} = 0$  or  $\tilde{A} = \infty$ , which are given by

$$r_{\text{m}}|_{\tilde{A}=0} = \left. \frac{c_{f,\text{m}}}{c_{g,\text{m}}} \right|_{\tilde{A}=0} = \epsilon \tilde{B} \left( 1 + \frac{C_{\Lambda}}{3C_{\Lambda} - \tilde{B}C'_{\Lambda}} \right), \quad (5.3.3)$$

$$r_{\text{m}}|_{\tilde{A}=\infty} = \left. \frac{c_{f,\text{m}}}{c_{g,\text{m}}} \right|_{\tilde{A}=\infty} = \epsilon \left( \tilde{B} - \frac{C_{\Lambda}}{C'_{\Lambda}} \right). \quad (5.3.4)$$

The extremal condition gives the equation for  $\tilde{B}$  at the critical point such that

$$(\kappa_g^2 b_1 - \kappa_f^2 b_3) \tilde{B}^2 + (\kappa_g^2 b_0 - 3\kappa_f^2 b_2) \tilde{B} - 2\kappa_f^2 b_1 = 0,$$

for  $\tilde{A} = 0$  or

$$2\kappa_g^2 b_3 \tilde{B}^2 + (3\kappa_g^2 b_2 - \kappa_f^2 b_4) \tilde{B} + (\kappa_g^2 b_1 - \kappa_f^2 b_3) = 0$$

for  $\tilde{A} = \infty$ , respectively. The roots of the above equation just provide a candidate for the critical value  $\tilde{B}_{\text{cr}}$ . Since the critical point must exist in the physically allowed region, we have to impose the additional constraint for the critical value as

$$V_g(\tilde{B}_{\text{cr}}, r_{\text{cr}}^{(\text{dS/M})}) < 0. \quad (5.3.5)$$

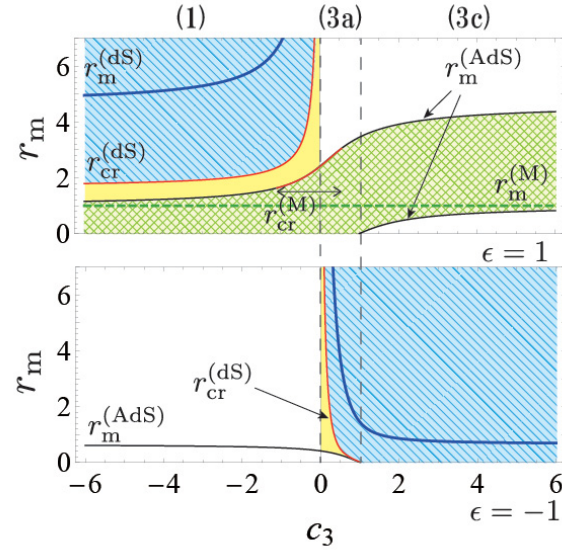
for  $\tilde{B}_{(\text{dS/M})} > \tilde{B}_{\text{cr}} > r_{\text{m}}$  or  $\tilde{B}_{(\text{dS/M})} < \tilde{B}_{\text{cr}} < r_{\text{m}}$ . These critical values  $r_{\text{cr}}^{(\text{dS/M})}$  are shown in Figs. 5.3-5.7.

We summarize the results in this subsection in Table 5.1.

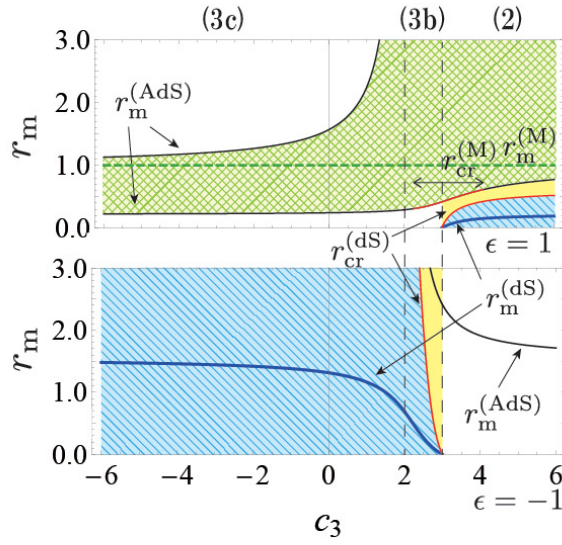
We show the conditions for the ratio  $r_{\text{m}}$  and the initial value of  $B$  under which every spacetime evolves into de Sitter universe or the matter dominant universe. The critical values depend on the coupling constants  $\{b_i\}$  (or  $c_3$  and  $c_4$ ) and  $\kappa_f^2/\kappa_g^2$ . When spacetimes do not satisfy these conditions, the universe will find a singularity unless we fine-tune the initial conditions.

## 5.4 Cosmic no hair conjecture

In the previous section, we discuss several examples, in which we showed that there are three possibilities for the fate of spacetime: de Sitter accelerating universe, the matter dominant universe, and spacetime with a future singularity, depending on the initial condition. Hence in the exact sense, the cosmic no-hair conjecture does not hold, but de Sitter universe can be obtained from a wide range of initial conditions. In this section, we shall further analyze how this result is generic by surveying the possible coupling parameters  $\{b_k\}$ , which are given by two free parameters  $c_3$  and  $c_4$  as (3.3.19).



(a) Case (I)



(b) Case (II)

Figure 5.11: The de Sitter solution (blue curves) and the necessary condition of  $r_m$  for self-acceleration (the stripe-shaded light-blue regions) are shown. We also shown the matter dominate universe (the crosshatched light-green curve) and its necessary condition of  $r_m$ . The dashed red curves show AdS solutions with  $\Lambda_g < 0$ . If the universe starts from the yellow region, it evolves into a singularity. The critical value  $r_{cr}^{(dS)}$  exists in the regions (1), (2), (3a) and (3b). The another critical value  $r_{cr}^{(M)}$  appear if  $-1.09 < c_3 < 0.55$  for Case (I) and  $2.27 < c_3 < 4.09$  for Case (II), respectively.

| region                          | $\epsilon$ | $r_m$   | $B$   |
|---------------------------------|------------|---|---|
| de Sitter accelerating universe |            |   |   |
| (1)                             | 1          | $r_m > r_{\text{cr}}^{(\text{dS})}$                                     | $B > r_m^{(\text{AdS}_2)}$  |
| (2)                             | 1          | $r_m < r_{\text{cr}}^{(\text{dS})}$                                     | $B < r_m^{(\text{AdS}_2)}$  |
| (3a)                            | -1         | $r_m > r_{\text{cr}}^{(\text{dS})}$                                     | $B > r_m^{(\text{AdS}_1)}$  |
| (3b)                            | -1         | $r_m < r_{\text{cr}}^{(\text{dS})}$                                     | $B < r_m^{(\text{AdS}_1)}$  |
| (3c)                            | -1         | no condition  | no condition  |
| matter dominant universe        |            |   |   |
| (1)                             | 1          | $r_m < r_{\text{cr}}^{(\text{M})}$                                      | $B < r_m^{(\text{AdS}_2)}$  |
| (2)                             | 1          | $r_m > r_{\text{cr}}^{(\text{M})}$                                      | $B > r_m^{(\text{AdS}_2)}$  |
| (3a)                            | 1          | $r_m < r_{\text{cr}}^{(\text{M})}$                                      | $B < r_m^{(\text{AdS}_2)}$  |
| (3b)                            | 1          | $r_m > r_{\text{cr}}^{(\text{M})}$                                      | $B > r_m^{(\text{AdS}_2)}$  |
| (3c)                            | 1          | $r_{\text{cr}}^{(\text{AdS}_1)} < r_m < r_{\text{cr}}^{(\text{AdS}_2)}$ | $r_{\text{cr}}^{(\text{AdS}_1)} < B < r_{\text{cr}}^{(\text{AdS}_2)}$ |

Table 5.1: The conditions for de Sitter accelerating universe or the matter dominant universe. Every spacetime evolves into de Sitter universe or the matter dominant universe, if the given conditions are satisfied for  $\epsilon$ ,  $r_m$  and the initial value of  $B$ .

Here, just for simplicity, we study two typical cases with one free parameter  $c_3$ : (I)  $b_4 = c_4 = 0$  and (II)  $b_0 = 4c_3 + c_4 - 6 = 0$ . The first and second cases include the region (1), (3a) and (3c), and the region (2), (3b) and (3c), respectively. (See the corresponding red dashed lines in Fig.3.1.)

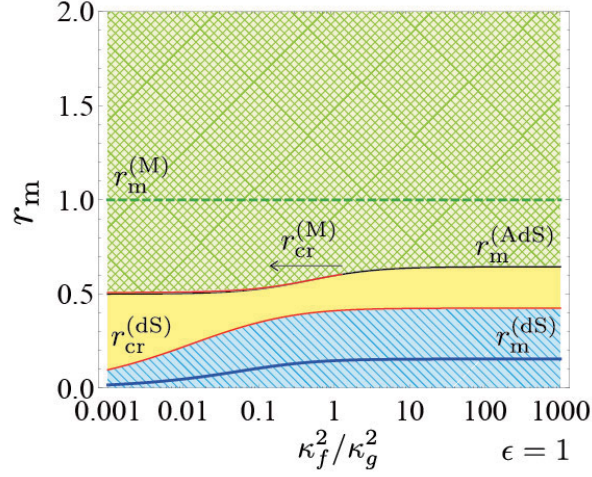
In Figs. 5.11 (a) and (b), for those two cases (I) and (II), we show which range of  $r_m$  can reach to de Sitter universe or the matter dominant universe, The blue solid curve and green dashed line denote de Sitter solution and the matter dominated universe, respectively. For the dS solutions, the value of  $\epsilon$  is negative in the regions (3a), (3b) and (3c) while it is positive in the regions (1) and (2).

In the region (3c), all spacetime evolves into either de Sitter self-accelerating universe or matter dominant universe, except for the time reversed ones, which collapse into a big crunch. On the other hand, in the regions (1), (2), (3a) and (3b), there exists a critical value  $r_{\text{cr}}^{(\text{dS})}$ , beyond (below) which spacetime with an appropriate initial condition evolves into de Sitter universe. However, the case with other initial data will evolve into either matter dominant universe or find a singularity. We note the critical values  $r_{\text{cr}}^{(\text{M})}$  are extremely close to  $r_m^{(\text{AdS})}$  and these appear only if  $-1.09 < c_3 < 0.55$  for Case (I) and  $2.27 < c_3 < 4.09$  for Case (II). Outside these regions, magnitude relation between  $B_{\text{cr}}$  and  $r_m$  is  $B_{\text{cr}} > r_m > r_m^{(\text{M})}$  or  $B_{\text{cr}} < r_m < r_m^{(\text{M})}$ , which dose not satisfy the additional constraint (5.3.5).

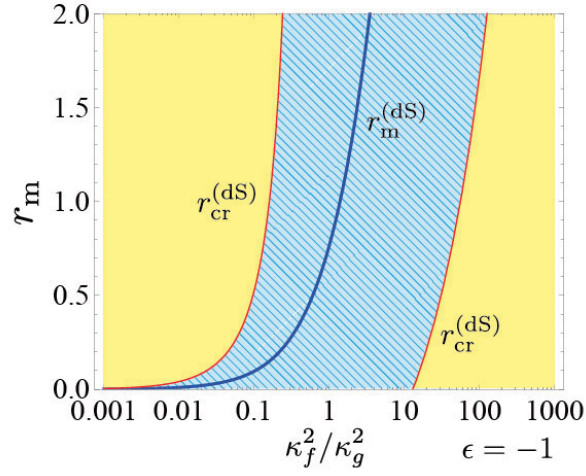
In order to see the dependence of gravitational constants  $\kappa_g$  and  $\kappa_f$ , we change the ratio of gravitational constants  $\kappa_f/\kappa_g$  by fixing the coupling constants  $\{b_i\}$ . In Figs.5.12 (a) and (b), we show the results for different values of the ratio  $\kappa_f^2/\kappa_g^2$  for Model B ( $c_3 = 4, c_4 = -10$ ) and Model E ( $c_3 = 3, c_4 = 0$ ), respectively. The result is qualitatively same in Model B except for the existence of  $r_{\text{cr}}^{(\text{M})}$ , while it is quite different in Model E. For Model B, the critical value  $r_{\text{cr}}^{(\text{M})}$  appears only if  $\kappa_f^2/\kappa_g^2 < 1.26$  as shown in Fig. 5.11. For Model E, all spacetime evolves into de Sitter universe if  $0.522408 < \kappa_f^2/\kappa_g^2 < 13.0711$ , otherwise a critical value appears as Model B.

Hence we can conclude that no hair conjecture does not always hold in the exact sense, but a self-accelerating universe can be found from natural (not fine-tuned) initial data for general coupling parameters and gravitational constants.

We should note the effect of radiation. Although the present radiation density is much less than matter density in our universe, it may not be the case for  $f$ -matter fields. Analyzing the case that  $f$ -radiation density is not ignorable, we find that the dynamics of the universe does not change so much from the matter dominated case.



(a)



(b)

Figure 5.12: The similar figures to Fig. 5.11 for different values of  $\kappa_f^2/\kappa_g^2$ . We plot the results for (a) Model B ( $c_3 = 4, c_4 = -10$ ) and (b) Model E ( $c_3 = 3, c_4 = 0$ ). For Model B, in addition to the critical value  $r_{\text{cr}}^{(\text{dS})}$  another critical value  $r_{\text{cr}}^{(\text{M})}$  appears if  $\kappa_f^2/\kappa_g^2 < 1.26$ . For Model E, no critical value appears if  $0.522408 < \kappa_f^2/\kappa_g^2 < 13.0711$ . All spacetime approach de Sitter universe.

## Chapter 6

# Stability in the early universe

When we obtain a homogeneous and isotropic solution, the next question is whether such a background dynamics is stable against small perturbations. In modified theories of the gravity, new gravitational degrees of freedom generally appear in addition to the usual tensor degrees of freedom. The extra degrees of freedom can be pathological if the extra mode suffers from the ghost instability and/or the gradient instability. When the instability exists only in IR regime, the instability is not so pathological, rather it can be recast in the Jeans-like instability [150]. In general, however, the existence of the ghost instability and/or the gradient instability suggests that the time scale of the instability can be arbitrarily fast and then the instability exists in UV regime. In order that the background dynamics is viable, the extra degrees of freedom have to be free from the ghost instability and the gradient instability.

In bigravity, although the solution can be free from the instability at the late stage of the universe, the instability exists at the early stage of the universe [57–62]. The instability should be related to the Higuchi-type instability discussed in Section 2.4. Since the bigravity contains the massive graviton and the Fierz-Pauli graviton becomes unstable when the background spacetime is the FLRW spacetime with  $H^2 \gtrsim m^2$ , the cosmology in bigravity may be also unstable when the Hubble expansion rate is larger than the graviton mass. Indeed, the perturbations around the homothetic background can be decomposed into the massless graviton mode and the massive graviton mode where the massive graviton is described by the Fierz-Pauli theory, thus the homothetic FLRW background must be unstable. Although perturbations around the general FLRW solution in bigravity are no longer reduced to the Fierz-Pauli theory, the instability at the early stage of the universe implies that the general FLRW solution also suffers from the Higuchi-type instability.

However, such an instability is quite obscure in the physical interpretation, since the natural expectation would be that one may not distinguish the massive theory from its corresponding massless theory when the horizon scale is larger than the Compton wavelength. Hence, the instability should be resolved without either a modification of the theory or an extra ingredient, if the bigravity theory is a reliable theory in such an energy scale. The instability may simply hint the possibility that the linear perturbations are no longer valid. Therefore, before we conclude the bigravity theory breaks down in the early stage of the Universe, it is instructive to take into account the nonlinear interactions. Indeed, in the paper [63], we found that a stable cosmological solution can exist even at the early stage of the universe when the nonlinearity of the scalar mode of the massive graviton is taken into account. We shall summarize the result of [63] in this chapter.

### 6.1 Ghost condensate and cosmological Vainshtein mechanism

The existence of the ghost instability usually destroys the viability of the theory since the energy of the unstable mode rapidly transfers to those of other modes and then the vacuum is unstable. Indeed, quantum mechanically, the ghost mode leads to a divergent decay rate [151].

However, the ghost instability is controllable if the ghost mode forms a condensed state. This

kind of models is dubbed the ghost condensate model [152]. A simple example is given by the Lagrangian  $\mathcal{L} = P(X)$  with

$$P(X) = -X + \frac{X^2}{M^4}. \quad (6.1.1)$$

where  $X = -\frac{1}{2}(\partial\phi)^2$  is the canonical kinetic term of the scalar field. The Lagrangian reads the equation of motion

$$\partial^\mu \left[ \partial_\mu \phi + \frac{1}{M^4} \partial_\mu \phi (\partial\phi)^2 \right] = 0. \quad (6.1.2)$$

When we assume the ansatz  $\phi = \phi(t)$ , the solutions are given by

$$\phi = 0, vt, \quad (6.1.3)$$

where  $v = M^2$ . Clearly, this Lagrangian contains the ghost around the vacuum  $\langle\phi\rangle = 0$  and then the vacuum  $\langle\phi\rangle = 0$  is unstable. On the other hand, when the velocity of the scalar field has a non-zero expectation value  $\langle\dot{\phi}\rangle = vt$ , the scalar field can be decomposed into the background and the fluctuations in the form

$$\phi = vt + \delta\phi(x). \quad (6.1.4)$$

Then the perturbed Hamiltonian reads

$$\delta\mathcal{H} = (\delta\dot{\phi})^2 \geq 0, \quad (6.1.5)$$

thus the perturbed Hamiltonian is bounded from below. Hence, the condensed state  $\langle\phi\rangle = vt$  does not suffer from the instability and give a stable homogeneous and isotropic solution when the gravitational effect is included.

As discussed in Section 2.4, the Fierz-Pauli theory on the FLRW spacetime is unstable in the early stage of the universe due to the ghost instability or the gradient instability depending on the dynamics of the universe. In bigravity, since the Fierz-Pauli theory is obtained around the homothetic spacetime, the homothetic FLRW spacetime is unstable. However, similarly to the ghost condensate, the existence of the instability is not a problem if the theory admits another stable FLRW spacetime.

In the ghost condensate, the homogeneous and isotropic solution can be found because the background value of the scalar field depends only on the time. In bigravity, however, it was shown that the general homogeneous and isotropic solutions are unstable [57–62], which suggests that the non-zero expectation value of the time derivative cannot give a stable solution. To obtain a condensed state, spatial derivatives must be non-zero but they may spoil the homogeneity of the spacetime in general.

The Higuchi-type instability arises from the scalar graviton which is encoded in the Stückelberg fields. The instability would lead to the growth of Stückelberg fields and then the nonlinear effects of Stückelberg fields have to be included. Although it seems that the spacetime becomes inhomogeneous due to the growth of Stückelberg fields, the spacetime can be homogeneous when the Vainshtein mechanism works in which the dynamics of the spacetime is decoupled from that of Stückelberg fields. Therefore, the cosmological Vainshtein mechanism could give a successful cosmology in which the Stückelberg fields are condensed with non-zero spatial derivatives but the inhomogeneity of Stückelberg fields does not affect the spacetime due to the Vainshtein screening.

The unstable era  $H \gg m$  is a viable region of the  $\Lambda_2$  decoupling limit. As discussed in Section 4.5, the  $\Lambda_2$  decoupling limit give an effective theory for the Vainshtein mechanism. The  $\Lambda_2$  decoupling limit can be taken if the curvature of the spacetime satisfies  $R \gg m^2$ . Indeed, by using the Einstein equation, the curvature is typically given by  $R \sim M_{\text{pl}}^{-2} T^4$  where  $T$  is the temperature of the matter fluid. Then the unstable era  $H \gg m$  reads  $T \gg \Lambda_2$ . Since the Stückelberg field does not give any effect on the spacetime in the  $\Lambda_2$  decoupling limit, the cosmological Vainshtein mechanism could be realized in the universe with  $T \gg \Lambda_2$ .

For this reason, we shall consider the perturbation around the flat FLRW background retaining nonlinearities of the Stückelberg fields. We then discuss whether the Stückelberg fields can be stabilized by nonlinear interactions of the scalar graviton and whether the fifth force can be screened in the early stage of the Universe.

## 6.2 Scalar graviton with nonlinear effects

To ease the difficulty in analyzing non-linear effects for a generic spacetime, we restrict our analysis to a spherically symmetric configuration of cosmological solutions. Even in a spherically symmetric system, however, it is still difficult to discuss full nonlinear effects without resorting to numerical simulations. Hence, we consider some simplified case.

We consider nonlinear perturbations on homothetic flat FLRW backgrounds:

$$d\bar{s}_g^2 = a^2(\eta)(-d\eta^2 + dr^2 + r^2 d\Omega^2), \quad (6.2.1)$$

$$d\bar{s}_f^2 = K^2 a^2(\eta)(-d\eta^2 + dr^2 + r^2 d\Omega^2). \quad (6.2.2)$$

where  $d\Omega^2 = d\theta^2 + \sin^2\theta d\varphi^2$ . This homothetic solution satisfies

$$3H^2 = \kappa_g^2 \bar{\rho}_g + \Lambda_g, \quad (6.2.3)$$

$$\frac{\dot{\bar{\rho}}_g}{a} + 3H(\bar{\rho}_g + \bar{P}_g) = 0, \quad (6.2.4)$$

with

$$\Lambda_g = K^2 \Lambda_f, \quad (6.2.5)$$

$$\kappa_g^2 \bar{\rho}_g = K^2 \kappa_f^2 \bar{\rho}_f, \quad \kappa_g^2 \bar{P}_g = K^2 \kappa_f^2 \bar{P}_f, \quad (6.2.6)$$

where  $H = \dot{a}/a^2$  and a dot is the derivative with respect to the conformal time  $\eta$ . We define the effective equation-of-state parameter  $w$  by

$$w := \frac{\kappa_g^2 \bar{P}_g - \Lambda_g}{\kappa_g^2 \bar{\rho}_g + \Lambda_g} = -1 - \frac{2\dot{H}}{3aH^2}. \quad (6.2.7)$$

For general nonlinear perturbations, it is difficult, if not impossible, to do an analysis even for spherically symmetric system without numerical simulations. Hence we discuss the following approximated model. First we impose spherical symmetry at full order and assume that the  $g$ - and  $f$ -spacetimes are approximated by the FLRW metric such that

$$ds_g^2 = a^2(\eta_g) [-e^{2\Phi_g} d\eta_g^2 + e^{2\Psi_g} dr_g^2 + r_g^2 d\Omega^2], \quad (6.2.8)$$

$$ds_f^2 = K^2 a^2(\eta_f) [-e^{2\Phi_f} d\eta_f^2 + e^{2\Psi_f} dr_f^2 + r_f^2 d\Omega^2], \quad (6.2.9)$$

where we introduce two coordinate systems  $(\eta_g, r_g)$  and  $(\eta_f, r_f)$  to describe the approximated FLRW spacetimes, which are given by different coordinate transformations from the original one coordinate system  $(\eta, r)$  as

$$\begin{aligned} \eta_g &= \eta_g(\eta, r), & r_g &= r_g(\eta, r), \\ \eta_f &= \eta_f(\eta, r), & r_f &= r_f(\eta, r). \end{aligned}$$

The approximated FLRW spacetimes mean that we assume  $|\Phi_g|, |\Psi_g| \ll 1$  and  $|\Phi_f|, |\Psi_f| \ll 1$  because the mass interaction term, which is proportional to  $m_{\text{eff}}^2/R_0$ , where  $R_0$  is the scale of the curvature, and gives the deviation from GR, is assumed be small. However they do not mean  $(\eta_g, r_g) \approx (\eta, r)$  and  $(\eta_f, r_f) \approx (\eta, r)$ , in which case the deviation from homothetic spacetimes is small and then can be described by the linear perturbations.

Although the bigravity theory allows one coordinate transformation, two independent coordinate transformations can be possible apparently by introducing the Stückelberg field such that

$$\eta_f = \eta_g + \mathcal{A}^\eta, \quad r_f = r_g + \mathcal{A}^r, \quad (6.2.10)$$

where  $(\mathcal{A}^\eta, \mathcal{A}^r)$  is the Stückelberg field in the spherically symmetric case. Using a gauge freedom, we can fix one coordinate system.

We also assume that for the unperturbed FLRW spacetimes,  $K$  and  $a$  are given by Eqs. (6.2.4), (6.2.5) and (6.2.6) although they are not homothetic. This is allowed as we obtain the consistent perturbation equations with this ansatz.

For the following discussions, we consider only a sub-horizon scale ( $aL \ll H^{-1}$ ) and a length smaller than the Compton wavelength of the massive graviton ( $aL \ll m_{\text{eff}}^{-1}$ ). This is because our interest is the sub-horizon physics during the epoch  $H > m_{\text{eff}}$  and such a solution provides us a stable cosmological Vainshtein mechanism. We define a dimensionless parameter as

$$\epsilon := \frac{aL}{H^{-1}} = aLH, \quad (6.2.11)$$

which satisfies  $\epsilon \ll 1$  for a sub-horizon scale.

For a spherically symmetric spacetime, we can divide the behavior of all variables into two: one is a slowly changing longitudinal mode mainly due to the background expansion and matter distributions, and the other is a fast changing wave-like oscillation mode of a scalar graviton. If the wave amplitude of the oscillation mode is small, when we take an average over the typical scale of the system  $aL$ , which is smaller than the horizon scale  $H^{-1}$ , we find only longitudinal-mode variables, which we call adiabatic modes. We then decompose all variables  $X$  into adiabatic and oscillation modes as

$$X = X^{\text{ad}} + \chi^{\text{osc}}, \quad (6.2.12)$$

with

$$X^{\text{ad}} \approx \langle X \rangle, \quad (6.2.13)$$

where  $\langle \rangle$  denotes an average over the typical scale of the system. Since we have assumed that the amplitude of the oscillation mode is sufficiently small, we will ignore the back-reaction from the oscillation mode to the adiabatic mode.

The dynamical time scale of the adiabatic mode is assumed to be the Hubble time scale, and then its evolution is caused by the expansion of the Universe and of the density perturbations. On the other hand, the oscillation mode comes from the degree of freedom of the scalar graviton. The time scale of the oscillation mode may be the same order of the inhomogeneity scale. Then each change rate is evaluated as

$$|\partial_\eta X^{\text{ad}}| \sim |aH X^{\text{ad}}|, \quad (6.2.14)$$

$$|\partial_\eta \chi^{\text{osc}}| \sim |\partial_r \chi^{\text{osc}}|. \quad (6.2.15)$$

Since we consider a sub-horizon scale ( $aL < H^{-1}$ ), the dynamical time scale of an oscillation mode is much shorter than the Hubble expansion time, i.e.,

$$|\partial_r \chi^{\text{osc}}| \gg |aH \chi^{\text{osc}}|. \quad (6.2.16)$$

Since the adiabatic mode may be obtained by taking the spatial average over the typical scale of the system, if the oscillation mode is small, we can assume that the dynamics of the adiabatic mode is decoupled from the dynamics of the oscillation mode. This assumption is valid if the small oscillation mode has no instability. Hence we first consider the evolution of the adiabatic modes without the oscillation modes. Then we study the dynamics of the oscillation modes around this adiabatic solution.

### 6.2.1 Adiabatic mode solution

We first discuss the time evolution of the adiabatic modes for the case without matter perturbations in order to see the behavior of non-linear Stückelberg field. The full analysis including matter perturbations will be discussed in Section 6.3, and the explicit expressions will be summarized in §. 6.3.1.

For the adiabatic modes, we fix the gauge freedom (6.2.10) by setting

$$\eta_g = \eta, \quad r_g = r, \quad (6.2.17)$$

and introduce the dimensionless variables  $\nu$  and  $\mu$  to parametrize  $\eta_f$  and  $r_f$  as

$$\eta_f = (1 + \nu)\eta, \quad r_f = (1 + \mu)r. \quad (6.2.18)$$



We assume that the time coordinate  $\eta_f$  and the radial coordinate  $r_f$  point the same directions of  $\eta_g$  and  $r_g$ , respectively, i.e.,

$$\nu > -1, \quad \mu > -1. \quad (6.2.19)$$

We have assumed the weak inhomogeneous gravitational fields around the FLRW spacetimes, i.e.,

$$|\Phi_g|, |\Psi_g|, |\Phi_f|, |\Psi_f| \ll 1, \quad (6.2.20)$$

and

$$|r\Phi'_g|, |r\Psi'_g|, |r\Phi'_f|, |r\Psi'_f| \ll 1, \quad (6.2.21)$$

which means that the perturbations from homogeneous and isotropic spacetimes are small. Note that this does not imply that the perturbations from the homothetic FLRW spacetime are small because of the existence of the non-linear Stückelberg field, i.e., either  $\nu$  or  $\mu$  are not necessarily small. The nonlinearities in the variables  $\nu$  and  $\mu$  must be retained. However we may assume those variables are not so large such that the perturbations of gravitational fields are still small, i.e.,

$$|\mu\Phi_g| \ll 1, \quad |r\mu'\Phi_g| \ll 1, \dots \quad (6.2.22)$$

The spatial derivative of the adiabatic mode may be evaluated by

$$|\partial_r X^{\text{ad}}| \sim L^{-1} |X^{\text{ad}}|, \quad L \lesssim r, \quad (6.2.23)$$

which leads with (6.2.14) to

$$|\partial_\eta X^{\text{ad}}| \sim \epsilon |\partial_r X^{\text{ad}}| \ll |\partial_r X^{\text{ad}}|. \quad (6.2.24)$$

Since the dynamical time scale of the adiabatic mode variables is given by  $H^{-1}$ , our spherically symmetric solution around the FLRW spacetimes must be restored to the static solution in the limit of  $H \rightarrow 0$ . The static and spherically symmetric solutions are explicitly shown in Chapter 8.

In a spherically symmetric static solution, the metric  $f_{\mu\nu}$  has no non-diagonal component in the coordinates  $(\eta, r)$ . Hence the non-diagonal component of  $f_{\mu\nu}$  is at most of the order of  $\epsilon$  in the present adiabatic solution around the FLRW spacetimes. The non-diagonal component is given by

$$f_{\eta r} = -K^2 a^2 [e^{2\Phi_f} (\eta + \eta\nu)' \eta\nu' - e^{2\Psi_f} (r + r\mu)' r\mu']. \quad (6.2.25)$$

where a prime denotes the derivative with respect to  $r$ . Because  $\dot{\nu} \sim aH\nu$ ,  $\dot{\mu} \sim aH\mu$  and  $|\Phi_f|, |\Psi_f| \ll 1$ , we find the leading contribution as, assuming  $K \sim \mathcal{O}(1)$ ,

$$f_{\eta r} \sim a^2 \mathcal{O}(\eta\nu', \epsilon\mu, \epsilon\mu^2) \quad (6.2.26)$$

which must be  $\mathcal{O}(\epsilon)$ . Since  $\eta\nu' \sim \nu/\epsilon \sim \mathcal{O}(\epsilon)$ , the Stückelberg variables  $\nu$  and  $\mu$  are evaluated as

$$|\nu| \lesssim \mathcal{O}(\epsilon^2), \quad |\mu| \lesssim \mathcal{O}(1). \quad (6.2.27)$$

We expand all basic equations up to the second order of  $\epsilon$ . The inhomogeneous gravitational fields  $\Phi_g, \Psi_g, \Phi_f, \Psi_f$  are determined by the Einstein equations, whose explicit solutions are given by Eqs. (6.3.2)-(6.3.5) in §. 6.3.1. The Stückelberg variable  $\nu$  is solved by the  $\eta$  component of the interaction conservation law  $\nabla_\alpha T^{[\gamma]\alpha}_\beta = 0$  as

$$\frac{\partial}{\partial r} \left[ \frac{r^2}{2 + (r\mu)'} \left( \eta\nu' + arH\mu(2 + (r\mu)') + r\dot{\mu} \right) \times (1 + 2\beta_2\mu + \beta_3\mu^2) \right] = 0, \quad (6.2.28)$$

where the parameters  $\beta_2$  and  $\beta_3$  are defined by

$$\beta_2 := \frac{b_2 K^2 + b_3 K^3}{b_1 K + 2b_2 K^2 + b_3 K^3}, \quad (6.2.29)$$

$$\beta_3 := \frac{b_3 K^3}{b_1 K + 2b_2 K^2 + b_3 K^3}. \quad (6.2.30)$$

Eq. (6.2.28) is integrable. An integral constant must be zero because of the regularity condition at  $r = 0$ . Hence we obtain two cases: The first parenthesis in the square brackets of (6.2.28) vanishes or the second one does so. If the second parenthesis vanishes,  $\mu$  is a constant. However, barring special tuning of model parameters, such a solution cannot reproduce the static result in the limit of  $H \rightarrow 0$ . Hence we conclude that the first parenthesis vanishes, i.e.,

$$\eta\nu' = -Har\mu(2 + (r\mu)') - r\dot{\mu}, \quad (6.2.31)$$

which determines  $\nu$  by giving  $\mu$ . This expression shows that the condition (6.2.27) is consistent.

Substituting (6.2.31), together with later obtained Eqs. (6.3.2)-(6.3.5), into the  $r$  component of  $\nabla_\alpha T^{[\gamma]\alpha}_\beta = 0$ , we obtain an algebraic equation for another Stückelberg variable  $\mu$  as

$$\mathcal{C}_{m^2}(\mu) + \mathcal{C}_{H^2}(\mu) = 0, \quad (6.2.32)$$

where both  $\mathcal{C}_{m^2}$  and  $\mathcal{C}_{H^2}$  are quintic functions of  $\mu$  (The explicit forms are given in §. 6.3.1). These terms have typical magnitudes given by

$$\mathcal{C}_{m^2} \sim m_{\text{eff}}^2 \times \mathcal{O}(\mu), \quad \mathcal{C}_{H^2} \sim H^2 \times \mathcal{O}(\mu).$$

The equation (6.2.32) reproduces the static result (8.2.12) in the limit of  $H \rightarrow 0$  thus the expression is consistent with our assumptions.

Since  $\mu$  is determined by the algebraic equation (6.2.32),  $\mu$  has no dynamical degree of freedom. It is not surprising because we have ignored the oscillation mode which corresponds to the dynamical degree of freedom of the scalar graviton. As a result, the Stückelberg fields do not have any dynamical freedom in the adiabatic mode solutions.

From now on, we focus on the period of the Universe with  $H \gg m_{\text{eff}}$ , which corresponds to the early stage of the Universe. The algebraic equation (6.2.32) reduces

$$\mathcal{C}_{H^2} \approx 0. \quad (6.2.33)$$

This equation has at most four roots, which are given by  $\mu = -1$  and

$$\mu_0 = 0, \text{ and } \mu_\pm, \quad (6.2.34)$$

where

$$\mu_\pm = \frac{1 + (1 - 3w)\beta_2 \pm \sqrt{1 - 4\beta_2 + (1 - 3w)^2\beta_2^2 + 3(1 - w)(1 + 3w)\beta_3}}{-2\beta_2 + (1 + 3w)\beta_3}. \quad (6.2.35)$$

Since the root  $\mu = -1$  gives  $r_f = 0$  for any  $r$ , we do not adopt this solution, and consider only the other three roots  $\mu_0 = 0, \mu_\pm$ . Since those roots are constants, which depend on the coupling constants and equation-of-state parameter, we can classify the solutions of Eq. (6.2.32) by those roots, which we call the  $\mu_0$ -branches.

When we do not include matter perturbations, neglecting the contributions from the interaction terms (which are much smaller than  $\epsilon^2$  for  $H \gg m_{\text{eff}}$ ), the metric perturbations are solved as

$$\Phi_g, \Psi_g, \Phi_f, \Psi_f \approx 0. \quad (6.2.36)$$

Then two metrics are given by

$$\begin{aligned} ds_g^2 &= a^2(\eta) [-d\eta^2 + dr^2 + r^2 d\Omega^2], \\ ds_f^2 &= K^2 a^2(\eta_f) [-d\eta_f^2 + dr_f^2 + r_f^2 d\Omega^2], \end{aligned} \quad (6.2.37)$$

where the coordinates  $(\eta_f, r_f)$ , which correspond to the nonlinear modulations due to the adiabatic Stückelberg fields, deviating from the physical coordinates as

$$\eta_f = \eta - \frac{1}{2}Har^2(2\mu_0 + \mu_0^2), \quad r_f = (1 + \mu_0)r, \quad (6.2.38)$$

where we have integrated Eq. (6.2.31) for  $\nu$  setting  $\mu = \mu_0$ .

The solution  $\mu_0 = 0$  corresponds to the homothetic FLRW spacetimes, while we can also find the other approximately homogeneous and isotropic solutions with  $\mu_0 = \mu_{\pm}$  in the massless limit, in which the coordinate transformation from  $(\eta, r)$  to  $(\eta_f, r_f)$  is nonlinear. The solutions with  $\mu_0 = \mu_{\pm}$  are valid up to the second order of  $\epsilon$  with  $\epsilon \ll 1$  when the interaction terms can be ignored. Thus the solutions with the nonlinear Stückelberg variable  $\mu$  are not exactly homogeneous and isotropic spacetimes, but approximate homogeneity and isotropy still hold in the sub-horizon scales.

The solutions  $\mu_0 = \mu_{\pm}$  with the limit  $H \gg m_{\text{eff}}$  are indeed same as the solutions obtained by the  $\Lambda_2$  decoupling limit. In the limit  $H \gg m_{\text{eff}}$ , we have ignored the back-reaction from the Stückelberg variables to the variables of the spacetime. In this case, the dynamics of the spacetime variables are determined by the Einstein equations in GR and the dynamics of the variables  $\mu$  and  $\nu$  are determined by the conservation equation  $\nabla_{\alpha} T^{[\gamma]\alpha}_{\beta} = 0$ . On the other hand, when we take the  $\Lambda_2$  decoupling limit first, the equations for Stückelberg variables are obtained by the variation of the massive gravity nonlinear sigma model with the homothetic FLRW spacetimes with respect to the Stückelberg variables. The equation of motion in the  $\Lambda_2$  decoupling limit actually coincides with the equation with the limit  $H \gg m_{\text{eff}}$ .

### 6.2.2 Stability conditions of scalar graviton

Next, we consider the oscillation modes of perturbations. In the previous calculation, we discussed a spherically symmetric solution based on the adiabatic potential approximation. It does not contain the dynamical degree of freedom of the scalar graviton. In this subsection, we analyze the stability of the solution against the fluctuations of the scalar graviton with the condition  $H \gg m_{\text{eff}}$ .

We consider the following perturbations:

$$ds_g^2 = a^2(\eta_g) \left[ -e^{2(\Phi_g + \phi_g)} d\eta_g^2 + e^{2(\Psi_g + \psi_g)} dr_g^2 + r_g^2 d\Omega^2 \right], \quad (6.2.39)$$

$$ds_f^2 = K^2 a^2(\eta_f) \left[ -e^{2(\Phi_f + \phi_f)} d\eta_f^2 + e^{2(\Psi_f + \psi_f)} dr_f^2 + r_f^2 d\Omega^2 \right]. \quad (6.2.40)$$

We divide the perturbations into the adiabatic and oscillation modes. When we take an average over the typical scale of the system, the oscillation-mode perturbations do not contribute, and the equations for the adiabatic equations are obtained. We solved them in the previous subsection. When the oscillation-mode perturbations are defined by

$$\chi^{\text{osc}} = X - X^{\text{ad}}, \quad (6.2.41)$$

the equations that govern their evolution are found by subtraction of the adiabatic modes from the full perturbation equations.

Using a gauge freedom of the oscillation-mode perturbations, as in (6.2.10), we set two coordinates as

$$\eta_g = \eta + \delta\eta(\eta, r), \quad r_g = r + \delta r(\eta, r), \quad (6.2.42)$$

$$\eta_f = \eta - \frac{1}{2}Har^2(2\mu_0 + \mu_0^2), \quad r_f = (1 + \mu_0)r, \quad (6.2.43)$$

where we have used the previous solutions for the adiabatic mode.

While  $(\Phi_g, \Psi_g, \Phi_f, \Psi_f)$  are the adiabatic modes,  $(\phi_g, \psi_g, \phi_f, \psi_f, \delta\eta, \delta r)$  are the oscillation modes of perturbations. We assume that all oscillation-mode variables have small amplitudes, i.e.,  $|\chi^{\text{osc}}| \ll 1$ , and the rate of their change in time is roughly  $|\partial_{\eta}\chi^{\text{osc}}| \sim |\partial_r\chi^{\text{osc}}|$ .

We find that the perturbed metric variables are not dynamical and they vanish in the limit of  $m_{\text{eff}}/H \rightarrow 0$ . This is easy to see from the equation of motion as follows: The Einstein curvature

tensors contain the terms proportional to  $H^2$ , while the energy-momentum tensors of the interaction term are proportional to  $m_{\text{eff}}^2$ . For instance, the  $(\eta_g, \eta_g)$ -component of the Einstein equations in the coordinates  $(\eta, r)$  gives

$$\begin{aligned} & 6H^2\phi_g - \frac{2}{a^2r^2} \frac{\partial(r\psi_g)}{\partial r} - \frac{2H}{a} \frac{\partial\psi_g}{\partial\eta} \\ &= m_{\text{eff}}^2 \frac{\kappa_g^2}{\kappa_-^2} \left[ \frac{(1 + 2\beta_2\mu_0 + \beta_3\mu_0^2)}{r^2} \frac{\partial(r^2\delta r)}{\partial r} + \dots \right]. \end{aligned} \quad (6.2.44)$$

Taking into account other components of the Einstein equations, we see that the energy-momentum tensors of the interaction term are negligible compared to the Einstein tensors when

$$|\phi_g|, |\psi_g| \gg \frac{\kappa_g^2}{\kappa_-^2} \frac{m_{\text{eff}}^2}{H^2} |\partial_a \delta r|, \frac{\kappa_g^2}{\kappa_-^2} \frac{m_{\text{eff}}^2}{H^2} |\partial_a \delta \eta|, \quad (6.2.45)$$

where  $\partial_a = (\partial_\eta, \partial_r)$ . When the conditions (6.2.45) hold, i.e., for the early stage of the Universe with  $m_{\text{eff}} \ll H$ , it is justified that the Einstein equations in bigravity is restored to the GR form. In such a stage, the Einstein equations for  $g_{\mu\nu}$  give the solution:

$$\phi_g \approx 0, \quad \psi_g \approx 0. \quad (6.2.46)$$

This result is convincing because there is no dynamical degree of freedom in a spherically symmetric system without matter perturbations in GR. By the same argument as above, we also find

$$\phi_f \approx 0, \quad \psi_f \approx 0, \quad (6.2.47)$$

from the Einstein equations for  $f_{\mu\nu}$ . This is, of course, the consequence that our limit  $m_{\text{eff}}/H \rightarrow 0$  is essentially same as the  $\Lambda_2$  decoupling limit and the dynamics of the spacetimes are restored into those in GR in the  $\Lambda_2$  decoupling limit.

In the limit of  $m_{\text{eff}}/H \rightarrow 0$ , we find that two metrics without matter perturbations are given by

$$ds_g^2 = a^2(\eta_g) [-d\eta_g^2 + dr_g^2 + r_g^2 d\Omega^2], \quad (6.2.48)$$

$$ds_f^2 = K^2 a^2(\eta_f) [-d\eta_f^2 + dr_f^2 + r_f^2 d\Omega^2]. \quad (6.2.49)$$

We then expand the action in terms of  $(\delta\eta, \delta r)$  up to the second order of  $\epsilon$ . The variations with respect to  $\delta\eta$  and  $\delta r$  give the constraint equations, which are solved such that the Stückelberg variables  $\delta\eta$  and  $\delta r$  are given by

$$\delta\eta = -\frac{\partial_\eta \pi}{a^2} + \frac{arH\mu_0}{1+\mu_0} \frac{\partial_r \pi}{a^2} + \mathcal{O}(\epsilon^2), \quad (6.2.50)$$

$$\delta r = \frac{\partial_r \pi}{a^2(1+\mu_0)} + \frac{arH\mu_0}{1+\mu_0} \frac{\partial_\eta \pi}{a^2} + \mathcal{O}(\epsilon^2), \quad (6.2.51)$$

in terms of a Stückelberg scalar  $\pi$ . For the analysis of stability, it is sufficient to determine  $\delta\eta$  and  $\delta r$  up to the first order of  $\epsilon$ .

Substituting (6.2.50) and (6.2.51) into the action, we obtain the quadratic action of  $\pi$  as

$$S_2 = \frac{m_{\text{eff}}^2}{\kappa_-^2} \int d\Omega \int d\eta dr (arH)^2 \mathcal{K}_S \left[ (\partial_\eta \pi)^2 - c_S^2 (\partial_r \pi)^2 \right], \quad (6.2.52)$$

where  $\Omega$  is the solid angle. The signs of these coefficients  $\mathcal{K}_S$  and  $c_S^2$  determine the stability of the Stückelberg scalar  $\pi$ , which corresponds to the scalar graviton.

For the  $\mu_0 = 0$ -branch, the coefficients are given by

$$\mathcal{K}_S|_{\mu_0=0} = \frac{3}{4}(1+3w), \quad (6.2.53)$$

$$c_S^2|_{\mu_0=0} = \frac{w-1}{1+3w}, \quad (6.2.54)$$

which is consistent with the result (2.4.15). On the other hand, for the  $\mu_0 = \mu_{\pm}$ -branches, after simplifying the expressions by using (6.2.35), we find

$$\mathcal{K}_S|_{\mu_0=\mu_{\pm}} = \frac{3}{4}(3w-1)(2+\mu_{\pm})(1+2\beta_2\mu_{\pm}+\beta_3\mu_{\pm}^2), \quad (6.2.55)$$

$$c_S^2|_{\mu_0=\mu_{\pm}} = \frac{2(3(1-w)+(1-(3w-1)\beta_2)\mu_{\pm})}{3(3w-1)(2+\mu_{\pm})(1+2\beta_2\mu_{\pm}+\beta_3\mu_{\pm}^2)}. \quad (6.2.56)$$

The no-ghost condition is given by  $\mathcal{K}_S > 0$  while the no-gradient instability condition is given by  $c_S^2 > 0$ . Hence, the stability condition of the scalar graviton is to have

$$\mathcal{K}_S > 0, \quad c_S^2 > 0. \quad (6.2.57)$$

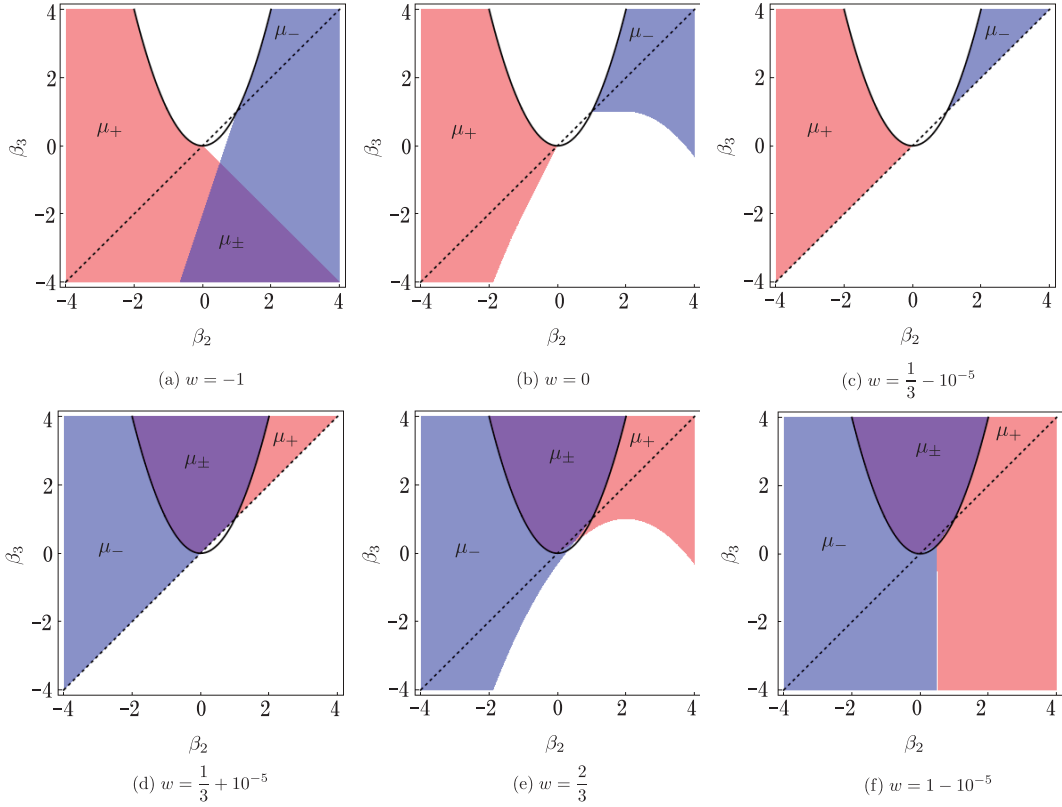


Figure 6.1: The stable regions of the coupling constants for flat FLRW backgrounds for the cases of  $w = -1$ ,  $w = 0$ ,  $w = 1/3 \pm 10^{-5}$ ,  $w = 2/3$  and  $w = 1 - 10^{-5}$ . The  $\mu_0 = \mu_+$ -branch is stable in the regions denoted by  $\mu_+$  (red regions), the  $\mu_0 = \mu_-$ -branch is stable in the regions denoted by  $\mu_-$  (blue regions), and both  $\mu_0 = \mu_{\pm}$  are stable in the regions denoted by  $\mu_{\pm}$  (purple regions). The black solid curves correspond to  $\beta_3 = \beta_2^2$  and the black dotted lines correspond to  $\beta_2 = \beta_3$ .

In the  $\mu_0 = 0$ -branch, either the ghost instability or the gradient instability appears for  $w < 1$ . So the instability is inevitable when the Universe consists of the standard matter, as shown in Section 2.4. Since the instability appears only in the relation between the two coordinate systems,  $(\eta_g, r_g)$  and  $(\eta_f, r_f)$ , two spacetimes still keep homogeneous approximately as long as the condition (6.2.45) holds. However, since  $\pi$  grows in time due to the instability in this branch, the condition (6.2.45) eventually breaks down.

On the other hand, the  $\mu_0 = \mu_{\pm}$ -branches can avoid the ghost instability as well as the gradient instability depending on the background dynamics and the coupling constants. In Fig. 6.1, we show the parameter regions where the solution is stable for the cases of  $w = -1$ ,  $w = 0$ ,  $w = 1/3 \pm 10^{-5}$ ,  $w = 2/3$  and  $w = 1 - 10^{-5}$ . Note that in the radiation dominant universe with  $w = 1/3$ , the action

is given by

$$S_2|_{w=1/3} = -\frac{m_{\text{eff}}^2(2+\mu_{\pm})}{2\kappa_-^2} \int d\Omega \int d\eta dr (arH)^2 (\partial_r \pi)^2, \quad (6.2.58)$$

which does not describe the dynamics of  $\pi$ <sup>1</sup>. Thus the expansions we have adopted in our calculation is invalidated in this limit, and in order to correctly study the dynamics of the scalar graviton, we must calculate either the higher-order terms of  $\pi$  or the higher-order corrections of  $\epsilon$ .

For  $w \simeq 1/3$ , the existence of the stable solution is guaranteed for the parameter region such that

$$\beta_2^2 > \beta_3 > \beta_2, \quad \text{for } w = \frac{1}{3} - |\delta w|, \quad (6.2.59)$$

$$\beta_3 > \beta_2, \quad \text{for } w = \frac{1}{3} + |\delta w|, \quad (6.2.60)$$

with  $|\delta w| \ll 1$ . In such a parameter region, at least one of  $\mu_{\pm}$  satisfies the stability condition (6.2.57) as well as our ansatz  $\mu_{\pm} > -1$ .

For  $w = 1$ ,  $\mu_{\pm}$  are given by

$$\mu_{\pm} = \frac{1 - 2\beta_2 \pm |1 - 2\beta_2|}{2(2\beta_3 - \beta_2)}. \quad (6.2.61)$$

Hence, one of  $\mu_{\pm}$  becomes zero, which gives the homothetic solution.

Since reducing the stability condition (6.2.57) to the allowed parameter region for arbitrary values of  $w$  is a nontrivial task due to the complicated dependence (6.2.35) of  $\mu_{\pm}$  on the model parameters, we analyze the stable region numerically. We conclude that the parameter region of

$$\beta_2^2 > \beta_3 > \beta_2, \quad (6.2.62)$$

guarantees the existence of a stable branch for any values of  $w$  except for  $w = 1/3$ . Even outside the region (6.2.62), we obtain stable branches for some values of  $w$ , but the instability always appears for near radiation dominant stage such that  $w = 1/3 - |\delta w|$ .

In the stable region (6.2.62), only one stable branch exists for any  $w$ . When the Universe consists of the usual matter field with  $w < 1$ , either  $\mu_0 = \mu_+$  or  $\mu_-$  gives a stable solution in the parameter region (6.2.62). While if the Universe is composed effectively of a ‘‘strange’’ matter field with  $w > 1$ , we find  $\mu_0 = \mu_{\pm}$ -branches are stable only in the region of  $\beta_3 > \beta_2^2$  (see Fig. 6.2), and the stable region disappears in the limit of  $w = \infty$  as shown in Fig. 6.2. As a result, only the  $\mu_0 = 0$ -branch becomes stable.

Although the condition (6.2.62) depends on the proportional factor  $K$ , we can derive the stability condition for the original coupling constants  $\{b_i\}$ . Since we assume  $m_{\text{eff}}^2 > 0$  (i.e.  $Kb_1 + 2K^2b_2 + K^3b_3 > 0$ ), the condition reduces to

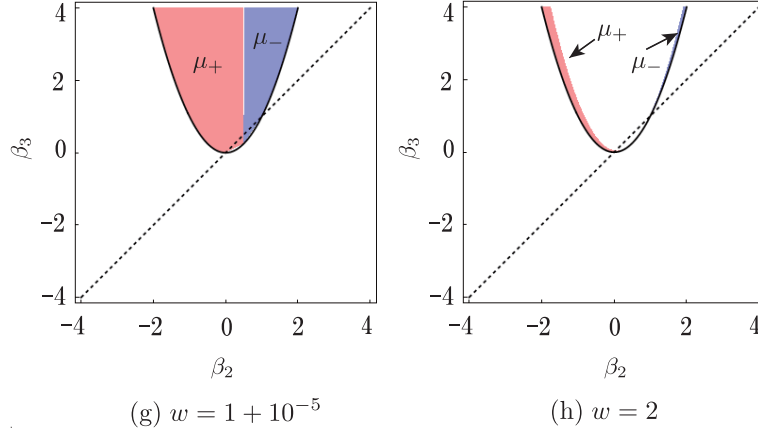
$$b_2^2 - b_1b_3 > 0, \quad b_2 < 0. \quad (6.2.63)$$

Therefore, if we choose the coupling constants in the above parameter regions (6.2.63), both ghost instability and gradient instability are avoided because of the nonlinear interactions, and then the early stage of the Universe described approximately by the solution in GR. That is, the big bang cosmology is stable.

### 6.3 Perturbations with matter effects

In this section, we consider the adiabatic modes retrieving matter perturbations and discuss the evolution history with the nonlinear effects of the Stückelberg fields. For the stable branch discussed in the previous section, the evolutions of the matter perturbations are approximated by the adiabatic modes. The oscillation modes of matter fluctuations decay in time [53]. Hence we can decouple the adiabatic and oscillation modes in this case as well.

<sup>1</sup> If we take into account the trace anomaly of quantum corrections, we find small deviation from  $w = 1/3$ . For example,  $w = \frac{1}{3} - \frac{5}{18\pi^2} \frac{g^4}{(4\pi)^2} \frac{(N_c + \frac{5}{2}N_f)(\frac{1}{3}N_c - \frac{2}{3}N_f)}{2 + \frac{g}{2}[N_c N_f / (N_c^2 - 1)]}$  for a plasma of the  $SU(N_c)$  gauge theory with coupling  $g$  and  $N_f$  flavors [153].

Figure 6.2: The same figures as Fig. 6.1 for the cases of  $w = 1 + 10^{-5}$  and  $w = 2$ .

### 6.3.1 Adiabatic mode with matter perturbations

Now we discuss the time evolution of the adiabatic modes with matter perturbations. The matter energy densities are perturbed as

$$\rho_g = \bar{\rho}_g(1 + \delta_g), \quad \rho_f = \bar{\rho}_f(1 + \delta_f). \quad (6.3.1)$$

We ignore pressure perturbations and spatial velocities compared to the density perturbations, just for simplicity.

All equations are expanded up to the second order in  $\epsilon$ . The Einstein equations for  $g_{\mu\nu}$  and  $f_{\mu\nu}$  give

$$2\Psi_g(\eta, r) = a^2(\eta)r^2 \left[ m_g^2 \left( \mu + \beta_2\mu^2 + \frac{\beta_3}{3}\mu^3 \right) + \frac{1}{3}\kappa_g^2\bar{\rho}_g\tilde{\delta}_g \right], \quad (6.3.2)$$

$$2r\frac{\partial\Phi_g}{\partial r}(\eta, r) = a^2(\eta)r^2 \left[ -m_g^2 \left( \mu - \frac{\beta_3}{3}\mu^3 \right) + \frac{1}{3}\kappa_g^2\bar{\rho}_g\tilde{\delta}_g \right], \quad (6.3.3)$$

and

$$2\Psi_f(\eta_f, r_f) = a^2(\eta_f)r_f^2 \left[ -\frac{m_f^2}{(1+\mu)^3} \left( \mu + (1+\beta_2)\mu^2 + \frac{1+\beta_2+\beta_3}{3}\mu^3 \right) + \frac{1}{3}K^2\kappa_f^2\bar{\rho}_f\tilde{\delta}_f \right], \quad (6.3.4)$$

$$2r_f\frac{\partial\Phi_f}{\partial r_f}(\eta_f, r_f) = a^2(\eta_f)r_f^2 \left[ \frac{m_f^2}{(1+\mu)^3} \left( \mu + 2\mu^2 + \frac{2+2\beta_2-\beta_3}{3}\mu^3 \right) + \frac{1}{3}K^2\kappa_f^2\bar{\rho}_f\tilde{\delta}_f \right], \quad (6.3.5)$$

respectively, where

$$\tilde{\delta}_g(\eta, r) := \frac{\int_0^r 4\pi\tilde{r}^2\delta_g d\tilde{r}}{\int_0^r 4\pi\tilde{r}^2 d\tilde{r}}, \quad \tilde{\delta}_f(\eta_f, r_f) := \frac{\int_0^{r_f} 4\pi\tilde{r}^2\delta_f d\tilde{r}}{\int_0^{r_f} 4\pi\tilde{r}^2 d\tilde{r}}, \quad (6.3.6)$$

are spatial averages of the density perturbations in the spheres with the radii  $r$  and  $r_f$ , respectively. The mass parameters are defined by (3.3.28)-(3.3.30).

Although the  $f$ -variables are given as the functions of  $(\eta_f, r_f)$ , it is easy to find them as the functions of  $(\eta, r)$  by use of the Stückelberg fields  $\nu$  and  $\mu$ . The variable  $\nu$  is determined by (6.2.31) even when the matter perturbations are included.

Substituting Eqs. (6.3.2)-(6.3.5) and (6.2.31) into the  $r$  component of  $\nabla_\alpha T^{[\gamma]\alpha}_\beta = 0$ , we obtain an algebraic equation for  $\mu$ :

$$\mathcal{C}_{m^2}(\mu) + \mathcal{C}_{H^2}(\mu) + \mathcal{C}_{\text{matter}}(\mu) = 0, \quad (6.3.7)$$

where we define each function as

$$\begin{aligned} \mathcal{C}_{m^2}(\mu) := & \mu \left\{ m_g^2 (1 + \mu)^2 [9 + 18\beta_2\mu + (6\beta_2^2 + 4\beta_3)\mu^2 - \beta_3^2\mu^4] \right. \\ & + m_f^2 \left[ 9 + 18(1 + \beta_2)\mu + (10 + 34\beta_2 + 4\beta_3 + 6\beta_2^2)\mu^2 \right. \\ & \left. \left. + (2 + 14\beta_2 + 8\beta_3 + 12\beta_2^2)\mu^3 + (2\beta_2 + 2\beta_3 + 2\beta_2^2 - \beta_3^2 + 4\beta_2\beta_3)\mu^4 \right] \right\}, \end{aligned} \quad (6.3.8)$$

$$\mathcal{C}_{H^2}(\mu) := -3H^2\mu(1 + \mu)^2 \left\{ 3(1 - w) + 2[1 + (1 - 3w)\beta_2]\mu + [2\beta_2 - (1 + 3w)\beta_3]\mu^2 \right\}, \quad (6.3.9)$$

$$\mathcal{C}_{\text{matter}}(\mu) := (1 + \mu)^2 \left\{ \kappa_g^2 \rho_g \tilde{\delta}_g (1 - \beta_3\mu^2) - K^2 \kappa_f^2 \rho_f \tilde{\delta}_f (1 + \mu) [1 + 2\mu + (2\beta_2 - \beta_3)\mu^2] \right\}. \quad (6.3.10)$$

Eq. (6.3.7) reproduces the static result (8.2.12) in the limit of  $H \rightarrow 0$ .

An important difference from the case without matter perturbations is that the variable  $\mu$  depends also on the matter perturbations. When the matter perturbations are not negligible, Eq. (6.2.32) should be replaced with Eq. (6.3.7), in which the typical value of the additional third term is evaluated by

$$\mathcal{C}_{\text{matter}} \sim \kappa_g^2 \rho_g \tilde{\delta}_g - K^2 \kappa_f^2 \rho_f \tilde{\delta}_f.$$

The metric perturbations are given by the GR results with the corrections coming from the interaction term, e.g., one of the perturbations of  $g_{\mu\nu}$  is given by

$$\Psi_g = \Psi_{\text{GR}} + a^2 r^2 m_{\text{eff}}^2 \times \frac{\kappa_g^2}{\kappa_-^2} \times \mathcal{O}(\mu). \quad (6.3.11)$$

When the second term is negligible compared to the first one, the metric perturbations are restored to the GR results. Since the equations of motion of twin matters are not modified from usual ones (e.g., see Eq. (3.3.10)), the restoration of the metric perturbations guarantees the dynamics of the matter is also restored to the GR result. Therefore we will discuss only the metric perturbations which are determined by  $\mu$  as in Eqs. (6.3.2)-(6.3.5).

### 6.3.2 GR phase

We discuss a stage when the Hubble parameter is larger than the effective graviton mass (i.e.,  $H^2 \gg m_{\text{eff}}^2$ ). Because  $\mathcal{C}_{H^2} \gg \mathcal{C}_{m^2}$ , Eq. (6.3.7) becomes

$$\mathcal{C}_{H^2} + \mathcal{C}_{\text{matter}} \approx 0. \quad (6.3.12)$$

Since the second term is much smaller than the first term, Eq. (6.3.12) is schematically solved as

$$\mu = \mu_0 + \mathcal{O}(\tilde{\delta}_g, \tilde{\delta}_f), \quad (6.3.13)$$

where  $|\tilde{\delta}_g|, |\tilde{\delta}_f| \ll 1$ . As discussed in the previous section, the stable branch is found with  $\mu_0 = \mu_{\pm}$  for  $w < 1$ , or with  $\mu_0 = 0$  for  $w > 1$ .

First, we consider the case of  $w < 1$ . The stable branch is given by one of  $\mu_{\pm}$ , and thus (6.3.12) is also solved as  $\mu \approx \mu_{\pm}$ . The gravitational sector is restored to the one in GR, when

$$\frac{\kappa_g^2}{\kappa_-^2} \times \frac{m_{\text{eff}}^2}{H^2} \ll \tilde{\delta}_g, \quad (6.3.14)$$

i.e., if the correction terms from the graviton mass are negligible compared to the GR terms in Eqs. (6.3.2)-(6.3.5). As a result, in the early stage of the Universe, the metric perturbations are restored to the GR results.

Next, we consider the case of  $w > 1$ , in which the stable branch is given by  $\mu_0 = 0$ . In this case, the solution is given by, assuming  $|\mu| \ll 1$ ,

$$\mu \approx \frac{\tilde{\delta}_g - \tilde{\delta}_f}{3(1 - w)}, \quad (6.3.15)$$



where we have used the background equations. One of the metric perturbations is described as

$$2\Psi_g = a^2 r^2 H^2 \tilde{\delta}_g + a^2 r^2 m_{\text{eff}}^2 \frac{\kappa_g^2}{\kappa_-^2} \frac{\tilde{\delta}_g - \tilde{\delta}_f}{3(1-w)}. \quad (6.3.16)$$

Since the second term is negligible compared to the first term in the case of  $H \gg m_{\text{eff}}$ , the metric perturbations are again restored to the GR results for  $w > 1$ .

Hence both cases show the GR limit in the early stage of the Universe ( $H \gg m_{\text{eff}}$ ). We shall call this stage the GR phase.

### 6.3.3 Bigravity phase

Secondly, we discuss the stage when the Hubble parameter is smaller than the effective graviton mass (i.e.,  $H^2 \ll m_{\text{eff}}^2$ ). In this stage, we find  $\mathcal{C}_{m^2} \gg \mathcal{C}_{H^2}$ . Hence, for the matter of our interest, Eq. (6.3.7) reduces to

$$\mathcal{C}_{m^2} + \mathcal{C}_{\text{matter}} \approx 0. \quad (6.3.17)$$

We denote the roots of  $\mathcal{C}_{m^2}(\mu) = 0$  by  $\mu_\infty$ , which are found to be zero and some constants of order unity. Similarly to the previous subsection, Eq. (6.3.17) is solved as

$$\mu = \mu_\infty + \frac{H^2}{m_{\text{eff}}^2} \times \mathcal{O}(\tilde{\delta}_g, \tilde{\delta}_f). \quad (6.3.18)$$

Since Eq. (6.3.17) is a polynomial equation of degree seven for  $\mu$ , there are seven solutions for  $\mu_\infty$ . We classify the solutions of Eq. (6.3.17) into two types: the linear branch and non-linear branches. Note that a branch here denotes one with  $\mu = \mu_\infty$  in the limit of  $H/m_{\text{eff}} \rightarrow 0$ .

The linear branch is realized by choosing  $\mu_\infty = 0$ . Eq. (6.3.17) gives the value of  $\mu$  as, assuming  $|\mu| \ll 1$ ,

$$\mu \approx -\frac{\kappa_g^2 \tilde{\rho}_g \tilde{\delta}_g - K^2 \kappa_f^2 \tilde{\rho}_f \tilde{\delta}_f}{9m_{\text{eff}}^2}. \quad (6.3.19)$$

Substituting this solution into the expression of the gravitational force (6.3.3), we find

$$\Phi'_g \approx \frac{a^2 r}{6} \left[ \left( 1 + \frac{m_g^2}{3m_{\text{eff}}^2} \right) \kappa_g^2 \tilde{\rho}_g - \frac{m_g^2}{3m_{\text{eff}}^2} K^2 \kappa_f^2 \tilde{\rho}_f \right]. \quad (6.3.20)$$

Hence the gravitational force in the  $g$ -sector is produced by the  $f$ -matter as well as the  $g$ -matter. We will detail why the  $f$ -matter affects the gravitational force in the  $g$ -spacetime in Section 7.1.

The nonlinear branches are obtained by choosing  $\mu_\infty \sim \mathcal{O}(1)$ . In this case, since  $|\mu_\infty| \gg |\tilde{\delta}_g|, |\tilde{\delta}_f|$ , the solutions are found to be

$$\mu \approx \mu_\infty, \quad (6.3.21)$$

giving the same as those without matter perturbations. For these nonlinear branches, the metric perturbations include the correction terms of the graviton masses as given in Eqs. (6.3.2)-(6.3.5). Hence, for these branches, there is a non-negligible inhomogeneity at large scale and the gravitational behavior deviate largely from GR's one beyond the Vainshtein radius. A question is the asymptotic structure of the nonlinear branch. In the bigravity phase, the limit  $H \rightarrow 0$  might be sufficient as a lowest-order approximation. In this limit, the adiabatic solutions turn to be the static ones. In the static case, as shown in [85], the nonlinear branches approaches a shell singularity or AdS spacetime when we introduce a negative cosmological constant. Hence, the nonlinear branch may not describe our Universe.

Since the gravitational behaviors are modified from the ones in GR due to the existence of the fifth force, mediated by the scalar mode of graviton, for both branches, we call this stage the bigravity phase.

## 6.4 Transition from GR to bigravity

As we have shown in the previous section, the universe in the bigravity theory has some stable branches in the both limits of  $H \gg m_{\text{eff}}$  and of  $H \ll m_{\text{eff}}$ , which correspond to the early and late stages of the universe, respectively. More precisely, in the early stage of the universe ( $H \gg m_{\text{eff}}$ ), the  $\mu_0 = 0$ -branch is unstable, while  $\mu_0 = \mu_{\pm}$ -branches can give the stable GR phase depending on the coupling constants. On the other hand, in the late stage of the universe ( $H \ll m_{\text{eff}}$ ), the branch with  $|\mu| \ll 1$ , which provide us the bigravity phase, is stable.

The question is whether any two stable branches with different limits can connect under our adiabatic approximation or not. We shall discuss this possibility in this section. Our Universe must start from the GR phase and transit to the bigravity phase. Then the Universe must pass through the period of  $H \sim m_{\text{eff}}$ , where the behavior of  $\mu$  becomes unclear.

One unknown in this period is the transition time scale, if the transition occurs. If the transition time scale is given by the Hubble time scale and the adiabatic mode is an attractor even in the period of  $H \sim m_{\text{eff}}$ , we can discuss the transition by considering only the adiabatic modes. However, if the transition time scale is faster than the Hubble time scale, the adiabatic approximation (6.2.24) is no longer valid, and a full analysis without approximation will be required.

Here, we only speculate some possible transitions based on the adiabatic approximation with the assumption (6.2.24). When the amplitudes of the density perturbations are given, one can obtain the Stückelberg modulation  $\mu$  in terms of  $H$  and  $\tilde{\delta}_{g/f}$  by solving the algebraic equation (6.3.7) together with the use of (6.2.3) and (6.2.6). Since  $H$  decreases in time, we find the evolution of  $\mu$  without solving the equations of motion, under the assumption that the solutions to (6.3.7) at different moments are continuously connected. Here we also assume that the density perturbations are constant in time; although they may evolve in time, the qualitative behavior does not change much.

We show several examples in Figs. 6.3 and 6.4. We have explored a wide range of the parameters with the stability condition (6.2.62).

As shown in Figs. 6.3 and 6.4, two stable branches in the limits of  $m_{\text{eff}}/H \ll 1$  and of  $m_{\text{eff}}/H \gg 1$  can be continuous or discontinuous depending on the equation-of-state parameter  $w$  and the density perturbations. For example, as shown in Fig. 6.3 (II), for  $w = 2/3$ , we find one continuous curve from the early stage to the late stage of the Universe, exhibiting the branch that is stable in both limits of  $m_{\text{eff}}/H \ll 1$  and of  $m_{\text{eff}}/H \gg 1$ , if  $\tilde{\delta}_g(= 10^{-2}) > \tilde{\delta}_f(= 10^{-3})$ . On the other hand, if  $\tilde{\delta}_g(= 10^{-3}) < \tilde{\delta}_f(= 10^{-2})$ , two (one stable and another unstable) continuous curves are splitted into two discontinuous curves as found in Fig. 6.3 (II). There are points at which two real roots of Eq. (6.3.7) degenerate and beyond which they become imaginary. At such points, the time derivative of  $\mu$  ( $d\mu/dH^{-1}$ ) diverges, but  $\mu$  itself is finite. At such a singular point, we argue that the scalar graviton is singular. This is because the variable  $\mu$  is basically related to the adiabatic mode of the scalar graviton  $\pi_0$  as  $\mu = a^{-2}\pi'_0/r$ . So when  $\partial\mu \rightarrow \pm\infty$  (or  $\partial\pi \rightarrow \infty$ ), a singular behavior of the scalar graviton may appear.

However, near such a singular point, our assumption (6.2.24) is no longer valid. This singular behavior may simply be an artifact of our adiabatic assumption, and if we analyze the full nonlinear dynamics without the adiabatic approximation, this singularity may not appear. Hence, when we find a discontinuity in the solution  $\mu(H)$ , what happens in the transition period is still an open problem. In what follows, we just discuss the adiabatic solutions given by the continuous curves.

We classify our results into two cases: Case A and Case B. Some examples of Case A are given in Fig. 6.3, while those of Case B are in Fig. 6.4. In both cases, there is a continuous curve from GR phase to bigravity phase when  $\tilde{\delta}_g > \tilde{\delta}_f$  with  $w > 1/3$  which may give a viable phase transition with the adiabatic approximation. However, either  $w < 1/3$  or  $\tilde{\delta}_g < \tilde{\delta}_f$  cannot give such a transition. In particular, when  $w < 1/3$ , the GR phase may transit to the nonlinear branch in the bigravity phase in Case A; while the GR phase approaches to the singularity in Case B.

From the above analysis, we conclude that for  $w > 1/3$ , there exists a stable adiabatic solution, which describes that the Universe evolves from a GR phase in the early stage to a linear bigravity phase in the late stage. For more realistic equation-of-state parameter  $w < 1/3$ , however, if the transition from the GR phase to the linear bigravity phase occurs, the transition time scale is likely to be faster than  $H^{-1}$  and then the adiabatic condition must no longer be valid <sup>2</sup>. In

<sup>2</sup>One may argue the possibility that the transition might occur with a Hubble time scale by taking into account

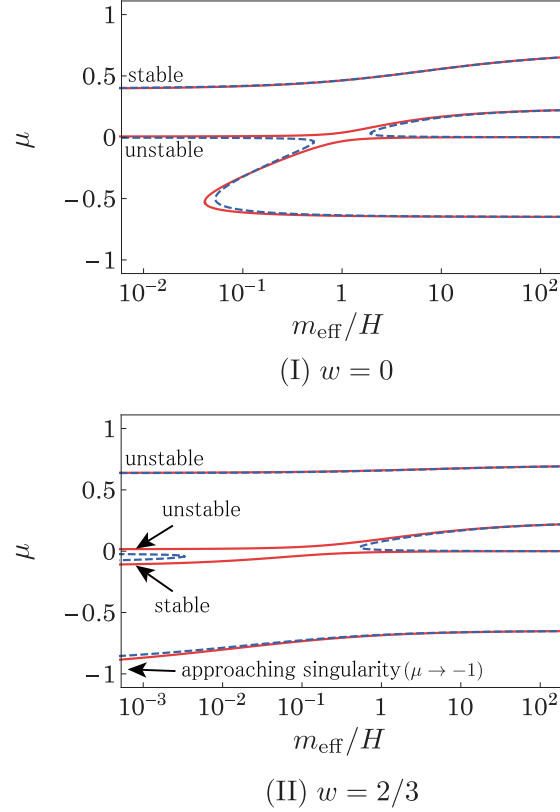


Figure 6.3: Case A: There exists a continuous curve from  $\mu_0$  to the branch with non-linear  $\mu_\infty$  ( $\sim O(1)$ ). We plot the roots of Eq. (6.3.7) for  $\tilde{\delta}_g = 10^{-2}, \tilde{\delta}_f = 10^{-3}$  (red curves) and for  $\tilde{\delta}_g = 10^{-3}, \tilde{\delta}_f = 10^{-2}$  (blue dashed curves). We set  $\beta_2 = -3, \beta_3 = 3, m_g^2 = m_f^2$ . The branch with  $\mu_0 \simeq 0.40$  for  $w = 0$  and  $\mu_0 \simeq -0.10$  for  $w = 2/3$  are stable in the early stage of the Universe ( $m_{\text{eff}}/H \ll 1$ ). The Universe may evolve from the stable  $\mu_0$ -branch to the  $\mu_\infty$ -branch. For example, for  $w = 0$ ,  $\mu$  changes from  $\mu_0 = 0.4$  (GR phase) to  $\mu_\infty = 0.7$  (nonlinear bigravity phase), while for  $w = 2/3$ , it does from  $\mu_0 = -0.1$  (GR phase) to  $\mu_\infty = 0$  (linear bigravity phase).

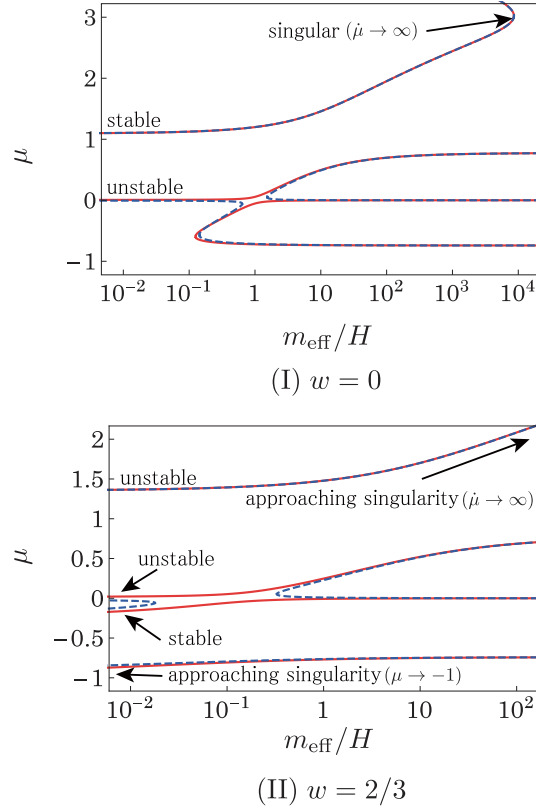


Figure 6.4: Case B: There exists no continuous curve from  $\mu_0$  to the branch with non-linear  $\mu_\infty (\sim O(1))$ . We plot the roots of Eq. (6.3.7) for  $\tilde{\delta}_g = 10^{-2}, \tilde{\delta}_f = 10^{-3}$  (red curves) and  $\tilde{\delta}_g = 10^{-3}, \tilde{\delta}_f = 10^{-2}$  (blue dashed curves). We set  $\beta_2 = -1, \beta_3 = 1/2, m_g^2 = m_f^2$ . The stable branches for  $m_{\text{eff}}/H \ll 1$  are given by  $\mu_0 \simeq 1.1$  for  $w = 0$ , and  $\mu_0 \simeq -0.21$  for  $w = 2/3$ . The Universe with  $w = 2/3$  may evolve from  $\mu_0 = -0.21$  (GR phase) to  $\mu_\infty = 0$  (linear bigravity phase), but for  $w = 0$ , there is no stable adiabatic solution.

order to conclusively analyze the full evolution history of the Universe for natural equation-of-state parameter  $w$ , the analysis beyond the adiabatic approximation is required, and a numerical treatment should be expected.

---

the evolutions of the density perturbations. However this is unlikely because the qualitative behaviors of Figs. 6.3 and 6.4 do not depend on the amplitudes of  $\tilde{\delta}_g$  and  $\tilde{\delta}_f$  but rather on their ratio  $\tilde{\delta}_g/\tilde{\delta}_f$ .



## Chapter 7

# On dark matter

The big mysteries in the modern cosmology are not only the origin of the accelerating expansion of the Universe but also the origin of dark matter. The existence of dark matter is confirmed in many situations, e.g., the abundance of non-relativistic particles in the Universe, the cosmological structure formation, and dark matter halos existing around galaxies. In order to realize the bottom-up scenario of the structure formation, dark matter must be cold (or warm). The standard candidates of cold dark matter are massive particles which are weakly coupled to standard model particles and dark matter particles are produced via a thermal process called weakly interacting massive particles (WIMPs). Since WIMPs are coupled to known particles, dark matter could be observed in the direct ways through particle productions in colliders or dark matter scattering off a nucleus, or in the indirect ways through dark matter annihilation to cosmic rays [32–37]. However, these experiments have not discovered dark matter particles so far; thus we have confirmed the existence of dark matter only by the gravitational interactions. The experimental null results would suggest that a paradigm shift is required.

In this chapter, we shall discuss two possibilities to explain the origin of dark matter in the context of bigravity: dark matter from  $f$ -sector matter [51, 53] and dark matter composed of massive graviton [54]. In the first case, the dark matter candidate is the matter field coupling to  $f$ -metric. By definition, the  $f$ -matter is not directly coupled to the  $g$ -matter field. Only possible interactions between the  $g$ -matter and the  $f$ -matter are through the gravitational interaction. Hence the  $g$ -matter observes the  $f$ -matter as a dark matter component. On the other hand, in the second possibility, the dark matter candidate is the massive graviton itself. In this case, we do not need to introduce any additional matter fields other than the  $g$ -matter fields.

In Section 7.1, we discuss the first possibility so we consider the effects of the  $f$ -matter field on three situations: the background dynamics of the Universe, the rotation curves of galaxies, and the structure formation.

The linear perturbations around a homothetic solution are decomposed into two eigenstates: the massless and massive graviton modes. Note that these are the mass eigenstates, whereas they are mixed up in the physical frame described by two metrics. That is, the massless and massive modes couple to both  $g$ - and  $f$ -matter fluids. As a result, the perturbations of our spacetime are described by the linear combinations of the massless and massive modes. Our  $g$ -spacetime is affected by  $f$ -matter fluids via the massless and massive graviton modes. The effects though the massless graviton mode should be the same as that in GR because the carrier of the gravitational interaction is the massless graviton in GR. The non-trivial effect would be obtained from the massive graviton mode. Indeed, we will show that the massive graviton mode gives a repulsive force rather than an attractive force in the  $g$ -spacetime while the massless graviton mode gives a standard attractive force. As a result, the gravitational force becomes weaker than the prediction of GR in some scale in bigravity.

In Section 7.2, on the other hand, we shall consider the scenario in which dark matter is explained by the massive gravitons. As shown in Section 3.4, the massive gravitons act as a gravitational source for the massless graviton. In the scales larger than the Compton wavelength the massive graviton is not relevant to the carrier of the gravitational force due to the Yukawa suppression. Since the massive graviton should be confined in galaxies, the de Broglie wavelength

of the massive graviton should be smaller than kpc scale in order to be a candidate for dark matter. Then the massive graviton behaves as just a massive particle (not as a carrier of gravitational force) in significant scales of dark matter.

In a scenario of massive graviton dark matter, the gravitational wave is an observational tool to explore our scenario. Since the  $g$ -metric to which ordinary matter fields couple is a linear combination of the two mass eigenstates, production of massive gravitons, i.e. the dark matter particles, is inevitably accompanied by generation of massless gravitons, i.e. the gravitational waves. Therefore, in this scenario, some information about dark matter in our Universe is encoded in gravitational waves. We can indirectly estimate some parameters of massive graviton by using the gravitational waves when observed.

## 7.1 Dark matter from $f$ -sector

In this section, we will analyze whether the  $f$ -matter field can be dark matter in our  $g$ -world.

Let us consider the linear perturbation around the homothetic background. The unperturbed solution is assumed to be homothetic, i.e.,

$${}^{(0)}g_{\mu\nu} \quad \text{and} \quad {}^{(0)}f_{\mu\nu} = K^2 {}^{(0)}g_{\mu\nu}, \quad (7.1.1)$$

which is the solution of two Einstein equations:

$${}^{(0)}G^\mu{}_\nu({}^{(0)}g) = -\Lambda_g(K)\delta^\mu{}_\nu + \kappa_g^2 T^{[m]\mu}{}_\nu, \quad (7.1.2)$$

$${}^{(0)}G^\mu{}_\nu({}^{(0)}f) = -\Lambda_f(K)\delta^\mu{}_\nu + \kappa_f^2 \mathcal{T}^{[m]\mu}{}_\nu, \quad (7.1.3)$$

A constant  $K$  is determined by the quartic equation (3.3.16), and the matter energy-momenta satisfy the following condition:

$$\kappa_f^2 \mathcal{T}^{[m]\mu}{}_\nu = \frac{1}{K^2} \kappa_g^2 T^{[m]\mu}{}_\nu. \quad (7.1.4)$$

We then consider the following perturbations:

$$g_{\mu\nu} = {}^{(0)}g_{\mu\nu} + \delta g_{\mu\nu}, \quad (7.1.5)$$

$$f_{\mu\nu} = {}^{(0)}f_{\mu\nu} + K^2 \delta f_{\mu\nu} = K^2 \left( {}^{(0)}g_{\mu\nu} + \delta f_{\mu\nu} \right) \quad (7.1.6)$$

where  $|\delta g_{\mu\nu}|, |\delta f_{\mu\nu}| \ll |{}^{(0)}g_{\mu\nu}|$ . The suffixes of  $\delta g_{\mu\nu}$  as well as  $\delta f_{\mu\nu}$  are raised and lowered by the background metric  ${}^{(0)}g_{\mu\nu}$ .

The energy-momentum tensors of twin matter fluid and  $\gamma$ -“energy-momentum” ones from the interaction terms can be expanded as

$$\kappa_g^2 T^{[m]\mu}{}_\nu = \kappa_g^2 \left[ T^{[m]\mu}{}_\nu + \delta T^{[m]\mu}{}_\nu \right], \quad (7.1.7)$$

$$K^2 \kappa_f^2 \mathcal{T}^{[m]\mu}{}_\nu = K^2 \kappa_f^2 \left[ \mathcal{T}^{[m]\mu}{}_\nu + \delta \mathcal{T}^{[m]\mu}{}_\nu \right] \quad (7.1.8)$$

and

$$\kappa_g^2 T^{[\gamma]\mu}{}_\nu = -\Lambda_g \delta^\mu{}_\nu + \frac{m_g^2}{2} (\hat{\varphi}^\mu{}_\nu - \hat{\varphi} \delta^\mu{}_\nu), \quad (7.1.9)$$

$$K^2 \kappa_f^2 T^{[\gamma]\mu}{}_\nu = -K^2 \Lambda_f \delta^\mu{}_\nu - \frac{m_f^2}{2} (\hat{\varphi}^\mu{}_\nu - \hat{\varphi} \delta^\mu{}_\nu), \quad (7.1.10)$$

respectively. Here we have introduced new variables  $\hat{\varphi}_{\mu\nu}$  and  $\hat{h}_{\mu\nu}$  from two metric perturbations as

$$\begin{aligned} \hat{\varphi}_{\mu\nu} &= \delta g_{\mu\nu} - \delta f_{\mu\nu}, \\ \hat{h}_{\mu\nu} &= \frac{m_f^2}{m_{\text{eff}}^2} \delta g_{\mu\nu} + \frac{m_g^2}{m_{\text{eff}}^2} \delta f_{\mu\nu} \end{aligned} \quad (7.1.11)$$



with (3.3.30). Note that, in this section, we use the dimensionless variables  $\hat{\varphi}_{\mu\nu}$  and  $\hat{h}_{\mu\nu}$  for convenience.

The linearized Einstein equations are given by

$$\delta G_{\mu\nu}^{(1)}(\hat{h}) = \frac{m_f^2}{m_{\text{eff}}^2} \kappa_g^2 \delta T_{\mu\nu}^{(1)} + \frac{m_g^2}{m_{\text{eff}}^2} K^2 \kappa_f^2 \delta \mathcal{T}_{\mu\nu}^{(1)}, \quad (7.1.12)$$

$$\delta G_{\mu\nu}^{(1)}(\hat{\varphi}) - \frac{m_{\text{eff}}^2}{2} (\hat{\varphi}_{\mu\nu} - \hat{\varphi} g_{\mu\nu}^{(0)}) = \kappa_g^2 \delta T_{\mu\nu}^{(1)} - K^2 \kappa_f^2 \delta \mathcal{T}_{\mu\nu}^{(1)}. \quad (7.1.13)$$

Note that, for the massive mode, we can derive following constraint equations from the linearized Einstein equation:

$$\overset{(0)}{\nabla}_\mu \hat{\varphi}^\mu{}_\nu = \overset{(0)}{\nabla}_\nu \hat{\varphi}, \quad (7.1.14)$$

$$(3m_{\text{eff}}^2 - 2\Lambda_g) \hat{\varphi} = \kappa_g^2 (2T_{\alpha\beta}^{(0)[\text{m}]} \hat{\varphi}^{\alpha\beta} - \overset{(0)}{T}^{[\text{m}]} \hat{\varphi}) - 2\kappa_g^2 \delta T^\mu{}_\mu + 2K^2 \kappa_f^2 \delta \mathcal{T}^\mu{}_\mu. \quad (7.1.15)$$

When we discuss the scales larger than the Compton wavelength of the massive graviton, we can ignore the equation (7.1.13) since the massive graviton does not give any effects on the gravitational force. The equation (7.1.12) suggests that the gravitational source for the massless graviton is given by the sum of both twin matters. The metric perturbations are represented as

$$\begin{aligned} \delta g_{\mu\nu} &= \hat{h}_{\mu\nu} + \frac{m_g^2}{m_{\text{eff}}^2} \hat{\varphi}_{\mu\nu}, \\ \delta f_{\mu\nu} &= \hat{h}_{\mu\nu} - \frac{m_f^2}{m_{\text{eff}}^2} \hat{\varphi}_{\mu\nu}, \end{aligned} \quad (7.1.16)$$

and then, in large scales, the  $g$ -spacetime perturbation is approximated by

$$\delta g_{\mu\nu} \simeq \hat{h}_{\mu\nu}. \quad (7.1.17)$$

The expression clearly shows that the  $f$ -matter field acts as a dark matter component in the  $g$ -spacetime in the scales larger than the Compton wavelength. It is worth noting that the linear perturbations around the homothetic background should be valid in the scales larger than the Compton wavelength since the Vainshtein radius is much shorter than the Compton wavelength in general.

The non-trivial effects may exist in the scales shorter than the Compton wavelength. We will discuss the effect of the  $f$ -matter in several scales. We believe from observation that the evidence of dark matter appears in three situations; (A) dark matter in the Friedmann equation, (B) a dark halo at a galaxy scale, and (C) CDM in cosmic structure formation. So we discuss them in order.

### 7.1.1 Cosmic pie

First, we discuss the pie chart of the content of the Universe. The amount of dark matter is about 5 times as large as the baryonic matter.

In order to explain the cosmic pie, we consider the homogeneous and isotropic spacetime, which metrics are given by

$$ds_g^2 = -N_g^2 dt^2 + a_g^2 \left( \frac{dr^2}{1 - kr^2} + r^2 d\Omega^2 \right), \quad (7.1.18)$$

$$ds_f^2 = -N_f^2 dt^2 + a_f^2 \left( \frac{dr^2}{1 - kr^2} + r^2 d\Omega^2 \right), \quad (7.1.19)$$

where  $N_g$  and  $N_f$  are lapse function, while  $a_g$  and  $a_f$  are scale factors for  $g_{\mu\nu}$  and  $f_{\mu\nu}$ , respectively. Using the gauge freedom, we can set  $N_g = 1$  without loss of generality. See Chapter 5 for details of dynamics of FLRW spacetime and notations.

For generic initial data, the ratios  $N_f/N_g$  and  $a_f/a_g$  can approach to the same constant  $K$  given by (3.3.16), as the universe expands, i.e., the homothetic solution is an attractor in the present

system. The dynamical time scale is about  $m_{\text{eff}}^{-1}$ . We can approximate the cosmological solution by small deviation of metrics from a homothetic background when

$$3m_{\text{eff}}^2 - 2\Lambda_g \gg |\kappa_g^2 \rho_g - K^2 \kappa_f^2 \rho_f|. \quad (7.1.20)$$

As a result, near the attractor, i.e., near the present stage of the universe, the evolution of the universe is described by the effective Friedmann equation

$$H_g^2 + \frac{k}{a_g^2} = \frac{\Lambda_g}{3} + \frac{\kappa_{\text{eff}}^2}{3} [\rho_g + \rho_D], \quad (7.1.21)$$

where

$$\kappa_{\text{eff}}^2 = \kappa_g^2 \left[ 1 - \frac{3m_g^2}{3m_{\text{eff}}^2 - 2\Lambda_g} \right], \quad (7.1.22)$$

$$\rho_D = \frac{3m_f^2}{3m_f^2 - 2\Lambda_g} K^4 \rho_f, \quad (7.1.23)$$

and  $\rho_g$  and  $\rho_f$  are energy densities of  $g$ - and  $f$ -matter, respectively.  $H_g = \dot{a}_g/a_g$  is the Hubble parameter where a dot denotes the derivative with respect to  $t$ .  $\kappa_{\text{eff}}^2$  is the effective gravitational constant, and  $\rho_D$  is regarded as the energy density of a dark component in the  $g$ -world, i.e., another one of twin matter fluids works as dark matter through the interaction term between two metrics. Note that the matter densities can deviate largely from those of the homothetic solution such that  $\rho_D \geq \rho_g$ , although the metric deviation is still small enough as long as  $m_{\text{eff}}^2 \geq \kappa_{\text{eff}}^2 \rho_D$ .

If both matter components are dominated by non-relativistic matter;

$$\rho_g = \frac{\rho_{g,0}}{a_g^3}, \quad \rho_f = \frac{\rho_{f,0}}{a_f^3}, \quad (7.1.24)$$

the density of dark component is approximated by

$$\begin{aligned} \rho_D &= \frac{3m_f^2}{3m_f^2 - 2\Lambda_g} \frac{K^4 \rho_{f,0}}{a_f^3} \\ &\approx \frac{3m_f^2}{3m_f^2 - 2\Lambda_g} \frac{K \rho_{f,0}}{a_g^3} + \mathcal{O}(a_g^{-6}). \end{aligned} \quad (7.1.25)$$

Hence if  $3m_f^2 > 2\Lambda_g$ ,  $\rho_D$  behaves as a dark matter component in the  $g$ -world. If  $\rho_g$  consists just of baryonic matter, in order to explain the observed amount of dark matter, we have to require

$$\frac{\rho_D}{\rho_g} = \frac{3m_f^2}{3m_f^2 - 2\Lambda_g} \frac{K \rho_{f,0}}{\rho_{g,0}} \sim 5. \quad (7.1.26)$$

With an appropriate choice of the coupling parameters, we find the above value, which may explain dark matter by the  $f$ -matter fluid.

To show a full dynamics of the density parameters beyond the approximation, we choose one model with the appropriate values of  $\kappa_f^2/\kappa_g^2$  and  $r_m = \rho_{f,0}/\rho_{g,0}$ . In Fig. 7.1, we show the results for those two models. The present time, which is shown by the dashed lines in the figures, is fixed by the observed value of the deceleration parameter  $q = -\ddot{a}_g a_g / \dot{a}_g^2 = -0.527 \pm 0.026$ . We find that the present total matter density  $(\Omega_D + \Omega_m)|_0$  is about 0.3 and the dark energy  $\Omega_\Lambda|_0$  is about 0.7, respectively, as shown in Fig. 7.1. This result does not depend on the choice of the initial value of  $\tilde{B}$ .

Since the ratio  $\rho_D/\rho_g \sim 5$  for both models, we find  $\Omega_D|_0 \sim 0.25$  and  $\Omega_m|_0 \sim 0.05$ , which must consist of baryonic matter because  $\Omega_b|_0 \sim 0.05$ . We need not introduce non-baryonic dark matter in  $g$ -spacetime. Another one of twin matter fluids plays a role of dark matter in the effective Friedmann equation.

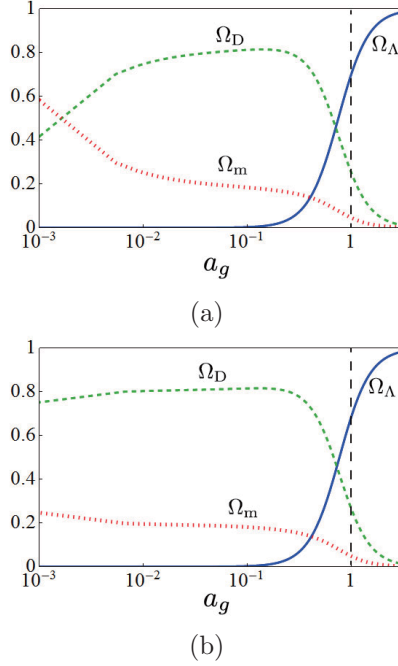


Figure 7.1: The time evolution of density parameters for Model  $\kappa_f^2/\kappa_g^2 = 60$  and  $r_m = 180$  with  $c_3 = -4, c_4 = -10$ , and for Model  $\kappa_f^2/\kappa_g^2 = 1000$  and  $r_m = 3000$  with  $c_3 = -4, c_4 = -10$ .  $a_g = 1$  is the present time.

### 7.1.2 Dark matter halo

Next, we discuss how to explain a dark matter halo around a galaxy by another one of twin matter fluids. The existence of dark matter halo is confirmed by observations such as a flat rotation curve of a galaxy [154].

To analyze the gravitational fields of a galaxy, we consider static Newtonian potentials  $\Phi_g$  and  $\Phi_f$  formed by non-relativistic mass densities  $\rho_g$  and  $\rho_f$ . We obtain the Poisson equation for the massive mode as

$$(\Delta - m_{\text{eff}}^2)\Phi_- = \frac{4}{3}(4\pi G\rho_g - 4\pi\mathcal{G}K^2\rho_f), \quad (7.1.27)$$

where  $\Delta = \partial^i\partial_i$  is the usual three-dimensional Laplacian operator and  $\Phi_- = -\varphi_{00}/2$  is the gravitational potential of the massive mode. The factor  $4/3$  comes from the vDVZ discontinuity. Note that the source term is described by the subtraction of two mass densities, and then it can be negative.

For the massless mode, we obtain the ordinary form of the Poisson equation:

$$\Delta\Phi_+ = 4\pi G\frac{m_f^2}{m_{\text{eff}}^2}\rho_g + 4\pi\mathcal{G}K^2\frac{m_g^2}{m_{\text{eff}}^2}\rho_f, \quad (7.1.28)$$

where  $\Phi_+ = -h_{00}/2$  is the gravitational potential of the massless mode. This source term is positive definite.

We find that both gravitational potentials are affected by both  $g$ - and  $f$ - matter fluids. This is main difference from the Newtonian gravity theory. It may make a possibility such that the  $f$ -matter can behave as dark matter in the  $g$ -worlds.

In a small scale such as the solar system, however, GR must be restored because GR has been well confirmed by the experiments and observations. The restoration could be realized via the Vainshtein mechanism. In this range (below the Vainshtein radius), the linear perturbation approach is broken down, and then non-linear effects must be taken into account. However, when

GR is restored from the bigravity theory, the effect on the  $g$ -world from the  $f$ -matter fluid must be screened. It indicates that the  $f$ -matter cannot be dark matter below the Vainshtein radius. Since we are interested in whether the  $f$ -matter plays a role of dark matter in the  $g$ -world, we shall only analyze the linear perturbations. The evaluation of the Vainshtein radius will be given in the last part of this subsection.

For a simplest case in which matter fluids are localized spherically, the Newtonian potentials outside matter distributions are solved as

$$\Phi_- = \frac{4}{3} \left( \frac{GM_g}{r} e^{-m_{\text{eff}} r} - \frac{K^2 \mathcal{G} \mathcal{M}_f}{r} e^{-m_{\text{eff}} r} \right), \quad (7.1.29)$$

$$\Phi_+ = \frac{m_f^2}{m_{\text{eff}}^2} \frac{GM_g}{r} + \frac{m_g^2}{m_{\text{eff}}^2} \frac{K^2 \mathcal{G} \mathcal{M}_f}{r}, \quad (7.1.30)$$

where the gravitational masses are defined by

$$M_g = \int 4\pi \rho_g r^2 dr, \quad \mathcal{M}_f = \int 4\pi \rho_f r^2 dr. \quad (7.1.31)$$

The Newtonian potentials in the  $g$ - and  $f$ -worlds are described as

$$\begin{aligned} \Phi_g &= \Phi_+ + \frac{m_g^2}{m_{\text{eff}}^2} \Phi_- \\ &= -\frac{GM_g}{r} \left( \frac{m_f^2}{m_{\text{eff}}^2} + \frac{4m_g^2}{3m_{\text{eff}}^2} e^{-m_{\text{eff}} r} \right) \\ &\quad - \frac{m_g^2}{m_{\text{eff}}^2} \frac{K^2 \mathcal{G} \mathcal{M}_f}{r} \left( 1 - \frac{4}{3} e^{-m_{\text{eff}} r} \right), \end{aligned} \quad (7.1.32)$$

$$\begin{aligned} \Phi_f &= \Phi_+ - \frac{m_f^2}{m_{\text{eff}}^2} \Phi_- \\ &= -\frac{K^2 \mathcal{G} \mathcal{M}_f}{r} \left( \frac{m_g^2}{m_{\text{eff}}^2} + \frac{4m_f^2}{3m_{\text{eff}}^2} e^{-m_{\text{eff}} r} \right) \\ &\quad - \frac{m_f^2}{m_{\text{eff}}^2} \frac{GM_g}{r} \left( 1 - \frac{4}{3} e^{-m_{\text{eff}} r} \right). \end{aligned} \quad (7.1.33)$$

where  $\Phi_g = -\delta g_{00}/2$ ,  $\Phi_f = -\delta f_{00}/2$ .

Let us consider the Newtonian potential in the  $g$ -world. Below the Compton wavelength of the massive graviton ( $r < m_{\text{eff}}^{-1}$ ), the potential becomes

$$\Phi_g = -\frac{GM_g}{r} \left( 1 + \frac{m_g^2}{3m_{\text{eff}}^2} \right) + \frac{m_g^2}{3m_{\text{eff}}^2} \frac{K^2 \mathcal{G} \mathcal{M}_f}{r}. \quad (7.1.34)$$

Note that the second term is positive definite. It means that the  $f$ -matter acts as a repulsive force in the  $g$ -world. It comes from the factor  $4/3$  in (7.1.32). To explain dark matter, of course, the gravitational force must be attractive. Therefore, the  $f$ -matter cannot behave as dark matter when the size of the localized system is smaller than the Compton wavelength.

The origin of this repulsive force is the massive mode, which cannot propagate in the large system such that  $m_{\text{eff}} r \gg 1$ . In fact, beyond the Compton wavelength ( $r > m_{\text{eff}}^{-1}$ ), the potential is approximated by

$$\Phi_g = -\frac{G_{\text{eff}}}{r} (M_g + K^4 \mathcal{M}_f) \quad (7.1.35)$$

where

$$G_{\text{eff}} = \frac{m_f^2}{m_{\text{eff}}^2} G \quad (7.1.36)$$

is the local effective gravitational constant. This potential is formed by the  $f$ -matter as well as the  $g$ -matter. Hence, it is possible to explain dark matter by another one of twin matter fluids.

Inside the Vainshtein radius, the gravitational constant is restored to the Newtonian gravitational constant. The effective gravitational constants at a galactic scale is same as the effective one in the Friedmann equation with  $m_{\text{eff}}^2 \gg \Lambda_g$ , which we assume to explain dark matter as well as dark energy. Since the difference between the effective gravitational constant in the Friedmann equation and the Newtonian one should not be so large from the CMB observation [155–157], we find a constraint such that

$$\frac{m_g^2}{m_f^2} = \frac{K^2 \kappa_g^2}{\kappa_f^2} \ll 1. \quad (7.1.37)$$

Now we return to the Poisson equations. (7.1.27) and (7.1.28), and study numerically whether  $f$ -matter can provide a flat rotation curve of a galaxy in  $g$ -world or not. We assume the dark matter halo is composed of only  $f$ -matter, and the distribution of  $\rho_f$  is assumed to be proportional to  $r^{-2}$  around the galactic disk. Although the rotation curve is sensitive to the matter distributions of  $\rho_f$  as well as  $\rho_g$ , for simplicity, we assume a spherically symmetric matter distribution as

$$\begin{aligned} \rho_g(r) &= \rho_g(0) \exp[-r/r_{\text{gal}}], \\ \rho_f(r) &= \frac{\rho_f(0)}{1 + (r/r_{\text{halo}})^2}. \end{aligned} \quad (7.1.38)$$

We show the resulting rotation curves for several values of  $m_{\text{eff}}$  in Fig. 7.2. The rotation velocity  $V$  is evaluated as  $V^2 = r d\Phi_g/dr$ . We find a flat rotation curve if  $m_{\text{eff}}^{-1} \sim \text{kpc}$ .

We then conclude that the  $f$ -matter behaves as dark matter in the  $g$ -world if the Compton wavelength of the massive graviton is less than a galaxy scale such as  $m_{\text{eff}}^{-1} \sim 1 \text{ kpc}$ . When the mass becomes lighter, then the rotation velocity decreases. It is due to a “repulsive force” induced by the massive mode because the Compton wavelength becomes larger. Note that in the shorter range than  $r \sim 10 \text{ kpc}$ , the rotational velocity with the  $f$ -matter (the green curve) is smaller than that without the  $f$ -matter (the black dotted curve), which is the evidence that the  $f$ -matter acts as a repulsive force.

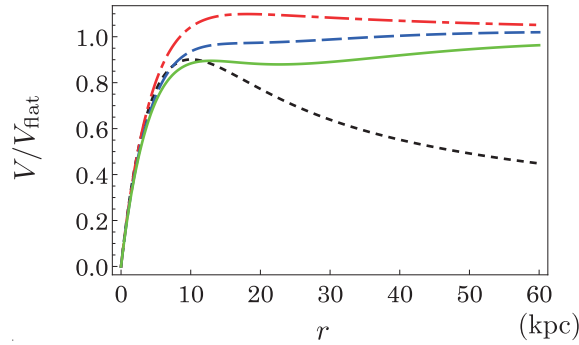


Figure 7.2: The rotation curve in the  $g$ -worlds. We plot three cases of  $m_{\text{eff}}^{-1} = 5$  (the red dashed-dotted curve), 10 (the blue dashed curve) and 15 kpc (the green solid curve). Matter distributions are given by  $\rho_g(r) = \rho_g(0) \exp[-r/r_{\text{gal}}]$ ,  $\rho_f(r) = \rho_f(0)(1 + (r/r_{\text{halo}})^2)^{-1}$ , where we set  $r_{\text{gal}} = r_{\text{halo}} = 3 \text{ kpc}$  and  $\rho_g(0) = \rho_f(0)$ . The effective gravitational constant is  $G_{\text{eff}}/G = 0.961538$  ( $m_g/m_f = 0.2$ ). The black dotted curve is the rotation curve without  $f$ -matter.

In order to justify the above analysis, we have to evaluate the Vainshtein radius below which the linear approximation is broken. We find the linear perturbation analysis for a spherically symmetric system is valid only when

$$m_{\text{eff}}^2 \gg \frac{GM_-(r)}{r^3}, \quad (7.1.39)$$

where

$$GM_-(r) := \left| G \int_0^r 4\pi \tilde{r}^2 \rho_g(\tilde{r}) d\tilde{r} - K^2 \mathcal{G} \int_0^r 4\pi \tilde{r}^2 \rho_f(\tilde{r}) d\tilde{r} \right|. \quad (7.1.40)$$

Here we have ignored a cosmological constant. The mass of galaxy is dominated by the dark matter component, and we have the constraint (7.1.37), we find  $K^2\mathcal{G}\mathcal{M}_f \gg GM_g$ , where  $M_g$  and  $\mathcal{M}_f$  are total masses of the  $g$ - and  $f$ -matter fluids, respectively. Hence the right hand side is bounded from the above as

$$GM_-(r) \leq K^2\mathcal{G}\mathcal{M}_f.$$

As a result, we conclude that the linear perturbation analysis is valid for

$$r \gg r_V := \left( \frac{K^2\mathcal{G}\mathcal{M}_f}{m_{\text{eff}}^2} \right)^{1/3}. \quad (7.1.41)$$

From Eq. (7.1.35), we find the effective mass of a galaxy in the  $g$ -world is

$$M_{\text{gal}} \approx \frac{m_f^2}{m_{\text{eff}}^2} K^4 \mathcal{M}_f. \quad (7.1.42)$$

For  $M_{\text{gal}} \sim 10^{12} M_\odot$ , we can evaluate the Vainshtein radius as

$$r_V \sim 0.04 \text{ kpc} \left( \frac{m_{\text{eff}}^{-1}}{1 \text{ kpc}} \right)^{2/3} \left( \frac{1}{1 - G_{\text{eff}}/G} \right)^{1/3}. \quad (7.1.43)$$

It guarantees that the linear perturbation approximation is valid in a galactic scale if  $m_{\text{eff}}^{-1} \lesssim \text{kpc}$ .

Note that, although the effective cosmological constant in bigravity typically given by the graviton mass squared, this value can be much smaller than the graviton mass squared [53]. Thus, when we fine-tune the coupling constant  $\{b_i\}$ , the models with  $m_{\text{eff}} \sim (\text{kpc})^{-1}$  and  $\Lambda_g \sim (\text{Gpc})^{-2}$  can be realized. In this case, the bigravity theory could explain both dark matter and dark energy, simultaneously. However, the bigravity explains either dark matter or dark energy in the case without the fine-tuning.

### 7.1.3 Cosmic structure formation

Finally, we discuss the evolution of cosmological density perturbations based on the linear perturbation theory. The basic equations for scalar-mode perturbations are summarized in the end of this subsection. For simplicity, we assume that the background flat FLRW spacetimes are given by the homothetic solution. In this subsection, we calculate the evolution of the density perturbations  $\delta_g$  and  $\delta_f$  in the  $g$ - and  $f$ -worlds, respectively. Those perturbations are given by the linear combinations of  $\delta_+$  and  $\delta_-$ , which are the density perturbations in the equations for the massless and the massive graviton modes, respectively. Since two modes are decoupled, we first solve numerically the perturbation equations for the massive graviton mode.

#### Numerical solutions

Since we are interested in formation of galaxies, we discuss only sub-horizon scale perturbations,  $a/k \ll H^{-1}$ . In this subsection, we first analyze the linear perturbation equations numerically. We assume that the matter component is dominated by non-relativistic matter ( $w = 0$ ). Since there is another scale of length, i.e., the Compton wave length of the massive graviton  $m_{\text{eff}}^{-1}$ , we can classify those three scales into three possibilities:

Case (a)  $a/k \ll H^{-1} \ll m_{\text{eff}}^{-1}$ ,

Case (b)  $a/k \ll m_{\text{eff}}^{-1} \ll H^{-1}$ ,

Case (c)  $m_{\text{eff}}^{-1} \ll a/k \ll H^{-1}$ .

Assuming the initial data at the decoupling time is given in each case, we solve numerically the perturbation equations (7.1.83)-(7.1.88) for the massive graviton mode.

We show the results for one metric component  $\beta_-^{(L)}$  and the density perturbation  $\delta_-$  in Fig. 7.3, where we have chosen the initial data as (a)  $a_{\text{in}}/k = 10^{-4} \times m_{\text{eff}}^{-1}$ ,  $H_{\text{in}}^{-1} = 10^{-2} \times m_{\text{eff}}^{-1}$ , (b)

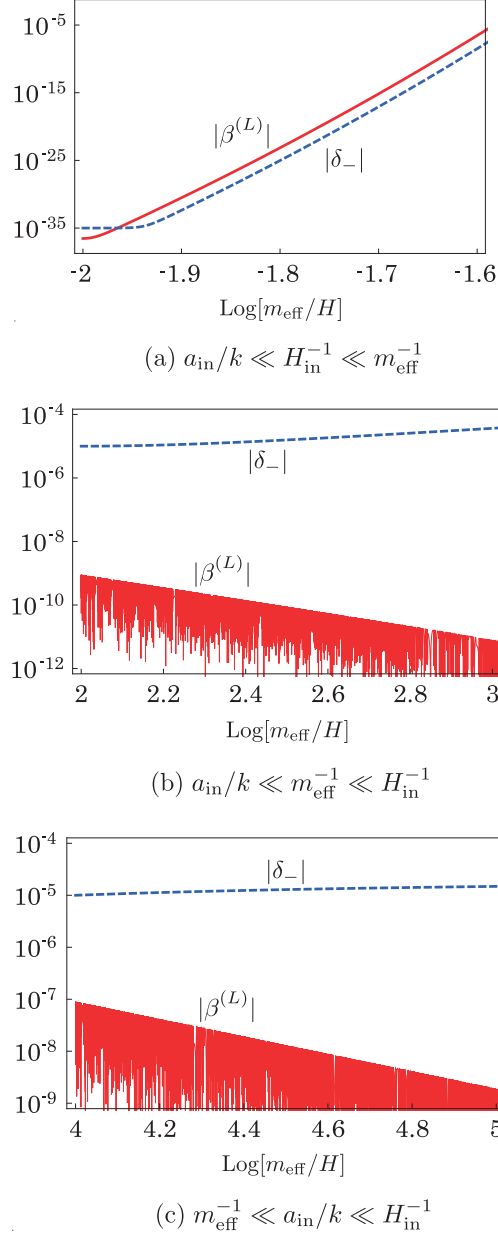


Figure 7.3: The time evolution of  $\beta_-^{(L)}$  and  $\delta_-$ . The background spacetime is the dust dominant universe ( $a \propto t^{2/3}$ ). We choose the initial data (a)  $a_{\text{in}}/k = 10^{-4} \times m_{\text{eff}}^{-1}$ ,  $H_{\text{in}}^{-1} = 10^{-2} \times m_{\text{eff}}^{-1}$ , (b)  $a_{\text{in}}/k = 10^{-2} \times m_{\text{eff}}^{-1}$ ,  $H_{\text{in}}^{-1} = 10^2 \times m_{\text{eff}}^{-1}$ , and (c)  $a_{\text{in}}/k = 10^2 \times m_{\text{eff}}^{-1}$ ,  $H_{\text{in}}^{-1} = 10^4 \times m_{\text{eff}}^{-1}$ . The perturbations grow exponentially for (a). For (b) and (c), the metric perturbation  $\beta_-^{(L)}$  decays with oscillations, while the density perturbation  $\delta_-$  increases slowly without oscillation.

$a_{\text{in}}/k = 10^{-2} \times m_{\text{eff}}^{-1}$ ,  $H_{\text{in}}^{-1} = 10^2 \times m_{\text{eff}}^{-1}$ , and (c)  $a_{\text{in}}/k = 10^2 \times m_{\text{eff}}^{-1}$ ,  $H_{\text{in}}^{-1} = 10^4 \times m_{\text{eff}}^{-1}$ . In the calculation, we have ignored the terms with the sound speed because we consider the perturbations larger than the Jeans length, i.e.  $k \ll k_J = a\sqrt{4\pi G\bar{\rho}}/c_s$ .

For the case (a), both perturbation variables ( $\beta_-^{(L)}, \delta_-$ ) grow exponentially due to the Higuchi type instability. Hence the linear perturbation is unstable. On the other hand, for the cases (b) and (c), the metric perturbation  $\beta_-^{(L)}$  decays with oscillations, which frequency is about  $\sqrt{(k/a)^2 + m_{\text{eff}}^2}$ , while the density perturbation  $\delta_-$  increases monotonically without oscillations. The increase rates are evaluated numerically by power-law functions of the scale factor  $a$  as  $\delta_- \propto a^{1.176}$  and  $a^{0.1077}$  for (b) and (c), respectively.

The Compton wavelength  $m_{\text{eff}}^{-1}$  is larger than the horizon scale  $H^{-1}$  for (a), while the relation is opposite for (b) and (c). The above result concludes that if  $m_{\text{eff}}^{-1} > H^{-1}$  (the case (a)), the perturbative approach is no longer valid. The non-linear effect must be taken into account as discussed in Section 6.

When  $m_{\text{eff}}^{-1} < H^{-1}$  (the case (b) and (c)), there are two important time scales: One is the Hubble expansion time  $H^{-1}$ , and the other is the oscillation time scale of the massive graviton  $m_{\text{eff}}^{-1}$ . We find that the metric variables  $\{\alpha_-, \beta_-^{(L)}, h_-^{(L)}, h_-^{(T)}\}$  are divided into two parts; the monotonically growing part and the oscillating part. The former part changes in the Hubble expansion time  $H^{-1}$ , while the latter part with the high frequency  $\sqrt{(k/a)^2 + m_{\text{eff}}^2}$  is always decaying. The metric component  $\beta_-^{(L)}$  has no former part, and then eventually vanishes as shown in In Fig. 7.3. On the other hand, the matter perturbations  $\{\delta_-, v_-^{(L)}\}$  grow slowly in the Hubble time scale  $H^{-1}$  without oscillation.

As a result, all variables asymptotically approach monotonic functions increasing in the Hubble time scale  $H^{-1}$ . There seems to exist an asymptotic solution which changes monotonically in the Hubble time scale  $H^{-1}$ . We then assume that the perturbation variables change in the Hubble time scale  $H^{-1}$ , i.e.,  $|\dot{X}_-| \sim |HX_-|$ , which provides the above asymptotic solution. We call such an approach an adiabatic potential approximation, since we ignore the oscillation parts of metric which correspond to the scalar gravitational waves.

### Adiabatic potential approximation

Under the adiabatic potential approximation, we look for a solution for sub-horizon scale perturbations. From the perturbation equations for the massive mode, (7.1.83), (7.1.87) and (7.1.88), we find

$$-\left(\frac{k^2}{a^2} + 3m_{\text{eff}}^2\right)\alpha_- = \kappa_g^2 \bar{\rho}_g \delta_- + 3m_{\text{eff}}^2 h_-^{(L)}, \quad (7.1.44)$$

$$\beta_-^{(L)} = 0, \quad h_-^{(T)} = -3\left(\frac{\alpha_-}{2} + h_-^{(L)}\right). \quad (7.1.45)$$

Substituting (7.1.89) into (7.1.44), we obtain

$$-\left(\frac{k^2}{a^2} + m_{\text{eff}}^2\right)\alpha_- = \frac{4}{3} \times \frac{\kappa_g^2 \bar{\rho}_g}{2} \delta_-, \quad (7.1.46)$$

where we have ignored a cosmological constant compared with the graviton mass term, because we are interested in the case with a rather large value of  $m_{\text{eff}}$ . This equation is interpreted as the massive Poisson equation. The factor 4/3 comes from the vDVZ discontinuity. Using Eq. (7.1.46) and ignoring the sound velocity term, the equation for the density perturbation  $\delta_-$  is described as

$$\ddot{\delta}_- + 2H\dot{\delta}_- - \frac{4k^2/a^2}{3(k^2/a^2 + m_{\text{eff}}^2)} \frac{\kappa_g^2 \bar{\rho}_g}{2} \delta_- = 0. \quad (7.1.47)$$

As we showed numerically, the solution of this equation is found as an attractor for generic initial data if  $m_{\text{eff}}^{-1} < H^{-1}$  is satisfied initially. However, the condition  $m_{\text{eff}}^{-1} < H^{-1}$  is not always true. In fact, when we go back to the past, since  $H^{-1} \sim t$ , then the condition is broken in the past epoch.



When we start from the epoch of  $m_{\text{eff}}^{-1} > H^{-1}$ , which corresponds to the case (a), the linear perturbation is unstable, and then nonlinear effect must be taken into account. As discussed in Section 6, we may find the stable universe by considering the condensation of the Stückelberg fields in that epoch. Since the results shown in Section 6 are obtained by the spherically symmetric system, the realization of the condensed state for a generic system is an open question. Furthermore, the transition from the condensed state is also unknown.

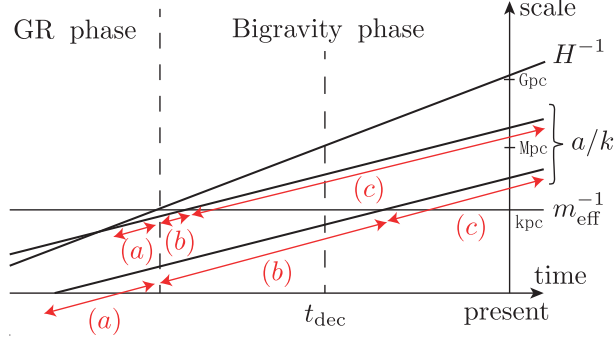


Figure 7.4: The schematic diagram of the growth history. In the early stage of the Universe ( $H^{-1} < m_{\text{eff}}^{-1}$ ), because of the Vainshtein mechanism, the standard big bang universe is recovered. However the Universe eventually evolves into the bigravity phase, in which there are two cases (b) and (c) depending on the perturbation scale compared with  $m_{\text{eff}}^{-1}$ .

We may assume the following scenario. In the early stage of the universe, because of the cosmological Vainshtein mechanism, gravity is described by GR and then the standard big bang scenario is found. However, the Universe eventually evolves into the bigravity phase at  $H^{-1} \sim m_{\text{eff}}^{-1}$  as shown in Fig. 7.4. When the universe reaches the decoupling time, we find the case (b) or (c) for the perturbations, in which the adiabatic potential approximation becomes valid as an attractor. For discussions about the structure formation, it is sufficient to discuss the case (b) and (c) only. We analyze whether the  $f$ -matter can be dark matter in the cosmic structure formation, using the above adiabatic potential approximation.

### Growth history of density perturbation

The evolution equation of density perturbation for the massless mode in a sub-horizon scale is given from Eq. (7.1.82) as

$$\ddot{\delta}_+ + 2H\dot{\delta}_+ - \frac{\kappa_g^2 \bar{\rho}_g}{2} \delta_+ = 0 \quad (7.1.48)$$

where we have ignored a cosmological constant and the term with a sound velocity as before. This equation for  $\delta_+$  is the same as that in GR. On the other hand, as found in Eq. (7.1.47), the evolution of the massive mode variable  $\delta_-$  depends on the Compton wavelength of the massive graviton as well as the scale of the perturbations.

From Eqs. (7.1.47) and (7.1.48) for  $\delta_+$  and  $\delta_-$ , we obtain the equations for the physical density perturbations ( $\delta_g$  and  $\delta_f$ ) as

$$\begin{aligned} \ddot{\delta}_g + 2H\dot{\delta}_g - 4\pi G_{\text{eff}}(\bar{\rho}_g \delta_g + \bar{\rho}_D \delta_D) &= 0, \\ \ddot{\delta}_f + 2H\dot{\delta}_f - 4\pi \mathcal{G}_{\text{eff}}(\bar{\rho}_f \delta_f + \bar{\rho}_G \delta_G) &= 0, \end{aligned} \quad (7.1.49)$$

where

$$G_{\text{eff}} = G \frac{m_f^2}{m_{\text{eff}}^2} \left( 1 + \frac{m_g^2}{m_f^2} F \right), \quad (7.1.50)$$

$$\bar{\rho}_D = K^4 \bar{\rho}_f, \quad (7.1.51)$$

$$\delta_D = \frac{1 - F}{1 + \frac{m_g^2}{m_f^2} F} \delta_f, \quad (7.1.52)$$

and

$$\mathcal{G}_{\text{eff}} = \mathcal{G} \frac{K^2 m_g^2}{m_{\text{eff}}^2} \left( 1 + \frac{m_f^2}{m_g^2} F \right), \quad (7.1.53)$$

$$\bar{\rho}_G = K^{-4} \bar{\rho}_g, \quad (7.1.54)$$

$$\delta_G = \frac{1 - F}{1 + \frac{m_f^2}{m_g^2} F} \delta_g, \quad (7.1.55)$$

with

$$F := \frac{4m_{\text{eff}}^{-2}}{3(m_{\text{eff}}^{-2} + a^2/k^2)}. \quad (7.1.56)$$

Beyond the Compton wavelength of the massive graviton, the effective gravitational constant becomes  $G_{\text{eff}}/G \approx m_f^2/m_{\text{eff}}^2$ . It is the same not only as the cosmological value but also as the local one if the graviton mass is large ( $m_{\text{eff}}^2 \gg \Lambda_g$ ). The perturbation of dark matter component coincides with that of the  $f$ -matter, i.e.,

$$\delta_D \approx \delta_f, \quad (7.1.57)$$

for  $a/k \gg m_{\text{eff}}^{-1}$ . Therefore, the  $f$ -matter perturbation behaves as the dark matter component in the  $g$ -world as §. 7.1.1 and §. 7.1.2.

Inside the Compton wavelength, the  $f$ -matter acts as a repulsive force as shown in §. 7.1.2. In the present case, it can be seen explicitly from the relation

$$\delta_D \sim -\frac{1}{3 + 4\frac{m_g^2}{m_f^2}} \delta_f \quad (7.1.58)$$

for  $a/k \ll m_{\text{eff}}^{-1}$ . It indicates that the  $g$ -matter accumulates in a low-density region of the  $f$ -matter.

We show the numerical result of the evolution of density perturbations for two different scales [ $k^{-1} = 10\text{Mpc}$  and  $100\text{kpc}$  at the present ( $a = 1$ )] in Fig. 7.5. We assume  $\delta_g = 10^{-5}$  and  $\delta_f = 10^{-1}$  at the decoupling time ( $a = 10^{-3}$ ). For the large scale perturbation, its scale is always larger than the Compton wavelength after the decoupling time. Hence the  $f$ -matter plays the role of dark matter in the  $g$ -world and helps small baryon perturbation  $\delta_g$  to grow rapidly as shown in Fig. 7.5 (a). The evolution of  $\delta_g$  is similar to the growth of density perturbations with CDM in GR.

On the other hand, for the small scale perturbation, its scale is shorter than the Compton wavelength at the decoupling time. During the period of  $a/k < m_{\text{eff}}^{-1}$ , the  $f$ -matter acts as a repulsive source in the  $g$ -world. Then the evolution of  $\delta_g$  is quite different due to the appearance of a repulsive force by the  $f$ -matter perturbations as shown in Fig. 7.5 (b).  $\delta_g$  changes its sign and then decreases to a negative value in the early stage. But the perturbation scale eventually exceeds  $m_{\text{eff}}^{-1}$  as the scale factor increases. In fact the perturbation scale becomes larger than the Compton wavelength after  $a = k/\sqrt{3} \times m_{\text{eff}}^{-1}$ , when  $\delta_D$  changes its sign. After then, the  $f$ -matter begins to act as dark matter. As shown in Fig. 7.5 (b),  $\delta_g$  changes its sign again to be positive.  $\delta_g$  then grow into a nonlinear regime via large density perturbations of the  $f$ -matter fluid.

We set  $m_g/m_f = 0.2$ , which satisfies the constraint (7.1.37). From Eq. (7.1.77), we find that the perturbations of the  $g$ -variables are dominated by the massless mode, while those of the  $f$ -variables have a significant influence by the massive mode. Since the massive mode can grow only when  $a/k \ll m_{\text{eff}}^{-1}$ ,  $\delta_f$  grows first and then  $\delta_g$  follows as shown in Fig. 7.5 (b). On the other hand, as shown in Fig. 7.5 (a),  $\delta_f$  cannot grow at first because the massive mode cannot grow for  $a/k \gg m_{\text{eff}}^{-1}$ .  $\delta_f$  starts to grow after the perturbation of the massless mode catches up to that of the massive mode.  $\delta_g$  grows rapidly by the increase of the massless mode even when  $\delta_f$  does not grow.

We conclude that the cosmic structure formation can also be explained by another one of twin matter fluids.

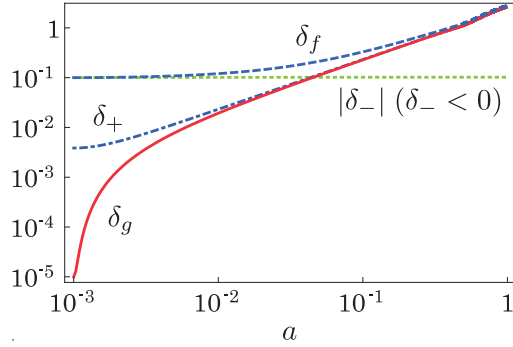
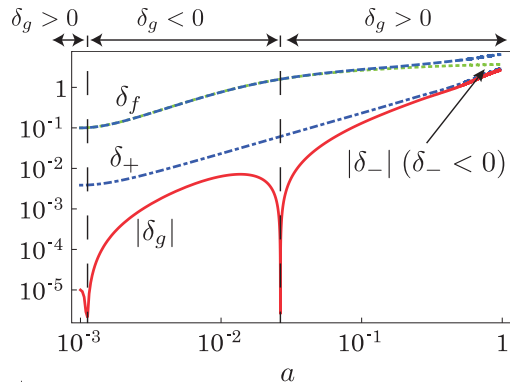
(a)  $k^{-1} = 10 \text{ Mpc}$ (b)  $k^{-1} = 10^2 \text{ kpc}$ 

Figure 7.5: The evolution of density perturbations for two scales [(a) 10Mpc and (b) 100kpc at the present ( $a = 1$ )]. We assume  $\delta_g = 10^{-5}$  and  $\delta_f = 10^{-1}$  at the decoupling time ( $a = 10^{-3}$ ). The blue dashed curve indicates the evolution of  $\delta_f$ , while the red solid curve indicates that of  $\delta_g$ . The  $\delta_+$  and  $\delta_-$  are the source terms for the massless graviton mode and the massive graviton mode, respectively. We set  $m_{\text{eff}}^{-1} = 1 \text{ kpc}$  and  $m_g/m_f = 0.2$ . The background spacetime is the dust dominant universe ( $a \propto t^{2/3}$ ).

### Cosmological linear perturbations

Here, we shortly summarize the linear perturbations of a flat FLRW universe in the bigravity theory. Just for simplicity, we assume that the background metrics are given by the homothetic flat FLRW spacetimes. The detail analysis for more generic background spacetime including vector and tensor modes was discussed in e.g., [59].

The background homothetic flat FLRW spacetimes are given by

$$g_{\mu\nu}^{(0)} dx^\mu dx^\nu = -dt^2 + a^2(t) \delta_{ij} dx^i dx^j, \quad (7.1.59)$$

$$f_{\mu\nu}^{(0)} = K^2 g_{\mu\nu}^{(0)}. \quad (7.1.60)$$

This background solution is determined by the standard Friedmann equation with a cosmological constant and the following constraints must be satisfied:

$$\kappa_g^2 T^{[m]\mu}{}_\nu = K^2 \kappa_f^2 \mathcal{T}^{[m]\mu}{}_\nu, \quad (7.1.61)$$

$$\Lambda_g = K^2 \Lambda_f. \quad (7.1.62)$$

We then consider the adiabatic scalar perturbations and ignore an anisotropic stress. The perturbed metrics are expressed as

$$\begin{aligned} g_{00} &= -(1 + 2\alpha_g Y), \\ g_{0i} &= -a\beta_g^{(L)} Y_i, \\ g_{ij} &= a^2(\delta_{ij} + 2h_g^{(L)} \delta_{ij} Y + 2h_g^{(T)} Y_{ij}), \end{aligned} \quad (7.1.63)$$

$$\begin{aligned} f_{00} &= -K^2(1 + 2\alpha_f Y), \\ f_{0i} &= -K^2 a\beta_f^{(L)} Y_i, \\ f_{ij} &= K^2 a^2(\delta_{ij} + 2h_f^{(L)} \delta_{ij} Y + 2h_f^{(T)} Y_{ij}), \end{aligned} \quad (7.1.64)$$

while the perturbed energy-momentum tensors are given by

$$\begin{aligned} T^0{}_0 &= -\bar{\rho}_g(1 + \delta_g), \\ T^0{}_i &= a(\bar{\rho}_g + \bar{P}_g)(v_g^{(L)} - \beta_g^{(L)})Y_i, \\ T^i{}_0 &= -a^{-1}(\bar{\rho}_g + \bar{P}_g)v_g^{(L)}Y^i, \\ T^i{}_j &= P_g(\delta^i{}_j + \pi_g^{(L)} \delta^i{}_j), \\ \mathcal{T}^0{}_0 &= -\bar{\rho}_f(1 + \delta_f), \\ \mathcal{T}^0{}_i &= a(\bar{\rho}_f + \bar{P}_f)(v_f^{(L)} - \beta_f^{(L)})Y_i, \\ \mathcal{T}^i{}_0 &= -a^{-1}(\bar{\rho}_f + \bar{P}_f)v_f^{(L)}Y^i, \\ \mathcal{T}^i{}_j &= P_f(\delta^i{}_j + \pi_f^{(L)} \delta^i{}_j), \end{aligned} \quad (7.1.65)$$

where the scalar harmonic function  $Y$  is defined by

$$(\Delta + k^2)Y = 0, \quad (7.1.67)$$

with  $-k^2$  being an eigenvalue of the usual three-dimensional Laplacian operator  $\Delta$ , and its vector and tensor harmonic functions are defined by:

$$\begin{aligned} Y_i &= -k^{-1} \partial_i Y, \\ Y_{ij} &= k^{-2} \left( \partial_i \partial_j - \frac{1}{3} \delta_{ij} \partial^a \partial_a \right) Y, \end{aligned} \quad (7.1.68)$$

respectively. The perturbation variables  $\{\alpha_{g/f}, \beta_{g/f}^{(L)}, h_{g/f}^{(L)}, h_{g/f}^{(T)}\}$  and  $\{\delta_{g/f}, v_{g/f}^{(L)}, \pi_{g/f}^{(L)}\}$  depend only on time. The unperturbed energy densities and pressures,  $\{\bar{\rho}_{g/f}, \bar{P}_{g/f}\}$ , must satisfy

$$\kappa_g^2 \bar{\rho}_g = K^2 \kappa_f^2 \bar{\rho}_f, \quad \kappa_g^2 \bar{P}_g = K^2 \kappa_f^2 \bar{P}_f. \quad (7.1.69)$$

For the perturbation variables in the  $g$ -world, we can define the gauge invariant variables as in GR:

$$\begin{aligned}\Phi_g &= \alpha_g - \dot{\sigma}_g^{(L)}, \\ \Psi_g &= \mathcal{R}_g - H\sigma_g^{(L)}, \\ \Delta_g &= \delta_g + 3(1+w)\frac{a}{k}H(\beta_g^{(L)} - v_g^{(L)})_g, \\ V_g &= v_g^{(L)} + \frac{a}{k}\dot{h}_g^{(T)},\end{aligned}\tag{7.1.70}$$

where

$$w = \bar{P}_g/\bar{\rho}_g, \quad c_s^2 = \dot{\bar{P}}_g/\dot{\bar{\rho}}_g.\tag{7.1.71}$$

$\mathcal{R}_g$  and  $\sigma_g$  are the curvature and the shear perturbations, respectively, which are defined by

$$\mathcal{R}_g = h_g^{(L)} + \frac{1}{3}h_g^{(T)},\tag{7.1.72}$$

$$\sigma_g^{(L)} = \frac{a^2}{k^2}\dot{h}_g^{(T)} - \frac{a}{k}\beta_g^{(L)}.\tag{7.1.73}$$

Similarly, we introduce the gauge invariant variables in the  $f$ -world, which are defined by those with the subscript  $f$ . We note  $w$  and  $c_s^2$  coincide in the  $g$ - and  $f$ -worlds because of (7.1.69).

The massless and massive mode perturbations,  $X_+$  and  $X_-$ , are described by the linear combination of the perturbed variables in the  $g$ - and  $f$ -worlds,  $X_g$  and  $X_f$ , as

$$X_+ = \frac{m_f^2}{m_{\text{eff}}^2}X_g + \frac{m_g^2}{m_{\text{eff}}^2}X_f,\tag{7.1.74}$$

$$X_- = X_g - X_f,\tag{7.1.75}$$

or inversely

$$X_g = X_+ + \frac{m_g^2}{m_{\text{eff}}^2}X_-,\tag{7.1.76}$$

$$X_f = X_+ - \frac{m_f^2}{m_{\text{eff}}^2}X_-.\tag{7.1.77}$$

For the massless mode, there are four independent equations

$$-\frac{k^2}{a^2}\Phi_+ = \frac{\kappa_g^2\bar{\rho}_g}{2}\Delta_+,\tag{7.1.78}$$

$$\Phi_+ + \Psi_+ = 0,\tag{7.1.79}$$

$$\dot{\Delta}_+ - 3wH\Delta_+ + (1+w)\frac{k}{a}V_+ = 0,\tag{7.1.80}$$

and

$$\dot{V}_+ + HV_+ - \frac{k}{a}\left[\frac{c_s^2\Delta_+}{1+w} + \Phi_+\right] = 0,\tag{7.1.81}$$

for four perturbation variables  $\{\Phi_+, \Psi_+, \Delta_+, V_+\}$ .

If both background matter densities ( $\bar{\rho}_g$  and  $\bar{\rho}_f$ ) are dominated by non-relativistic matter ( $w = 0$ ), the equation for the density perturbation  $\Delta_+$  is given by

$$\ddot{\Delta}_+ + 2H\dot{\Delta}_+ + \left(\frac{k^2c_s^2}{a^2} - \frac{\kappa_g^2\bar{\rho}_g}{2}\right)\Delta_+ = 0,\tag{7.1.82}$$

which is the same as that in GR. Then we will not discuss it furthermore.

Unlike the massless mode, there are six independent equations of motion for the massive mode variables  $\{\alpha_-, \beta_-^{(L)}, h_-^{(L)}, h_-^{(T)}, \delta_-, v_-^{(L)}\}$ . By use of  $\Phi_-, \Psi_-$ , which are given by the above six variable, we find the similar four equations to those of the massless mode as

$$-\frac{k^2}{a^2}\Phi_- + m_{\text{eff}}^2 \left( \frac{3}{2}h_-^{(L)} + \frac{3}{4}\frac{a}{k}H\beta_-^{(L)} + h_-^{(T)} \right) = \frac{\kappa_g^2 \bar{\rho}_g}{2}\Delta_-, \quad (7.1.83)$$

$$\Phi_- + \Psi_- = m_{\text{eff}}^2 \frac{a^2}{k^2} h_-^{(T)}, \quad (7.1.84)$$

$$\begin{aligned} \dot{\Delta}_- - 3wH\Delta_- + (1+w)\frac{k}{a}V_- \\ + \frac{3}{4}(1+w)m_{\text{eff}}^2 \frac{a}{k}\beta_-^{(L)} = 0, \end{aligned} \quad (7.1.85)$$

$$\dot{V}_- + HV_- - \frac{k}{a} \left[ \frac{c_s^2 \Delta_-}{1+w} + \Phi_- \right] = 0, \quad (7.1.86)$$

in which the extra terms come from the interactions between two metrics. In addition, we have two more independent equations from (7.1.14) as

$$6\dot{h}_-^{(L)} + 6Hh_-^{(L)} - 6H\alpha_- + \frac{k}{a}\beta_-^{(L)} = 0, \quad (7.1.87)$$

$$\frac{a}{k} \left( \frac{3}{2}\dot{\beta}_-^{(L)} + 6H\beta_-^{(L)} \right) + 3\alpha_- + 6h_-^{(L)} + 2h_-^{(T)} = 0. \quad (7.1.88)$$

Note that although the massive mode variables are gauge invariant in themselves, we also use  $\Phi_-, \Psi_-, \Delta_-$  and  $V_-$  just for the similar description to those of the massless mode.

Once the equation of state are given, since the above six dynamical equations are independent, we can solve the six variables  $\{\alpha_-, \beta_-^{(L)}, h_-^{(L)}, h_-^{(T)}, \delta_-, v_-^{(L)}\}$  for given appropriate initial data.

In order to set up initial data, we have the additional constraint equations:

$$(3m_{\text{eff}}^2 - 2\Lambda_g) \left( \alpha_- + 3h_-^{(L)} \right) = \kappa_g^2 \bar{\rho}_g \left( \delta_- - 3w\pi_-^{(L)} - (1+3w)\alpha_- + 3(1-w)h_-^{(L)} \right), \quad (7.1.89)$$

$$-H\Phi_- + \dot{\Psi}_- = \frac{a}{k}\dot{H}V_- + \frac{1}{4}m_{\text{eff}}^2 \frac{a}{k}\beta_-^{(L)}, \quad (7.1.90)$$

which are obtained from (7.1.15) and 0- $i$  component of the Einstein equations.

From the above basic equations, we find that the variables consist of two parts: One is an oscillating wave part and the other is a monotonically changing part in time. As an example, we show the equation for  $h_-^{(T)}$ :

$$\begin{aligned} \ddot{h}_-^{(T)} + 3H\dot{h}_-^{(T)} + \left( \frac{k^2}{a^2} + m_{\text{eff}}^2 \right) h_-^{(T)} \\ = -\frac{k^2}{a^2} \left( \alpha_- + 3h_-^{(L)} \right) + 12H \left( \dot{h}_-^{(L)} + Hh_-^{(L)} - H\alpha_- \right) \\ \approx -\frac{k^2}{a^2} \left( \alpha_- + 3h_-^{(L)} \right) \quad \left( \text{for } \frac{a}{k} \ll H^{-1} \right). \end{aligned} \quad (7.1.91)$$

Furthermore, when we focus on the epoch such as  $m_{\text{eff}}^2 \gg H^2$ , Eq. (7.1.89) reads  $\alpha_- + 3h_-^{(L)} \approx 0$ . Then we obtain

$$\ddot{h}_-^{(T)} + 3H\dot{h}_-^{(T)} + \left( \frac{k^2}{a^2} + m_{\text{eff}}^2 \right) h_-^{(T)} \approx 0. \quad (7.1.92)$$

This equation naively shows that  $h_-^{(T)}$  oscillates with the frequency  $\omega \sim \sqrt{k^2/a^2 + m_{\text{eff}}^2}$  with the damping amplitude due to the expansion of the universe. As a result, the metric variable will approach a monotonically changing part with damping oscillations.

## 7.2 Massive graviton as dark matter

In this section, we shall consider the massive graviton as a candidate of dark matter. We assume that the Compton wavelength is sufficiently smaller than the galactic scale and that the matter field is minimally coupled to only the  $g$ -metric. In this situation, gravity is basically mediated by the massless graviton: while matter fields propagate on the metric  $g_{\mu\nu}$  and its perturbation is a linear combination of the massless and massive graviton modes, the latter mode is exponentially suppressed at the length scale of the background. Hence, only the Einstein equation of the massless graviton is relevant. Including the energy-momentum tensors of massless and massive gravitons, the equation of motion for the massless graviton, after averaging over a spacetime region with the size larger than the scales of the perturbation but smaller than the scales of the background, is given by

$$\mathcal{E}^{\mu\nu,\alpha\beta}h_{\alpha\beta} = \frac{1}{M_{\text{pl}}}(T_{\text{m}}^{\mu\nu} + T_{\text{gw}}^{\mu\nu} + T_G^{\mu\nu}), \quad (7.2.1)$$

where  $T_{\text{gw}}^{\mu\nu}$  is the usual energy-momentum tensor of the massless graviton, while  $T_G^{\mu\nu}$  is the energy-momentum tensor of the massive graviton. As shown in Section 3.4, they are given by

$$T_{\text{gw}}^{\mu\nu} = \frac{1}{4}\langle h^{\alpha\beta,\mu}h_{\alpha\beta}{}^{,\nu} \rangle, \quad (7.2.2)$$

$$T_G^{\mu\nu} = \frac{1}{4}\langle \varphi^{\alpha\beta,\mu}\varphi_{\alpha\beta}{}^{,\nu} \rangle, \quad (7.2.3)$$

where  ${}_{,\mu}$  denotes a partial derivative and  $h_{\mu\nu}$  is fixed in the transverse-traceless gauge. We notice that the Planck mass used here is defined by (3.4.2) which does not coincide with the mass scale defined by  $\kappa_g$ . Note also that, in this section, we use the dimensionful perturbations  $h_{\mu\nu}$  and  $\varphi_{\mu\nu}$  defined by (3.3.26) and (3.3.27), respectively.

When the massive graviton is non-relativistic, the massive graviton indeed behaves like a dust as a source of the massless graviton. At the rest frame of the massive graviton, the energy-momentum tensor is indeed given by

$$T_G^{\mu\nu} = \frac{m^2}{4}\text{diag}[\langle \varphi^{\alpha\beta}\varphi_{\alpha\beta} \rangle, 0, 0, 0]. \quad (7.2.4)$$

If the massive graviton is the dark matter, the massive gravitons have to survive until today. However, since the graviton couples universally to matter fields, the massive graviton can decay to light particles. The total decay rate of massive graviton [158–160] is given by

$$\Gamma_G \sim 0.1 \frac{m^3}{M_G^2}. \quad (7.2.5)$$

If the decay rate of massive graviton is larger than the present Hubble parameter, the massive graviton cannot be relict at present. By demanding that the decay rate be lower than the present Hubble parameter, an upper bound on the graviton mass is thus given by

$$m \lesssim 0.01 \left( \frac{M_G}{M_{\text{pl}}} \right)^{2/3} \text{ GeV}. \quad (7.2.6)$$

On the other hand, the existence of dark matter in galaxies gives a lower bound on the graviton mass. Since the massive graviton should be confined in galaxies, the de Broglie wavelength of the massive graviton  $2\pi/(mv)$  should be smaller than kpc scale. Using a typical velocity  $v \sim 10^{-3}$  in the halo, a lower bound of the graviton mass is given by

$$m \gtrsim 10^{-23} \text{ eV}. \quad (7.2.7)$$

In summary, when the mass is in the range

$$10^{-23} \text{ eV} \lesssim m \lesssim 0.01 \left( \frac{M_G}{M_{\text{pl}}} \right)^{2/3} \text{ GeV}, \quad (7.2.8)$$

the massive graviton can be a candidate of dark matter.

### 7.2.1 Production of massive gravitons

One of the simplest scenarios of the generation of the massive graviton in the early universe would be through inflation as discussed in [161, 162]. In this case, however, the Hubble expansion rate during inflation must be larger than the graviton mass to produce sufficient amount of massive gravitons for dark matter. In this case, our perturbative approach is no longer used (see Section 6) and thus we shall not consider the generation of massive graviton during inflation.

Instead of the production by inflation, we thus consider the generation of the massive graviton through the preheating after inflation. During preheating, the inflaton decays to inhomogeneous modes of itself and/or some other fields and then large inhomogeneities can be created. This kind of field bubble is a classical source of gravitational waves. The gravitational waves from the preheating have been discussed in [163–171]. The peak momentum  $k_* = |\mathbf{k}_*|$  and the energy density  $\rho_{\text{gw}}^*$  of the generated massless gravitational wave are roughly estimated as

$$k_* \sim 1/R_*, \quad \rho_{\text{gw}}^* \sim \alpha (R_* H_*)^2 \rho_* \quad (7.2.9)$$

where  $R_*$ ,  $H_*$  and  $\rho_*$  are the typical size of the field bubble, the Hubble expansion rate, and the energy density at the time of production, respectively, and we have included a numerical factor  $\alpha$  that varies from one model to another ( $\alpha \simeq 0.1$  for chaotic inflation, for example) [166, 167, 170]. The typical size  $R_*$  and the numerical factor  $\alpha$  can be evaluated when we assume a concrete preheating model. However, we take a phenomenological attitude and treat  $R_*$  and  $\alpha$  as a free parameter to discuss a model independent prediction. The present frequency and the density parameter of the gravitational wave background are then given by

$$f \sim \frac{4 \times 10^{10}}{R_* \rho_*^{1/4}} \text{Hz}, \quad h^2 \Omega_{\text{gw}} \sim 10^{-5} \alpha (R_* H_*)^2. \quad (7.2.10)$$

Note that in this model, the gravitational waves are created at the sub-horizon scale which remain the sub-Horizon scale until today. We can assume the graviton mass is larger than the Hubble expansion rate at the time of production of gravitational waves so that the Higuchi instability is avoided. Therefore, the cosmic history of the amplitude of gravitational waves can be discussed by using the linear theory until today.

In the sub-horizon scale, we can ignore the effect of the expansion of the Universe to discuss the generations of the massless and the massive gravitons. Hence we can use the equations on the Minkowski background. For the massless graviton, the equation of motion with a source is expressed by

$$\partial^2 h^{\mu\nu} = -\frac{2}{M_{\text{pl}}} S^{\mu\nu}, \quad (7.2.11)$$

where  $S^{\mu\nu}$  will be specified in (7.2.15) below and we have chosen the harmonic gauge

$$\partial_\mu h^\mu{}_\nu = \frac{1}{2} \partial_\nu h. \quad (7.2.12)$$

On the other hand, the equation of motion for the massive graviton is given by

$$(\partial^2 - m^2)\varphi^{\mu\nu} = -\frac{2}{M_G} J^{\mu\nu}, \quad (7.2.13)$$

where the massive graviton must satisfy the constraint equations

$$\partial_\mu \varphi^{\mu\nu} = \partial^\nu \varphi, \quad \frac{m^2}{2} \varphi = -\frac{1}{3M_G} T_{\text{m}}. \quad (7.2.14)$$

The source terms for massless and massive gravitons are given by

$$S^{\mu\nu} := T_{\text{m}}^{\mu\nu} - \frac{1}{2} \eta^{\mu\nu} T_{\text{m}}, \quad (7.2.15)$$

$$J^{\mu\nu} := T_{\text{m}}^{\mu\nu} - \frac{1}{3} \left( \eta^{\mu\nu} - \frac{\partial^\mu \partial^\nu}{m^2} \right) T_{\text{m}}. \quad (7.2.16)$$



Using the retarded Green's function

$$G_R(x-y; p) = \theta(x^0 - y^0) \int \frac{d^3 \mathbf{p}}{(2\pi)^3} \frac{-i}{2p^0} \left( e^{ip(x-y)} - e^{-ip(x-y)} \right), \quad (7.2.17)$$

the solutions of Eqs. (7.2.11) and (7.2.13) can be constructed. We denote  $k^\mu$  as the four-momentum of the massless graviton and  $p^\mu$  as the four-momentum of the massive graviton with  $p^\mu p_\mu = -m^2$ . We evaluate the solutions after the source vanishes, i.e., after the preheating. Choosing the coordinate  $u^\mu = \delta_0^\mu$  in the transverse-traceless gauge, the solutions are given by

$$h_{0\mu}(x) = 0, \\ h_{ij}(x) = \frac{2}{M_{\text{pl}}} \int \frac{d^3 \mathbf{k}}{(2\pi)^3} \frac{i}{2k^0} \mathcal{O}_{ijlm}(k) \mathcal{T}_m^{lm}(k) e^{ikx} + \text{c.c.}, \quad (7.2.18)$$

$$\varphi_{\mu\nu}(x) = \frac{2}{M_G} \int \frac{d^3 \mathbf{p}}{(2\pi)^3} \frac{i}{2p^0} \mathcal{J}_{\mu\nu}(p) e^{ipx} + \text{c.c.}, \quad (7.2.19)$$

where

$$\mathcal{O}_{ijlm} = P_{l(i} P_{j)m} - \frac{1}{2} P_{ij} P_{lm}, \quad P_{ij} = \delta_{ij} - k_i k_j / \mathbf{k}^2, \quad (7.2.20)$$

is the transverse-traceless projection operator which is introduced to satisfy the transverse-traceless gauge. Note that the source terms

$$\mathcal{T}_m^{ij}(k) = \int d^4 y e^{-iky} T_m^{ij}(y), \quad (7.2.21)$$

$$\mathcal{J}^{\alpha\beta}(p) = \int d^4 y e^{-ipy} J^{\alpha\beta}(y) \\ = \mathcal{T}_m^{\alpha\beta}(p) - \frac{1}{3} \left( \eta^{\alpha\beta} + \frac{p^\alpha p^\beta}{m^2} \right) \mathcal{T}_m(p), \quad (7.2.22)$$

are evaluated at only  $k^2 = 0$  and  $p^2 = -m^2$ , respectively. The on-shell condition for the massive graviton leads  $p^\mu \mathcal{J}_{\mu\nu} = 0, \mathcal{J}^\mu{}_\mu = 0$ , thus the massive graviton automatically satisfies the transverse-traceless condition after the source vanishes. As a result, we find

$$\langle h_{\alpha\beta}{}^{,\mu} h^{\alpha\beta, \nu} \rangle = \frac{4}{M_{\text{pl}}^2} \left\langle \int \frac{d^3 \mathbf{k}}{(2\pi)^3} \int \frac{d^3 \mathbf{k}'}{(2\pi)^3} \frac{k^\mu k'^\nu}{2k^0 k'^0} \mathcal{T}_m^{kl}(k) \mathcal{O}_{kl}^{ij}(k) \mathcal{O}_{ijnm}(k') \mathcal{T}_m^{*nm}(k') e^{i(k-k')x} \right\rangle, \quad (7.2.23)$$

$$\langle \varphi_{\alpha\beta}{}^{,\mu} \varphi^{\alpha\beta, \nu} \rangle = \frac{4}{M_G^2} \left\langle \int \frac{d^3 \mathbf{p}}{(2\pi)^3} \int \frac{d^3 \mathbf{p}'}{(2\pi)^3} \frac{p^\mu p'^\nu}{2p^0 p'^0} \mathcal{J}^{\alpha\beta}(p) \mathcal{J}_{\alpha\beta}^*(p') e^{i(p-p')x} \right\rangle \\ \approx \frac{4}{M_G^2} \left\langle \int \frac{d^3 \mathbf{p}}{(2\pi)^3} \int \frac{d^3 \mathbf{p}'}{(2\pi)^3} \frac{p^\mu p'^\nu}{2p^0 p'^0} \left( \mathcal{T}_m^{\alpha\beta}(p) \mathcal{T}_{m\alpha\beta}^*(p') - \frac{1}{3} \mathcal{T}_m(p) \mathcal{T}_m^*(p') \right) e^{i(p-p')x} \right\rangle, \quad (7.2.24)$$

where  $*$  denotes the complex conjugate and we have used the on-shell condition  $p^2 = -m^2$ . While the last term in (7.2.16) would diverge in the limit  $m^2 \rightarrow 0$ , (7.2.24) is finite in the same limit.

The result indicates that, if most of the produced massive gravitons are relativistic, i.e.,  $k_* > m$ , the amount of the gravitons are simply evaluated by

$$\langle \varphi_{\alpha\beta}{}^{,\mu} \varphi^{\alpha\beta, \nu} \rangle \sim \frac{M_{\text{pl}}^2}{M_G^2} \langle h_{\alpha\beta}{}^{,\mu} h^{\alpha\beta, \nu} \rangle. \quad (7.2.25)$$

In this case, the massive gravitons behave like a cold, warm, or hot dark matter depending on the free-streaming scale as far as the structure formation is concerned.

We then discuss the case where the peak momentum  $k_*$  is smaller than the graviton mass, i.e.,  $m > k_* \sim 1/R_*$ , where  $R_*$  is the scale of the field bubble. In this case, the massive graviton is produced with non-relativistic velocity and continues to be non-relativistic afterward. Therefore, the massive graviton behaves like a cold dark matter.

In order to relate the abundance of massive gravitons as dark matter to the amount of gravitational waves, we are interested in the ratio of the stress-energy tensors for the massive and massless gravitons. In the case under consideration, i.e. for  $m > k_* \sim 1/R_*$ , the ratio strongly depends on the value of  $mR_*$ . Since the bubbly stage of the preheating is significantly non-Gaussian, the estimate of the abundance of massive gravitons requires detailed numerical simulations, in general.

Nevertheless, we could roughly estimate the produced abundance of the massive gravitons when we know the spectrum of gravitational waves. We focus on only the tensor mode of the massive graviton, for simplicity. Since we focus on only the produced amount, we will omit the index  $*$  to represent the production time until the end of this subsection. The equations of motion for the transverse-traceless components are given by

$$\ddot{h}_{ij}^{\text{TT}} + \mathbf{k}^2 h_{ij}^{\text{TT}} = \frac{2}{M_{\text{pl}}} \Pi_{ij}, \quad (7.2.26)$$

$$\ddot{\varphi}_{ij}^{\text{TT}} + (\mathbf{p}^2 + m^2) \varphi_{ij}^{\text{TT}} = \frac{2}{M_G} \Pi_{ij}, \quad (7.2.27)$$

where  $h_{ij}^{\text{TT}}$  and  $\varphi_{ij}^{\text{TT}}$  are the transverse-traceless components of the massless graviton and the massive graviton, respectively, and  $\Pi_{ij} = \mathcal{O}_{ijlm} T_m^{lm}$ . We assume the source exists only  $t_{\text{start}} < t < t_{\text{end}}$  and there were no gravitons before  $t_{\text{start}}$ . The source are assumed to be statistically homogeneous and isotropic. The energy densities are expressed by

$$\begin{aligned} \rho_{\text{gw}} &= \frac{1}{4} \langle \dot{h}_{\text{TT}}^{ij} \dot{h}_{ij}^{\text{TT}} \rangle_{\text{ens}} \\ &= \frac{1}{4} \frac{1}{(2\pi)^3} \int d^3 \mathbf{k} P_h(t, k), \end{aligned} \quad (7.2.28)$$

$$\begin{aligned} \rho_G^{\text{TT}} &= \frac{1}{4} \langle \dot{\varphi}_{\text{TT}}^{ij} \dot{\varphi}_{ij}^{\text{TT}} \rangle_{\text{ens}} \\ &= \frac{1}{4} \frac{1}{(2\pi)^3} \int d^3 \mathbf{p} P_\varphi(t, p), \end{aligned} \quad (7.2.29)$$

where  $\rho_G^{\text{TT}}$  is the energy density of the massive gravitons contributed from only the tensor mode and  $k = |\mathbf{k}|$  and  $p = |\mathbf{p}|$ . We have replaced the spacetime average  $\langle \dots \rangle$  with the ensemble average  $\langle \dots \rangle_{\text{ens}}$  to define the energy densities of gravitons. This replacement can be taken when the ergodic assumption is valid. The power spectra are defined by

$$\langle \dot{h}_{\text{TT}}^{ij}(t, \mathbf{k}) \dot{h}_{ij}^{\text{TT}*}(t, \mathbf{k}') \rangle_{\text{ens}} = (2\pi)^3 \delta^{(3)}(\mathbf{k} - \mathbf{k}') P_h(t, k), \quad (7.2.30)$$

$$\langle \dot{\varphi}_{\text{TT}}^{ij}(t, \mathbf{p}) \dot{\varphi}_{ij}^{\text{TT}*}(t, \mathbf{p}') \rangle_{\text{ens}} = (2\pi)^3 \delta^{(3)}(\mathbf{p} - \mathbf{p}') P_\varphi(t, p), \quad (7.2.31)$$

where  $*$  represents the complex conjugate. Substituting the solutions of (7.2.26) and (7.2.27) into the expressions of power spectra, they are expressed by

$$P_h = \frac{2}{M_{\text{pl}}^2} \int_{t_{\text{start}}}^{t_{\text{end}}} dt_x \int_{t_{\text{start}}}^{t_{\text{end}}} dt_y \cos[k(t_x - t_y)] \Pi(t_x, t_y, k), \quad (7.2.32)$$

$$P_\varphi = \frac{2}{M_G^2} \int_{t_{\text{start}}}^{t_{\text{end}}} dt_x \int_{t_{\text{start}}}^{t_{\text{end}}} dt_y \cos[\omega(t_x - t_y)] \Pi(t_x, t_y, p) \quad (7.2.33)$$

where  $\omega = \sqrt{\mathbf{p}^2 + m^2}$  and  $\Pi$  is defined by

$$\langle \Pi^{ij}(t_x, \mathbf{k}) \Pi_{ij}^*(t_y, \mathbf{k}') \rangle = (2\pi)^3 \delta^{(3)}(\mathbf{k} - \mathbf{k}') \Pi(t_x, t_y, k). \quad (7.2.34)$$

It is worth noting that the two point correlators are proportional to the delta function due to the statistical homogeneity and the quantities  $P_h, P_\varphi$  and  $\Pi$  depend on  $k$  (or  $p$ ) due to the statistical isotropy.

Conventionally, spectra of energy densities are expressed by using the densities per logarithmic frequency. For the massive graviton, it is more convenient to use the density per logarithmic momentum  $p$  instead of the frequency  $\omega$ . The densities per logarithmic interval are calculated as

$$\frac{d\rho_{\text{gw}}}{d \ln k} = \frac{k^3}{4\pi^2 M_{\text{pl}}^2} \int_{t_{\text{start}}}^{t_{\text{end}}} dt_x \int_{t_{\text{start}}}^{t_{\text{end}}} dt_y \cos[k(t_x - t_y)] \Pi(t_x, t_y, k), \quad (7.2.35)$$

$$\frac{d\rho_G^{\text{TF}}}{d \ln p} = \frac{p^3}{4\pi^2 M_G^2} \int_{t_{\text{start}}}^{t_{\text{end}}} dt_x \int_{t_{\text{start}}}^{t_{\text{end}}} dt_y \cos[\omega(t_x - t_y)] \Pi(t_x, t_y, p). \quad (7.2.36)$$

Note that, when the source is uncollated, namely white noise, the integrations of these expressions are constant and then the momentum dependence of the spectrum is given by  $k^3$  (or  $p^3$ ). Since our source is generated by a causal process, the source is uncollated in scales beyond the causal connected region. For the massive gravitons, the gravitational interaction exists only within the Compton wavelength. Hence, the integration of Eq. (7.2.36) will read constant for  $p^{-1} > m^{-1}$  because the source is effectively uncollated for massive gravitons in that scale.

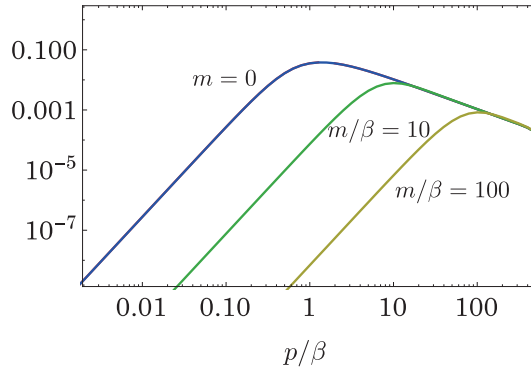


Figure 7.6: The energy spectra of gravitons from bubble collision. We use the formula [172] to model the two-point correlator of the source where  $\beta^{-1}$  is the duration of the production process. The amplitude is scale free since we do not specify the background energy density. All IR tails of spectra are given by  $p^3$ .

We show the energy spectra generated by bubble collisions in Fig. 7.6. Gravitational waves from bubble collision have been discussed in the context of cosmic phase transitions because the vacuum bubbles are produced during first-order phase transitions (see e.g., [173,174] for reviews). Although the electroweak phase transition or QCD phase transition may not be first-order, models beyond the standard model can lead to the first-order phase transition. The gravitational waves from those are good tools to explore a signature of beyond standard models. An analytic formula to express the two-point correlator of the bubble collisions is discussed in [172]. The spectrum depends on the wall velocity and the duration of the phase transition, however, we only consider the case when the wall velocity is the speed of light, for simplicity.

The spectra shown in Fig. 7.6 are calculated by the formula given by [172] where  $\beta^{-1}$  is the duration of the phase transition. Since the source does not exist beyond the time scale  $\beta^{-1}$ , the source is uncollated beyond the length scale  $\beta^{-1}$ . Hence, the IR tail of the spectrum is given by  $p^3$  for  $p/\beta < 1$ . For the massive gravitons, additionally, the tail of spectrum is given by  $p^3$  for  $p/m < 1$ . This dependence is, indeed, the consequence of that the gravitational interaction exists only within the Compton wavelength and then the source is effectively uncollated in large scales for massive gravitons.

The above results are obtained from a simple source; thus, it may not be directly applied to gravitons produced by other sources, e.g., preheating interested in here. However, the  $p^3$  dependence at large scales must be a generic feature of the energy spectrum of massive gravitons. If the peak momentum of the massless gravitons is smaller than the graviton mass, the peak momentum of the massive graviton is  $p_{\text{peak}} = m$  as shown in Fig. 7.6. Since the spectrum of the massive graviton for  $p > m$  should be the same as that of the massless graviton, the generated energy

density of massive graviton is evaluated by

$$\left. \frac{d\rho_G^{\text{TT}}}{d \ln p} \right|_{\text{peak}} \simeq \frac{M_{\text{pl}}^2}{M_G^2} \left. \frac{d\rho_{\text{gw}}}{d \ln k} \right|_{k=m}, \quad (7.2.37)$$

for  $k_{\text{peak}} < m$  when the spectrum of  $d\rho_{\text{gw}}/d \ln k$  decreases for  $k > m$ . When we know the details of the spectrum of massless gravitons, we can estimate the spectrum of massive gravitons.

Since we have concentrated on the tensor mode in the above arguments, the produced energies of vector and scalar modes are not clear yet. When the source is a complicated random field, all polarization modes of the massive graviton may be equally produced. Hence, we do not consider the difference depending on the polarizations furthermore.

## 7.2.2 Present abundance and gravitational waves

The UV behavior of spectrum should strongly depend on the production mechanism (see Fig. 7.7); thus we will restrict our analysis to the case where the peak momentum of the gravitational wave is higher than the graviton mass, i.e.  $m < k_* \sim 1/R_*$ , where  $R_*$  is the scale of the field bubble and the index  $*$  represent the quantities at the production. In this case, the massive graviton is produced with relativistic velocities. In order to realize the bottom-up scenario of the structure formation, we thus need to make it sure that the free streaming scale due to the massive graviton is less than about 0.1 Mpc [175]. The free streaming due to the relativistic motion of massive gravitons continues until the peak momentum is redshifted down to  $m$ . Therefore, The free streaming scale is estimated as

$$\begin{aligned} L_{\text{fs}} &\sim \frac{a_0}{a_{\text{nr}} H_{\text{nr}}} \sim \frac{a_{\text{nr}}}{a_*} \frac{a_0}{a_* H_*} \sim \frac{1}{m R_*} \frac{a_0}{a_* H_*} \\ &\sim \frac{2\pi f}{m} 10^7 \text{ Mpc}, \end{aligned} \quad (7.2.38)$$

where  $a_{\text{nr}}$  and  $H_{\text{nr}}$  are the scale factor and the Hubble expansion rate, respectively, at the time when the massive graviton becomes non-relativistic and  $a_0$  is the scale factor today. By requiring that  $L_{\text{fs}}$  be less than 0.1 Mpc, we thus obtain the constraint

$$\frac{m}{2\pi f} > 10^8. \quad (7.2.39)$$

Therefore, in the case of the relativistic production, if the characteristic frequency of the gravitational wave from preheating is determined by observation, we can obtain a lower bound on the graviton mass.

In this case, most of the generated massive gravitons are relativistic with the momentum  $\sim k_* > m$ , thus both massive and massless gravitons are created by the sources with almost the same four-momenta. As shown in (7.2.25), the energy densities are thus evaluated as

$$\frac{\rho_G^*}{\rho_{\text{gw}}^*} \sim \frac{M_{\text{pl}}^2}{M_G^2}, \quad (7.2.40)$$

where  $\rho_G^*$  and  $\rho_{\text{gw}}^*$  are the energy densities of the massive graviton and the massless graviton at the production time. When the massive graviton is relativistic, the energy densities of both gravitons decrease as  $a^{-4}$ , where  $a$  is the scale factor of the Universe. As the Universe expands, the massive graviton becomes non-relativistic, and then the energy density of the massive graviton decreases as  $a^{-3}$ . Hence the energy density of the massive graviton at the present is

$$\Omega_G \sim \frac{M_{\text{pl}}^2}{M_G^2} \frac{m}{2\pi f} \Omega_{\text{gw}}, \quad (7.2.41)$$

where  $\Omega_G$  is the density parameter of the massive graviton. Hence if the massive graviton is the dominant component of dark matter, the combination  $(M_{\text{pl}}/M_G)^2 \times m$  can be estimated by the gravitational wave background as shown in Fig. 7.7.

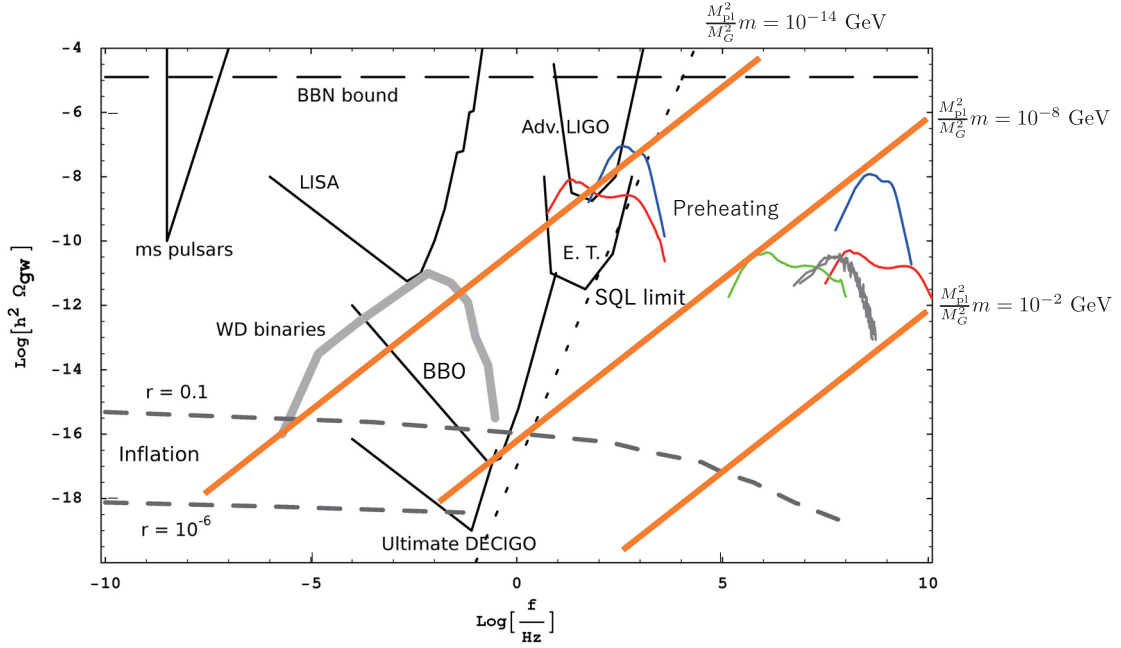


Figure 7.7: The sensitivities of gravitational wave detectors and the expected gravitational wave spectra from the preheating (red, blue, green and gray curves at the right), adopted from [170]. The orange lines then represent expected frequency and amplitude of the gravitational wave background corresponding to the massive graviton dark matter model for  $(M_{\text{pl}}/M_G)^2 \times m = 10^{-14}\text{GeV}$ ,  $10^{-8}\text{GeV}$  and  $10^{-2}\text{GeV}$ . The gravitational wave background thus determines the combination  $(M_{\text{pl}}/M_G)^2 \times m$ . In particular, some of gravitational wave spectra are detectable by LIGO, for which the massive graviton can be the dominant component of dark matter when  $(M_{\text{pl}}/M_G)^2 \times m \sim 10^{-14}\text{ GeV}$ .

Since the present abundance and the frequency of the gravitational wave background can be evaluated by (7.2.10), the present abundance and the free streaming scale of the massive graviton can be estimated by using  $\rho_*$  and  $R_*$ . We now focus on gravitational waves to be sensitive in the LIGO range. For instance, the preheating of

$$\rho_*^{1/4} \sim 10^8 \text{ GeV}, \quad R_*^{-1} \sim 0.1 \text{ GeV}, \quad (7.2.42)$$

predicts the gravitational wave background with

$$f \sim 40 \text{ Hz}, \quad h^2 \Omega_{\text{gw}} \sim \alpha 10^{-8}. \quad (7.2.43)$$

Note that the graviton mass has been assumed to be consistent with the Higuchi bound, i.e.  $m > \sqrt{2}H_*$ , to avoid the Higuchi instability, while the relativistic production is realized only when  $m < R_*^{-1}$ . Hence, the consistency of our assumptions reads  $R_*^{-1} > m > \sqrt{2}H_*$ . A set of consistent parameters is

$$m \sim 0.01 \text{ GeV}, \quad M_G \sim 10^6 M_{\text{pl}}, \quad (7.2.44)$$

in which the massive graviton can explain the observed amount of the dark matter. Since  $\sqrt{2}H_* \sim 0.005 \text{ GeV}$ , the Higuchi bound is barely satisfied. The corresponding free streaming scale is about  $10^{-7} \text{ pc}$ , so the massive graviton behaves like a cold dark matter. Therefore if the gravitational detectors observe the stochastic gravitational wave background with (7.2.43), the massive graviton with (7.2.44) is a viable candidate of dark matter.

## Chapter 8

# Astrophysical objects and Vainshtein screening

In the previous chapters, we discussed the cosmological solutions in bigravity and found the bigravity theory admits a viable cosmological solution and yield various phenomenological features. Therefore, the bigravity theory is phenomenologically a good candidate for an alternative theory of gravity. However the modification of the gravity is strongly constrained by Solar System tests of the gravity which agree with the predictions of GR (see e.g., [1]). Hence the effect of the modification of gravity must be screened at Solar System and must admit viable solutions for astrophysical objects.

In bigravity, there are a massive graviton as well as a massless graviton. If the graviton mass is heavy enough, the massive graviton does not give any effect on the gravitational field because of the Yukawa suppression. Therefore, we will not discuss such a heavy massive graviton in this chapter. On the other hand, in the present chapter, we shall focus on the sufficiently light massive graviton such that the graviton mass is  $m < 10^{-23}$  eV. The gravitational field and the structure of the astrophysical objects would be changed by the existence of the massive graviton. Intuitively, the massive graviton is restored into the massless graviton by taking the massless limit. However, the linear massive gravity, namely Fierz-Pauli theory [6], cannot be restored to the linearized GR even in the massless limit (vDVZ discontinuity) [7,8]. Vainshtein proposed that the vDVZ discontinuity can be evaded by taking into account nonlinear mass terms [9]. Therefore, the non-linear bigravity theory may have no discontinuity in the massless limit.

To discuss the restoration to GR, one of the simplest system is the static and spherically symmetric spacetime. Indeed, stars and black holes could be well-approximated by static and spherical objects except for rapidly rotating cases. In bigravity, the static and spherically symmetric solutions are classified into non-diagonal ansatz [67–69], and bi-diagonal ansatz. In the former type ansatz, there are only trivial solutions, which are the same as those in GR. Additionally, the perturbation around the non-diagonal solution is also identical to GR [176–178]. Hence, the massive graviton does not appear in the non-diagonal ansatz. To find a non-trivial solution, if it exists, we should assume both metrics can be simultaneously diagonal in a same coordinate system. Based on the bi-diagonal ansatz, the solutions with Vainshtein screening for stars were found in the weak gravity region [76,79,82] and also in the strong gravity region [85], in which the behavior in GR is recovered inside the Vainshtein radius but the modification appears outside the Vainshtein radius.

The black hole geometry in bigravity is a open question. There exists some special case of the bi-diagonal ansatz such that two metrics are proportional, which we have called a homothetic spacetime. The solutions are also given by those in GR. However, in this case, the massive graviton appears in the perturbation around the solutions. As a result, the homothetic Schwarzschild black hole becomes unstable against the radial perturbations if the graviton mass is sufficiently small [179–181]. The instability of this black hole implies that there would be a hairy black hole solution as well, and that the homothetic Schwarzschild black hole may transit to the hairy black hole. However, the paper [182] showed numerically that such a hairy black hole does not exist unless the coupling constants satisfy a special condition. One may wonder what we will find in the

final stage of gravitational collapse of a compact relativistic star.

In the paper [85] we show the coupling constants are classified into two classes: Class [I] and Class [II]. In Class [I], a curvature singularity appears when a mass of a neutron star exceeds a critical value. On the other hand, the Vainshtein screening holds even for a neutron star in Class [II]; however, the stability condition in the early universe discussed in Chapter 6 exclude this possibility. Hence, the problem arises in the astrophysical scale in Class [I], while the problem arises in the cosmological scale in Class [II].

The existence of the singularity and the non-existence of the hairy black hole may imply that the static and spherical symmetry is not sufficient to describe an astrophysical objects. It seems that the problems exist only in the strong gravitational field. However, we also show the static and spherically symmetric solutions obtained in the weak gravitational field are unstable against small perturbations [86]. Therefore, the static and spherical symmetry should not be sufficient even in the weak gravitational field regime. Indeed, as already discussed in §. 4.5.3, the scalar graviton generally suffers from an instability in Ricci flat spacetime when the vector graviton is not excited. If we assume the spherical symmetry, there is no vector type freedom; thus the spherically symmetric solutions would be unstable outside astrophysical objects. To discuss any astrophysical objects, we should relax the spherical symmetry in bigravity but non-spherical solutions have not been found so far. The existence of a viable astrophysical solution (not only black holes but also stars) is an open question in bigravity.

This chapter is organized as follows. We summarize the basic equations for the bi-diagonal static and spherically symmetric solution in Section 8.1. We review the weak field results obtained by [79, 82] in Section 8.2. In Section 8.3 we then summarize our result [85] in which we have focused on the strong gravitational field such as a neutron star. In this section, we also verify the  $\Lambda_2$  decoupling limit indeed gives an approximated solution deep inside the Vainshtein radius. Finally, we discuss the stability of the static and spherically symmetric solution [86] in Section 8.4.

## 8.1 Static and spherically symmetric spacetime

To find a non-trivial static and spherically symmetric regular solution, we assume two metrics are bi-diagonal in a same coordinate system. Thus, we consider the following metric forms:

$$ds_g^2 = -N_g^2 dt^2 + \frac{r_g'^2}{F_g^2} dr^2 + r_g^2 d\Omega^2, \quad (8.1.1)$$

$$ds_f^2 = K^2 \left[ -N_f^2 dt^2 + \frac{r_f'^2}{F_f^2} dr^2 + r_f^2 d\Omega^2 \right], \quad (8.1.2)$$

where the variables  $\{N_g, F_g, r_g, N_f, F_f, r_f\}$  are functions of a radial coordinate  $r$ , and a prime denotes the derivative with respect to  $r$ . The ansatz has two residual gauge freedoms: One is a rescaling of time coordinate ( $t \rightarrow \hat{t} = ct$  with  $c$  being a constant), and the other is redefinition of the radial coordinate ( $r \rightarrow \tilde{r}(r)$ ). The proportional constant factor  $K$  is introduced just for convenience. When  $N_g/N_f = F_g/F_f = r_g/r_f = 1$ ,  $g$ - and  $f$ -spacetimes are homothetic and the  $\gamma$  energy-momentum tensors turn to be just “effective” cosmological terms, where the  $g$ - and  $f$ -cosmological constants are given by

$$\begin{aligned} \Lambda_g(K) &= m^2 \frac{\kappa_g^2}{\kappa^2} (b_0 + 3b_1 K + 3b_2 K^2 + b_3 K^3), \\ \Lambda_f(K) &= m^2 \frac{\kappa_f^2}{\kappa^2} (b_4 + 3b_3 K^{-1} + 3b_2 K^{-2} + b_1 K^{-3}). \end{aligned} \quad (8.1.3)$$

Since two metrics are proportional, the Einstein equations reads

$$\Lambda_g(K) = K^2 \Lambda_f(K), \quad (8.1.4)$$



which determines  $K$  as one of the real roots of this quartic equation. We focus on asymptotically homothetic Minkowski solutions<sup>1</sup>, i.e., we assume the boundary condition

$$N_g/N_f, F_g/F_f, r_g/r_f \rightarrow 1, \quad (8.1.5)$$

with  $\Lambda_g(1) = \Lambda_f(1) = 0$ .

We introduce new variable  $\mu$  defined by

$$\mu := \frac{r_f}{r_g} - 1 \quad (8.1.6)$$

with  $\mu > -1$ , which determines the relation between two radial coordinates  $r_g$  and  $r_f$ . From the boundary condition,  $\mu$  should approach zero at infinity.

Introducing new parameters as

$$m_g^2 := \frac{m^2 \kappa_g^2}{\kappa^2} (b_1 K + 2b_2 K^2 + b_3 K^3), \quad (8.1.7)$$

$$m_f^2 := \frac{m^2 \kappa_f^2}{K^2 \kappa^2} (b_1 K + 2b_2 K^2 + b_3 K^3), \quad (8.1.8)$$

$$\beta_2 := \frac{b_2 K^2 + b_3 K^3}{b_1 K + 2b_2 K^2 + b_3 K^3}, \quad (8.1.9)$$

$$\beta_3 := \frac{b_3 K^3}{b_1 K + 2b_2 K^2 + b_3 K^3}, \quad (8.1.10)$$

the Einstein equations are reduced to

$$\frac{2F_g F'_g}{r_g r'_g} + \frac{F_g^2 - 1}{r_g^2} = -\kappa_g^2 \rho_g - \Lambda_g + m_g^2 \left( 1 + 2(\beta_2 - 1)\mu + (\beta_3 - \beta_2)\mu^2 - (1 + 2\beta_2\mu + \beta_3\mu^2) \frac{r'_f F_g}{r'_g F_f} \right), \quad (8.1.11)$$

$$\frac{2F_g^2 N'_g}{r_g r'_g N_g} + \frac{F_g^2 - 1}{r_g^2} = \kappa_g^2 P_g - \Lambda_g + m_g^2 \left( 1 + 2(\beta_2 - 1)\mu + (\beta_3 - \beta_2)\mu^2 - (1 + 2\beta_2\mu + \beta_3\mu^2) \frac{N_f}{N_g} \right), \quad (8.1.12)$$

$$\begin{aligned} \frac{2F_f F'_f}{r_f r'_f} + \frac{F_f^2 - 1}{r_f^2} &= -K^2 \kappa_f^2 \rho_f - \Lambda_g \\ &+ \frac{m_f^2}{(1 + \mu)^2} \left( 1 + 2(1 + \beta_2)\mu + (1 + \beta_2 + \beta_3)\mu^2 - (1 + 2\beta_2\mu + \beta_3\mu^2) \frac{r'_g F_f}{r'_f F_g} \right), \end{aligned} \quad (8.1.13)$$

$$\begin{aligned} \frac{2F_f^2 N'_f}{r_f r'_f N_f} + \frac{F_f^2 - 1}{r_f^2} &= K^2 \kappa_f^2 P_f - \Lambda_g \\ &+ \frac{m_f^2}{(1 + \mu)^2} \left( 1 + 2(1 + \beta_2)\mu + (1 + \beta_2 + \beta_3)\mu^2 - (1 + 2\beta_2\mu + \beta_3\mu^2) \frac{N_g}{N_f} \right), \end{aligned} \quad (8.1.14)$$

We have two more Einstein equations, which are automatically satisfied since we have two Bianchi identities for  $g_{\mu\nu}$  and  $f_{\mu\nu}$ .

In the original Lagrangian, we have six unfixed coupling constants  $\{\kappa_f, b_i\}$ , where  $m$  is not independent because it is just a normalization factor of  $b_i$ . We use six different combinations of those constants;  $\{m_g, m_f, \Lambda_g, K, \beta_2, \beta_3\}$ , in stead of  $\{\kappa_f, b_i\}$ , because the behaviors of the solutions within the Vainshtein radius are characterized by  $\beta_2$  and  $\beta_3$  as we will see later. The original coupling constants  $\{\kappa_f, b_i\}$  are found from  $\{m_g, m_f, \Lambda_g, K, \beta_2, \beta_3\}$ .

<sup>1</sup>Non-asymptotically homothetic solutions and non-asymptotically flat solutions can be found which are shown in Appendix of [85]. However, these are not relevant for our discussion so we shall not discuss them furthermore.

The energy-momentum conservation laws of twin matters give

$$P'_g + \frac{N'_g}{N_g}(\rho_g + P_g) = 0, \quad (8.1.15)$$

$$P'_f + \frac{N'_f}{N_f}(\rho_f + P_f) = 0, \quad (8.1.16)$$

where we assume that twin matters are perfect fluids. The energy-momentum conservation laws of the interaction terms, which are equivalent to the Bianchi identities, reduce to one constraint equation;

$$2(F_g - F_f) \left( N_g(1 - \beta_2 + (\beta_2 - \beta_3)\mu) + N_f(\beta_2 + \beta_3\mu) \right) + r_g(1 + 2\beta_2\mu + \beta_3\mu^2) \left( \frac{F_g N'_g}{r'_g} - \frac{F_f N'_f}{r'_f} \right) = 0. \quad (8.1.17)$$

Substituting the Einstein equations (8.1.12) and (8.1.14) into Eq. (8.1.17), we obtain one algebraic equation:

$$\mathcal{C}[N_g, N_f, F_g, F_f, \mu, P_g, P_f] = 0. \quad (8.1.18)$$

Note that the proportional factor  $K$  is not necessary to be unity. Since  $K$  appears only in the form of  $K^2\rho_f$  and  $K^2P_f$ , however, unless  $f$  matter exists, the basic equations are free from the value of  $K$ . In what follows, we assume that there is no  $f$ -matter just for simplicity; thus we can set  $K = 1$  without loss of generality. Some discussions on the effects from  $f$ -matter are done in Appendixes of [63, 85].

## 8.2 Weak field approximation

First, we consider the weak gravitational field such that the variables  $\{N_g, N_f, F_g, F_f\}$  are approximated by

$$N_g = e^{\Phi_g} \simeq 1 + \Phi_g, \quad F_g^{-1} = e^{\Psi_g} \simeq 1 + \Psi_g, \quad (8.2.1)$$

$$N_f = e^{\Phi_f} \simeq 1 + \Phi_f, \quad F_f^{-1} = e^{\Psi_f} \simeq 1 + \Psi_f, \quad (8.2.2)$$

where  $\{\Phi_g, \Phi_f, \Psi_g, \Psi_f\}$  and their first derivatives are assumed to be small quantities:

$$|\Phi_g|, |\Psi_g|, |\Phi_f|, |\Psi_f| \ll 1, \quad (8.2.3)$$

$$|r\Phi'_g|, |r\Psi'_g|, |r\Phi'_f|, |r\Psi'_f| \ll 1, \quad (8.2.4)$$

We shall fix the radial coordinate as  $r = r_g$  in which the areal radial coordinate in  $f$ -spacetime is given by

$$r_f = (1 + \mu)r. \quad (8.2.5)$$

Note that the weak gravity approximation does not guarantee the smallness of the variable  $\mu$ . The variable  $\mu$  can be large and then the nonlinearity of  $\mu$  must be retained. We have assumed the spacetime is asymptotically homothetic which implies the linear approximation even for  $\mu$  can be taken in the space regions sufficiently far from the source. Then the space regions could be separated into two regions: linear regime and nonlinear regime. The variable  $\mu$  is assumed to be small in the linear regime, while we retain all nonlinear terms of  $\mu$  in the nonlinear regime. The boundary between these regions must be given by the Vainshtein radius. The variable  $\mu$  determines the deviation between two areal radial coordinates; thus it is related to the scalar Stüeckelberg field  $\pi$  in the way

$$\mu = \frac{\pi'(r)}{r}. \quad (8.2.6)$$

Hence, the nonlinear regime must correspond to the space region in which the scalar graviton is nonlinearly excited, i.e., the space region inside the Vainshtein radius.

In the linear regime, the spacetime is approximated by linear perturbations around the homothetic spacetime. These perturbations are decomposed into two independent modes: the massless graviton mode and the massive graviton mode. The massless graviton mode obeys the linearized Einstein equation while the massive graviton mode obeys the Fierz-Pauli theory. Since the point source solutions for these modes have been already discussed in Section 2.2, we do not discuss the details about the solutions in the linear regime.

The purpose in this section is to discuss the space regions around the Vainshtein radius. In general cases, the Vainshtein radius is much smaller than the Compton wavelength of the massive graviton. Therefore, we shall focus on only the space regions deep inside the Compton wavelength. Then the Einstein equations read

$$\frac{\Psi_g}{r^2} = \frac{1}{6}\kappa_g^2\tilde{\rho}_g + \frac{m_g^2}{2}\left(\mu + \beta_2\mu^2 + \frac{\beta_3}{3}\mu^3\right), \quad (8.2.7)$$

$$\frac{\Psi_f}{r_f^2} = -\frac{m_f^2}{2(1+\mu)^3}\left[\mu + (1+\beta_2)\mu^2 + \frac{1+\beta_2+\beta_3}{3}\mu^3\right], \quad (8.2.8)$$

$$\frac{1}{r}\frac{d\Phi_g}{dr} = \frac{1}{6}\kappa_g^2\tilde{\rho}_g - \frac{m_g^2}{2}\left(\mu - \frac{\beta_3}{3}\mu^3\right), \quad (8.2.9)$$

$$\frac{1}{r_f}\frac{d\Phi_f}{dr_f} = \frac{m_f^2}{2(1+\mu)^3}\left(\mu + 2\mu^2 + \frac{2+2\beta_2-\beta_3}{3}\mu^3\right), \quad (8.2.10)$$

where we introduce the mean density in the sphere with the radius  $r$  by

$$\tilde{\rho}_g(r) = \frac{\int_0^r 4\pi\tilde{r}^2\rho_g(\tilde{r})d\tilde{r}}{\int_0^r 4\pi\tilde{r}^2d\tilde{r}}, \quad (8.2.11)$$

with  $\rho_g = -T_g^{[m]0}$ . We ignore the pressures of the matter here because we have considered Newtonian stars.

Substituting them into  $\nabla_\mu T^{[\gamma]\mu}_\nu = 0$ , in the weak field limit, we find an algebraic equation for  $\mu$  as

$$\mathcal{C}_{m^2}(\mu) + \mathcal{C}_{\text{matter}}(\mu) = 0 \quad (8.2.12)$$

where  $\mathcal{C}_{m^2}$  and  $\mathcal{C}_{\text{matter}}$  are given by Eqs. (6.3.8) and (6.3.10) without  $f$ -matter. The exterior region of the source, the function  $\mathcal{C}_{\text{matter}}$  is given by

$$\mathcal{C}_{\text{matter}} = \frac{6GM_\star}{r^3}(1+\mu)^2(1-\beta_3\mu^2), \quad (8.2.13)$$

where  $M_\star$  is the gravitational mass of the  $g$ -matter. We show a root of this algebraic equation and the behaviors of  $\Phi'_g, \Psi_g$  in Fig. 8.1

The Figure 8.1 explicitly shows the existence of the Vainshtein screening inside the Vainshtein radius  $R_V$  defined by

$$R_V := \left(\frac{GM_\star}{m_{\text{eff}}^2}\right)^{1/3}, \quad (8.2.14)$$

where  $m_{\text{eff}}^2 = m_g^2 + m_f^2$ . The  $\mu$  approaches the constant  $-1/\sqrt{\beta_3}$  deep inside the Vainshtein radius in which  $\Phi'_g$  and  $\Psi_g$  recover the behavior in GR. On the other hand, in  $r \gg R_V$ , the  $\mu$  approaches zero which suggests that the linear approximation is indeed valid in the regions beyond the Vainshtein radius.

There is a root of Eq. (8.2.12) with  $\mu \rightarrow 0$  as  $r \rightarrow \infty$ , which is the asymptotically homothetic branch. Such a branch should be extended inward without any singularity. As shown in Fig. 8.1,

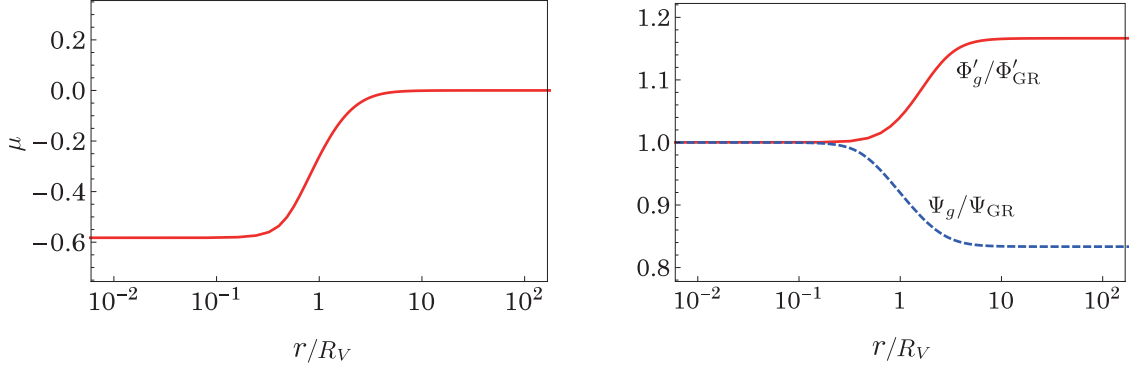


Figure 8.1: The left figure shows asymptotically homothetic branches ( $\mu \rightarrow 0$ ) of Eq. (8.2.12). We set  $\beta_2 = -3, \beta_3 = 3, m_g^2 = m_f^2, \Lambda_g = 0$ . The right figure shows the existence of the Vainshtein screening, i.e., GR is recovered for  $r < r_V$ , where we define  $\Phi'_{\text{GR}} = \Phi'_g|_{m_g=0}$  and  $\Psi_{\text{GR}} = \Psi_g|_{m_g=0}$ .

the branch with  $\mu = 0$  at  $r = \infty$  reaches to  $\mu \rightarrow -1/\sqrt{\beta_3}$  in the range of  $r \ll R_V$ , where we find a successful Vainshtein screening.

Although we cannot find analytic roots  $\mu(r)$  of the septic equation (8.2.12), we can easily find an inverse function  $r(\mu)$  because  $r$  appears only in  $\mathcal{C}_{\text{matter}}$  as the form (8.2.13). The result indicates that the function  $r(\mu)$  is a single-valued function. However, the function  $\mu(r)$  is not a single-valued function, if there is an extremal value of the function  $r(\mu)$ , i.e.,  $dr/d\mu = 0$ . The point of  $dr/d\mu = 0$  corresponds to a curvature singularity. Hence a regular solution must be given by a monotonic function  $\mu(r)$  in the domain  $0 < r < \infty$ .

As discussed in [82], one can find the parameter constraint as follows: Since the function  $\mu(r)$  should be monotonic, the function is approximated by

$$\mu = -1/\sqrt{\beta_3} + \delta\mu(r), \quad (8.2.15)$$

with  $1 \gg \delta\mu > 0$  in  $r \ll R_V$ . Substituting this expression into (8.2.12), we find

$$\begin{aligned} & \mathcal{C}_{m^2}|_{\mu=-1/\sqrt{\beta_3}} + \mathcal{C}_{\Lambda}|_{\mu=-1/\sqrt{\beta_3}} \\ & \approx -\frac{12GM_\star}{r^3} (1 - 1/\sqrt{\beta_3})^2 \sqrt{\beta_3} \delta\mu. \end{aligned} \quad (8.2.16)$$

Since the right hand side is negative, the necessary condition is given by

$$\begin{aligned} & - \left( \mathcal{C}_{m^2}|_{\mu=-1/\sqrt{\beta_3}} + \mathcal{C}_{\Lambda}|_{\mu=-1/\sqrt{\beta_3}} \right) \\ & = \frac{2}{\beta_3^{5/2}} (\beta_2 - \sqrt{\beta_3})(d_1 + \beta_2 d_2) > 0, \end{aligned} \quad (8.2.17)$$

where

$$d_1 := -6m_g^2 \sqrt{\beta_3} (1 - \sqrt{\beta_3})^2 + m_f^2 (1 - 6\sqrt{\beta_3} + 13\beta_3 - 6\beta_3^{3/2}) \quad (8.2.18)$$

$$d_2 := 3m_g^2 (1 - \sqrt{\beta_3})^2 + m_f^2 (1 - 6\sqrt{\beta_3} + 3\beta_3). \quad (8.2.19)$$

However the constraint (8.2.17) is not sufficient, because it does not guarantee that the function  $\mu(r)$  is a single-valued function in the domain  $0 < r < \infty$ , which is guaranteed by  $r(\mu)$  has no extremal value in  $-1/\sqrt{\beta_3} < \mu < 0$ . We must impose  $dr(\mu)/d\mu > 0$  for any  $\mu$  with  $-1/\sqrt{\beta_3} < \mu < 0$  which gives further constraint on the coupling constants.

Three examples of the solution  $\mu(r)$  are shown in Fig. 8.2: (a)  $\beta_2 = -3, \beta_3 = 3$ , (b)  $\beta_2 = 1.73, \beta_3 = 3$ , and (c)  $\beta_2 = 7, \beta_3 = 3$ . The case (a) and (b) satisfy

$$\beta_2 - \sqrt{\beta_3} < 0, \quad d_1 + \beta_2 d_2 < 0, \quad (8.2.20)$$

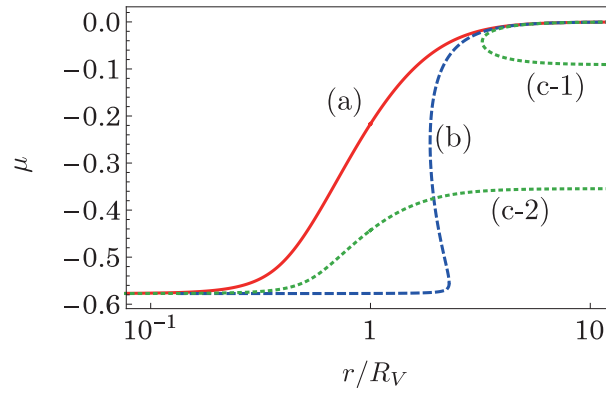


Figure 8.2: Examples of the root of (8.2.12). We set  $m_g = m_f$  and (a)  $\beta_2 = -3, \beta_3 = 3$  (red solid curve), (b)  $\beta_2 = 1.73, \beta_3 = 3$  (blue dashed curve), and (c)  $\beta_2 = 7, \beta_3 = 3$  (green dotted curves). Only the case (a) gives a regular asymptotically flat solution.

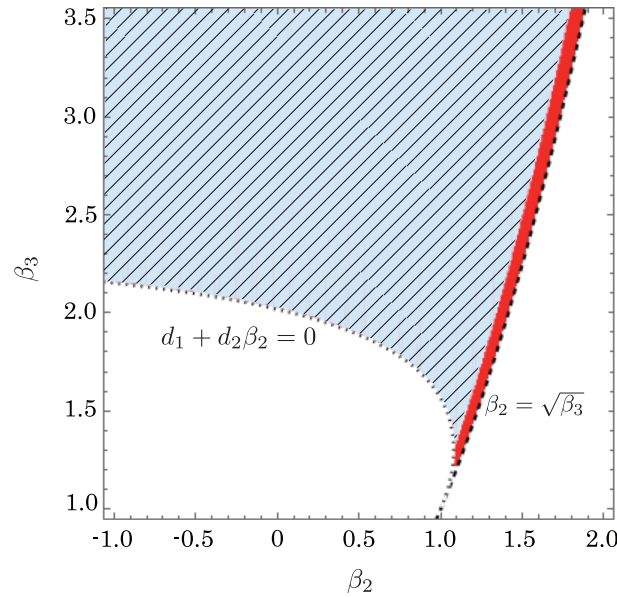


Figure 8.3: The parameter space for a successful Vainshtein screening. We set  $m_g = m_f$ . The colored (the light-blue and red) regions satisfy  $\beta_2 - \sqrt{\beta_3} < 0, d_1 + \beta_2 d_2 < 0$ . However, only the hatched light-blue region satisfies the condition such that  $\mu(r)$  is a single-valued function.

while the case (c) satisfies

$$\beta_2 - \sqrt{\beta_3} > 0, \quad d_1 + \beta_2 d_2 > 0. \quad (8.2.21)$$

For both (a) and (b), the branch of  $\mu \simeq -1/\sqrt{\beta_3}$  in  $r \ll R_V$  connects the branch of  $\mu = 0$  at  $r = \infty$ . However, the case (a) gives the single-valued function  $\mu(r)$ , while the case (b) is not. It indicates that the ratio of two radial coordinates are not single-valued function. For the case (c), there are two curves (c-1) and (c-2) and these are disconnected. Note that, the branch (c-2) can be extended to infinity. This branch is not an asymptotically Minkowski solution, but an asymptotically AdS solution [85].

As a result, the parameter constraint is approximately given by

$$\beta_2 - \sqrt{\beta_3} \lesssim 0, \quad d_1 + \beta_2 d_2 < 0, \quad (8.2.22)$$

as shown in Fig. 8.3. The hatched light-blue region gives a successful Vainshtein screening solution. We can show numerically that there is no regular asymptotically homothetic solution in the narrow region along  $\beta_2 = \sqrt{\beta_3}$  (the red region), in which  $\mu(r)$  is not a single-valued function such as (b) in Fig. 8.2, and should then be excluded.

### 8.3 Relativistic stars

For Newtonian stars, the static and spherically symmetric solution admits a successful Vainshtein screening at the background level when the coupling constants satisfy (8.2.22). On the other hand, as pointed out in [85], the parameter space is classified into two spaces: Class [I] and Class [II]. In Class [I], the curvature singularity appears when the gravitational field becomes strong, i.e., the mass of the neutron star exceeds a critical value.

To discuss a neutron star, we may not find an analytic solution. We will perform a numerical calculation to find a solution describing a compact object. However, deep inside the Vainshtein radius, we can use an approximation,  $\Lambda_2$  decoupling limit. As discussed in Section 4.5, the  $\Lambda_2$  decoupling limit gives an effective theory to describe dynamics of the Stückelberg fields deep inside the Vainshtein radius. In the spherically symmetric spacetime, the variable  $\mu$  is the Stückelberg field. Therefore, the behavior of  $\mu$  can be discussed by the effective action deep inside the Vainshtein radius. Indeed, we shall verify this approximation is valid in this section.

#### 8.3.1 Regular compact objects in $\Lambda_2$ decoupling limit

Before we present our numerical solutions, we shall discuss some analytic features of a compact object. The radius of neutron star is about  $10^6$ cm, while the Vainshtein radius is given typically by  $10^{20}$ cm when the Compton wave length of the graviton mass is the cosmological scale ( $m_{\text{eff}}^{-1} \sim 10^{28}$ cm). The magnitude of the interaction term, which is proportional to the graviton mass squared, is much smaller than the density of a neutron star. Hence, the interaction term seems not to affect the structure of a neutron star. If we ignore the interaction terms in the Einstein equations (3.3.4) and (3.3.5) (or Eqs. (8.1.11)-(8.1.14)), we just find two independent Einstein equations in GR. Then both spacetimes are given approximately by GR solutions, which we can solve easily. In bigravity theory, however, we have one additional non-trivial constraint equation (3.3.11) (or (8.1.18) for a static and spherically symmetric case) even in the massless limit. This constraint will restrict the existence of the solutions.

In the  $\Lambda_2$  decoupling limit, the effective action to determine the Stückelberg variable  $\mu$  is given by

$$S_{\text{eff}} = -\Lambda_2^4 \int d^4x \sqrt{-g} \mathcal{U}(\mu; g_{\text{GR}}, f_{\text{GR}}), \quad (8.3.1)$$

where  $\Lambda_2 = \sqrt{m/\kappa}$ , and  $g_{\text{GR}}$  and  $f_{\text{GR}}$  are solutions in GR which act as like external forces to the Stückelberg field <sup>2</sup>. The variation of the effective action with respect to  $\mu$  yields the same equation

<sup>2</sup> If both metrics are Minkowski ones, this action becomes a total divergence term. Hence it is necessary that one of them is at least a curved metric.

as (8.1.18). As we will see, the  $\Lambda_2$  decoupling limit is valid deep inside the Vainshtein radius. It implies that, inside the Vainshtein radius, the non-compact nonlinear sigma model with a curved metric is indeed obtained as the effective theory for the Stückelberg field.

We analyze two models: one is a simple toy model of a relativistic star, i.e., a uniform-density star, and the other is a more realistic polytropic star with an appropriate equation of state for a neutron star.

### The boundary condition at “infinity” in the massless limit

The boundary condition at spatial infinity, which is outside of the Vainshtein radius, is given by Eq. (8.1.5). Since the radius of a neutron star is much smaller than the Vainshtein radius, there exists the weak gravity region even inside of the Vainshtein radius. We then introduce an intermediate scale  $R_I$  with  $R_\star \ll R_I \ll R_V$ , where  $R_\star$  and  $R_V$  are the radius of a star and the Vainshtein radius, respectively. The space inside the Vainshtein radius can be divided into two regions: the region deep inside the Vainshtein radius ( $r < R_I$ ) and the weak gravity region ( $R_I < r < R_V$ ), where the gravitational force is described by a linear gravitational potential.

From the analysis for the Vainshtein screening in the weak gravity system, we find that GR (or Newtonian) gravity is recovered in  $r < R_V$ , while the homothetic solution is obtained outside the Vainshtein radius  $r \gg R_V$ . The function  $\mu(r)$  changes from  $-1/\sqrt{\beta_3}$  at small distance ( $r \ll R_V$ ) to 0 at large distance ( $r \gg R_V$ ). When gravity is weak, we find  $\mu \approx -1/\sqrt{\beta_3}$  deep inside of the Vainshtein radius. Hence we expect that  $\mu \approx -1/\sqrt{\beta_3}$  at  $r \approx R_I$  for a relativistic star.

We then obtain the boundary condition for a relativistic star in the massless limit as

$$\frac{N_g}{N_f} \rightarrow 1 - \frac{GM_g}{R_I} \approx 1, \quad \mu \rightarrow -\frac{1}{\sqrt{\beta_3}}, \quad (8.3.2)$$

as  $r \rightarrow R_I$ , which we can assume  $R_I \approx \infty$  because  $R_I \gg R_\star$ . Note that in the  $\Lambda_2$  decoupling limit, the Vainshtein radius turns to be infinite since the effective theory is viable only in the local region deep inside the Vainshtein radius.

### Uniform-density star

First, we consider a uniform-density star. Since the basic equations in the massless limit are just the Einstein equations, we can easily solve them. The  $g$ -metric of this  $g$ -star is given by the interior and exterior Schwarzschild solutions, while the  $f$ -metric is just a Minkowski spacetime: For the interior ( $r < R_\star$ ),

$$F_g = \left(1 - \frac{2GM_\star r^2}{R_\star^3}\right)^{1/2}, \quad (8.3.3)$$

$$N_g = N_g(0) \frac{3F_g(R_\star) - F_g(r)}{3F_g(R_\star) - 1}, \quad (8.3.4)$$

$$\frac{P_g(r)}{\rho_g} = \frac{F_g(r) - F_g(R_\star)}{3F_g(R_\star) - 1}, \quad (8.3.5)$$

$$F_f = 1, \quad N_f = N_f(0), \quad (8.3.6)$$

while for the exterior ( $r > R_\star$ ),

$$F_g = \left(1 - \frac{2GM_\star}{r}\right)^{1/2}, \quad (8.3.7)$$

$$N_g = \frac{2N_g(0)}{3F_g(R_\star) - 1} F_g(r), \quad (8.3.8)$$

$$F_f = 1, \quad N_f = N_f(0), \quad (8.3.9)$$

where  $R_\star$  and

$$M_\star := \frac{4\pi}{3} \rho_g R_\star^3 \quad (8.3.10)$$

are the  $g$ -star radius and the gravitational mass, respectively.

Although we can choose  $N_g(0)$  (or  $N_f(0)$ ) any value by the rescaling of time coordinate, from the boundary condition  $N_g/N_f = 1$  at infinity ( $R_I$ ), we find the ratio as

$$\frac{N_f(0)}{N_g(0)} = \frac{2}{3F_g(R_\star) - 1}. \quad (8.3.11)$$

Only one variable  $\mu$  has not been solved. When we find a regular solution of  $\mu(r)$  for the constraint (8.1.18) in the whole coordinate region ( $0 \leq r < \infty$ ) with the boundary condition  $\mu \rightarrow -1/\sqrt{\beta_3}$  as  $r \rightarrow \infty$ , we can construct a relativistic star in the bigravity theory.

First we analyze the constraint (8.1.18) at the center  $r = 0$  ( $r_f = 0$ ), which gives

$$\beta_3(3P_g(0) + \rho_g)\mu_0^2 + 6P_g(0)(\beta_2 - \beta_3)\mu_0 + 3P_g(0)(1 - 2\beta_2) - \rho_g = 0, \quad (8.3.12)$$

where  $\mu_0 := \mu(0)$ . This is the quadratic equation of  $\mu_0$ , which does not guarantee the existence of a real root of  $\mu_0$ . In order to have a real root  $\mu_0$ , we have one additional constraint as

$$9(\beta_2^2 + \beta_3^2 - \beta_3) \left( \frac{P_g(0)}{\rho_g} \right)^2 + 6\beta_2\beta_3 \left( \frac{P_g(0)}{\rho_g} \right) + \beta_3 \geq 0.$$

We then classify the coupling constants  $\beta_2$  and  $\beta_3$  into three cases: (1)  $\beta_2 < -\sqrt{\beta_3}$ , (2)  $\beta_2 > \sqrt{\beta_3}$ , and (3)  $-\sqrt{\beta_3} < \beta_2 < \sqrt{\beta_3}$ .

In the case (1), the real root  $\mu_0$  exists only for the restricted range of  $P_g(0)/\rho_g$ . In fact, there are two critical values;  $w_-$  and  $w_+$  ( $w_+ > w_-$ ), which are defined by

$$w_{\pm} = \frac{-\beta_2\beta_3 \pm \sqrt{(\beta_2^2 - \beta_3)(-1 + \beta_3)\beta_3}}{3[\beta_2^2 + (-1 + \beta_3)\beta_3]}, \quad (8.3.13)$$

and the real root exists either if  $P_g(0)/\rho_g < w_-$  or if  $P_g(0)/\rho_g > w_+$ .

On the other hand, for the case (2) and (3), the real root  $\mu_0$  always exists for any value of  $P_g(0)/\rho_g$ .

Furthermore, when we take into account the finiteness of the graviton mass, even if it is very small, we find an additional constraint on the coupling constants  $\{\beta_2, \beta_3\}$  from the existence of non-relativistic star with asymptotically homothetic spacetime (see Section 8.2).

Since the case (2) is completely excluded, we find two classes of the coupling parameters, which provide a relativistic star with asymptotically homothetic spacetime, as follows:

**Class [I]:**  $\beta_2 < -\sqrt{\beta_3}$  and  $d_1 + d_2\beta_2 < 0$

**Class [II]:**  $-\sqrt{\beta_3} \leq \beta_2 \lesssim \sqrt{\beta_3}$  and  $d_1 + d_2\beta_2 < 0$ ,

where  $d_1$  and  $d_2$  are some complicated functions of  $\beta_3$ , which are defined by (8.2.18) and (8.2.19), respectively.

Assuming  $\beta_3 > 1$ , which is necessary for the existence of asymptotically homothetic solution, we show the ranges of Class [I] and Class [II] with this constraint by the shaded light-red region and the hatched light-blue region in Fig. 8.4, respectively. For its outside (the white region), there exists neither non-relativistic star nor relativistic one.

Even if a real  $\mu_0$  exists, we may not find a regular solution of  $\mu(r)$  in the whole coordinate range ( $0 \leq r < \infty$ ) because the real root of (8.1.18) may disappear at some finite radius. In Figs. 8.5 and 8.6, we present some examples of Class [I] and Class [II], respectively. As the example of Class [I], we choose

$$m_g = m_f, \quad \beta_2 = -3, \quad \beta_3 = 3, \quad (8.3.14)$$

while for Class [II], the parameters are chosen as

$$m_g = m_f, \quad \beta_2 = 1, \quad \beta_3 = 3, \quad (8.3.15)$$



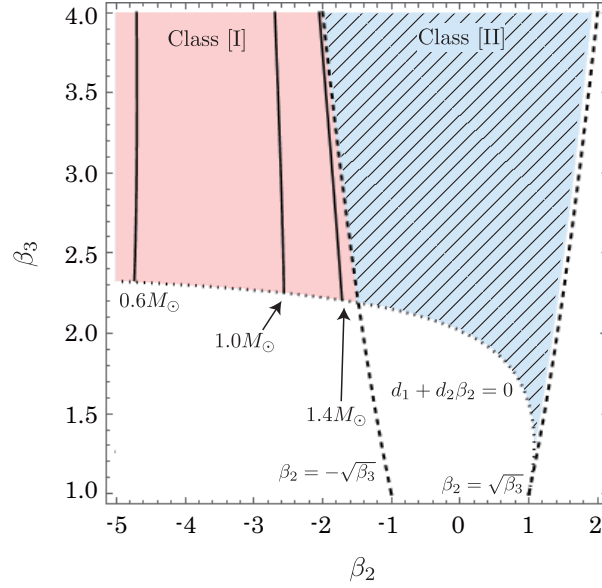


Figure 8.4: The constraint on the coupling constants from the existence of the static spherically symmetric solution in bigravity where we assume  $m_g = m_f$  and  $\Lambda_g = 0$ . The parameters are classified into two classes: Class [I] (the light-red region) and Class [II] (the hatched light-blue region). Although there is a regular solution with Vainshtein screening mechanism in the weak gravitational approximation for both classes, the difference appears in the case of relativistic star. For Class [I], the maximum mass of a neutron star is constrained stronger than the case of GR, while the star exists as in the case of GR for Class [II]. The contour lines of maximum mass are presented in the figure, where the maximum mass increases as  $\{\beta_2, \beta_3\}$  are close to  $\beta_2 = -\sqrt{\beta_3}$ .

and

$$m_g = m_f, \quad \beta_2 = -2, \quad \beta_3 = 4. \quad (8.3.16)$$

Note that there are two real roots for  $\mu_0$ . Then we find two branches of  $\mu(r)$ , which we call the branch A and the branch B. The branch A approaches a homothetic solution ( $\mu \rightarrow -1/\sqrt{\beta_3}$ ) as  $r \rightarrow \infty$  in the massless limit, while the branch B ( $\mu \rightarrow 1/\sqrt{\beta_3}$ ) does not become homothetic at infinity. A few discussions about the asymptotically non-homothetic branch are presented in [85].

For the Class [I] example (8.3.14),  $\mu_0$  exists only if  $P_g(0)/\rho_g < w_- = 1/15$  (the top figure of Fig. 8.5) or  $P_g(0)/\rho_g > w_+ = 1/3$  (the bottom figure). We find a regular solution for both branches if  $P_g(0)/\rho_g < 1/15$ . The branch A solutions provide relativistic stars with asymptotically homothetic spacetime, while the branch B solutions are not asymptotically flat.

For  $1/15 < P_g(0)/\rho_g < 1/3$ ,  $\mu_0$  does not exist. We find the solution  $\mu(r)$  only for the region larger than some finite radius, and two branches A and B are connected. The topology of this spacetime is similar to a wormhole, but it has a curvature singularity at the throat (the turning point of  $\mu(r)$ ). For the large value of  $P_g(0)/\rho_g$ , the turning point appears outside of the “star”, which means the “wormhole” structure exists even for the vacuum case [85]. Therefore, the existence of such a wormhole type solution may be caused by the strong gravity effect rather than the effect of the pressure.

The wormhole throat corresponds to the point  $d\mu/dr_g = \infty$  (i.e.,  $dr_f/dr_g = \infty$ ). When we have  $dr_f/dr_g = \infty$ , the interaction terms diverges at the point. As a result, the contribution from the interaction term should not be ignored even for the case with a very small graviton mass, and then our assumption is no longer valid at a wormhole throat. Hence, we have to re-investigate whether a relativistic star does not exist for the coupling constants of Class [I]. We shall analyze it in next subsection.

When  $P_g(0)/\rho_g$  becomes larger, i.e., if  $P_g(0)/\rho_g > 1/3$ , we again find a real  $\mu_0$ , but there exists no regular  $\mu(r)$  for the whole range of  $r$ .  $\mu(r)$  exists in two separated regions; one is smaller than

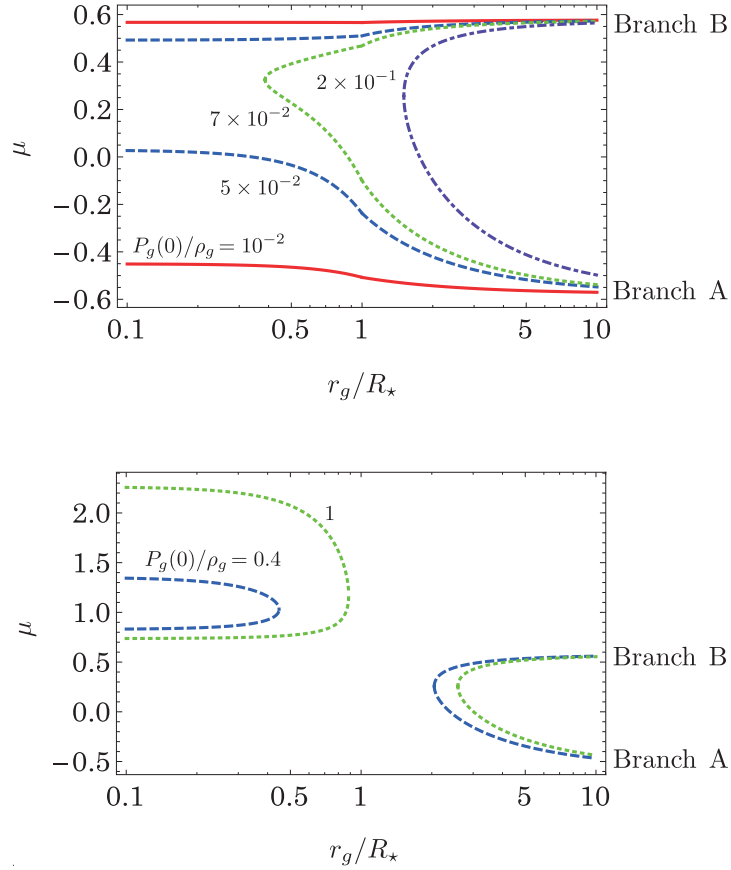


Figure 8.5: We set  $m_g = m_f, \beta_2 = -3, \beta_3 = 3$ . The top and the bottom figures denote the cases of  $P_g(0)/\rho_g < 1/15$  and of  $P_g(0)/\rho_g > 1/3$ , respectively. When  $1/3 > P_g(0)/\rho_g > 1/15$ , there is no real root of  $\mu_0$ . Although there exists a real root of  $\mu_0$  for  $P_g(0)/\rho_g > 1/3$ , the solutions are disconnected between the region of  $r \lesssim R_*$  and that of  $r \gg R_*$ . As a result, there exist a relativistic star for  $P_g(0)/\rho_g < 1/15 \approx 0.06667$ .

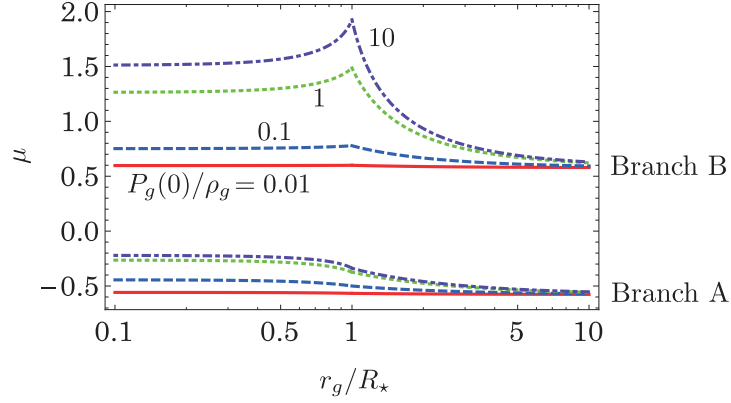
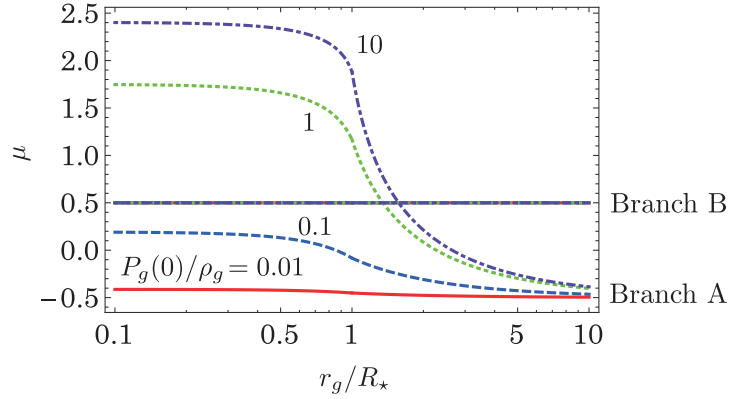
(a)  $\beta_2 = 1, \beta_3 = 3$ (b)  $\beta_2 = -2, \beta_3 = 4$ 

Figure 8.6: We set  $m_g = m_f$ , and (a)  $\beta_2 = 1, \beta_3 = 3$ , and (b)  $\beta_2 = -2, \beta_3 = 4$ . We choose the central pressure as  $P_g(0)/\rho_g = 0.01, 0.1, 1, 10$ . In the figure (a) ( $\beta_2^2 - \beta_3 < 0$ ), there are two branches, and these do not connect for a large pressure of the star. For the figure (b) ( $\beta_2^2 - \beta_3 = 0$ ), there are a non-trivial root (the branch A) as well as a trivial root  $\mu = 1/\sqrt{\beta_3}$  (the branch B). Although these two roots intersect beyond a critical pressure, there is a regular star beyond it in the branch A.

some finite radius ( $< R_*$ ) and the other is larger than another finite radius ( $> R_*$ ), In both regions, two branches A and B are connected. We find a kind of closed universe for the smaller-radius inner region, and a kind of wormhole structure for the larger radius outer region. Both spacetime structures contain a curvature singularity at the throats (the turning points of  $\mu(r)$ ).

On the other hand, for the Class [II] example, both branch A and B solutions exist for any value of  $P_g(0)$  (Fig. 8.6), and they are not connected each other. Hence we always find a relativistic star with asymptotically homothetic spacetime structure (the branch A solution).

We note that at the boundary of Class [I] and Class [II] (i.e.,  $\beta_2 = -\sqrt{\beta_3}$ ). The trivial solution  $\mu = 1/\sqrt{\beta_3}$  gives the branch B. While the branch A has a non-trivial solution shown in Fig. 8.6 (b), which gives a relativistic star for any value of  $P_g(0)$ .

Hence we may conclude that a relativistic star always exists a regular solution for the coupling constants of Class [II]. On the other hand, there does not exist a relativistic star beyond a critical value of the pressure for the coupling constants of Class [I], i.e., for  $P_g(0)/\rho_g > w_-$ . Instead, the spacetime may turn to a wormhole geometry with a singularity (or a closed universe with a singularity).

The existence condition of  $P_g(0)/\rho_g < w_-$  can be rewritten by the compactness of a star,  $GM_*/R_*$ . Using the internal solution (8.3.3) and (8.3.5), we find

$$\frac{GM_*}{R_*} = \frac{2 \frac{P_g(0)}{\rho_g} \left(1 + 2 \frac{P_g(0)}{\rho_g}\right)}{\left(1 + 3 \frac{P_g(0)}{\rho_g}\right)^2}. \quad (8.3.17)$$

Then we obtain the existence condition for Class [I] as

$$\frac{GM_*}{R_*} < \frac{GM_*}{R_*} \Big|_{\max} := \frac{2w_- (1 + 2w_-)}{(1 + 3w_-)^2}. \quad (8.3.18)$$

This gives the maximum value of the compactness of a relativistic star for given coupling constants  $\beta_2$  and  $\beta_3$ . Since  $\beta_2$  and  $\beta_3$ , are restricted as shown in Fig. 8.4, we can evaluate the upper bound of the compactness for Class [I] as

$$\frac{GM_*}{R_*} \Big|_{\text{ub}} := \sup_{\text{Class [I]}} \left\{ \frac{GM_*}{R_*} \Big|_{\max} \right\} \approx 0.23, \quad (8.3.19)$$

which is realized for  $\beta_2 \simeq -1.48, \beta_3 \simeq 2.19$ .

While in Class [II], any coupling constants give the same maximum value of the compactness, that is,

$$\frac{GM_*}{R_*} \Big|_{\max} = \frac{4}{9}, \quad (8.3.20)$$

which is obtained from the existence condition for a regular interior solution in GR because there is no additional constraint in this class.

The upper bound of the compactness in Class [I] is almost the same as the observed value (e.g., the compactness is about 0.3 when a radius of a two solar mass neutron star is 10 km, while it is about 0.21 for a two solar mass star with a radius of 14 km [183–185]). In order to give a stringent constraint on the theory by observations, we have to analyze more realistic star, which will be discussed below.

### Polytropic star

Giving a more realistic equation of state, we present a neutron star solution in the bigravity theory. We then discuss its mass and radius in order to give a constraint on the theory or the coupling constants by comparing them with observed values.

We assume a simple polytropic-type equation of state

$$P = \mathcal{K}\rho^2, \quad (8.3.21)$$

where we set  $\mathcal{K} = 1.5 \times 10^5$  [cgs]. In the massless limit of the graviton, we have two decoupled Einstein equations. Then the  $f$ -metric is given by the Minkowski spacetime because there is no  $f$ -matter, For  $g$ -spacetime, we have the same neutron star solution as that in GR. We present  $\rho_c$ - $M_\star$  and  $R_\star$ - $M_\star$  relations in Fig. 8.7, where  $\rho_c = \rho_g(0)$  is the central density. We find that the maximum mass of a neutron star is about  $2M_\odot$ , where  $M_\odot$  is the solar mass, for the above equation of state. This result is obtained in GR but also it is the case for Class [II] in bigravity because we always find the regular solution for  $\mu(r)$  in the whole coordinate range ( $0 \leq r < \infty$ ). We show some examples for the same coupling constants (8.3.15) with several values of the central density  $\rho_c$  in Fig. 8.8.

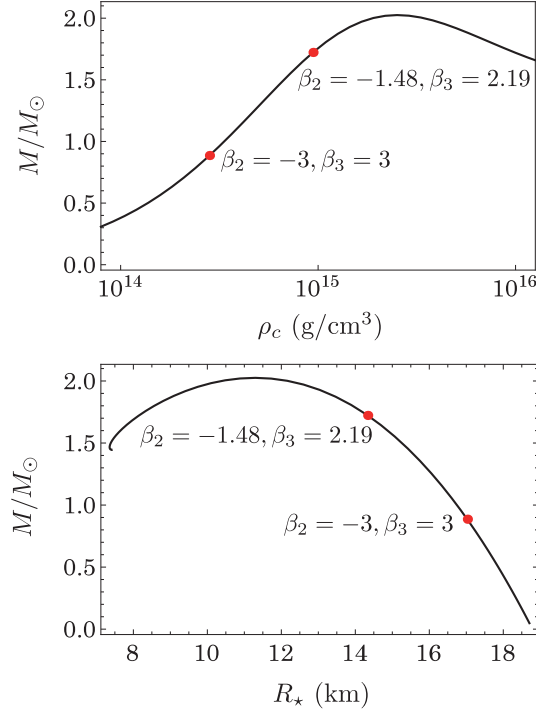


Figure 8.7:  $\rho_c$ - $M_\star$  and  $R_\star$ - $M_\star$  relations for neutron stars with the polytropic equation of state (8.3.21). The black solid lines are obtained in GR or in Class [II]. The maximum mass in Class [I], which is shown by the red dots with  $\beta_2 = -3, \beta_3 = 3$  and  $\beta_2 = -1.48, \beta_3 = 2.19$ , depends on the coupling constants,

However, for Class [I], we find the additional constraint to find the regular  $\mu(r)$  as we expect from the result in the previous discussion. We also present some examples of  $\mu(r)$  for the same coupling constants (8.3.14) with several values of  $\rho_c$  in Fig. 8.8. This figure shows there is no regular solution of  $\mu(r)$  in the whole region if the density  $\rho_c$  is larger than  $2.8 \times 10^{14}$  g/cm<sup>3</sup>. This upper limit of the density does not reach the central density with the maximum mass of neutron star in GR (see Fig. 8.7). Hence this limit of  $\rho_c$  provides the maximum mass of a neutron star in Class [I], which is much smaller than that in GR (or in Class [II]). In Fig. 8.4, the maximum masses in Class [I] are shown by the contour lines. The maximum mass is larger as the parameters  $\{\beta_2, \beta_3\}$  come close to  $\beta_2 = -\sqrt{\beta_3}$ . The upper bound of the maximum mass in Class [I] is at most  $1.72M_\odot$ , which is realized at  $\beta_2 \simeq -1.48$  and  $\beta_3 \simeq 2.19$ . Hence the maximum mass in Class [I] does not reach  $2M_\odot$ , which may be inconsistent with the existence of the  $2M_\odot$  neutron star [186–189]. One might find a  $2M_\odot$  neutron star in Class [I] if we modify the equation of state, but it will give a strong constraint on the coupling constants in the theory.

As for the compactness, we find

$$\begin{aligned} \left. \frac{GM_\star}{R_\star} \right|_{\text{ub}} &= 0.18 && \text{for Class [I]}, \\ \left. \frac{GM_\star}{R_\star} \right|_{\text{max}} &= 0.31 && \text{for Class [II]}. \end{aligned} \quad (8.3.22)$$

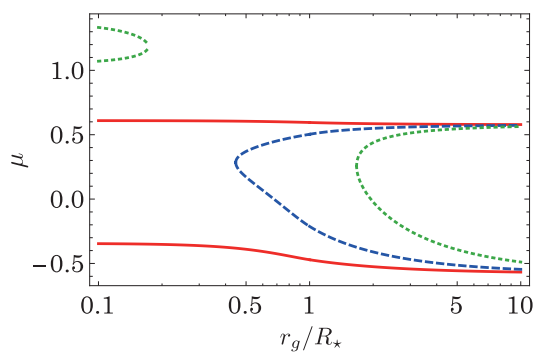
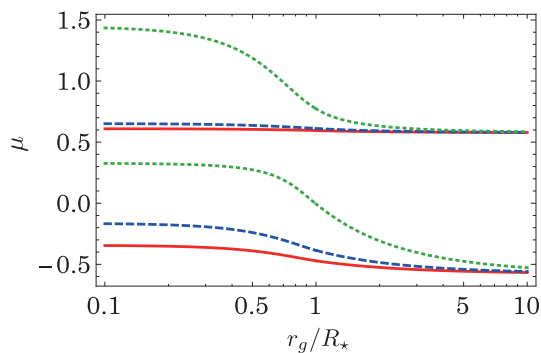
(a)  $\beta_2 = -3, \beta_3 = 3$ (b)  $\beta_2 = -1, \beta_3 = 3$ 

Figure 8.8: We set  $m_g = m_f$ , and (a)  $\beta_2 = -3, \beta_3 = 3$  (Class [I]) and (b)  $\beta_2 = -1, \beta_3 = 3$  (Class [II]). We choose  $\rho_c = 1.71 \times 10^{14} \text{ g/cm}^3$  (red solid curves),  $3.35 \times 10^{14} \text{ g/cm}^3$  (blue dashed curves) and  $18.9 \times 10^{14} \text{ g/cm}^3$  (green dotted curves), whose star masses are  $0.6M_\odot$ ,  $1.0M_\odot$  and  $2.0M_\odot$ , respectively.

Although both values are so far consistent with observations, the coupling constants in Class [I] may be restricted again because the above value is just the upper bound.

### 8.3.2 Regular compact objects: numerical results

In this subsection, we numerically solve the basic equations under the metric ansatz (8.1.1) and (8.1.2) with a  $g$ -matter field. We find a relativistic star solution and confirm the previous results obtained in the  $\Lambda_2$  decoupling limit when the graviton mass is sufficiently small.

In general, we have nine variables  $N_g, N_f, F_g, F_f, \mu, \rho_g$ , and  $P_g$ , and six ordinary differential equations (8.1.11)-(8.1.14), (8.1.15), and one algebraic equation (8.1.18) with an equation of state  $P_g = P_g(\rho_g)$ . In order to solve those equations numerically, we first take the derivative of (8.1.18), and then find seven first-order ordinary differential equations:

$$\frac{dX}{dr} = \mathcal{F}_X[N_g, N_f, F_g, F_f, \mu, \rho_g, P_g, r], \quad (8.3.23)$$

$$\begin{aligned} \frac{dr_f}{dr} &= r \frac{d\mu}{dr} + \mu + 1 \\ &= J[N_g, N_f, F_g, F_f, \mu, \rho_g, P_g, r]. \end{aligned} \quad (8.3.24)$$

where  $X = \{N_g, N_f, F_g, F_f, P_g\}$ , and  $\mathcal{F}_X$  and  $J$  do not contain any derivatives. Here we have fixed the radial coordinate as  $r_g = r$  by use of the gauge freedom. We solve these differential equations from the center of a star ( $r = 0$ ). In order to guarantee that the above set up gives a correct solution of our system, we have to impose the constraint (8.1.18) on the variables at the center.

We numerically integrate Eqs. (8.3.23) and (8.3.24) outwards from the center  $r = 0$ . The constraint equation (8.1.18) is used to evaluate the boundary values at the center. Since it must be satisfied in the region of  $r > 0$  too, we use this constraint to check the accuracy of our numerical solutions in  $r > 0$ .

Since the equations are seemingly singular at  $r = 0$ , we start our calculations from  $r = 0 + \delta r$  with  $\delta r \ll 1$ . All variables are expanded around  $r = 0$  as

$$X = \sum_{n=0} \frac{1}{n!} X^{(n)}(0) r^n, \quad (8.3.25)$$

where  $X^{(n)}(0)$  is the  $n$ -th derivative of the variable  $X$  at  $r = 0$ .

Here, by use of the freedom of time coordinate rescaling, we choose  $N_g(0) = 1$  without loss of generality<sup>3</sup>. We determine the values of variables at  $r = \delta r$  by using up to second order of (8.3.25).

As mentioned, we focus only on the asymptotically flat solution with only  $g$ -matter, i.e., the branch A solution.

#### A uniform density star

We first discuss a uniform density star, i.e.,  $\rho_g = \text{constant}$ . The dimensionless parameters characterizing the star are

$$\kappa_g^2 \rho_g / m_{\text{eff}}^2, \quad P_g^{(0)}(0) / \rho_g, \quad (8.3.28)$$

where we have defined

$$m_{\text{eff}}^2 = m_g^2 + m_f^2, \quad (8.3.29)$$

<sup>3</sup> Although it gives  $N_g(\infty) \neq 1$ , if we wish to find the boundary condition  $N_g(\infty) = 1$ , we redefine new lapse functions as

$$\tilde{N}_g(r) = \frac{N_g(r)}{N_g(\infty)}, \quad \tilde{N}_f(r) = \frac{N_f(r)}{N_g(\infty)} \quad (8.3.26)$$

and new time coordinate as

$$\tilde{t} = N_g(\infty) t \quad (8.3.27)$$

New metrics defined by  $\tilde{N}_g, \tilde{N}_f$  and  $\tilde{t}$  satisfy the boundary condition  $\tilde{N}_g(\infty) = 1$  at infinity. In this case, the time coordinate  $t$  corresponds to the proper time for the observer at the spatial infinity.

which gives the effective graviton mass on the homothetic spacetime. The first parameter in (8.3.28) is evaluated as

$$\frac{\kappa_g^2 \rho_g}{m_{\text{eff}}^2} = \frac{6GM_\star}{R_\star} \left( \frac{m_{\text{eff}}^{-1}}{R_\star} \right)^2, \quad (8.3.30)$$

which is much larger than unity because  $m_{\text{eff}}^{-1}$  is the Compton wavelength of the graviton and then it must be a cosmological scale.

Once the parameters (8.3.28) are given, the proper value of  $\mu(0)$  is determined by a shooting method to adjust the correct boundary condition (8.1.5) at infinity as well as the asymptotic flatness. Then all coefficients in Eq. (8.3.25) are fixed by this  $\mu(0)$  from the expanded basic equations order by order,

We use  $\mu_0$  as the center value of  $\mu(0)$  in the case of  $\Lambda_2$  decoupling limit. When the value of the graviton mass is sufficiently small, the proper value of  $\mu(0)$  is close to  $\mu_0$ . Hence, we start to search for  $\mu(0)$  near  $\mu_0$  to find a regular solution with the correct boundary condition.

To check the boundary conditions at infinity, we evaluate the eigenvalues of  $\gamma^\mu{}_\nu$ , i.e.,

$$\lambda_0 := \frac{N_f}{N_g}, \quad (8.3.31)$$

$$\lambda_1 := \frac{r'_f/F_f}{1/F_g}, \quad (8.3.32)$$

$$\lambda_2 = \lambda_3 := \frac{r_f}{r} = 1 + \mu. \quad (8.3.33)$$

If all eigenvalues approach unity as  $r \rightarrow \infty$ , the solution is asymptotically homothetic. Then the  $\gamma$  energy-momentum tensor will become a ‘‘cosmological’’ constant ( $\Lambda_g$ ) term at infinity. We find our solution with an asymptotic flatness, if  $\Lambda_g = 0$ , which we have assumed for our coupling constants.

### Class [I]

As an example in Class [I], we choose the same coupling constants as before, i.e.,

$$\Lambda_g = 0, \quad m_g = m_f, \quad \beta_3 = -3, \quad \beta_4 = 3. \quad (8.3.34)$$

The branch A solution approaches an asymptotically flat homothetic spacetime. In Fig. 8.9, we show a numerical solution by setting  $\kappa_g^2 \rho_g / m_{\text{eff}}^2 = 2.5 \times 10^5$ ,<sup>4</sup> for which the typical value of the Vainshtein radius is given by

$$R_V := (GM_\star / m_{\text{eff}}^2)^{1/3} \sim 30R_\star. \quad (8.3.35)$$

GR is recovered within the Vainshtein radius.

We note  $\lambda_1$  is discontinuous at the star surface  $R_\star$ . It is because the discontinuity of the matter distribution leads to the discontinuity of  $r'_f$  as seen in Eq. (8.3.24). This discontinuity disappears when we discuss a continuous matter distribution such as a polytropic star (8.3.21) as shown in Fig. 8.11.

Changing the central value of the pressure  $P_g(0)/\rho_g$ , we find the solution disappears for  $P_g(0)/\rho_g > 0.0665$ . It is consistent with the argument in the  $\Lambda_2$  decoupling limit, in which the critical value is given by  $P_g(0)/\rho_g = 1/15 \approx 0.06667$ . Hence even in the case with a finite graviton mass, there exists a critical value of the pressure beyond which a regular star solution does not exist.

If we choose the larger value of the parameter as  $\kappa_g^2 \rho_g / m_{\text{eff}}^2 = 2.5 \times 10^7$ , the solution exists for  $P_g(0)/\rho_g > 0.0666$ , which is closer to the value in the  $\Lambda_2$  decoupling limit. Hence, we expect that the  $\Lambda_2$  decoupling limit approximation is valid for the realistic value  $\kappa_g^2 \rho_g / m_{\text{eff}}^2 \sim 10^{43}$ .

<sup>4</sup>This value is too small for a realistic neutron star with a massive graviton responsible for the present accelerating expansion of the Universe, for which we have  $\kappa_g^2 \rho_g / m_{\text{eff}}^2 \sim 10^{43}$ . However, because of the technical reason for numerical calculation, we choose the above value. For the realistic value, we expect that the solution may be closer to the case of the  $\Lambda_2$  decoupling limit.



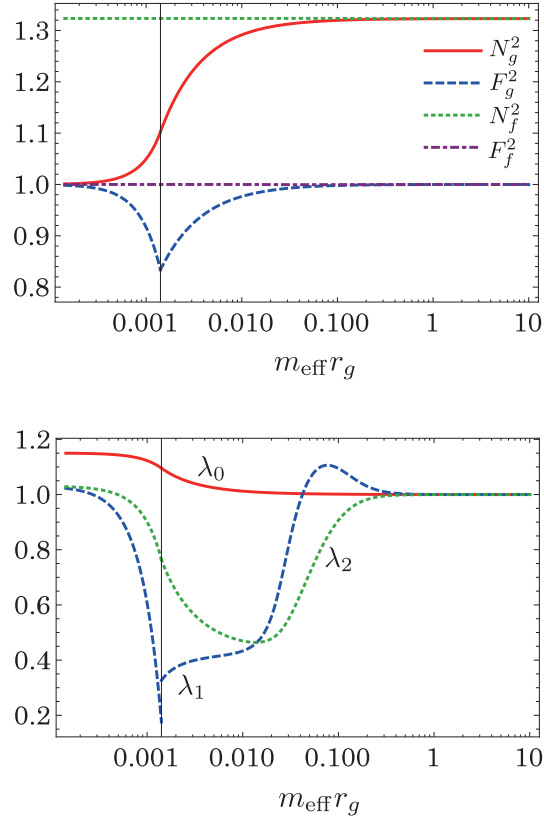


Figure 8.9: A typical solution for the branch A. We set  $P_g(0)/\rho_g = 5 \times 10^{-2}$ . The shooting parameter is tuned to be  $\mu(0) = 0.03093$ . The vertical bar represents the star surface ( $R_\star/m_{\text{eff}}^{-1} = 0.00141288$ ).

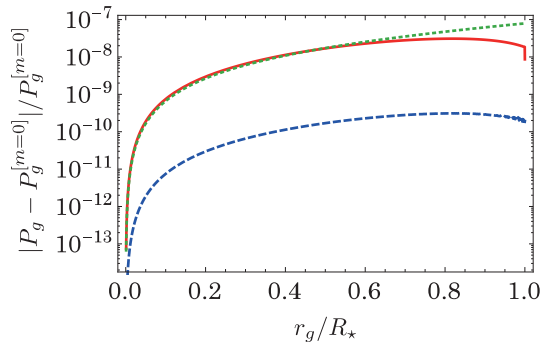


Figure 8.10:  $|P_g - P_g^{[m=0]}|/P_g^{[m=0]}$  where  $P_g$  is the numerical solution with a finite mass and  $P_g^{[m=0]}$  is the solution in  $\Lambda_2$  decoupling limit. We set  $P_g(0)/\rho_g = 5 \times 10^{-2}$  and (8.3.34) with  $\kappa_g^2 \rho_g / m_{\text{eff}}^2 = 2.5 \times 10^5$  (the red solid curve),  $\kappa_g^2 \rho_g / m_{\text{eff}}^2 = 2.5 \times 10^7$  (the blue dashed curve) and (8.3.36) with  $\kappa_g^2 \rho_g / m_{\text{eff}}^2 = 2.5 \times 10^5$  (the green dotted curve). We note  $P_g - P_g^{[m=0]} > 0$  for (8.3.34), while  $P_g - P_g^{[m=0]} < 0$  for (8.3.36).

If the solution exists, the inner structure of star as well as the gravitational field are restored to the result of GR because of the Vainshtein mechanism. We find differences between our numerical solution and the semi-analytic solution in the  $\Lambda_2$  decoupling limit are very small as shown one example of the pressure  $P_g$  in Fig. 8.10. This fact also confirms the validity of the  $\Lambda_2$  decoupling limit approximation if the graviton mass is sufficiently small. We conclude that the bigravity for Class [I] cannot reproduce the result in GR beyond the critical value of  $P_g(0)/\rho_g$ .

### Class [II]

As an example in Class [II], we choose one of the previous coupling constants, i.e.,

$$\Lambda_g = 0, \quad m_g = m_f, \quad \beta_3 = 1, \quad \beta_3 = 3 \quad (8.3.36)$$

and we set

$$\kappa_g^2 \rho_g / m_{\text{eff}}^2 = 2.5 \times 10^5. \quad (8.3.37)$$

In this case, we can find a regular star for any values of  $P_g(0)$ . The solution is almost the same as the  $\Lambda_2$  decoupling limit (or GR) as shown in Fig. 8.10. We conclude that in the bigravity theory in Class [II] the results in GR are recovered and the Vainshtein mechanism holds even in a strong gravity limit.

### Polytropic star

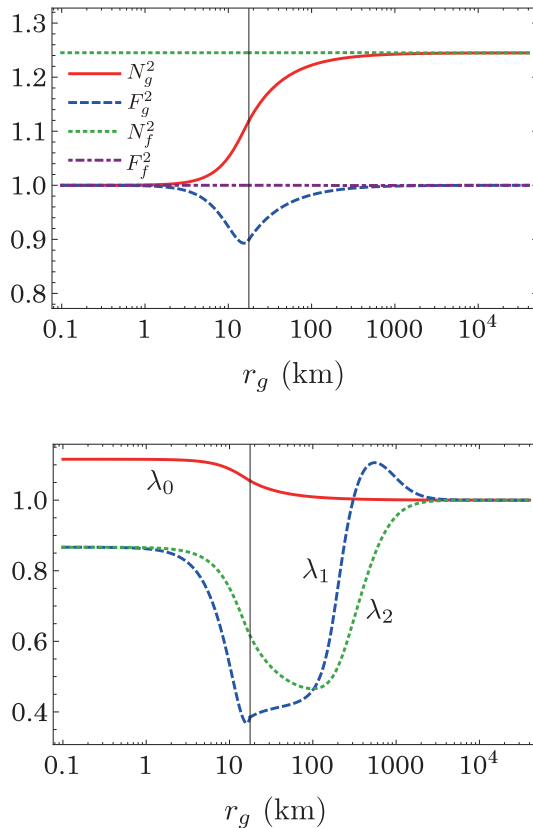


Figure 8.11: We set  $\rho_c = 1.71 \times 10^{14} \text{ g/cm}^3$  and  $m_{\text{eff}}^{-1} = 10^4 \text{ km}$ , for which the mass of the neutron star is  $0.601M_\odot$ . The shooting parameter is tuned to be  $\mu(0) = -0.13334$ . The vertical bar represents the star surface ( $R_\star = 17.7 \text{ km}$ ).

For a neutron star with a realistic equation of state, we can also confirm the above results, i.e. the  $\Lambda_2$  decoupling limit is valid to discuss an astrophysical object. Here we again assume the polytropic equation of state (8.3.21).

One typical example of the solutions in Class [I] is shown in Fig. 8.11, where we choose the coupling constants as (8.3.34) and

$$\rho_c = 1.71 \times 10^{14} \text{ g/cm}^3, \quad m_{\text{eff}}^{-1} = 10^4 \text{ km}, \quad (8.3.38)$$

We find a neutron star solution with

$$M_\star = 0.601M_\odot, \quad R_\star = 17.7 \text{ km}, \quad (8.3.39)$$

which is the same as those in the  $\Lambda_2$  decoupling limit. Our numerical calculation shows that increasing the central density  $\rho_c$ , the solution exists only for  $M_\star \lesssim 0.882M_\odot$  for the coupling constants (8.3.34). We have obtained  $M_\star \lesssim 0.886M_\odot$  in the  $\Lambda_2$  decoupling limit. If we choose the larger value of the Compton wavelength of the graviton as  $m_{\text{eff}}^{-1} = 10^5 \text{ km}$ , the mass upper limit increases as  $M_\star \lesssim 0.884M_\odot$ , which is closer to the value in the  $\Lambda_2$  decoupling limit. Beyond the critical value, the curvature singularity appears since the  $T_{\mu\nu}^{[\gamma]}$  diverges at the point  $\mu' \rightarrow \infty$ .

For Class [II], we always find the same solution as that in GR. As a result, as the case of a uniform-density star, we confirm that the  $\Lambda_2$  decoupling limit solution is a good approximation for the sufficiently small graviton mass.

## 8.4 Perturbations around static and spherically symmetric solution

In the previous sections we have considered the static and spherically symmetric solutions and discussed whether there is a viable astrophysical solution or not. As a result, although there is a constraint on the parameters of the theory, the bigravity theory seems to admit a viable solution with the Vainshtein mechanism. However, the previous analysis is not sufficient since realistic solutions must be stable over the age of the Universe.

In §. 4.5.3, we have shown that the Vainshtein screening solutions cannot be supported only by the excitation of the scalar graviton. However since the massive gravity nonlinear sigma model contains the degrees of freedom of the vector graviton as well, one cannot still conclude the solution is indeed unstable. In this section, thus, we study the general perturbations around the static and spherically symmetric solutions with Vainshtein screening given by the previous sections in which there exists only the scalar graviton in the background solution.

Indeed, we will show the static and spherically symmetric solutions are unstable; thus these solutions may not be realized in the Universe. The existence of a viable astrophysical object in bigravity is an open problem.

For simplicity, we only focus on outside the source ( $r > R_\star > 2GM$ ) thus the  $g$ -spacetime is given by Schwarzschild spacetime. We choose the spherical coordinate

$$g_{\mu\nu}^{\text{GR}} = \text{diag}[-F_g^2, F_g^{-2}, r^2, r^2 \sin^2 \theta], \quad (8.4.1)$$

$$\eta_{\mu\nu} = \text{diag}[-1, 1, r^2, r^2 \sin^2 \theta], \quad (8.4.2)$$

with  $F_g^2 = 1 - \frac{2GM}{r}$  where  $M$  and  $R_\star$  is a gravitational mass and a radius of the star, respectively.

First, we give the static and spherically symmetric solution. The solution can be found by assuming the Stückelberg field as

$$\pi_\mu = \bar{\pi}_\mu = (0, r\mu(r), 0, 0). \quad (8.4.3)$$

The basic equation can be derived by varying the action with respect to  $\mu$ . Then the solution is given by

$$\begin{aligned} \mu &= \frac{-(1 - F_g)(\beta_2 - 2\beta_3) + \epsilon \sqrt{(\beta_2 - 2\beta_3)^2 (1 - F_g)^2 + \beta_3(1 + F_g)(4\beta_2 - 1 + (3 - 4\beta_2)F_g)}}{\beta_3(1 + F_g)} \\ &= \frac{\epsilon}{\sqrt{\beta_3}} + \mathcal{O}(GM/r), \end{aligned} \quad (8.4.4)$$

where  $\epsilon = \pm 1$ . Note that although  $\beta_2$  and  $\beta_3$  are originally free parameters, it was shown that this solution exists only for  $\beta_3 > 1$  with some other constraints (8.2.22). Here the minus branch ( $\epsilon = -1$ ) is the asymptotically flat branch. On the other hand, the plus branch ( $\epsilon = 1$ ) is not regular in general, however the plus branch can describe a regular asymptotically AdS solution when we introduce a negative cosmological constant [85].

We shall study the stability of this solution. Since the background spacetime is spherically symmetric, perturbations can be decomposed into odd parity perturbations and even parity perturbations, that is,

$$\pi_\mu = \bar{\pi}_\mu + \delta\pi_\mu^{\text{odd}} + \delta\pi_\mu^{\text{even}}. \quad (8.4.5)$$

These perturbations are decoupled at the linear order equation of motion (or equivalently at the quadratic order Lagrangian). Hence we separately discuss the odd and even parity perturbations, in order.

### 8.4.1 Odd parity perturbations

First, we discuss the odd parity perturbations. Because of the spherical symmetry of the background solution, we can separate the variables and then  $x^i = (\theta, \varphi)$  dependence can be expanded in terms of the vector spherical harmonics  $Y_i$ , which is defined by

$$[D^2 + \ell(\ell + 1) - 1]Y_i = 0, \quad (\ell = 1, 2, \dots), \quad (8.4.6)$$

$$D^i Y_i = 0. \quad (8.4.7)$$

Here,  $D_i$  is the covariant derivative on the 2-sphere and  $D^2 = D_i D^i$ . The explicit form of  $Y_i$  is given by

$$Y_i = \epsilon_{ij} D^j Y, \quad (8.4.8)$$

where  $\epsilon_{ij}$  is the Levi-Civita tensor and  $Y$  is the spherical harmonics satisfying

$$[D^2 + \ell(\ell + 1)]Y = 0, \quad (\ell = 0, 1, 2, \dots). \quad (8.4.9)$$

By using the vector harmonics, the perturbation of the Stüeckelberg field is expressed by

$$\delta\pi_\mu^{\text{odd}} = (0, 0, r\chi_\Omega Y_i), \quad (8.4.10)$$

where  $\chi_\Omega$  is a function of  $(t, r)$ .

The quadratic order action is given by

$$S^{\text{odd}} = \int r^2 dt dr d\Omega \frac{\Lambda^4}{4} (\sqrt{\beta_3} + \epsilon\beta_2) \left[ \frac{4}{2\sqrt{\beta_3} + \epsilon} \dot{\chi}_\Omega^2 - \frac{1}{\sqrt{\beta_3} + \epsilon} \left( \chi_\Omega'^2 + \frac{\ell(\ell+1)}{r^2} \chi_\Omega^2 \right) \right] Y_i Y^i + \mathcal{O}(GM/r), \quad (8.4.11)$$

where a dot and a prime denote the time derivative and the radial derivative, respectively. Since each eigenmode of the harmonics does not couple with the other eigenmodes, we drop the summation sign. The stability condition (no-ghost and no-gradient instability) is given by

$$\sqrt{\beta_3} + \beta_2 > 0. \quad (8.4.12)$$

for the plus branch, while for the minus branch the condition is

$$\sqrt{\beta_3} - \beta_2 > 0. \quad (8.4.13)$$

### 8.4.2 Even parity perturbations

Next we consider the even parity perturbations. By using the spherical harmonics, the perturbation of the Stüeckelberg field is expressed by

$$\delta\pi_\mu^{\text{even}} = (\xi_t Y, \xi_r Y, r\xi_\Omega D_i Y), \quad (8.4.14)$$

where  $\xi_t$ ,  $\xi_r$  and  $\xi_\Omega$  are functions of  $(t, r)$ . Note that for the  $\ell = 0$  mode, the variable  $\xi_\Omega$  is undefined because  $D_i Y = 0$ . Hence we should discuss  $\ell = 0$  mode and  $\ell \geq 1$  modes, separately.

**Radial perturbation** ( $\ell = 0$ )

For  $\ell = 0$ , the spherical harmonics is simply given by  $Y|_{\ell=0} = 1/\sqrt{4\pi}$ . The quadratic order action can be schematically expressed by

$$S^{\ell=0} = S^{\ell=0}(\dot{\xi}_r, \xi'_t, \xi'_r, \xi_t, \xi_r), \quad (8.4.15)$$

from which  $\xi_t$  is non-dynamical and it can be integrated out. The variation with respect to  $\xi_t$  yields a constraint equation

$$\partial_t [2rF_g^{-1}(F_g - 1)(\beta_2 + \beta_3\mu)\xi_r] - \partial_r \left[ \frac{r^2 F_g (1 + 2\beta_2\mu + \beta_3\mu^2)(F_g^2 \xi'_t - \dot{\xi}_r)}{1 + F_g^2(r + r\mu)'} \right] = 0, \quad (8.4.16)$$

where the solution is given by

$$\xi'_t = -2GM(\beta_2 + \epsilon\sqrt{\beta_3}) \left[ \frac{\dot{\Xi}'}{2rF_g(F_g - 1)(\beta_2 + \beta_3\mu)} + \frac{1 + F_g^2(r + r\mu)'}{r^2 F_g^3(1 + 2\beta_2\mu + \beta_3\mu^2)} \dot{\Xi} \right], \quad (8.4.17)$$

$$\xi_r = -2GM(\beta_2 + \epsilon\sqrt{\beta_3}) \frac{F_g}{2r(F_g - 1)(\beta_2 + \beta_3\mu)} \Xi', \quad (8.4.18)$$

with some function  $\Xi(t, r)$ . Here the factor is introduced so that  $\xi_t$  and  $\xi_r$  can be expressed by

$$\xi_t = \dot{\Xi} + \mathcal{O}(GM/r), \quad (8.4.19)$$

$$\xi_r = \Xi' + \mathcal{O}(GM/r), \quad (8.4.20)$$

at the leading order of  $GM/r$ . Then the quadratic action is expressed by

$$S^{\ell=0} = \Lambda_2^4 \int r^2 dt dr \left[ K_t \dot{\Xi}^2 - K_r \Xi'^2 \right], \quad (8.4.21)$$

where

$$K_t = -\epsilon \left( \frac{GM}{r} \right)^2 \frac{3\sqrt{\beta_3}(\beta_2 + \epsilon\sqrt{\beta_3})}{r^2} + \mathcal{O} \left( \left( \frac{GM}{r} \right)^3 \right) \quad (8.4.22)$$

$$K_r = -\epsilon \frac{GM}{r} \frac{\sqrt{\beta_3}}{r^2} + \mathcal{O} \left( \left( \frac{GM}{r} \right)^2 \right). \quad (8.4.23)$$

Note that, while the gradient term appears at the first order of  $GM/r$  (i.e., the first order of the metric perturbation around the Minkowski spacetime), the kinetic term appears at the second order of  $GM/r$ . Hence the scalar graviton is not infinitely strong coupled although the propagation speed is superluminal.

From the second order action, we can see that the plus branch suffers from the gradient instability. Even for the minus branch, the stability condition is given by

$$\beta_2 - \sqrt{\beta_3} > 0, \quad (8.4.24)$$

which has a sign opposite to the stability condition of the odd parity perturbations. As a result, we conclude that the static spherically symmetric solution is unstable for any parameters of  $\beta_2$  and  $\beta_3$ .

**General modes** ( $\ell \geq 1$ )

Although we have shown the instability of the background solution, we discuss general modes of the even parity perturbations for completeness. The quadratic action can be expressed by

$$S^{\text{even}} = \int Y^2 d\Omega \int dt dr \mathcal{L}^{\text{even}}(\dot{\xi}_r, \dot{\xi}_\Omega, \xi'_A, \xi_A), \quad (8.4.25)$$

where  $A = (t, r, \Omega)$ , thus  $\xi_t$  is a non-dynamical variable, same as the case of  $\ell = 0$  mode. However, contrary to the case of  $\ell = 0$  mode, the constraint equation, which is derived by the variation with respect to  $\xi_t$ , is not easily solved. We notice however that the constraint equation has a particular solution

$$\delta\pi_\mu^{\text{even}} = \partial_\mu(\Xi(t, r)Y(\theta, \varphi)) + \mathcal{O}(GM/r), \quad (8.4.26)$$

in which there is no degree of freedom of the vector graviton. Since the stability of the case of the purely scalar graviton has already been discussed, we shall not discuss this case furthermore here.

To discuss the stability of the general perturbations, we use the Hamiltonian formulation and calculate the on-shell Hamiltonian. The canonical momenta are defined by

$$\pi_A = \frac{\delta\mathcal{L}^{\text{even}}}{\delta\dot{\xi}_A}, \quad (8.4.27)$$

Since the Lagrangian does not contain  $\dot{\xi}_t$ , there is a primary constraint

$$\Phi^1 := \pi_t \approx 0, \quad (8.4.28)$$

where the symbol “ $\approx$ ” is the weak equality which holds on shell.  $\dot{\xi}_r$  and  $\dot{\xi}_\Omega$  can be expressed in terms of canonical variables. Then the total Hamiltonian is given by

$$\begin{aligned} \mathcal{H}_T^{\text{even}} &= \pi_r \dot{\xi}_r + \pi_\Omega \dot{\xi}_\Omega - \mathcal{L}^{\text{even}} + \lambda \pi_t \\ &= \mathcal{H}^{\text{even}}[\pi_r, \pi_\Omega, \xi_A] + \lambda \pi_t \end{aligned} \quad (8.4.29)$$

where  $\lambda$  is the Lagrangian multiplier. The preservation of the primary constraint yields

$$\Phi^2 := \{\Phi^1, \mathcal{H}_T^{\text{even}}\} \approx 0, \quad (8.4.30)$$

where

$$H_T^{\text{even}} = \int dr \mathcal{H}_T^{\text{even}}. \quad (8.4.31)$$

Note that since  $\Phi^2$  contains only  $\xi_t, \pi_r, \pi_r', \pi_\Omega$ , the secondary constraint  $\Phi^2 \approx 0$  is the constraint equation on the canonical variables, from which we can easily express  $\xi_t$  in terms of  $\pi_r, \pi_r', \pi_\Omega$ . This system has only these two constraints. Indeed, the condition  $\{\Phi^2, H_T^{\text{even}}\} \approx 0$  contains the Lagrangian multiplier  $\lambda$  and it does not generate a constraint equation, but an equation to determine the Lagrangian multiplier. As a result, we have two constraint equations on the canonical variables which are second class. Hence the degree of freedom of this system in the phase space is

$$\text{d.o.f.} = 6 - 2 = 2 \times 2,$$

which indicates that the even parity perturbations contain one scalar graviton and one vector graviton.

Substituting the solutions of constraint equations into the Hamiltonian, the on-shell Hamiltonian is given by

$$\begin{aligned} H_{\text{on-shell}}^{\text{even}} &= \int dr \mathcal{H}_{\text{on-shell}}^{\text{even}}(\pi_r, \pi_r', \pi_\Omega, \xi_r, \xi_\Omega, \xi_\Omega'), \\ &= \int dr \Lambda_2^4 \left[ \frac{K_1}{r^2} (\pi_r + A_1 \pi_\Omega)^2 + \frac{K_2}{r^2} (r \pi_r' + A_2 \pi_\Omega)^2 + \frac{K_3}{r^2} \pi_\Omega^2 \right. \\ &\quad \left. + K_4 (\xi_\Omega + A_4 \xi_r)^2 + K_5 (r \xi_\Omega' + A_5 \xi_r)^2 + K_6 \xi_r^2 \right], \end{aligned} \quad (8.4.32)$$

where the dimensionless coefficients are expanded as

$$K_1 = \epsilon \frac{\mathcal{B}_1}{48\beta_3^{3/2}(\beta_2 + \epsilon\sqrt{\beta_3})} + \mathcal{O}\left(\frac{GM}{r}\right), \quad (8.4.33)$$

$$K_2 = -\epsilon \left(\frac{GM}{r}\right)^{-2} \frac{1}{12\sqrt{\beta_3}(\beta_2 + \epsilon\sqrt{\beta_3})} + \mathcal{O}\left(\left(\frac{GM}{r}\right)^{-1}\right), \quad (8.4.34)$$

$$K_3 = -\epsilon \left(\frac{GM}{r}\right)^{-2} \frac{\sqrt{\beta_3}(1 - 2\epsilon\sqrt{\beta_3})^2}{3\mathcal{B}_1(\beta_2 + \epsilon\sqrt{\beta_3})} + \mathcal{O}\left(\left(\frac{GM}{r}\right)^{-1}\right), \quad (8.4.35)$$

$$K_4 = -\epsilon\ell(\ell+1) \frac{GM}{r} \frac{\mathcal{B}_2}{16\sqrt{\beta_3}(\epsilon + \sqrt{\beta_3})^2} + \mathcal{O}\left(\left(\frac{GM}{r}\right)^2\right), \quad (8.4.36)$$

$$K_5 = \epsilon\ell(\ell+1) \frac{\beta_2 + \epsilon\sqrt{\beta_3}}{4(\epsilon + \sqrt{\beta_3})} + \mathcal{O}\left(\frac{GM}{r}\right), \quad (8.4.37)$$

$$K_6 = \epsilon\ell(\ell+1) \left(\frac{GM}{r}\right)^{-1} \sqrt{\beta_3}\mathcal{B}_2^{-1}(\beta_2 + \epsilon\sqrt{\beta_3})^2 + \mathcal{O}(1), \quad (8.4.38)$$

and

$$A_1 = \left(\frac{GM}{r}\right)^{-1} 4\beta_3\mathcal{B}_1^{-1}(1 - 2\epsilon\sqrt{\beta_3}) + \mathcal{O}(1), \quad (8.4.39)$$

$$A_2 = -1 + \mathcal{O}\left(\frac{GM}{r}\right), \quad (8.4.40)$$

$$A_4 = \left(\frac{GM}{r}\right)^{-1} 4\sqrt{\beta_3}\mathcal{B}_2^{-1}(\epsilon + \sqrt{\beta_3})(\beta_2 + \epsilon\sqrt{\beta_3}) + \mathcal{O}(1), \quad (8.4.41)$$

$$A_5 = -1 + \mathcal{O}\left(\frac{GM}{r}\right) \quad (8.4.42)$$

with

$$\mathcal{B}_1 := \beta_2 + 8\beta_3 - 4\beta_2\beta_3 + \epsilon\sqrt{\beta_3}(4\beta_3 - 3), \quad (8.4.43)$$

$$\mathcal{B}_2 := \beta_2^2(1 - 4\beta_3) + \beta_3(5 + 4\beta_3) - 4\beta_2\beta_4 + 2\epsilon\sqrt{\beta_3}(6\beta_3 - \beta_2(1 + 4\beta_3)) \quad (8.4.44)$$

One can find  $K_1K_3 < 0$  and  $K_4K_6 < 0$  for any parameters  $(\beta_2, \beta_3)$ , thus the Hamiltonian is unbounded from the below, which means that the perturbations suffer from the instability.





# Chapter 9

## Summary

The discoveries of the accelerating expansion of the Universe as well as dark matter may reveal that a new physics beyond the standard one exists in nature. Phenomenologically, the  $\Lambda$ CDM model provides a consistent scenario with cosmological observations. However, the origins of dark components of the Universe have not been cleared and various scenarios have been proposed. One possibility is that the dark components might be due to a modification of GR. Some of modified theories of gravity indeed yield the accelerating expansion without dark matter or a dark matter candidate from the gravitational origin. Among many modified gravity theories, one natural modification of GR is to consider the possibility of a massive graviton. Especially, in this thesis, we have focused the bigravity theory which contains both massless and massive gravitons and discussed cosmological and astrophysical aspects of this theory. In this theory, the graviton mass in the range  $10^{-2}$  eV  $\lesssim m \lesssim 10^{-23}$  eV may be excluded from observations, in general.

In Chapter 5, we have studied the dynamics of the homogeneous and isotropic universe in the bigravity theory. The vacuum solution of bigravity is not uniquely determined. The bigravity theory can admit the de Sitter solution as a vacuum solution (and also anti-de Sitter solution) even if we assume the existence of the Minkowski vacuum. We find two stable attractors for the FLRW spacetime with twin dust matter fields: One is de Sitter accelerating universe ( $\Lambda_g > 0$ ) and the other is matter dominated universe ( $\Lambda_g = 0$ ). The present accelerating expansion can be naturally obtained by the tiny graviton mass such as  $m \sim 10^{-33}$  eV.

We have also discussed the stability of the cosmological solution in Chapter 6. It has been known that, when the graviton mass is smaller than the Hubble parameter, homogeneous and isotropic spacetimes suffer from the Higuchi type instability against the linear perturbation in the bigravity. However, we find a cosmological solution in which the instabilities can be resolved by the cosmological Vainshtein mechanism for an appropriate parameter space of coupling constants. The growth history of the perturbations can be restored into that in GR. However, it has not been cleared whether or not this cosmological solution transits to the cosmological solution discussed in Chapter 5. We show the transition may not occur at least adiabatically in the universe with the standard matter components.

In Chapter 7, we have studied two possibilities to explain dark matter in the context of bigravity:  $f$ -matter as dark matter, and massive graviton as dark matter. In the former case, the dark matter candidate is matter fields which couple with  $f_{\mu\nu}$ . The standard matter fields are assumed to couple with  $g_{\mu\nu}$ . Although there are no direct interactions between the  $g$ -matter and the  $f$ -matter, the  $f$ -matter can affect the  $g$ -matter through the gravitational interactions because the bigravity theory has the interaction between  $g_{\mu\nu}$  and  $f_{\mu\nu}$ . An observational signature is that the  $f$ -matter can produce a repulsive force in the scales between the Vainshtein radius and the Compton wavelength. In particular, if the graviton mass is  $\sim 10^{-27}$  eV, the repulsive force may be observed as that the gravity is effectively weak at galactic scales. On the other hand, the second possibility is that the massive graviton itself is a dark matter candidate. We obtain a general bound on the graviton mass to be dark matter which is typically given by  $10^{-23}$  eV  $\lesssim m \lesssim 10^7$  eV. We have constructed a scenario in which the production of massive gravitons is accompanied by the production of the gravitational waves. In this scenario, we can estimate a suitable value of the graviton mass from the observations of the gravitational waves.

In Chapter 8, we have shown that the Vainshtein mechanism would be unsuccessful around an astrophysical object. First, we have studied static and spherically symmetric solutions and discussed the solutions describing a neutron star. As a result, a curvature singularity is found beyond a critical value of the mass of the neutron star in some parameter space. Hence, the Vainshtein mechanism is broken in the strong gravitational field. In this study, there is still a parameter space to yield the successful Vainshtein screening in the strong gravitational field. However, we then find that the static and spherically symmetric solutions are unstable against small perturbations within the Vainshtein radius. To evade the instability the excitation of the vector graviton would be needed. In the spherically symmetric spacetimes, the vector graviton may not be excited. Studies beyond the spherically symmetric would be required to obtain a successful Vainshtein mechanism. Note that the instability is problematic only for the light massive graviton ( $m \lesssim 10^{-23}$  eV) because the Vainshtein radius is much smaller than the astrophysical scales in the case of the heavy massive graviton ( $m \gtrsim 10^{-2}$  eV).

In conclusion, the bigravity theory yields some explanations of the acceleration of the Universe or dark matter depending on the graviton mass. For instance, the massive graviton with  $m \sim 10^{-33}$  eV can explain the present accelerating expansion. However, if the graviton mass is small ( $m \lesssim 10^{-23}$  eV), the consistency with the Solar System tests of gravity is an open question because there is no stable solution describing an astrophysical object.

## Future issues

Phenomenologically, we may classify the bigravity theory into two cases: the small mass ( $m \lesssim 10^{-23}$  eV) or the large mass ( $m \gtrsim 10^{-2}$  eV). Regarding the former case, an important remaining problem is to find a viable solution of an astrophysical object. In a local region of the spacetime, the  $\Lambda_2$  decoupling limit can yield an effective theory which is originally obtained by considering the nonlinear excitation of the vector graviton [83, 84]. The limit also gives the effective theory even when the vector graviton is not excited but the spacetime is curved [86]. However, we show that the effective theory only with the scalar graviton excitation leads to the instability in Ricci flat spacetimes. As a result, the static and spherically symmetric ansatz does not give a viable astrophysical solution which would be caused by that we have taken into account the excitation of the scalar graviton only. When we relax the spherical symmetry, the vector graviton could be excited and then it will dramatically change the behavior of the spacetime.

As for the large mass graviton, the bigravity may give a new paradigm for dark matter. Although we have already discussed two ways to explain dark matter, other possibilities would remain. For instance, the energy density of the anisotropy of the Bianchi type universe decreases as a dust fluid in the bigravity theory although that in GR decreases as a stiff matter [48]. This fact could be explained by that the anisotropy is a consequence of a condensation of massive gravitons with some direction and the energy density of the non-relativistic massive gravitons decreases as a dust. If the condensed massive graviton indeed behaves like dark matter, we will observe a deformation of the spacetime as dark matter in bigravity.

Although the graviton mass is phenomenologically significant, theoretical predictions about the origin of the mass are still insufficient. The massive graviton would be reduced from a fundamental theory as a low-energy effective theory [112, 190–197]. We should know the precise mechanism generating the graviton mass in order to discuss more fundamental problems of massive spin-2 field. Furthermore, the number of gravitons is not clear. We have considered the case of two gravitons; however, the multi-gravity extension is also possible in which the number of the gravitons is larger than two [18]. For instance, if massive graviton gravitons are obtained as Kaluza-Klein modes from a higher dimensional picture, it would be natural that there exist several massive gravitons in four dimensions. At the linear level, since the gravitons propagate independently, the qualitative behavior in multi-gravity would not be changed from that in bigravity. On the other hand, nonlinear interactions of the multi-gravitons may lead to other features than bi-gravitons.

The massive graviton has been received much attention from both theoretical and phenomenological prospects. The success of the ghost-free nonlinear extension of the Fierz-Pauli theory gives a new paradigm for theories of gravity and also the cosmological problems. Nevertheless, there are still interesting open questions in the theories of massive spin-2 fields.

## Acknowledgments

First of all, I would like to thank my supervisor Kei-ichi Maeda for his guidances, suggestions and encourages throughout my master and PhD courses. I cannot imagine myself to get a PhD degree without his supports. I am grateful to Shoichi Yamada for pedagogical teaching and discussions. I am also thankful to Hiroyuki Abe for letting me skip half of a grade of my master course. I would like to thank also Shinji Mukohyama for invaluable discussions and hospitality during my visit to Yukawa Institute for Theoretical Physics (YITP) at Kyoto University. It was a grateful opportunity to develop my research. As for writing the papers and this thesis I have benefited much from the collaborations with Ryo Namba and Shuntaro Mizuno. The papers including the thesis have not been completed without discussions with them. I thank Antonio De Felice, Kotaro Fujisawa, Tomohiro Harada, Kazunori Kohri, Tsutomu Kobayashi, Hideo Kodama, Takashi Nakamura, Shin'ichi Nojiri, Jiro Soda, Ryo Sito, Norihiro Tanahashi, Takahiro Tanaka, Ayumu Terukina, Masahide Yamaguchi, Junichi Yokoyama, Mikhail S. Volkov for useful discussions and comment. I am grateful to the colleagues at Waseda University. Finally, I would like to express my gratitude to my parents and friends for their supports and encourages.



# Appendix A

## Constrained systems

In this chapter, we briefly summarize Lagrangian and Hamiltonian formulations in constrained systems. We mainly consider only mechanics with finite degrees of freedom, for simplicity.

### A.1 Lagrangian formulation

Let us consider the action

$$S = \int L(q^i, \dot{q}^i, t) dt, \quad (\text{A.1.1})$$

where  $q^i$  are generalized coordinates for point particles ( $i = 1, 2, \dots, N$ ). We assume the action contains up to first order time derivatives of  $q^i$  until Section B.4. The variation principle leads to the Euler-Lagrange equation

$$A_{ij} \ddot{q}^j + \frac{\partial^2 L}{\partial \dot{q}^i \partial q^j} \dot{q}^j - \frac{\partial L}{\partial q^i} = 0, \quad (\text{A.1.2})$$

where

$$\xi^i := \dot{q}^i, \quad (\text{A.1.3})$$

and

$$A_{ij} := \frac{\partial^2 L}{\partial \xi^i \partial \xi^j}. \quad (\text{A.1.4})$$

The matrix  $A_{ij}$  is called Hessian.

If the Hessian has no zero eigenvalues, that is

$$\det(A_{ij}) \neq 0, \quad (\text{A.1.5})$$

there exists an inverse matrix  $(A^{-1})^{ij}$  and the equation of motion is then

$$\dot{\xi}^i + (A^{-1})^{ij} \frac{\partial^2 L}{\partial \xi^j \partial q^k} \xi^k - (A^{-1})^{ij} \frac{\partial L}{\partial q^j} = 0. \quad (\text{A.1.6})$$

This expression explicitly shows that there are  $N$  independent equations of motion. To determine the dynamics of this system, one requires  $2N$  independent initial data. The number of degrees of freedom of the system is  $2N$  in the phase space.

On the other hand, if the determinant of the Hessian is zero,  $A_{ij}$  is not invertible and then all  $N$  equations are no longer independent. Supposing

$$\text{rank}(A_{ij}) = N - R, \quad (\text{A.1.7})$$

there exist  $(N - R)$  independent eigenvectors such that

$$A_{ij}\tau_\alpha^j = 0, \quad (\text{A.1.8})$$

where  $\alpha = 1, 2, \dots, R$ . The constraint equations are obtained by multiplying the equations by the eigenvectors:

$$\tau_\alpha^i \left( \frac{\partial^2 L}{\partial \xi^i \partial q^j} \xi^j - \frac{\partial L}{\partial q^i} \right) = 0. \quad (\text{A.1.9})$$

In this system, one cannot set  $2N$  initial data, independently, due to the constraint equations. The number of physical degrees of freedom is less than  $2N$ . To count the number of degrees of freedom, the Hamiltonian formulation is more useful than the Lagrangian formulation.

## A.2 Hamiltonian formulation

Let us define the conjugate momenta

$$p_i(q, \xi) := \frac{\partial L(q, \xi)}{\partial \xi^i}. \quad (\text{A.2.1})$$

The Hessian is the Jacobian for the conjugate momenta since

$$A_{ij} = \frac{\partial^2 L}{\partial \xi^i \partial \xi^j} = \frac{\partial p_i}{\partial \xi^j}. \quad (\text{A.2.2})$$

If the Hessian is inverted ( $\det(A_{ij}) \neq 0$ ), one can solve all  $\xi^i$  in terms of canonical variables  $q^i$  and  $p_i$ . However, some of  $\xi^i$  are not inverted in constrained systems since the transformation from  $\xi^i$  to  $p_i$  is singular. Some of  $\xi^i$  are not expressed in terms of the canonical variables.

First, we consider the case that  $A_{ij}$  is invertible. In this case, all  $\xi^i$  are expressed in terms of the canonical variables and then all canonical variables  $(q^i, p_i)$  are independent. The variation of the action reads

$$\delta S = \int \left[ - \left( \dot{p}_i + \frac{\partial H}{\partial q^i} \right) \delta q^i + \left( \dot{q}^i - \frac{\partial H}{\partial p_i} \right) \delta p_i \right] dt = 0, \quad (\text{A.2.3})$$

where we define the Hamiltonian

$$H(q, p) := p_i \dot{q}^i(q, p) - L(q, p). \quad (\text{A.2.4})$$

Supposing all canonical variables are independent, one obtains the Hamilton's equations of motion

$$\dot{q}^i = \frac{\partial H}{\partial p_i}, \quad \dot{p}_i = - \frac{\partial H}{\partial q^i}. \quad (\text{A.2.5})$$

Time evolution of generic function  $f(q^i, p_i, t)$  is given by

$$\frac{df(p, q, t)}{dt} = \{f, H\} + \frac{\partial f}{\partial t} \quad (\text{A.2.6})$$

where

$$\{f, g\} := \frac{\partial f}{\partial q^i} \frac{\partial g}{\partial p_i} - \frac{\partial f}{\partial p_i} \frac{\partial g}{\partial q^i} \quad (\text{A.2.7})$$

is the Poisson bracket.

In constrained systems, contrarily to unconstrained systems, all canonical variables are not independent. Due to the singularity of the Hessian, there exist primary constraints on the canonical variables

$$\Phi_\alpha^1(q, p) = 0, \quad (\text{A.2.8})$$

where  $\alpha = 1, 2, \dots, R$  when  $\text{rank}(A_{ij}) = N - R$ . For instance, when the Lagrangian does not contain  $\xi^\alpha$ , the conjugate momenta are

$$p_\alpha = \frac{\partial L}{\partial \xi^\alpha} = 0,$$

which gives constraint equations on  $p_\alpha$  and then  $\xi^\alpha$  are not solvable in terms of canonical variables. The constraint equations restrict  $2N$  dimensional phase space into lower dimensional space, which space we call the constraint surface.

As a result, when the Hessian has  $R$  zero eigenvalues, there exists  $R$  primary constraint  $\Phi_\alpha^1 \approx 0$ , where we introduce the weak equality denoted by “ $\approx$ ” which holds on the constraint surface. In unconstrained systems, we have used the independence of the canonical variables to derive the Hamilton’s equations of motion. In the constrained systems, however, the canonical variables  $(q^i, p_i)$  are no longer independent. The variations of canonical variables have to satisfy

$$\frac{\partial \Phi_\alpha^1}{\partial q^i} \delta q^i + \frac{\partial \Phi_\alpha^1}{\partial p_i} \delta p_i \approx 0. \quad (\text{A.2.9})$$

To hold the constraint equations, we introduce Lagrangian multipliers  $v^\alpha$  and rewrite the action as

$$S = \int [p_i \dot{q}^i - H - v^\alpha \Phi_\alpha^1] dt. \quad (\text{A.2.10})$$

The variation reads

$$\delta S = \int \left[ - \left( \dot{p}_i + \frac{\partial H}{\partial q^i} + v^\alpha \frac{\partial \Phi_\alpha^1}{\partial q^i} \right) \delta q^i + \left( \dot{q}^i - \frac{\partial H}{\partial p_i} - v^\alpha \frac{\partial \Phi_\alpha^1}{\partial p_i} \right) \delta p_i \right] dt. \quad (\text{A.2.11})$$

By choosing  $v^\alpha$  appropriately, each parenthesis in front of  $\delta q^i$  or  $\delta p_i$  is independently zero. Then one obtains the  $2N$  independent Hamilton’s equations of motion

$$\dot{q}^i = \frac{\partial H}{\partial p_i} + v^\alpha \frac{\partial \Phi_\alpha^1}{\partial p_i} = \{q^i, H_T\}, \quad (\text{A.2.12})$$

$$\dot{p}_i = - \frac{\partial H}{\partial q^i} - v^\alpha \frac{\partial \Phi_\alpha^1}{\partial q^i} = \{p_i, H_T\}, \quad (\text{A.2.13})$$

where we define the total Hamiltonian

$$H_T := H + v^\alpha \Phi_\alpha^1. \quad (\text{A.2.14})$$

It is worth noting that, in the constrained systems, time evolution of a variable is given by the total Hamiltonian instead of the Hamiltonian. The time derivative of a function  $f(q^i, p_i, t)$  is calculated as

$$\dot{f} = \{f, H_T\} + \frac{\partial f}{\partial t}. \quad (\text{A.2.15})$$

The singularity of the Hessian leads to the primary constraints. The primary constraints does not have any information about a time evolution of the system since we have not used the dynamical equations, namely the Hamilton’s equations. Even if we assume the primary constraints initially hold, it is not guaranteed to satisfy the primary constraints after a time evolution. The preservations of the primary constraints yield secondary constraints

$$\Phi_\alpha^2 = \dot{\Phi}_\alpha^1 = \{\Phi_\alpha^1, H_T\} \approx \{\Phi_\alpha^1, H\} + v^\beta L_{\alpha\beta} \approx 0, \quad (\text{A.2.16})$$

where

$$L_{\alpha\beta} := \{\Phi_\alpha^1, \Phi_\beta^1\}. \quad (\text{A.2.17})$$

If the matrix  $L_{\alpha\beta}$  is invertible even on the constrained surface, the secondary constraints are no longer the constraints on the canonical variables. The equation (A.2.16) is just an equation

to determine the Lagrangian multipliers. By using the inverse matrix  $(L^{-1})^{\alpha\beta}$ , the Lagrangian multipliers are determined by

$$v^\alpha \approx -(L^{-1})^{\alpha\beta} \{\Phi_\alpha^1, H\}. \quad (\text{A.2.18})$$

The preservations of (A.2.16) do not also yield constrains on the canonical variables since they are equations in terms of  $\dot{v}^\alpha$ .

If the matrix  $L_{\alpha\beta}$  is not invertible, some of (A.2.16) indeed give constraints on the canonical variables. A simple case is  $L_{\alpha\beta} \approx 0$  in which the secondary constraints are given by

$$\Phi_\alpha^2 = \{\Phi_\alpha^1, H\} \approx 0.$$

In general, the number of the secondary constraint is less than or equal to that of the primary constraints. We assume there exist  $R'$  secondary constraints  $\Phi_\mu^2$  where  $\mu = 1, 2, \dots, R'$  with  $R' \leq R$ . Then, the preservations of those yield

$$\Phi_\mu^3 = \{\Phi_\mu^2, H_T\} \approx \{\Phi_\mu^2, H\} + v^\beta \{\Phi_\mu^2, \Phi_\beta^1\}. \quad (\text{A.2.19})$$

If some of these equations are constraints on the canonical variables, we should calculate the preservations of those which may yield further constraints. This procedure must continue till either all  $v^\alpha$  are determined or the preservations trivially hold by using other constraints.

Note that it is not guaranteed that all  $v^\alpha$  are determined. For instance, let us consider following case: the matrix  $\{\Phi_\alpha^1, \Phi_\beta^1\}$  is weakly zero and the preservations of the secondary constraints are expressed in terms of the primary and secondary constraints, that is

$$\Phi_\alpha^3 = a^\alpha \Phi_\alpha^1 + b^\alpha \Phi_\alpha^2, \quad (\text{A.2.20})$$

where  $a^\alpha$  and  $b^\alpha$  are some functions of the canonical variables. In this case, the equation  $\Phi_\alpha^3 \approx 0$  trivially hold and then the Lagrangian multipliers  $v^\alpha$  are undetermined. Even if we consider  $\dot{\Phi}_\alpha^3 \approx 0$ , it is also trivially satisfied on the constraint surface.

The constraints on the canonical variables are classified into two classes: first class constraints  $\psi_a$  and second class constraints  $\theta_s$ . The first class constraints have a weakly vanishing Poisson bracket with all constraints,

$$\{\psi_a, \theta_s\} \approx 0, \quad \{\psi_a, \psi_b\} \approx 0, \quad (\text{A.2.21})$$

and the second class constraints are others; that is,  $\theta_s$  is a second class constraint if

$$\exists t \quad \text{s.t.} \quad \{\theta_s, \theta_t\} \not\approx 0. \quad (\text{A.2.22})$$

The total number of constraints is fixed in a given system; however the number of the first class constraints (or the second class constraints) is not unique. We denote all constraints  $\Phi_\alpha$  and define the matrix

$$M_{\alpha\beta} := \{\Phi_\alpha, \Phi_\beta\}. \quad (\text{A.2.23})$$

If the matrix  $M_{\alpha\beta}$  has zero eigenvalues on the constraint surface, we denote the corresponding eigenvectors  $u_a^\alpha$ . Even if each  $\Phi_\alpha$  is not a first class constraint, each linear combination  $u_a^\alpha \Phi_\alpha$  is a first class constraint since

$$0 = u_a^\alpha M_{\alpha\beta} = u_a^\alpha \{\Phi_\alpha, \Phi_\beta\} \approx \{u_a^\alpha \Phi_\alpha, \Phi_\beta\}. \quad (\text{A.2.24})$$

This suggests that the maximum number of the first class constraints is given by the number of the zero eigenvalues of the matrix  $M_{\alpha\beta}$ . One redefine the constraints such that new constraints  $\Phi_{\alpha'}$  satisfy

$$M_{\alpha'\beta'} = \{\Phi_{\alpha'}, \Phi_{\beta'}\} \approx \begin{pmatrix} 0 & 0 \\ 0 & C_{st} \end{pmatrix}, \quad (\text{A.2.25})$$



where

$$\det(C_{st}) \neq 0. \quad (\text{A.2.26})$$

After this redefinition, the number of the first class constraints is maximized, or, equivalently, the number of the second class constraints is minimized. Note that, while the number of the first class constraints is odd or even, the number of the second class constraints is even. This fact is easily shown by using that  $C_{st}$  is an antisymmetric matrix and (A.2.26).

If the system has first class constraints, some of  $v^\alpha$  are undetermined. In the constrained system, the time evolution is determined by the total Hamiltonian which contains  $v^\alpha$ . Therefore, the undetermined  $v^\alpha$  suggests that the dynamics is not uniquely determined. This kind of theory is called gauge theory. The existence of the first class constraints is related to the gauge symmetry. The number of the gauge symmetry is given by the number of the first class primary constraints since the number of the first class primary constraints coincides with the number of the undetermined  $v^\alpha$ . The linear combinations of the first class constraints give generating functions of the gauge transformation.

Let us count the number of degrees of freedom of the system with  $A$  primary constraints  $\psi_a$  and  $2S$  secondary constraints  $\theta_s$ . The total number of the constraints is  $A + 2S$ . We notice again that the number of the secondary constraints is even. The second class constraints reduce the physical degrees of freedom, directly. On the other hand, when the system has the first class constraints, the degrees of freedom are reduced by not only the constraints themselves but also the gauge freedom. The gauge fixing conditions  $\chi_a$  are introduced in order that all first class constraints are recast in second class constraints regarding the gauge fixing condition as additional constraints, i.e.,  $\det\{\psi_a, \chi_b\} \neq 0$ . Then the degrees of freedom are reduced by  $\psi_a$  and  $\chi_a$ . As a result, the number of the total degrees of freedom of the system is given by

$$2N - 2S - 2A = 2(N - S - A),$$

in the phase space. The dynamics of the system is characterized by  $N - S - A$  independent positions and  $N - S - A$  independent velocities.

### A.3 Field theory

The generalization to field theories are straightforwardly done. For fields  $\phi^a$ <sup>1</sup>, the  $d + 1$  dimensional action is given by

$$S = \int dt L, \quad L := \int d^d \mathbf{x} \mathcal{L}(\phi^a, \phi^a_{;\mu}), \quad (\text{A.3.1})$$

where  $\mathcal{L}$  is the Lagrangian density. The Hamiltonian density and the Hamiltonian are defined by

$$\mathcal{H} := \pi_a \dot{\phi}^a - \mathcal{L}, \quad (\text{A.3.2})$$

$$H := \int d^d \mathbf{x} \mathcal{H}, \quad (\text{A.3.3})$$

where the conjugate momenta are defined by

$$\pi_a(t, \mathbf{x}) := \frac{\partial \mathcal{L}(t, \mathbf{x})}{\partial \dot{\phi}^a(t, \mathbf{x})}. \quad (\text{A.3.4})$$

The time derivative of a functional  $f[\phi, \pi; t]$  is given by

$$\dot{f}(t, \mathbf{x}) = \{f(t, \mathbf{x}), H\} + \frac{\partial f(t, \mathbf{x})}{\partial t}, \quad (\text{A.3.5})$$

---

<sup>1</sup>The index  $a$  labels independent components of fields. For example, when we consider  $N$  scalar fields, the label runs from 1 to  $N$ . For a vector field  $A^\mu$  in four dimensions, the index  $a$  runs from one to four.

where

$$\{f(t, \mathbf{x}), g(t, \mathbf{y})\} = \int d^d \mathbf{z} \left[ \frac{\delta f(t, \mathbf{x})}{\delta \pi_a(t, \mathbf{z})} \frac{\delta g(t, \mathbf{y})}{\delta \phi^a(t, \mathbf{z})} - \frac{\delta f(t, \mathbf{x})}{\delta \phi^a(t, \mathbf{z})} \frac{\delta g(t, \mathbf{y})}{\delta \pi_a(t, \mathbf{z})} \right], \quad (\text{A.3.6})$$

is the Poisson bracket between two functionals  $f$  and  $g$ .  $\frac{\delta}{\delta \phi^a}$  and  $\frac{\delta}{\delta \pi_a}$  are the functional derivatives with respect to the fields  $\phi^a$  and  $\pi_a$ , respectively. Then, the discussions in a field theory are done in a similar way to mechanics.

# Appendix B

## Instabilities

### B.1 Ghost instability

The ghost instability arises when the kinetic term has a wrong sign (see [198] for a review). Let us consider the following Lagrangian with the ghost field  $\phi$ :

$$\mathcal{L} = +\frac{1}{2}(\partial\phi)^2 - \frac{1}{2}(\partial\psi)^2 + \mathcal{L}_{\text{int}}(\phi, \psi). \quad (\text{B.1.1})$$

The field  $\psi$  has the correct sign kinetic term. When the interaction between the ghost field and other fields vanishes, the field  $\phi$  does not exhibit any instability either classically or quantum mechanically. However, the wrong sign kinetic term leads to that the kinetic energy of the field  $\phi$  is negative. The energy of the ghost field is rapidly transferred to the other field via the interaction  $\mathcal{L}_{\text{int}}$  and then the vacuum  $\langle\phi\rangle = \langle\psi\rangle = 0$  is unstable. Quantum mechanically, the ghost field leads to a divergent decay rate [151].

The existence of a ghost field implies that the theory is ill-defined. However, as discussed in Section 6.1, the ghost mode is controllable in the context of the ghost condensate. The vacuum  $\langle\phi\rangle = 0$  is unstable, however, there may be a stable condensed state  $\langle\phi\rangle \neq 0$  when higher order kinetic terms are introduced.

### B.2 Gradient instability

Another instability originated from kinetic terms is the gradient instability. The gradient instability arises from wrong spatial derivatives. A typical example of the Lagrangian with the gradient instability is given by

$$\mathcal{L} = \frac{1}{2}\dot{\phi}^2 + \frac{1}{2}(\partial_i\phi)^2. \quad (\text{B.2.1})$$

In the Fourier space, the solutions are

$$\phi(t) \sim e^{\pm kt}, \quad (\text{B.2.2})$$

where  $k = |\mathbf{k}|$ . Hence, the solution has a exponentially growing mode. The time scale of the growing mode is

$$t_{\text{inst}} \sim k^{-1}, \quad (\text{B.2.3})$$

thus the high energy mode leads to the rapid growth of the mode.

Clearly, the gradient instability can appear in the theory without the Lorentz invariance. Even for Lorentz invariant theories, the Lorentz invariance for perturbations is effectively lost due to the non-zero background configuration. For instance, the perturbations have no Lorentz invariance around the FLRW background. To verify the stability of some background, we have to confirm non-existence of not only the ghost instability but also the gradient instability.

### B.3 Tachyonic instability

Finally, we discuss an instability arising from a mass term instead of the kinetic term. A tachyonic instability appears in a field with a wrong sign mass term. A typical Lagrangian is

$$\mathcal{L} = -\frac{1}{2}(\partial\phi)^2 + \frac{m^2}{2}\phi^2. \quad (\text{B.3.1})$$

The long wavelength mode ( $k \rightarrow 0$ ) tends to

$$\phi(t) \sim e^{\pm mt}, \quad (\text{B.3.2})$$

thus the solution exhibits an unstable mode. The time scale of the instability is given by

$$t_{\text{inst}} \sim m^{-1}. \quad (\text{B.3.3})$$

Differently from previous two instabilities, the time scale of tachyonic instability is bounded. Furthermore, in the short wavelength mode, we may ignore the mass term compared with the kinetic term. Hence, the tachyonic instability is not sensitive for high energy modes.

### B.4 Ostrogradsky instability

It is known that, when the equations of motion contain a third derivative or higher than it, the system is unstable. In other words, a Lagrangian with higher derivatives gives an unstable system. The instability associated with higher derivatives are called Ostrogradsky instability (see [199, 200] for reviews). In this section, we show why such higher derivatives lead to the instability. For simplicity, we shall only consider a point particle in one dimensional space whose Lagrangian is assumed to be  $L = L(q, \dot{q}, \ddot{q})$ .

In the Lagrangian formulation, the Euler-Lagrange equation is given by

$$\frac{\partial L}{\partial q} - \frac{d}{dt} \frac{\partial L}{\partial \dot{q}} + \frac{d^2}{dt^2} \frac{\partial L}{\partial \ddot{q}} = 0. \quad (\text{B.4.1})$$

This equation may contain fourth derivatives of  $q$  which reads that 4 independent initial data are required to determine the dynamics of the system.

In the Hamiltonian formulation, we may need four independent canonical variables due to higher derivatives. The Ostrogradsky's choices are

$$\begin{aligned} Q_1 &= q, & P_1 &= \frac{\partial L}{\partial \dot{q}} - \frac{d}{dt} \frac{\partial L}{\partial \ddot{q}}, \\ Q_2 &= \dot{q}, & P_2 &= \frac{\partial L}{\partial \ddot{q}}. \end{aligned} \quad (\text{B.4.2})$$

An assumption of the Ostrogradsky's theorem is the Lagrangian is non-degenerated:  $\ddot{q}$  can be expressed in terms of the canonical variables by solving the equations (B.4.2); that is, there exists a function  $a(Q_1, Q_2, P_2)$  such that

$$P_2 = \left. \frac{\partial L}{\partial \ddot{q}}(q, \dot{q}, \ddot{q}) \right|_{q=Q_1, \dot{q}=Q_2, \ddot{q}=a}. \quad (\text{B.4.3})$$

Under the non-degeneracy of the Lagrangian, the Hamiltonian is expressed as

$$\begin{aligned} H(Q_1, Q_2, P_1, P_2) &= P_1 \dot{q} + P_2 \ddot{q} - L \\ &= P_1 Q_2 + P_2 a(Q_1, Q_2, P_2) - L(Q_1, Q_2, a(Q_1, Q_2, P_2)). \end{aligned} \quad (\text{B.4.4})$$

The Hamilton's equations derived from the Hamiltonian indeed reproduce the result obtained from the Euler-Lagrange equation.

The Ostrogradsky's Hamiltonian is linear in the variable  $P_2$ . Therefore, the Hamiltonian is unbounded from below (and above), which leads to the system has no stable state. This is the

consequence of higher derivative theories. The Lagrangian with higher derivatives describes a system with unbounded energy; thus the system is unstable.

An example is a higher derivative generalization of the harmonic oscillator described by the Lagrangian

$$L = -\frac{g}{2\omega^2}\ddot{q}^2 + \frac{1}{2}\dot{q}^2 - \frac{\omega^2}{2}q^2, \quad (\text{B.4.5})$$

where  $g, \omega$  are constant. The Euler-Lagrange equation admits a solution

$$q(t) = A_+ \cos(k_+ t) + B_+ \sin(k_+ t) + A_- \cos(k_- t) + B_- \sin(k_- t), \quad (\text{B.4.6})$$

where

$$k_{\pm} = \omega \sqrt{\frac{1 \pm \sqrt{1 - 4g}}{2g}}. \quad (\text{B.4.7})$$

For this system, the Ostrogradsky's canonical momenta are given by

$$P_1 = \dot{q} + \frac{g}{\omega^2}q^{(3)}, \quad (\text{B.4.8})$$

$$P_2 = -\frac{g}{\omega^2}\ddot{q}. \quad (\text{B.4.9})$$

Then the Hamiltonian is

$$H = P_1 Q_2 - \frac{\omega^2}{2g}P_2^2 - \frac{1}{2}Q_2^2 + \frac{\omega^2}{2}Q_1^2. \quad (\text{B.4.10})$$

The energy of the system is evaluated by substituting the solution of the Euler-Lagrange equation into the Hamiltonian. The on-shell Hamiltonian is

$$H = \frac{1}{2}\sqrt{1 - 4g}k_+^2(A_+^2 + B_+^2) - \frac{1}{2}\sqrt{1 - 4g}k_-^2(A_-^2 + B_-^2), \quad (\text{B.4.11})$$

which clearly shows that the  $-$  mode is the ghost state since it has a negative energy.

The Ostrogradsky's theorem is derived under the assumption that the Lagrangian is non-degenerated. The non-degeneracy suggests that the system has no constraint. However, when the Lagrangian is degenerated, i.e., the Hessian is degenerated, zero eigenvalues of the Hessian leads to constraints and then the unstable mode can be eliminated by the constraints (see [201] for an explicit example). The degenerated Lagrangian with higher derivatives can evade the Ostrogradsky instability.



# Bibliography

- [1] C. M. Will, *The Confrontation between General Relativity and Experiment*, *Living Rev. Rel.* **17** (2014) 4, [1403.7377].
- [2] VIRGO, LIGO SCIENTIFIC collaboration, B. P. Abbott et al., *Tests of general relativity with GW150914*, *Phys. Rev. Lett.* **116** (2016) 221101, [1602.03841].
- [3] D. Lovelock, *The Einstein tensor and its generalizations*, *J. Math. Phys.* **12** (1971) 498–501.
- [4] J. Murata and S. Tanaka, *A review of short-range gravity experiments in the LHC era*, *Class. Quant. Grav.* **32** (2015) 033001, [1408.3588].
- [5] C. de Rham, J. T. Deskins, A. J. Tolley and S.-Y. Zhou, *Graviton Mass Bounds*, 1606.08462.
- [6] M. Fierz and W. Pauli, *On relativistic wave equations for particles of arbitrary spin in an electromagnetic field*, *Proc. Roy. Soc. Lond.* **A173** (1939) 211–232.
- [7] H. van Dam and M. J. G. Veltman, *Massive and massless Yang-Mills and gravitational fields*, *Nucl. Phys.* **B22** (1970) 397–411.
- [8] V. I. Zakharov, *Linearized gravitation theory and the graviton mass*, *JETP Lett.* **12** (1970) 312.
- [9] A. I. Vainshtein, *To the problem of nonvanishing gravitation mass*, *Phys. Lett.* **B39** (1972) 393–394.
- [10] D. G. Boulware and S. Deser, *Can gravitation have a finite range?*, *Phys. Rev.* **D6** (1972) 3368–3382.
- [11] C. de Rham and G. Gabadadze, *Generalization of the Fierz-Pauli Action*, *Phys. Rev.* **D82** (2010) 044020, [1007.0443].
- [12] C. de Rham, G. Gabadadze and A. J. Tolley, *Resummation of Massive Gravity*, *Phys. Rev. Lett.* **106** (2011) 231101, [1011.1232].
- [13] S. F. Hassan and R. A. Rosen, *Resolving the Ghost Problem in non-Linear Massive Gravity*, *Phys. Rev. Lett.* **108** (2012) 041101, [1106.3344].
- [14] S. F. Hassan, R. A. Rosen and A. Schmidt-May, *Ghost-free Massive Gravity with a General Reference Metric*, *JHEP* **02** (2012) 026, [1109.3230].
- [15] S. F. Hassan and R. A. Rosen, *Confirmation of the Secondary Constraint and Absence of Ghost in Massive Gravity and Bimetric Gravity*, *JHEP* **04** (2012) 123, [1111.2070].
- [16] S. F. Hassan, A. Schmidt-May and M. von Strauss, *Proof of Consistency of Nonlinear Massive Gravity in the Stückelberg Formulation*, *Phys. Lett.* **B715** (2012) 335–339, [1203.5283].
- [17] S. F. Hassan and R. A. Rosen, *Bimetric Gravity from Ghost-free Massive Gravity*, *JHEP* **02** (2012) 126, [1109.3515].

- [18] K. Hinterbichler and R. A. Rosen, *Interacting Spin-2 Fields*, *JHEP* **07** (2012) 047, [1203.5783].
- [19] K. Hinterbichler, *Theoretical Aspects of Massive Gravity*, *Rev. Mod. Phys.* **84** (2012) 671–710, [1105.3735].
- [20] E. Babichev and C. Deffayet, *An introduction to the Vainshtein mechanism*, *Class. Quant. Grav.* **30** (2013) 184001, [1304.7240].
- [21] C. de Rham, *Massive Gravity*, *Living Rev. Rel.* **17** (2014) 7, [1401.4173].
- [22] A. Schmidt-May and M. von Strauss, *Recent developments in bimetric theory*, *J. Phys.* **A49** (2016) 183001, [1512.00021].
- [23] PLANCK collaboration, P. A. R. Ade et al., *Planck 2015 results. XIII. Cosmological parameters*, *Astron. Astrophys.* **594** (2016) A13, [1502.01589].
- [24] S. Weinberg, *The Cosmological Constant Problem*, *Rev. Mod. Phys.* **61** (1989) 1–23.
- [25] SUPERNOVA COSMOLOGY PROJECT collaboration, S. Perlmutter et al., *Measurements of Omega and Lambda from 42 high redshift supernovae*, *Astrophys. J.* **517** (1999) 565–586, [astro-ph/9812133].
- [26] SUPERNOVA SEARCH TEAM collaboration, A. G. Riess et al., *Observational evidence from supernovae for an accelerating universe and a cosmological constant*, *Astron. J.* **116** (1998) 1009–1038, [astro-ph/9805201].
- [27] T. Clifton, P. G. Ferreira, A. Padilla and C. Skordis, *Modified Gravity and Cosmology*, *Phys. Rept.* **513** (2012) 1–189, [1106.2476].
- [28] A. Joyce, B. Jain, J. Khoury and M. Trodden, *Beyond the Cosmological Standard Model*, *Phys. Rept.* **568** (2015) 1–98, [1407.0059].
- [29] K. Koyama, *Cosmological Tests of Modified Gravity*, *Rept. Prog. Phys.* **79** (2016) 046902, [1504.04623].
- [30] G. Bertone, D. Hooper and J. Silk, *Particle dark matter: Evidence, candidates and constraints*, *Phys. Rept.* **405** (2005) 279–390, [hep-ph/0404175].
- [31] J. L. Feng, *Dark Matter Candidates from Particle Physics and Methods of Detection*, *Ann. Rev. Astron. Astrophys.* **48** (2010) 495–545, [1003.0904].
- [32] PARTICLE DATA GROUP collaboration, K. A. Olive et al., *Review of Particle Physics*, *Chin. Phys.* **C38** (2014) 090001.
- [33] FERMI-LAT collaboration, M. Ackermann et al., *Searching for Dark Matter Annihilation from Milky Way Dwarf Spheroidal Galaxies with Six Years of Fermi Large Area Telescope Data*, *Phys. Rev. Lett.* **115** (2015) 231301, [1503.02641].
- [34] FERMI-LAT, MAGIC collaboration, M. L. Ahnen et al., *Limits to dark matter annihilation cross-section from a combined analysis of MAGIC and Fermi-LAT observations of dwarf satellite galaxies*, *JCAP* **1602** (2016) 039, [1601.06590].
- [35] FERMI-LAT collaboration, M. Ackermann et al., *Updated search for spectral lines from Galactic dark matter interactions with pass 8 data from the Fermi Large Area Telescope*, *Phys. Rev.* **D91** (2015) 122002, [1506.00013].
- [36] CMS collaboration, V. Khachatryan et al., *Search for dark matter, extra dimensions, and unparticles in monojet events in proton-proton collisions at  $\sqrt{s} = 8$  TeV*, *Eur. Phys. J.* **C75** (2015) 235, [1408.3583].
- [37] J. M. Gaskins, *A review of indirect searches for particle dark matter*, 1604.00014.



- [38] A. Higuchi, *Forbidden Mass Range for Spin-2 Field Theory in De Sitter Space-time*, *Nucl. Phys.* **B282** (1987) 397.
- [39] A. Higuchi, *Massive Symmetric Tensor Field in Space-times With a Positive Cosmological Constant*, *Nucl. Phys.* **B325** (1989) 745–765.
- [40] M. Porrati, *No van Dam-Veltman-Zakharov discontinuity in AdS space*, *Phys. Lett.* **B498** (2001) 92–96, [[hep-th/0011152](#)].
- [41] I. I. Kogan, S. Mouslopoulos and A. Papazoglou, *The  $m \rightarrow 0$  limit for massive graviton in  $dS(4)$  and  $AdS(4)$ : How to circumvent the van Dam-Veltman-Zakharov discontinuity*, *Phys. Lett.* **B503** (2001) 173–180, [[hep-th/0011138](#)].
- [42] L. Grisa and L. Sorbo, *Pauli-Fierz Gravitons on Friedmann-Robertson-Walker Background*, *Phys. Lett.* **B686** (2010) 273–278, [[0905.3391](#)].
- [43] M. S. Volkov, *Cosmological solutions with massive gravitons in the bigravity theory*, *JHEP* **01** (2012) 035, [[1110.6153](#)].
- [44] M. von Strauss, A. Schmidt-May, J. Enander, E. Mortsell and S. F. Hassan, *Cosmological Solutions in Bimetric Gravity and their Observational Tests*, *JCAP* **1203** (2012) 042, [[1111.1655](#)].
- [45] M. Berg, I. Buchberger, J. Enander, E. Mortsell and S. Sjors, *Growth Histories in Bimetric Massive Gravity*, *JCAP* **1212** (2012) 021, [[1206.3496](#)].
- [46] D. Comelli, M. Crisostomi, F. Nesti and L. Pilo, *FRW Cosmology in Ghost Free Massive Gravity*, *JHEP* **03** (2012) 067, [[1111.1983](#)].
- [47] Y. Sakakihara, J. Soda and T. Takahashi, *On Cosmic No-hair in Bimetric Gravity and the Higuchi Bound*, *PTEP* **2013** (2013) 033E02, [[1211.5976](#)].
- [48] K.-i. Maeda and M. S. Volkov, *Anisotropic universes in the ghost-free bigravity*, *Phys. Rev.* **D87** (2013) 104009, [[1302.6198](#)].
- [49] Y. Akrami, T. S. Koivisto and M. Sandstad, *Accelerated expansion from ghost-free bigravity: a statistical analysis with improved generality*, *JHEP* **03** (2013) 099, [[1209.0457](#)].
- [50] Y. Akrami, T. S. Koivisto, D. F. Mota and M. Sandstad, *Bimetric gravity doubly coupled to matter: theory and cosmological implications*, *JCAP* **1310** (2013) 046, [[1306.0004](#)].
- [51] K. Aoki and K.-i. Maeda, *Cosmology in ghost-free bigravity theory with twin matter fluids: The origin of dark matter*, *Phys. Rev.* **D89** (2014) 064051, [[1312.7040](#)].
- [52] D. Comelli, M. Crisostomi, K. Koyama, L. Pilo and G. Tasinato, *Cosmology of bigravity with doubly coupled matter*, *JCAP* **1504** (2015) 026, [[1501.00864](#)].
- [53] K. Aoki and K.-i. Maeda, *Dark matter in ghost-free bigravity theory: From a galaxy scale to the universe*, *Phys. Rev.* **D90** (2014) 124089, [[1409.0202](#)].
- [54] K. Aoki and S. Mukohyama, *Massive gravitons as dark matter and gravitational waves*, *Phys. Rev.* **D94** (2016) 024001, [[1604.06704](#)].
- [55] E. Babichev, L. Marzola, M. Raidal, A. Schmidt-May, F. Urban, H. Veermäe et al., *Bigravitational origin of dark matter*, *Phys. Rev.* **D94** (2016) 084055, [[1604.08564](#)].
- [56] E. Babichev, L. Marzola, M. Raidal, A. Schmidt-May, F. Urban, H. Veermäe et al., *Heavy spin-2 Dark Matter*, *JCAP* **1609** (2016) 016, [[1607.03497](#)].
- [57] D. Comelli, M. Crisostomi and L. Pilo, *Perturbations in Massive Gravity Cosmology*, *JHEP* **06** (2012) 085, [[1202.1986](#)].
- [58] D. Comelli, M. Crisostomi and L. Pilo, *FRW Cosmological Perturbations in Massive Bigravity*, *Phys. Rev.* **D90** (2014) 084003, [[1403.5679](#)].

- [59] A. De Felice, A. E. Gümrükçüoğlu, S. Mukohyama, N. Tanahashi and T. Tanaka, *Viable cosmology in bimetric theory*, *JCAP* **1406** (2014) 037, [1404.0008].
- [60] F. Koennig, Y. Akrami, L. Amendola, M. Motta and A. R. Solomon, *Stable and unstable cosmological models in bimetric massive gravity*, *Phys. Rev.* **D90** (2014) 124014, [1407.4331].
- [61] Y. Akrami, S. F. Hassan, F. Könnig, A. Schmidt-May and A. R. Solomon, *Bimetric gravity is cosmologically viable*, *Phys. Lett.* **B748** (2015) 37–44, [1503.07521].
- [62] M. Fasiello and R. H. Ribeiro, *Mild bounds on bigravity from primordial gravitational waves*, *JCAP* **1507** (2015) 027, [1505.00404].
- [63] K. Aoki, K.-i. Maeda and R. Namba, *Stability of the Early Universe in Bigravity Theory*, *Phys. Rev.* **D92** (2015) 044054, [1506.04543].
- [64] E. Babichev, C. Deffayet and R. Ziour, *The Vainshtein mechanism in the Decoupling Limit of massive gravity*, *JHEP* **05** (2009) 098, [0901.0393].
- [65] E. Babichev, C. Deffayet and R. Ziour, *Recovering General Relativity from massive gravity*, *Phys. Rev. Lett.* **103** (2009) 201102, [0907.4103].
- [66] E. Babichev, C. Deffayet and R. Ziour, *The Recovery of General Relativity in massive gravity via the Vainshtein mechanism*, *Phys. Rev.* **D82** (2010) 104008, [1007.4506].
- [67] K. Koyama, G. Niz and G. Tasinato, *Analytic solutions in non-linear massive gravity*, *Phys. Rev. Lett.* **107** (2011) 131101, [1103.4708].
- [68] T. M. Nieuwenhuizen, *Exact Schwarzschild-de Sitter black holes in a family of massive gravity models*, *Phys. Rev.* **D84** (2011) 024038, [1103.5912].
- [69] K. Koyama, G. Niz and G. Tasinato, *Strong interactions and exact solutions in non-linear massive gravity*, *Phys. Rev.* **D84** (2011) 064033, [1104.2143].
- [70] G. Chkareuli and D. Pirtskhalava, *Vainshtein Mechanism In  $\Lambda_3$  - Theories*, *Phys. Lett.* **B713** (2012) 99–103, [1105.1783].
- [71] A. Gruzinov and M. Mirbabayi, *Stars and Black Holes in Massive Gravity*, *Phys. Rev.* **D84** (2011) 124019, [1106.2551].
- [72] E. Babichev, C. Deffayet and G. Esposito-Farese, *Constraints on Shift-Symmetric Scalar-Tensor Theories with a Vainshtein Mechanism from Bounds on the Time Variation of  $G$* , *Phys. Rev. Lett.* **107** (2011) 251102, [1107.1569].
- [73] D. Comelli, M. Crisostomi, F. Nesti and L. Pilo, *Spherically Symmetric Solutions in Ghost-Free Massive Gravity*, *Phys. Rev.* **D85** (2012) 024044, [1110.4967].
- [74] L. Berezhiani, G. Chkareuli, C. de Rham, G. Gabadadze and A. J. Tolley, *On Black Holes in Massive Gravity*, *Phys. Rev.* **D85** (2012) 044024, [1111.3613].
- [75] S. Sjors and E. Mortsell, *Spherically Symmetric Solutions in Massive Gravity and Constraints from Galaxies*, *JHEP* **02** (2013) 080, [1111.5961].
- [76] M. S. Volkov, *Hairy black holes in the ghost-free bigravity theory*, *Phys. Rev.* **D85** (2012) 124043, [1202.6682].
- [77] F. Sbisà, G. Niz, K. Koyama and G. Tasinato, *Characterising Vainshtein Solutions in Massive Gravity*, *Phys. Rev.* **D86** (2012) 024033, [1204.1193].
- [78] M. S. Volkov, *Self-accelerating cosmologies and hairy black holes in ghost-free bigravity and massive gravity*, *Class. Quant. Grav.* **30** (2013) 184009, [1304.0238].
- [79] E. Babichev and M. Crisostomi, *Restoring general relativity in massive bigravity theory*, *Phys. Rev.* **D88** (2013) 084002, [1307.3640].

- [80] N. Kaloper, A. Padilla, P. Saffin and D. Stefanyszyn, *Unitarity and the Vainshtein Mechanism*, *Phys. Rev.* **D91** (2015) 045017, [1409.3243].
- [81] S. Renaux-Petel, *On the Vainshtein mechanism in the minimal model of massive gravity*, *JCAP* **1403** (2014) 043, [1401.0497].
- [82] J. Enander and E. Mortsell, *On stars, galaxies and black holes in massive bigravity*, *JCAP* **1511** (2015) 023, [1507.00912].
- [83] C. de Rham, A. J. Tolley and S.-Y. Zhou, *Non-compact nonlinear sigma models*, *Phys. Lett.* **B760** (2016) 579–583, [1512.06838].
- [84] C. de Rham, A. J. Tolley and S.-Y. Zhou, *The  $\Lambda_2$  limit of massive gravity*, *JHEP* **04** (2016) 188, [1602.03721].
- [85] K. Aoki, K.-i. Maeda and M. Tanabe, *Relativistic stars in bigravity theory*, *Phys. Rev.* **D93** (2016) 064054, [1602.02227].
- [86] K. Aoki and S. Mizuno, *Vainshtein mechanism in massive gravity nonlinear sigma models*, *Phys. Rev.* **D94** (2016) 064054, [1607.00173].
- [87] S. Deser and A. Waldron, *Gauge invariances and phases of massive higher spins in (A)dS*, *Phys. Rev. Lett.* **87** (2001) 031601, [hep-th/0102166].
- [88] S. Deser and A. Waldron, *Partial masslessness of higher spins in (A)dS*, *Nucl. Phys.* **B607** (2001) 577–604, [hep-th/0103198].
- [89] A. S. Goldhaber and M. M. Nieto, *Mass of the graviton*, *Phys. Rev.* **D9** (1974) 1119–1121.
- [90] C. Talmadge, J. P. Berthias, R. W. Hellings and E. M. Standish, *Model Independent Constraints on Possible Modifications of Newtonian Gravity*, *Phys. Rev. Lett.* **61** (1988) 1159–1162.
- [91] VIRGO, LIGO SCIENTIFIC collaboration, B. P. Abbott et al., *Observation of Gravitational Waves from a Binary Black Hole Merger*, *Phys. Rev. Lett.* **116** (2016) 061102, [1602.03837].
- [92] N. Yunes, K. Yagi and F. Pretorius, *Theoretical Physics Implications of the Binary Black-Hole Mergers GW150914 and GW151226*, *Phys. Rev.* **D94** (2016) 084002, [1603.08955].
- [93] K. Hinterbichler and R. A. Rosen, *Note on ghost-free matter couplings in massive gravity and multigravity*, *Phys. Rev.* **D92** (2015) 024030, [1503.06796].
- [94] G. D’Amico, C. de Rham, S. Dubovsky, G. Gabadadze, D. Pirtskhalava and A. J. Tolley, *Massive Cosmologies*, *Phys. Rev.* **D84** (2011) 124046, [1108.5231].
- [95] A. E. Gümrükçüoğlu, C. Lin and S. Mukohyama, *Open FRW universes and self-acceleration from nonlinear massive gravity*, *JCAP* **1111** (2011) 030, [1109.3845].
- [96] A. E. Gümrükçüoğlu, C. Lin and S. Mukohyama, *Cosmological perturbations of self-accelerating universe in nonlinear massive gravity*, *JCAP* **1203** (2012) 006, [1111.4107].
- [97] A. De Felice, A. E. Gümrükçüoğlu and S. Mukohyama, *Massive gravity: nonlinear instability of the homogeneous and isotropic universe*, *Phys. Rev. Lett.* **109** (2012) 171101, [1206.2080].
- [98] A. E. Gümrükçüoğlu, C. Lin and S. Mukohyama, *Anisotropic Friedmann-Robertson-Walker universe from nonlinear massive gravity*, *Phys. Lett.* **B717** (2012) 295–298, [1206.2723].
- [99] A. De Felice, A. E. Gümrükçüoğlu, C. Lin and S. Mukohyama, *Nonlinear stability of cosmological solutions in massive gravity*, *JCAP* **1305** (2013) 035, [1303.4154].

- [100] Y. Yamashita, A. De Felice and T. Tanaka, *Appearance of Boulware-Deser ghost in bigravity with doubly coupled matter*, *Int. J. Mod. Phys. D* **D23** (2014) 1443003, [1408.0487].
- [101] C. de Rham, L. Heisenberg and R. H. Ribeiro, *Ghosts and matter couplings in massive gravity, bigravity and multigravity*, *Phys. Rev. D* **D90** (2014) 124042, [1409.3834].
- [102] C. de Rham, L. Heisenberg and R. H. Ribeiro, *On couplings to matter in massive (bi-)gravity*, *Class. Quant. Grav.* **32** (2015) 035022, [1408.1678].
- [103] L. Heisenberg, *Quantum corrections in massive bigravity and new effective composite metrics*, *Class. Quant. Grav.* **32** (2015) 105011, [1410.4239].
- [104] L. Heisenberg, *More on effective composite metrics*, *Phys. Rev. D* **D92** (2015) 023525, [1505.02966].
- [105] C. de Rham and A. J. Tolley, *Vielbein to the rescue? Breaking the symmetric vielbein condition in massive gravity and multigravity*, *Phys. Rev. D* **D92** (2015) 024024, [1505.01450].
- [106] Q.-G. Huang, R. H. Ribeiro, Y.-H. Xing, K.-C. Zhang and S.-Y. Zhou, *On the uniqueness of the non-minimal matter coupling in massive gravity and bigravity*, *Phys. Lett. B* **B748** (2015) 356–360, [1505.02616].
- [107] A. De Felice, A. E. Gümrükçüoğlu, L. Heisenberg and S. Mukohyama, *Matter coupling in partially constrained vielbein formulation of massive gravity*, *JCAP* **1601** (2016) 003, [1509.05978].
- [108] T. Katsuragawa, *Properties of Bigravity Solutions in a Solvable Class*, *Phys. Rev. D* **D89** (2014) 124007, [1312.1550].
- [109] R. A. Isaacson, *Gravitational Radiation in the Limit of High Frequency. II. Nonlinear Terms and the Effective Stress Tensor*, *Phys. Rev.* **166** (1968) 1272–1279.
- [110] C. Deffayet and J.-W. Rombouts, *Ghosts, strong coupling and accidental symmetries in massive gravity*, *Phys. Rev. D* **D72** (2005) 044003, [gr-qc/0505134].
- [111] P. Creminelli, A. Nicolis, M. Papucci and E. Trincherini, *Ghosts in massive gravity*, *JHEP* **09** (2005) 003, [hep-th/0505147].
- [112] N. Arkani-Hamed, H. Georgi and M. D. Schwartz, *Effective field theory for massive gravitons and gravity in theory space*, *Annals Phys.* **305** (2003) 96–118, [hep-th/0210184].
- [113] N. A. Ondo and A. J. Tolley, *Complete Decoupling Limit of Ghost-free Massive Gravity*, *JHEP* **11** (2013) 059, [1307.4769].
- [114] M. Fasiello and A. J. Tolley, *Cosmological Stability Bound in Massive Gravity and Bigravity*, *JCAP* **1312** (2013) 002, [1308.1647].
- [115] A. Nicolis, R. Rattazzi and E. Trincherini, *The Galileon as a local modification of gravity*, *Phys. Rev. D* **D79** (2009) 064036, [0811.2197].
- [116] G. R. Dvali, G. Gabadadze and M. Porrati, *Metastable gravitons and infinite volume extra dimensions*, *Phys. Lett. B* **B484** (2000) 112–118, [hep-th/0002190].
- [117] G. R. Dvali, G. Gabadadze and M. Porrati, *4-D gravity on a brane in 5-D Minkowski space*, *Phys. Lett. B* **B485** (2000) 208–214, [hep-th/0005016].
- [118] G. R. Dvali and G. Gabadadze, *Gravity on a brane in infinite volume extra space*, *Phys. Rev. D* **D63** (2001) 065007, [hep-th/0008054].
- [119] C. Deffayet, G. Esposito-Farese and A. Vikman, *Covariant Galileon*, *Phys. Rev. D* **D79** (2009) 084003, [0901.1314].

- [120] C. Deffayet, S. Deser and G. Esposito-Farese, *Generalized Galileons: All scalar models whose curved background extensions maintain second-order field equations and stress-tensors*, *Phys. Rev.* **D80** (2009) 064015, [0906.1967].
- [121] C. Deffayet, X. Gao, D. A. Steer and G. Zahariade, *From k-essence to generalised Galileons*, *Phys. Rev.* **D84** (2011) 064039, [1103.3260].
- [122] T. Kobayashi, M. Yamaguchi and J. Yokoyama, *Generalized G-inflation: Inflation with the most general second-order field equations*, *Prog. Theor. Phys.* **126** (2011) 511–529, [1105.5723].
- [123] G. W. Horndeski, *Second-order scalar-tensor field equations in a four-dimensional space*, *Int. J. Theor. Phys.* **10** (1974) 363–384.
- [124] J. Gleyzes, D. Langlois, F. Piazza and F. Vernizzi, *Healthy theories beyond Horndeski*, *Phys. Rev. Lett.* **114** (2015) 211101, [1404.6495].
- [125] J. Gleyzes, D. Langlois, F. Piazza and F. Vernizzi, *Exploring gravitational theories beyond Horndeski*, *JCAP* **1502** (2015) 018, [1408.1952].
- [126] K. Koyama, G. Niz and G. Tasinato, *Effective theory for the Vainshtein mechanism from the Horndeski action*, *Phys. Rev.* **D88** (2013) 021502, [1305.0279].
- [127] R. Kimura, T. Kobayashi and K. Yamamoto, *Vainshtein screening in a cosmological background in the most general second-order scalar-tensor theory*, *Phys. Rev.* **D85** (2012) 024023, [1111.6749].
- [128] T. Kobayashi, Y. Watanabe and D. Yamauchi, *Breaking of Vainshtein screening in scalar-tensor theories beyond Horndeski*, *Phys. Rev.* **D91** (2015) 064013, [1411.4130].
- [129] R. Saito, D. Yamauchi, S. Mizuno, J. Gleyzes and D. Langlois, *Modified gravity inside astrophysical bodies*, *JCAP* **1506** (2015) 008, [1503.01448].
- [130] M. Gell-Mann and M. Levy, *The axial vector current in beta decay*, *Nuovo Cim.* **16** (1960) 705.
- [131] S. Weinberg, *Phenomenological Lagrangians*, *Physica* **A96** (1979) 327–340.
- [132] V. Baccetti, P. Martin-Moruno and M. Visser, *Massive gravity from bimetric gravity*, *Class. Quant. Grav.* **30** (2013) 015004, [1205.2158].
- [133] A. H. Chamseddine and M. S. Volkov, *Cosmological solutions with massive gravitons*, *Phys. Lett.* **B704** (2011) 652–654, [1107.5504].
- [134] P. Gratia, W. Hu and M. Wyman, *Self-accelerating Massive Gravity: Exact solutions for any isotropic matter distribution*, *Phys. Rev.* **D86** (2012) 061504, [1205.4241].
- [135] T. Kobayashi, M. Siino, M. Yamaguchi and D. Yoshida, *New Cosmological Solutions in Massive Gravity*, *Phys. Rev.* **D86** (2012) 061505, [1205.4938].
- [136] T. Q. Do and W. F. Kao, *Anisotropically expanding universe in massive gravity*, *Phys. Rev.* **D88** (2013) 063006.
- [137] A. E. Gümrukçüoğlu, L. Heisenberg, S. Mukohyama and N. Tanahashi, *Cosmology in bimetric theory with an effective composite coupling to matter*, *JCAP* **1504** (2015) 008, [1501.02790].
- [138] G. W. Gibbons and S. W. Hawking, *Cosmological Event Horizons, Thermodynamics, and Particle Creation*, *Phys. Rev.* **D15** (1977) 2738–2751.
- [139] S. W. Hawking and I. G. Moss, *Supercooled Phase Transitions in the Very Early Universe*, *Phys. Lett.* **B110** (1982) 35.

- [140] R. M. Wald, *Asymptotic behavior of homogeneous cosmological models in the presence of a positive cosmological constant*, *Phys. Rev.* **D28** (1983) 2118–2120.
- [141] A. A. Starobinsky, *Spectrum of relict gravitational radiation and the early state of the universe*, *JETP Lett.* **30** (1979) 682–685.
- [142] A. A. Starobinsky, *Isotropization of arbitrary cosmological expansion given an effective cosmological constant*, *JETP Lett.* **37** (1983) 66–69.
- [143] J. D. Barrow and J. Stein-Schabes, *Inhomogeneous cosmologies with cosmological constant*, *Phys. Lett.* **A103** (1984) 315.
- [144] Y. Kitada and K.-i. Maeda, *Cosmic no hair theorem in power law inflation*, *Phys. Rev.* **D45** (1992) 1416–1419.
- [145] Y. Kitada and K.-i. Maeda, *Cosmic no hair theorem in homogeneous space-times. 1. Bianchi models*, *Class. Quant. Grav.* **10** (1993) 703–734.
- [146] K.-i. Nakao, T. Nakamura, K.-i. Oohara and K.-i. Maeda, *Numerical study of cosmic no hair conjecture. 1. Formalism and linear analysis*, *Phys. Rev.* **D43** (1991) 1788–1797.
- [147] K. Nakao, T. Nakamura, K.-I. Maeda and K. Oohara, *Numerical study of cosmic no hair conjecture. 2: Analysis of initial data*, *Phys. Rev.* **D47** (1993) 3194–3202.
- [148] K.-i. Nakao, T. Shiromizu and K.-i. Maeda, *Gravitational mass in asymptotically de Sitter space-times*, *Class. Quant. Grav.* **11** (1994) 2059–2072.
- [149] M. Shibata, K.-i. Nakao, T. Nakamura and K.-i. Maeda, *Dynamical evolution of gravitational waves in the asymptotically de Sitter space-time*, *Phys. Rev.* **D50** (1994) 708–719.
- [150] A. E. Gümrükçüoğlu, S. Mukohyama and T. P. Sotiriou, *Low energy ghosts and the Jeans’ instability*, *Phys. Rev.* **D94** (2016) 064001, [1606.00618].
- [151] J. M. Cline, S. Jeon and G. D. Moore, *The Phantom menaced: Constraints on low-energy effective ghosts*, *Phys. Rev.* **D70** (2004) 043543, [hep-ph/0311312].
- [152] N. Arkani-Hamed, H.-C. Cheng, M. A. Luty and S. Mukohyama, *Ghost condensation and a consistent infrared modification of gravity*, *JHEP* **05** (2004) 074, [hep-th/0312099].
- [153] K. Kajantie, M. Laine, K. Rummukainen and Y. Schroder, *The Pressure of hot QCD up to  $g_6 \ln(1/g)$* , *Phys. Rev.* **D67** (2003) 105008, [hep-ph/0211321].
- [154] T. S. van Albada, J. N. Bahcall, K. Begeman and R. Sancisi, *The Distribution of Dark Matter in the Spiral Galaxy NGC-3198*, *Astrophys. J.* **295** (1985) 305–313.
- [155] O. Zahn and M. Zaldarriaga, *Probing the Friedmann equation during recombination with future CMB experiments*, *Phys. Rev.* **D67** (2003) 063002, [astro-ph/0212360].
- [156] S. Galli, A. Melchiorri, G. F. Smoot and O. Zahn, *From Cavendish to PLANCK: Constraining Newton’s Gravitational Constant with CMB Temperature and Polarization Anisotropy*, *Phys. Rev.* **D80** (2009) 023508, [0905.1808].
- [157] C. J. A. P. Martins, E. Menegoni, S. Galli, G. Mangano and A. Melchiorri, *Varying couplings in the early universe: correlated variations of  $\alpha$  and  $G$* , *Phys. Rev.* **D82** (2010) 023532, [1001.3418].
- [158] T. Han, J. D. Lykken and R.-J. Zhang, *On Kaluza-Klein states from large extra dimensions*, *Phys. Rev.* **D59** (1999) 105006, [hep-ph/9811350].
- [159] G. F. Giudice, R. Rattazzi and J. D. Wells, *Quantum gravity and extra dimensions at high-energy colliders*, *Nucl. Phys.* **B544** (1999) 3–38, [hep-ph/9811291].

- [160] J. L. Hewett, *Indirect collider signals for extra dimensions*, *Phys. Rev. Lett.* **82** (1999) 4765–4768, [hep-ph/9811356].
- [161] S. L. Dubovsky, P. G. Tinyakov and I. I. Tkachev, *Massive graviton as a testable cold dark matter candidate*, *Phys. Rev. Lett.* **94** (2005) 181102, [hep-th/0411158].
- [162] M. Pshirkov, A. Tuntsov and K. A. Postnov, *Constraints on the massive graviton dark matter from pulsar timing and precision astrometry*, *Phys. Rev. Lett.* **101** (2008) 261101, [0805.1519].
- [163] S. Y. Khlebnikov and I. I. Tkachev, *Relic gravitational waves produced after preheating*, *Phys. Rev.* **D56** (1997) 653–660, [hep-ph/9701423].
- [164] R. Easther and E. A. Lim, *Stochastic gravitational wave production after inflation*, *JCAP* **0604** (2006) 010, [astro-ph/0601617].
- [165] R. Easther, J. T. Giblin, Jr. and E. A. Lim, *Gravitational Wave Production At The End Of Inflation*, *Phys. Rev. Lett.* **99** (2007) 221301, [astro-ph/0612294].
- [166] G. N. Felder and L. Kofman, *Nonlinear inflaton fragmentation after preheating*, *Phys. Rev.* **D75** (2007) 043518, [hep-ph/0606256].
- [167] J. F. Dufaux, A. Bergman, G. N. Felder, L. Kofman and J.-P. Uzan, *Theory and Numerics of Gravitational Waves from Preheating after Inflation*, *Phys. Rev.* **D76** (2007) 123517, [0707.0875].
- [168] J. Garcia-Bellido, D. G. Figueroa and A. Sastre, *A Gravitational Wave Background from Reheating after Hybrid Inflation*, *Phys. Rev.* **D77** (2008) 043517, [0707.0839].
- [169] J. Garcia-Bellido and D. G. Figueroa, *A stochastic background of gravitational waves from hybrid preheating*, *Phys. Rev. Lett.* **98** (2007) 061302, [astro-ph/0701014].
- [170] J.-F. Dufaux, G. Felder, L. Kofman and O. Navros, *Gravity Waves from Tachyonic Preheating after Hybrid Inflation*, *JCAP* **0903** (2009) 001, [0812.2917].
- [171] L. R. Price and X. Siemens, *Stochastic Backgrounds of Gravitational Waves from Cosmological Sources: Techniques and Applications to Preheating*, *Phys. Rev.* **D78** (2008) 063541, [0805.3570].
- [172] R. Jinno and M. Takimoto, *Gravitational waves from bubble collisions: analytic derivation*, 1605.01403.
- [173] P. Binetruy, A. Bohe, C. Caprini and J.-F. Dufaux, *Cosmological Backgrounds of Gravitational Waves and eLISA/NGO: Phase Transitions, Cosmic Strings and Other Sources*, *JCAP* **1206** (2012) 027, [1201.0983].
- [174] C. Caprini et al., *Science with the space-based interferometer eLISA. II: Gravitational waves from cosmological phase transitions*, *JCAP* **1604** (2016) 001, [1512.06239].
- [175] M. Viel, G. D. Becker, J. S. Bolton and M. G. Haehnelt, *Warm dark matter as a solution to the small scale crisis: New constraints from high redshift Lyman- $\alpha$  forest data*, *Phys. Rev.* **D88** (2013) 043502, [1306.2314].
- [176] H. Kodama and I. Arraut, *Stability of the Schwarzschild de Sitter black hole in the dRGT massive gravity theory*, *PTEP* **2014** (2014) 023E02, [1312.0370].
- [177] T. Kobayashi, M. Siino, M. Yamaguchi and D. Yoshida, *Perturbations of Cosmological and Black Hole Solutions in Massive gravity and Bi-gravity*, *PTEP* **2016** (2016) 103E02, [1509.02096].
- [178] E. Babichev, R. Brito and P. Pani, *Linear stability of nonbidiagonal black holes in massive gravity*, *Phys. Rev.* **D93** (2016) 044041, [1512.04058].

- [179] E. Babichev and A. Fabbri, *Instability of black holes in massive gravity*, *Class. Quant. Grav.* **30** (2013) 152001, [1304.5992].
- [180] R. Brito, V. Cardoso and P. Pani, *Massive spin-2 fields on black hole spacetimes: Instability of the Schwarzschild and Kerr solutions and bounds on the graviton mass*, *Phys. Rev.* **D88** (2013) 023514, [1304.6725].
- [181] E. Babichev and A. Fabbri, *Stability analysis of black holes in massive gravity: a unified treatment*, *Phys. Rev.* **D89** (2014) 081502, [1401.6871].
- [182] R. Brito, V. Cardoso and P. Pani, *Black holes with massive graviton hair*, *Phys. Rev.* **D88** (2013) 064006, [1309.0818].
- [183] F. Ozel, G. Baym and T. Guver, *Astrophysical Measurement of the Equation of State of Neutron Star Matter*, *Phys. Rev.* **D82** (2010) 101301, [1002.3153].
- [184] A. W. Steiner, J. M. Lattimer and E. F. Brown, *The Equation of State from Observed Masses and Radii of Neutron Stars*, *Astrophys. J.* **722** (2010) 33–54, [1005.0811].
- [185] V. Suleimanov, J. Poutanen, M. Revnivtsev and K. Werner, *Neutron star stiff equation of state derived from cooling phases of the X-ray burster 4U 1724-307*, *Astrophys. J.* **742** (2011) 122, [1004.4871].
- [186] O. Barziv, L. Kaper, M. H. van Kerkwijk, J. H. Telting and J. van Paradijs, *The mass of the neutron star in vela x-1*, *Astron. Astrophys.* **377** (2001) 925, [astro-ph/0108237].
- [187] M. L. Rawls, J. A. Orosz, J. E. McClintock, M. A. P. Torres, C. D. Bailyn and M. M. Buxton, *Refined Neutron-Star Mass Determinations for Six Eclipsing X-Ray Pulsar Binaries*, *Astrophys. J.* **730** (2011) 25, [1101.2465].
- [188] D. J. Nice, E. M. Splaver, I. H. Stairs, O. Loehmer, A. Jessner, M. Kramer, 2 et al., *A 2.1 solar mass pulsar measured by relativistic orbital decay*, *Astrophys. J.* **634** (2005) 1242–1249, [astro-ph/0508050].
- [189] P. Demorest, T. Pennucci, S. Ransom, M. Roberts and J. Hessels, *Shapiro Delay Measurement of A Two Solar Mass Neutron Star*, *Nature* **467** (2010) 1081–1083, [1010.5788].
- [190] N. Arkani-Hamed, A. G. Cohen and H. Georgi, *(De)constructing dimensions*, *Phys. Rev. Lett.* **86** (2001) 4757–4761, [hep-th/0104005].
- [191] N. Arkani-Hamed, A. G. Cohen and H. Georgi, *Electroweak symmetry breaking from dimensional deconstruction*, *Phys. Lett.* **B513** (2001) 232–240, [hep-ph/0105239].
- [192] C. Deffayet and J. Mourad, *Deconstruction of gravity*, *Int. J. Theor. Phys.* **44** (2005) 1743–1752.
- [193] C. Deffayet and J. Mourad, *Multigravity from a discrete extra dimension*, *Phys. Lett.* **B589** (2004) 48–58, [hep-th/0311124].
- [194] N. Arkani-Hamed and M. D. Schwartz, *Discrete gravitational dimensions*, *Phys. Rev.* **D69** (2004) 104001, [hep-th/0302110].
- [195] C. de Rham, A. Matas and A. J. Tolley, *Deconstructing Dimensions and Massive Gravity*, *Class. Quant. Grav.* **31** (2014) 025004, [1308.4136].
- [196] Y. Yamashita and T. Tanaka, *Mapping the ghost free bigravity into braneworld setup*, *JCAP* **1406** (2014) 004, [1401.4336].
- [197] Y. Yamashita and T. Tanaka, *Bigravity from gradient expansion*, *JCAP* **1605** (2016) 011, [1510.07551].
- [198] F. Sbisà, *Classical and quantum ghosts*, *Eur. J. Phys.* **36** (2015) 015009, [1406.4550].



- [199] R. P. Woodard, *Avoiding dark energy with  $1/r$  modifications of gravity*, *Lect. Notes Phys.* **720** (2007) 403–433, [astro-ph/0601672].
- [200] R. P. Woodard, *Ostrogradsky's theorem on Hamiltonian instability*, *Scholarpedia* **10** (2015) 32243, [1506.02210].
- [201] D. Langlois and K. Noui, *Degenerate higher derivative theories beyond Horndeski: evading the Ostrogradski instability*, *JCAP* **1602** (2016) 034, [1510.06930].

## 早稲田大学 博士（理学） 学位申請 研究業績書

氏名 青木 勝輝 印

(2016年 12月 現在)

| 種 類 別 | 題名、 発表・発行掲載誌名、 発表・発行年月、 連名者（申請者含む）  |
|-------|---|
| ○論文   | 著者：Katsuki Aoki and Kei-ichi Maeda<br>題名：Cosmology in ghost-free bigravity theory with twin matter fluids: The origin of dark matter<br>掲載誌名：Physical Review D 86, 064051<br>発表年月：2014年3月 |
| ○論文   | 著者：Katsuki Aoki and Kei-ichi Maeda<br>題名：Dark matter in ghost-free bigravity theory: From a galaxy scale to the universe<br>掲載誌名：Physical Review D 90, 124089<br>発表年月：2014年12月            |
| ○論文   | 著者：Katsuki Aoki, Kei-ichi Maeda, and Ryo Namba<br>題名：Stability of the early Universe in bigravity<br>掲載誌名：Physical Review D 92, 044054<br>発表年月：2015年8月                                    |
| ○論文   | 著者：Katsuki Aoki, Kei-ichi Maeda, and Makoto Tanabe<br>題名：Relativistic stars in bigravity theory<br>掲載誌名：Physical Review D 93, 064054<br>発表年月：2016年3月                                      |
| ○論文   | 著者：Katsuki Aoki and Shinji Mukohyama<br>題名：Massive gravitons as dark matter and gravitational waves<br>掲載誌名：Physical Review D 94, 024001<br>発表年月：2016年7月                                  |
| ○論文   | 著者：Katsuki Aoki and Shuntaro Mizno<br>題名：Vainshtein mechanism in massive gravity nonlinear sigma models<br>掲載誌名：Physical Review D 94, 064054<br>発表年月：2016年9月                              |

## 早稲田大学 博士（理学） 学位申請 研究業績書

| 種 類 別 | 題名、 発表・発行掲載誌名、 発表・発行年月、 連名者（申請者含む）  |
|-------|---|
| 講演    | <p>講演者：青木勝輝、前田恵一<br/>           題目：bigravity 理論に基づく宇宙論とダークエネルギー問題<br/>           会議名：日本物理学会年次大会<br/>           開催場所：高知大学<br/>           開催年月：2013年9月</p>  |
| 講演    | <p>講演者：青木勝輝、前田恵一<br/>           題目：Cosmology in ghost-free bigravity theory with twin matter fluid<br/>           会議名：The 23rd Workshop on General Relativity and Gravitation in Japan<br/>           開催場所：弘前大学<br/>           開催年月：2013年11月</p>      |
| 講演    | <p>講演者：青木勝輝、前田恵一<br/>           題目：Bigravity 理論とダークマター問題への応用<br/>           会議名：日本物理学会年次大会<br/>           開催場所：東海大学<br/>           開催年月：2014年3月</p>   |
| 講演    | <p>講演者：青木勝輝、前田恵一<br/>           題目：Dark matter in ghost-free bigravity theory<br/>           会議名：The 24th Workshop on General Relativity and Gravitation in Japan<br/>           開催場所：Kavli IPMU<br/>           開催年月：2014年11月</p>                     |
| 講演    | <p>講演者：青木勝輝、前田恵一、難波亮<br/>           題目：Time-dependent screening and stability around FLRW background in bigravity<br/>           会議名：日本物理学会年次大会<br/>           開催場所：早稲田大学<br/>           開催年月：2015年3月</p>   |
| 講演    | <p>講演者：青木勝輝、前田恵一、難波亮、田邊誠<br/>           題目：Cosmological and Astrophysical Vainshtein mechanism in bigravity<br/>           会議名：Fourteenth Marcel Grossmann Meeting<br/>           開催場所：University of Rome La Sapienza<br/>           開催年月：2015年7月</p> |
| 講演    | <p>講演者：青木勝輝、前田恵一、難波亮、田邊誠<br/>           題目：Cosmological and Astrophysical Vainshtein mechanism in bigravity<br/>           会議名：2nd APCTP-TUS workshop on Dark Energy<br/>           開催場所：東京理科大学<br/>           開催年月：2015年8月</p>                       |

## 早稲田大学 博士（理学） 学位申請 研究業績書

| 種 類 別 | 題名、 発表・発行掲載誌名、 発表・発行年月、 連名者（申請者含む）  |
|-------|---|
| 講演    | <p>講演者：青木勝輝、前田恵一、田邊誠<br/>           題目：Relativistic stars in bigravity<br/>           会議名：日本物理学会年次大会<br/>           開催場所：大阪市立大学<br/>           開催年月：2015年9月</p>   |
| 講演    | <p>講演者：青木勝輝、前田恵一、田邊誠<br/>           題目：Relativistic stars in the bigravity theory<br/>           会議名：The 25th Workshop on General Relativity and Gravitation in Japan<br/>           開催場所：京都大学<br/>           開催年月：2015年12月</p>                       |
| 講演    | <p>講演者：青木勝輝、水野俊太郎<br/>           題目：修正重力理論における Vainshtein 機構の安定性解析<br/>           会議名：日本物理学会年次大会<br/>           開催場所：東北学院大学<br/>           開催年月：2016年3月</p>   |
| 講演    | <p>講演者：青木勝輝、向山信治<br/>           題目：Bigravitons as dark matter and gravitational waves<br/>           会議名：21st International Conference and General Relativity and Gravitation<br/>           開催場所：Columbia University<br/>           開催年月：2016年7月</p> |
| 講演    | <p>講演者：青木勝輝、向山信治<br/>           題目：Bigravitons as dark matter and gravitational waves<br/>           会議名：日本物理学会年次大会<br/>           開催場所：宮崎大学<br/>           開催年月：2016年9月</p>  |
| 講演    | <p>講演者：青木勝輝、水野俊太郎<br/>           題目：Vainshtein mechanism in massive gravity nonlinear sigma models<br/>           会議名：The 26th Workshop on General Relativity and Gravitation in Japan<br/>           開催場所：大阪市立大学<br/>           開催年月：2016年10月</p>    |